Studies on the Synthesis of Strained Azaphosphiridine Complexes and their Reactivity towards Small Molecules

Dissertation

zur

Erlangung des Doktorgrades (Dr. rer. nat.)

der

Mathematisch-Naturwissenschaftlichen Fakultät

der

Rheinischen Friedrich-Wilhelms-Universität Bonn

vorgelegt von

José Manuel Villalba Franco

aus

Murcia, Spanien

Bonn, 2015

Angefertigt mit Genehmigung der Mathematisch-Naturwissenschaftlichen Fakultät der Rheinischen Friedrich-Wilhelms-Universität Bonn

1. Gutachter Prof. Dr. R. Streubel

2. Gutachter Prof. Dr. R. Glaum

3. Gutachter Prof. Dr. A. Lützen

4. Gutachter Prof. Dr. M. Wiese

Eingereicht am: 15.10.2015

Tag der Promotion: 7.12.2015

Erscheinungsjahr: 2015

TO MY PARENTS

WHO CONSTRUCTED THE FUNDATIONS OF WHO I AM

AND

TO MY WIFE

WHO MAKES ME A BETTER PERSON

Somewhere, something incredible is waiting to be known.

Carl Sagan

Some of the results of this PhD Thesis were previously published

1. "Stimuli-Responsive Frustrated Lewis-Pair-Type Reactivity ""of a Tungsten Iminoazaphosphiridine Complex", J.M. Villalba Franco, G. Schnakenburg, T. Sasamori, A. Espinosa Ferao, R. Streubel, *Chem. Eur. J.* **2015**, *21*, 9650-9655.

2. "Unprecedented ring-ring interconversion of N,P,C-cage ligands", J.M. Villalba Franco, G. Schnakenburg, A. Espinosa Ferao, R. Streubel, *Chem. Eur. J.* **2015**, *21*, 3727-2735.

3. "Going for strain: synthesis of the first 3-imino-azaphosphiridine complexes and their conversion into oxaphosphirane complex valence isomers", J.M. Villalba Franco, T. Sasamori, G. Schnakenburg, A. Espinosa Ferao, R. Streubel, *Chem. Commun.* **2015**, *51*, 3878-3881.

4. "The azaphosphiridine to terminal phosphinidene complex rearrangement - looking for non-covalent interactions of a highly reactive species", J.M. Villalba Franco, A. Espinosa Ferao, G. Schnakenburg, R. Streubel, *Chem. Commun*. **2013**, *49*, 9648-9650.

Publications related to other works

1. "Generation of Selenium-substituted Phosphaalkenes via the 1,2- Elimination of Chlorosilanes", Takahiro Sasamori, José Manuel Villalba Franco, Jing-Dong Guo, Koh Sugamata, Shigeru Nagase, Rainer Streubel, Norihiro Tokitoh, *Eur. J. Inorg. Chem.* **2015**, *submited*.

2. "Reactivity of terminal phosphinidene versus Li-Cl phosphinidenoid complexes in cycloaddition chemistry", R. Streubel, J.M. Villalba Franco, A. Espinosa Ferao, G. Schnakenburg, *Chem. Commun*. **2012**, *48*, 5986-5988.

Conferences and workshops

1. J. M. Villalba Franco and R. Streubel, MHC-7 Deutsch-Österreichischer Workshop, Freiberg/Germany, September 19.-21. **2014**: *"Synthesis and reactivity of "Super-Strained" Azaphosphiridine Complexes"* (Vortrag).
2. J. M. Villalba Franco, A. Espinosa Ferao and R. Streubel, 11th European Workshop on Phosphorus Chemistry, Sofia, Bulgaria, März 24.-26. **2014**: *"The Azaphosphiridine to Phosphinidene Complex Rearrangement"* (Poster Beitrag).
3. J. M. Villalba Franco, A. Espinosa Ferao and R. Streubel, 9th Meeting of Organoelement Chemistry, Kyoto University, Kyoto, Japan, 29-30 November **2013**: *"The Electrophilic Phosphinidene Complex Stabilized by Non Covalent Interactions"* (Poster Beitrag).
4. J. M. Villalba Franco, A. Espinosa Ferao and R. Streubel, 48th Meeting of Young Chemist, Tsukuba University, Japan, July 29-31, **2013**: *"Non Covalent Interactions of a Transient Electrophilic Terminal Phosphinidene Complex"* (Poster Beitrag).

5. J. M. Villalba Franco, A. Espinosa Ferao and R. Streubel, Kyoto University, Kyoto Japan, July 12th **2013**:*"Complexes with novel N,P,C-heterocyclic cage ligands derived from an azaphosphiridine complex"* (Vortrag beim Arbeitskreis Prof. N. Tokitoh).
6. J. M. Villalba Franco, R. Streubel, MHC-6 PhD Workshop, Bonn/Germany, April 5-7, **2013**: *"N,P,C heterocyclic cage complexes derived from an azaphosphiridine complex"* (Vortrag).
7. J. M. Villalba Franco, R. Streubel, 10th European Workshop on Phosphorus Chemistry, Regensburg/Germany, March 18.-20., **2013**: *"Complexes with novel N,P,C-heterocyclic cage ligands derived from an azaphosphiridine complex"* (Vortrag).
8. J. M. Villalba Franco, R. Streubel, AC Kolloquium, University of Bonn, Bonn, Germany, 31.01.**2013**: *"Complexes with novel N,P,C-heterocyclic cage ligands"* (Vortrag).
9. J. M. Villalba Franco, R. Streubel, The 13th International Symposium on Inorganic Ring Systems, Victoria/Canada, July 29 to August 2. **2012**: *"Novel P,N cage ligands via rearrangement of azaphosphiridine complexes"* (Poster Beitrag).
10. J. M. Villalba Franco, C. Murcia, V. Nesterov, R. Streubel, 9th European Workshop on Phosphorus Chemistry, Rennes/France, March 22.-24. **2012**: "*P-Functional azaphosphiridine and oxaphosphirane complexes"* (Poster Beitrag).
11. J. M: Villalba Franco, R. Streubel, SFB 813 Winter School 2012 on Electrochemistry, Hirschegg/Österreich, Februar 22-26. **2012**: *"Novel P,N-cage complexes with "strange" NMR properties",* (Poster Beitrag).
12. J. M. Villalba Franco, A. Espinosa Ferao, R. Streubel, 5. Deutsch-Österreichischer Mitarbeiter-Workshop, Graz/Österreich, September 23.-25. **2011**: *"Azaphosphiridine complexes: Synthesis and mechanistic considerations",* (Vortrag).
13. J. M. Villalba Franco, R. Streubel, 8th European Workshop on Phosphorus Chemistry, Münster/Germany, March 28.-29. **2011:** "*Synthesis and ring expansion of 3-thienyl-substituted 2H-azaphosphirene and azaphosphiridine tungsten complexes",* (Poster Beitrag).
14. J. M. Villalba Franco, R. Streubel, MHC-4 Deutsch-Österreichischer Mitarbeiter-Workshop, Blaubeuren/Germany, September 24.-26. **2010**: *"Surprising competitive formation of an azaphosphiridine complex and a bicyclic azaphospholene complex",* (Vortrag).

Die vorliegende Arbeit wurde im Zeitraum von Januar 2011 bis Juli 2015 im Arbeitskreis von Prof. Dr. R. Streubel am Institut für Anorganische Chemie der Rheinischen Friedrich-Wilhelms-Universität in Bonn angefertigt.

Hiermit versichere ich, dass ich diese Arbeit selbst verfasst und keine anderen als die angegebenen Quellen und Hilfsmittel verwendet habe.

Bonn, den 30. September 2015

Danksagung

Bei Herrn Prof. Dr. Rainer Streubel bedanke ich mich herzlich für die Themenstellung, die hervorragenden Arbeitsbedingungen, seine wertvollen Ratschläge und Anregungen, die großzügige Bereitstellung von Mitteln zur Anfertigung dieser Arbeit, sowie das Ermöglichen meiner Auslandsaufenthalte und der Teilnahme an diversen Tagungen.

Bei Herrn Prof. Robert Glaum bedanke ich mich herzlich für sein Interesse und die Übernahme des Koreferates.

Herrn Prof. Norihiro Tokitoh und Prof. Takahiro Sasamori danke ich für die freundliche Aufnahme in seiner Arbeitsgruppe in der Institute for Chemical Research, Kyoto University. Darüber hinaus danke ich allen Mitarbeitern der Arbeitsgruppe für die gute Zusammenarbeit, insbesondere Dr. Koh Sugamata für die Einarbeitung in die Phosphenium-Kationenchemie, sowie Dr. Hideaki Miyake, Dr. Tomohiro Agou und Dr. Yoshiyuki Mizuhata für die Lösung von alltäglichen technischen Schwierigkeiten. Prof. Takahiro Sasamori und seine Familie danke ich für ihre Freundschaft.

Prof. Arturo Espinosa Ferao und Prof. Takahiro Sasamori danke ich für die theoretischen Untersuchungen und für die Anregungen und vielen Diskussionen.

Für die Anfertigung von Einkristallröntgenstrukturanalysen gilt mein Dank Herrn Dr. Gregor Schnakenburg, Frau Charlotte Rödde und Prof. Takahiro Sasamori.

Weiterhin danke ich allen Mitarbeitern der Zentralanalytik der Chemischen Institute. Vor allem geht mein Dank für die Aufnahme zahlreicher Spektren und die Durchführung der NMR-Sondermessungen an Frau Karin Prochnicki. Darüber hinaus danke ich Frau Hannelore Spitz, Frau Ulrike Weynand für die Aufnahme von NMR-Spektren. Herrn Claus Schmidt und Frau Dr. Senada Nocinovic danke ich für viele hilfreiche Diskussionen und Anregungen. Frau Christine Sondag und Frau Dr. Marianne Engeser danke ich für die Aufnahme von MS-Spektren, Frau Anna Martens für die Durchführung der Elementaranalysen sowie den Mitarbeitern des Chemikalienlagers, Glasbläserei, der Mechanik- und der Elektrowerkstatt.

Mein Dank gilt auch allen aktuellen und vorherigen Mitarbeiter des AK Streubel: Gerd von Frantzius, Aysel Özbolat-Schön, Holger Helten, Maren Bode, Stefan Fankel, Christian Schulten, Janaina Marinas Pérez, Carolin Albrecht, Vitaly Nesterov, Lili Duan, Susanne Sauerbrey, Melina Klein, Andreas Kyri, Paresh Kumar Majhi, Abhishek Koner, Jan Faßbender, Imtiaz Begum, Cristina Murcia García und Tobias Heurich für die hervorragende Zusammenarbeit und auch für die ausserhalb des Labors vorhandene Unterstützung.

Außerdem danke ich auch allen ACF- und Bachelor-Praktikanten, die mich bei meiner Arbeit unterstützt haben.

Mein besonderer Dank gilt meinen Eltern und meine Ehefrau, Marianna, die mich ständig unterstützt haben.

Table of Contents

Chemical abbreviations:

12-c-4	12-crown-4
AIM	Atoms-In-Molecules
Ar	Aryl
aver.	Average
BCP	Bond Critical Point
BDE	Bond Dissociation Energy
dmp	2,6-Dimesitylphenyl
dtbpe	1,2-bis(di-*tert*-butylphosphanyl)ethane
Bu	Butyl
c	Cyclo
can	Canonical
conf.	Configuration
Cp	Cyclopentadienyl
Cp*	1,2,3,4,5-Pentamethylcyclopentadienyl
Cy	Cyclohexyl
DFT	Density Functional Theory
E	Heteroatom or Energy
Et	Ethyl
Fc	Ferrocene or ferrocenyl
FLP	Frustrated Lewis Pair
Fur	Furyl
G(r)	Lagrange kinetic energy
$\Delta G^{\neq}_{c}$	Free activation energy at coalescence temperature
HB	Hydrogen Bond
HMPT	Hexamethyl phosphorus triamide
HOMO	Highest Occuped Molecular Orbital
J	Coupling constant
K_c	Rate constant
LA	Lewis Acid
LB	Lewis Base
LBO	Löwdin Bond Order
LDA	Lithium diisopropylamide
LUMO	Lowest Unoccupied Molecular Orbital
M	Metal
Me	Methyl
Mes	Mesityl (2,4,6-trimethylphenyl)
Mes*	Super mesityl (2,4,6-tritertbutylphenyl)
MBO	Mayer Bond Order
MS	Mass Spectrometry
n	normal

NBO	Natural Bond Orbital
NCI	Non-Covalent Interaction
NMR	Nuclear Magnetic Resonance
OTf	Triflate
Ph	Phenyl
^{i}Pr	iso-Propyl
Res	Resonance
RCP	Ring Critical Point
RDG	Reduced Density Gradient
RSE	Ring Strain Energy
solv.	Solvent
SOPT	Second Order Perturbation Theory
t, tert	Tertiary
Tc	Coalescence temperature
TfOH	Triflic acid
Th	Thienyl
THF	Tetrahydrofurane
TS	Transition State
WBI	Wiberg Bond Index
X	Halogen

Units:

Å	Angstrom
a_o	Bohr Radius
°	Angle degree
cm	Centimetre
°C	Degree Celsius
e	electron
eV	Electron volt
Hz	Hertz
kcal	Kilocalories
mg	milligram
mL	Millilitre
mmol	Millimol
ppm	Parts per million
pm	Picometre

Analyticals abbreviations:

Br	Broad
Calcd.	Calculated
d	Doublet or bond length

EI	Electronic Impact
ESI	Electrospry Ionization
IR	Infra Red
m	Multiplet
m / z	Mass to charge ratio
q	Quintet
r. t.	Room Temperature
s	Singlet
Sat	Satellites
sep	Septet
t	Triplet
w	Weak
$\Delta\nu_o$	Difference in Hz between resonances
$\rho(r)$	Electron density
δ	Chemical shift
ũ	Wave number

1. Introduction

1.1. Low-coordinate phosphorus compounds

As asserted by Scherer and Regitz in their renowned book *Multiple Bonds and Low Coordination in Phosphorus Chemistry* "the preparation of HCP (phosphaacetylene) **I**[1] by Gier and $Me_3P{=}P{-}CF_3$ **II**[2] by Burg and Mahler in 1961, although being unstable under ambient conditions, provided the starting point for a second heyday of phosphorus chemistry, namely the chemistry of low-coordinate phosphorus compounds" (Scheme 1.1.1.).[3]

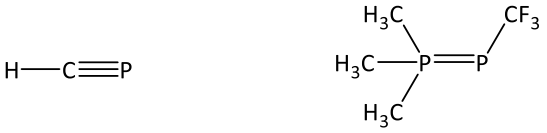

I **II**

Scheme 1.1.1. Phosphaacetylene **I** and P^{V},P^{III} diphosphene **II**.

$\sigma^2\lambda^3$–Phosphorus derivatives, where σ and λ stand for coordination and oxidation number respectively, are often compared to their C–C carbon analogous. The fact that phosphorus is reluctant to hybridize is due to the weak overlap between 3s and 3p atomic orbitals (AO).[3] This weak hybridization implies that the orbital which describes the phosphorus lone pair, for example in $HP{=}CH_2$, is not the highest in energy and features a very high 3s character (66% of the 3s atomic orbital and 34% of the 3p atomic orbital). These data are not specific to phosphaalkenes, and other low-coordinate phosphorus compounds display similar properties. As a consequence, the basicity of the lone pair is very low in low-coordinate phosphorus derivatives.[4] Due to the fact that the P=C π-bond strength (in CH_2=PH) is ca. 20 Kcal/mol weaker than that of the olefinic system (CH_2=CH_2),[4] most of these low-coordinate phosphorus compounds require kinetic stabilization to prevent oligomerization and be isolated. For example Mes*P=CH_2 (Mes* = 2,4,6-tris-*tert*-butylbenzene) could be isolated in the group of Appel thanks to the kinetic stabilization provided by the bulky Mes* group.[5] Thermodynamic stabilization can be achieved by introducing the P=C bond in a delocalized system as shown by Dimroth and Hoffmann in 1964 with the preparation of the first example of a stable two-coordinated, three valent phosphorus atom, the phosphamethine cyanine

cation **III**,[6] by Märkl with the 2,4,6-triphenylphosphinine **IV**[7] in 1966 and by Ashe with the parent phosphabenzene **V**[8] in 1971.

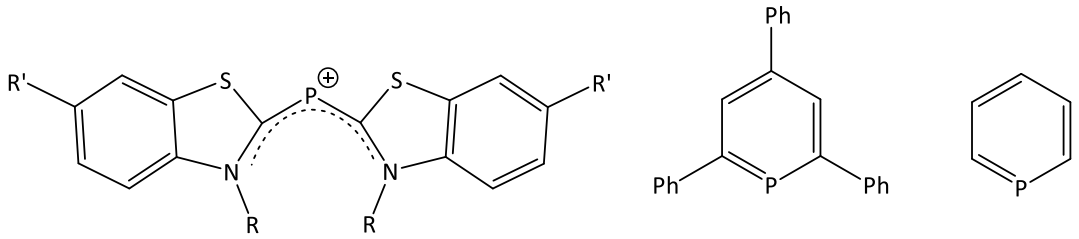

III[6] **IV**[7] **V**[8]

Scheme 1.1.2. Phosphamethine cyanine cation **III**, 2,4,6-triphenylphosphabenzene **IV** and phosphabenzene **V**.

Among the low-coordinate phosphorus compounds, phosphinidenes[9–11] are unique since they carry only a singly, σ–bonded substituent at the phosphorus atom. They are related with carbenes,[12] nitrenes[13] and silylenes[14] and, hence, can exist as singlet and triplet species depending on its substituent. Alike the parent carbene (H_2C) and nitrene (HN) and in contrast to silylene (H_2Si), the parent phosphinidene (HP) (according to IUPAC: phosphanediyl) largely prefers the triplet ground state. Alkyl or aryl substitution does not have a large influence on its ground state, while addition of a transition metal complex lead to a phosphinidene complex, which can exist as nucleophilic or electrophilic species.

1.2. Phosphinidene complexes

According to a proposal of Mathey,[11] electrophilic phosphinidene complexes can be seen as a combination of a singlet phosphinidene and a singlet transition metal moiety and, hence it has been related to the corresponding Fischer-type carbene complexes. The nucleophilic species can be considered as a combination of a triplet phosphinidene with a triplet transition metal moiety leading to a genuine P=M double bond with the more electronegative phosphorus atom carrying the negative charge and a LUMO that is mainly located at the metal center.[15] They have been related, for their part, to the Schrock-type carbene complexes (Figure 1.2.1).[16]

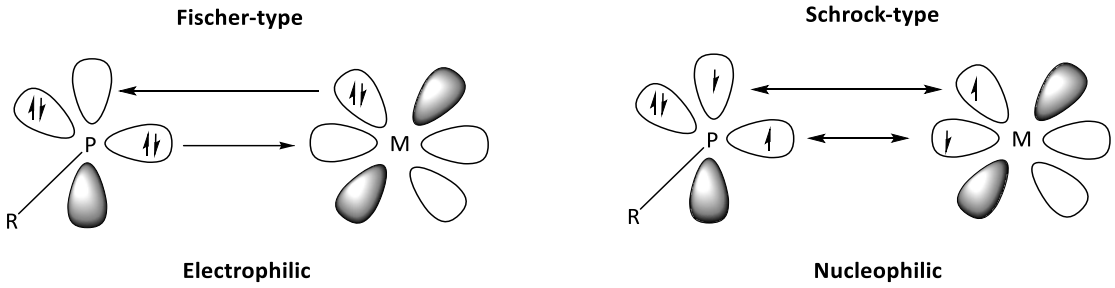

Figure 1.2.1. Representation of the electronic structures of electrophilic and nucleophilic terminal phosphinidene complexes (according to Mathey).[17]

The most characteristic reactions of the nucleophilic species are the phospha-Wittig reaction with carbonyl compounds[18], 1,2-additions of protic reagents[19], and [2+2] cycloadditions with alkynes (Scheme 1.2.1).[20]

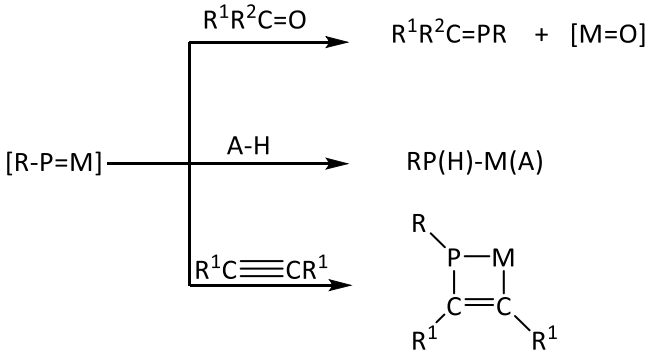

Scheme 1.2.1. Typical reactivity of nucleophilic terminal phosphinidene complexes.[17]

Since the first report of a transient electrophilic terminal phosphinidene pentacarbonylmetal(0) complex **IX** (Scheme 1.2.3), generated from 7-phosphanorbornadiene complexes (**VI**)[21] (Scheme 1.2.2) in toluene at about 110 °C (or at 55 °C if the reaction is performed in presence of CuCl),[22] these highly reactive species have been established as important RP_1 building blocks in organometallic synthesis.[9–11][23] Since then, several attempts have been made to develop methodologies to generate them in solution under milder conditions while keeping their high reactivity. In this regard, 2*H*-azaphosphirene (**VII**)[24-26] and benzophosphepine (**VIII**)[27] complexes (Scheme 1.2.2) were shown to be useful precursors for **XIX** at about 45-75 °C and 75-80 °C respectively.

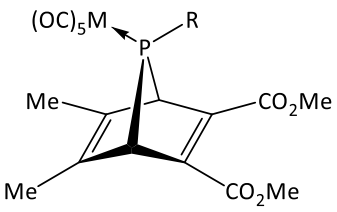

VI[20]

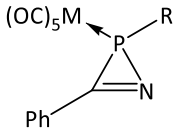

VII[25,26]

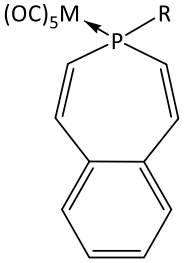

VIII[27]

Scheme 1.2.2. Commonly used electrophilic phosphinidene transfer reagents **VI**,[21] **VII**,[25,26] **VIII**[27] (M = Cr, Mo, W; R = alkyl or aryl).

It was then shown that transient *P*-amino phosphinidene complexes **X**[28] can be obtained via cycloreversion of phosphirane complexes at temperatures of *about* 70-90 °C. *P*-Amino phosphinidene iron complex **XI**, stable at room temperature, represented a breakthrough. However, strong back-donation from the iron and the additional intramolecular *N*-donor centre led to over-stabilization and, hence, loss of reactivity.[29] More recently, this quandary was solved to some extent as tetracarbonyliron(0) phosphinidene complexes of type **X** displayed a somewhat reduced phosphinidene complex reactivity in *intermolecular*[30] reactions, but which appeared to be enhanced for *intramolecular*[31] processes. Recently, a different strategy was reported using trileptic cationic phosphinidene metal(I) complexes[32] possessing cyclopentadienyl (Cp) or 1,2,3,4,5-pentamethylcyclopentadienyl (Cp*) ligands (**XII**), thus taking advantage of effective π-donor ligand effects. Stable, neutral, electrophilic phosphinidene vanadium[33] and niquel[34] complexes were prepared *via* halide abstraction from Cl_2PNR_2 and $[Na]_2[CpV(CO)_3]$ or deprotonation of cationic phosphido Ni complex ($[(dtbpe)Ni\{P(H)(dmp)\}^+][PF_6^-]$) respectively.

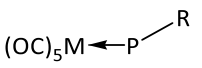

IX

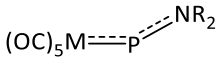

X

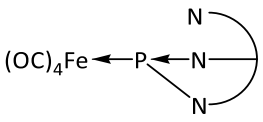

XI

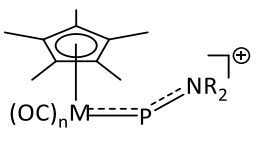

XII

Scheme 1.2.3. Terminal phosphinidene complexes **IX-XII** (M = transition metal, R = alkyl, aryl, amino group in **XI** = tris-(pyrazolyl)borato).

1.3. M/X phosphinidenoid complexes in heterocyclic chemistry

Already in 1985 Huttner visualized the synthetic potential of a species generated by a lithium/halogen exchange in a dichloro(organo)phosphane complex. Attempts where performed on dichloro(organo)phosphane complexes having sterically demanding organo substituents such as *t*-butyl, *c*-hexyl, or $(CH_3)_3SiCH_2$ using methyl lithium or *n*-butyl lithium as base but, here, only substitution reaction where obtained. When the size of the base was increased and *t*-butyl lithium was used, the result of the reaction was either a mixture of non-identified products or dinuclear phosphinidene complexes, depending on the transition metal. Although it could neither be isolated nor directly observed, a lithium/halogen exchange product was proposed as reactive intermediate.[35] Two decades later, a fluorophosphido tungsten(0) complex was proposed by Mathey to be generated in the reaction of 7-phosphanorbornadiene with cesium fluoride which readily reacted with another molecule of 7-phosphanorbornadiene forming a *P*-fluoro diphosphine complex.[36] An efficient methodology to achieve a lithium/halogen exchange in a dichloro(organo)phosphane complex was then reported in 2007 by Streubel.[37] Nowadays, such structures are named as Li/Cl phosphinidenoid complexes[37] among the scientific community. Meanwhile, this new and unique class of transition metal coordination compounds having unusual anionic *P*-ligands with a dicoordinate phosphorus atom and a bulky organic substituent such as bis(trimethylsilyl)methyl[38] (bisyl), 1,2,3,4,5-pentamethylcyclopentadienyl[39] (Cp*) or triphenylmethyl[40] (trityl) can be obtained (in some cases) bearing electron-withdrawing groups at phosphorus such as an halogen,[41] cyano,[42] alkoxide,[43] or amido.[44] Out of these four types of phosphinidenoid complexes, the Li/Cl derivatives **XV** have shown to be the most synthetically useful, because of their easy preparation and high reactivity. Chlorine/lithium exchange of dichloro(organo)phosphane complexes **XIII** using *tert*-butyl lithium or deprotonation of chloro(organo)phosphane complexes **XIV** with lithium diisopropylamide (LDA), in the presence of [12]crown-4 at low temperatures (-78 °C) in ethereal solvents have appeared as the two successful routes for the generation of these reactive intermediates. As well as M/X carbenoids resemble the reactivity of carbenes,[45] a multitude of examples have shown a similar parallelism of Li/Cl phosphinidenoid complexes and terminal electrophilic phosphinidene complexes in cycloaddition chemistry. For example, $\sigma^3\lambda^3$–oxaphosphirane complexes **XVI**, which were first reported by Mathey in 1990 by epoxidation of phosphaalkene complexes,[46] can be also obtained *via* reaction of an electrophilic terminal phosphinidene

complex generated thermally from 2*H*-azaphosphirene complex with aldehydes,[26] or *via* a Li/Cl phosphinidenoid complex with the same substrates.[38,47,48] Additionally, this so-called "low-temperature" route turned out to be extremely efficient because of its high yield and high functional group tolerance thus, in some cases, making the Li/Cl phosphinidenoid complex synthetically superior to the electrophilic phosphinidene complex in ring forming reactions. In the same vein, $1,2\lambda^3$–azaphosphiridine complexes **XVII** having the bisyl group at phosphorus can be synthesized making use of the electrophilic terminal phosphinidene complex and aromatic carbaldimines[49] as well as by reaction of Li/Cl phosphinidenoid complex and the same substrates.[50] Synthesis of $1,2\lambda^3$–azaphosphiridine complexes having the Cp* group at phosphorus has been one of the main objectives in this PhD thesis, which will be denoted hereafter as azaphosphiridines for simplicity. Nevertheless, occasionally different reactivity of these two kinds of reactive intermediates was observed toward the same substrates (Scheme 1.3.1).[51]

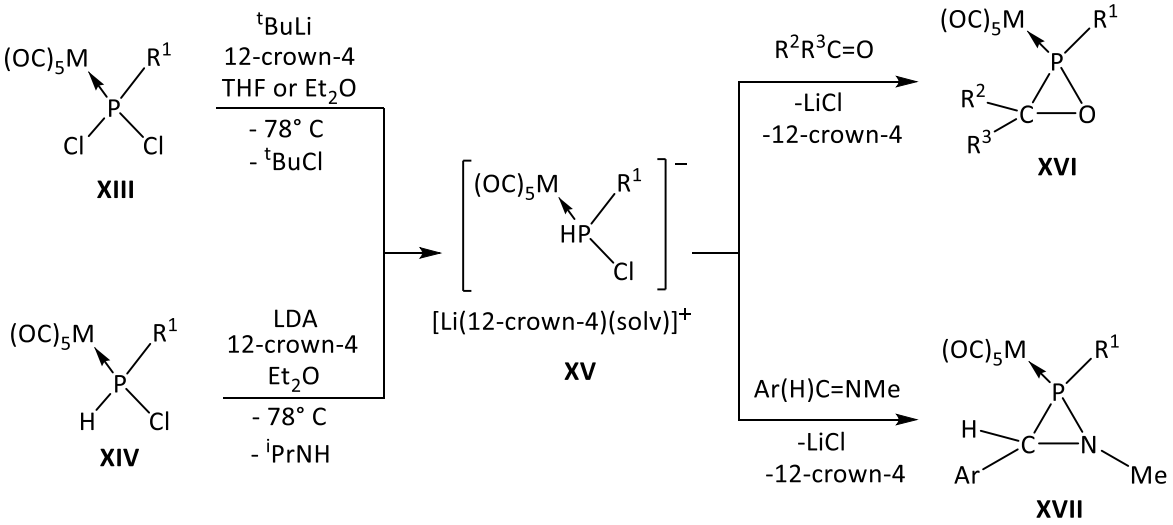

For oxaphosphirane complexes **XVI**: R^1 = $CH(SiMe_3)_2$,[37,47] Cp*,[38,48] CPh_3[40];
R_2, R_3 = H, aryl, alkyl
For azaphosphiridine complexes **XVII**: R^1 = $CH(SiMe_3)_2$[50]
Ar[50] = pheny, 2-furyl, 3-furyl, 2-thienyl, 2-(N-methylpirryl), ferrocenyl

Scheme 1.3.1. Generation of phosphinidenoid complex **XV** and formation of oxaphosphirane complex **XVI** and azaphosphiridine complex **XVII**.

1.4. Azaphosphiridines and their complexes

Three-membered heterocycles including one (**XVIII**) or two (**XIX**) heteroatoms such as oxygen, nitrogen or sulfur (Scheme 1.4.1) are very well known as versatile building blocks in organic synthesis.[52] Although related *P*-heterocycles, such as oxaphosphiranes (**XX**)[53] and azaphosphiridines (**IV**)[54] having four- and/or five-coordinate phosphorus centers received early attention in the late 1970s and early 1980s, reports on derivatives with a three-coordinate phosphorus center are still scarce for **XXI**[55] or even unknown for **XX**. Recently, computational studies on **XX**[56] and **XXI**[57] on the relative energies of the three-membered heterocycle and its isomers (and their $Cr(CO)_5$ in case of **XX** and **XXI**), the ring stability towards valence isomerization, and the ring strain, as well as the kinetics and thermodynamics of possible ring-opening reactions of P(III) (and P(V) chalcogenides for **XXI**) derivatives, were reported.

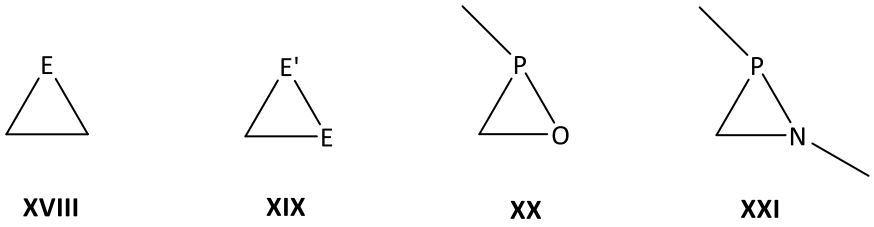

XVIII **XIX** **XX** **XXI**

E, E' = NR, O, S

Scheme 1.4.1. Three-membered rings having one (**XVIII**) or two (**XIX**) heteroatoms such as oxaphosphiranes (**XX**) and azaphosphiridines (**XXI**).

The question of electrocyclic ring opening and closing of symmetrical three-membered *P*-heterocycles was explored theoretically by Schoeller,[3] (Scheme 1.4.2) focusing on the thermochemistry of the E–E bond breaking and bond forming reactions, and the influence of substituents at E and P as being largely responsible for the relative stabilities of the rings with respect to their acyclic isomers, the bis(ylene)phosphoranes. Schoeller theoretically showed that species **XXIIb,c,f** tend to be more stable in form of their open valence isomers than as three-membered rings.[3] Experimentally, Niecke[58] studied the diazaphosphiridine system and demonstrated that the closed form can be obtained if bulky substituent such as *tert*-butyl are used at N atom.

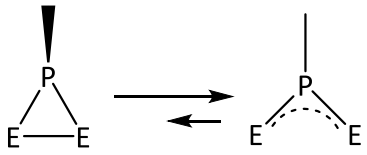

XXII **XXIII**

E = CH_2 (a), O (b), NH (c), SiH_2 (d), PH (e), S (f)

Scheme 1.4.2. Electrocyclic ring opening/closure for symmetrical three-membered phosphorus heterocycles according to Schoeller.[3]

The first example of an azaphosphiridine **XXVIII** was reported by Niecke in 1981. There, diisopropylamino(*tert*-butylimino)phosphane **XXIV** reacted with 1-diazo-2,2-dimethylpropane **XXV** to give the λ^3–triazaphospholene **XXVI** upon [2+3]-cycloaddition. The elimination of N_2 from **XXVI** leads to the corresponding imino(methylene)phosphorane **XXVII**. Then, valence isomerization of **XXVII** occurred yielding the final three-membered heterocycle **XXVIII**. This compound possesses a ^{31}P NMR chemical shift of -73.3 ppm, and was described to be a colorless liquid with a boiling point of 53-55 °C (0.01 torr)(Scheme 1.4.3).[55]

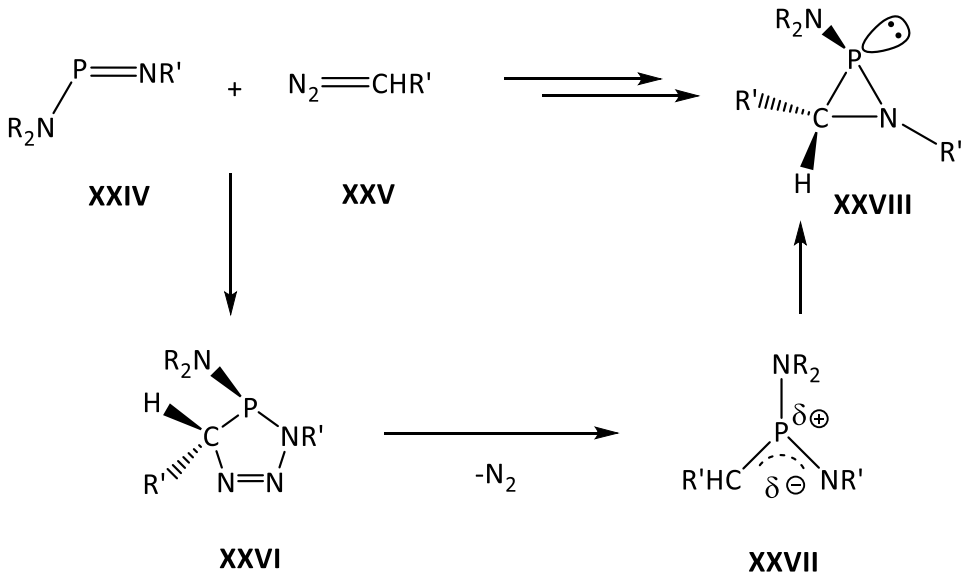

XXIV **XXV** **XXVIII**

XXVI **XXVII**

R = $CHMe_2$, R' = CMe_3

Scheme 1.4.3. Niecke´s synthesis of $1,2\lambda^3$–azaphosphiridine **XXVIII**.[55]

A second example was reported by Majoral and co-workers in 1989. In this case, addition of two equivalents of lithium bis(trimethylsilyl)amide **XXX** to the *C,C'*-dichloro phosphaalkene **XXIX** in THF at -7O °C led to the phosphaalkene **XXXI** (δ ^{31}P = +95). However, **XXXI** rearranged to the azaphosphiridine **XXXIII** which was obtained as a mixture of two isomers (δ ^{31}P = -49.5 and -47.4) (Scheme 1.4.4).[59]

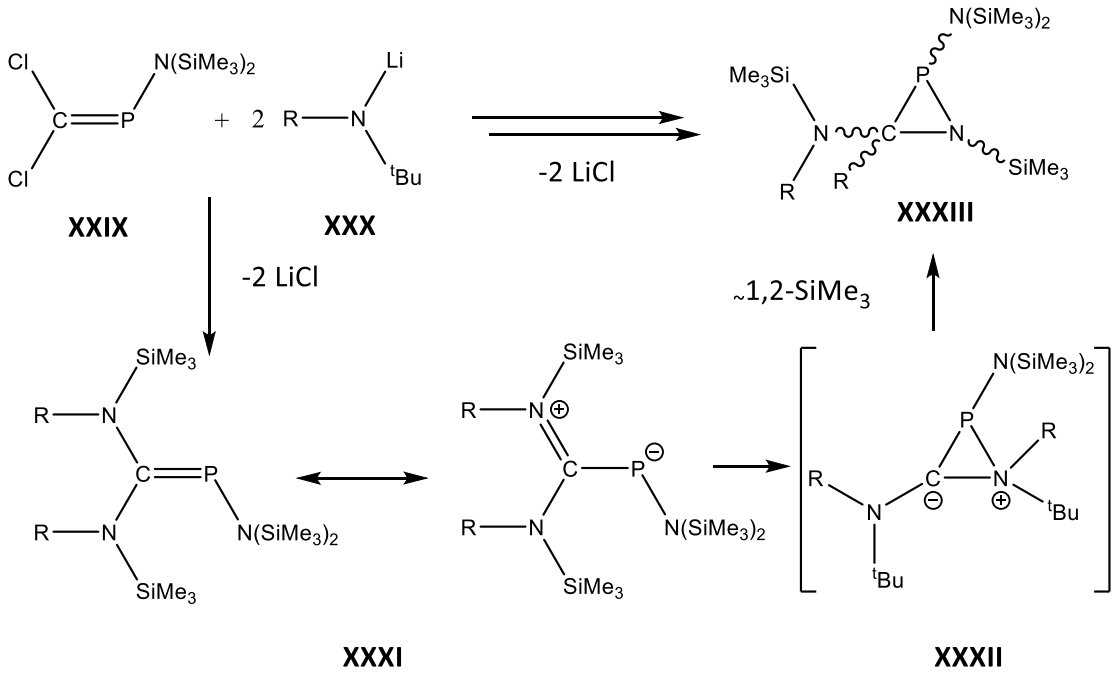

R = $SiMe_3$, ^tBu

Scheme 1.4.4. Majoral´s synthesis of $1,2\lambda^3$–azaphosphiridine **XXXIII**.[59]

The azaphosphiridine metal complex **XVIIa** was the first example ever to be reported (Streubel, 1997) using the reaction of the electrophilic terminal phosphinidene complex **XXXV**, generated thermally from the 2*H*-azaphosphirene complex **XXXIV**, and benzylidene(methyl)amine **XXXVIa**.[49] Later, Lammertsma and co-workers reported strong experimental[60] and computational[61] evidence for the intermediacy of azaphosphiridine complexes in thermal reactions of 7-phosphanorbornadiene complexes with imines, thus confirming the proposal by Mathey and co-workers made earlier in case of *P*-Ph and *P*-Me derivatives.[62] Recently, in 2010, a new methodology for the synthesis of this kind of three-membered heterocycles was developed using a Li/Cl phosphinidenoid metal(0) complex (**XV**) as the reactive intermediate in reaction with aldimines (**XXXVIa-c**) (Scheme 1.4.4).[50] Depending on the aryl substituent of the azaphosphiridine tungsten(0) complexes they display

^{31}P NMR chemical shifts between -35 and -41 ppm and $^{1}J_{W,P}$ coupling constants between 265 and 272 Hz (Scheme 1.4.4).

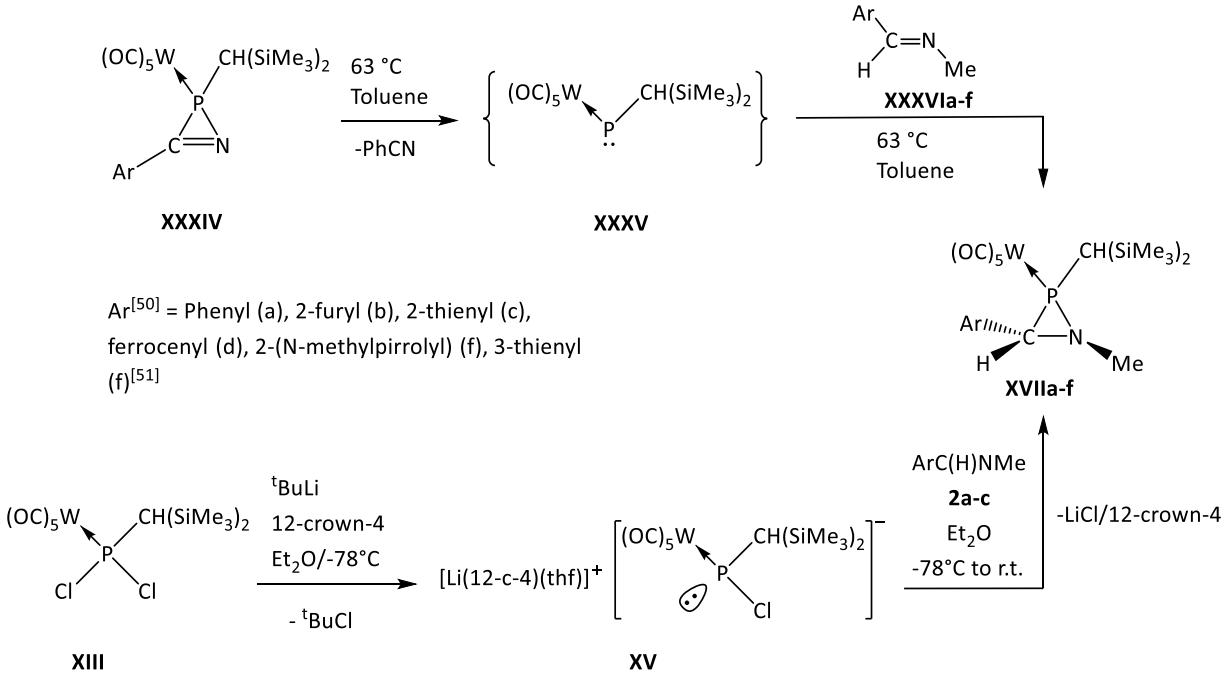

Scheme 1.4.4. Synthesis of azaphosphiridine tungsten(0) complexes **XVIIa-f** *via* reaction of an electrophilic phosphinidene complex (top) or a phosphinidenoid complex (bottom) with aldimines.[50,51]

Azaphosphiridine tungsten(0) complexes **XVIIa,d**, were shown to undergo regioselective ring expansion reactions with trifluoromethane sulfonic acid in the presence of dimethyl cyanamide, followed by deprotonation with triethylamine, thus leading to 1,3,4-$\sigma^3\lambda^3$-diazaphosphol-2-ene complexes (**XXXIX**) (Scheme 1.4.5).[50]

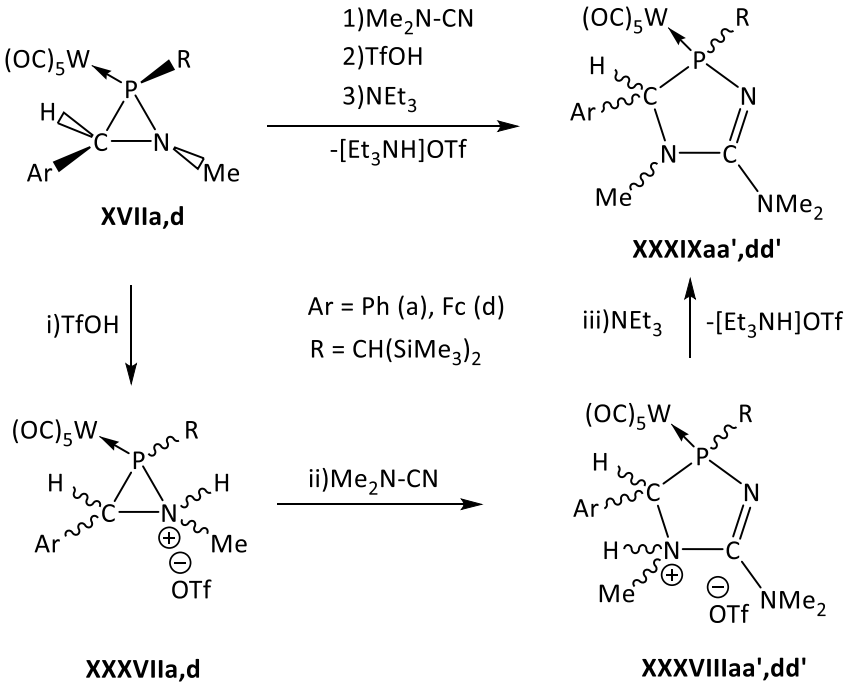

Scheme 1.4.5. Ring expansion reaction of complexes **XVIIa,d**.[50]

2. Aim of the thesis

The objective of this PhD Thesis was to build up a three-membered ring system containing phosphorus, carbon and nitrogen atoms, namely azaphosphiridines, which would exhibit higher reactivity than those azaphosphiridine systems reported before, and to study its ability to react with various, rather unreactive small molecules. This objective was approached from two different angles: i) the employment of a phosphorus bound pentamethyl cyclopentadienyl (Cp*) group and ii) the presence of an exocyclic imino bond at the ring carbon atom.

3. Complexes with N,P,C-cage ligands

In this chapter a comparative study on the reactivity of *P*-Cp* substituted terminal phosphinidene and Li/Cl phosphinidenoid complexes towards a series of *N*-methyl-*C*-aryl carbaldimines is reported. Despite intense studies on the reactivity of Li/Cl phosphinidenoid complexes, revealing their high versatility, occasionally, a different reactivity of these reactive intermediates towards the same substrates was observed. In addition, high-level DFT calculations were performed by Espinosa to study the path of formation of the products, revealing, *e.g.* an unprecedented ring-ring interconversion of a polycyclic ligand.

3.1. P,C-Cage ligand complexes having further heteroatoms

Since tetraphosphacubane[63] (**XL**) was obtained by phosphaalkyne cyclooligomerization in the late 1980s, the chemistry of P,C-cage compounds has expanded significantly. Despite this, few synthetic methods have been devised to prepare P,C-cage derivatives, incorporating further heteroatoms such as oxygen in **XLI**,[64] nitrogen in **XLII**[65-68] or phosphorus in **XLIII**.[69] For example O,P,C-cage complex **XLI** was obtained regioselectively upon thermal reaction of an oxaphosphirane complex and acetaldehyde. Here, an oxaphosphirane C–O ring opening was postulated to occur as the first step of the reaction mechanism.[64,70] Phosphaazabarbaralane **XLII**[71] named by Grützmacher *et. al.* as BARBAR-Phos, was elegantly synthesized by dehalogenation of dibenzotropylamino(dichloro)phosphane with magnesium in THF solutions. They showed that this kinds of ligands allow the synthesis of low-valent platinum(0) and copper(I) complexes.[71] N,P,C-Cage complexes with related structures were reported by the group of Streubel in the following years.[67,68] Hexaphosphapentaprismane cage **XLIII** could be prepared either by light-induced valence isomerization of an unsaturated precursor $^{t}Bu_4C_4P_6$ or by metal elimination of the trimeric mercury complex $[(^{t}Bu_4C_4P_6)Hg]_3$.[69] **XLIII** readily reacted with sulfur, selenium, and tellurium at its P–P bond to quantitatively afford new cage molecules of the type $EC_4{}^{t}Bu_4P_6$ (E = S, Se, Te).[72] Some of these structures were obtained only within the coordination sphere of a transition metal and/or by using *P*-pentamethylcyclopentadienyl substituted reactive species such as terminal and bridging[73] phosphinidene complexes. Recently, access to ionic cages such as **XLIV**, which were obtained by reducing pentamethylcyclopentadienyl dichlorophosphine with low oxidation state group XIII halides like indium chloride, was also reported.[74,75]

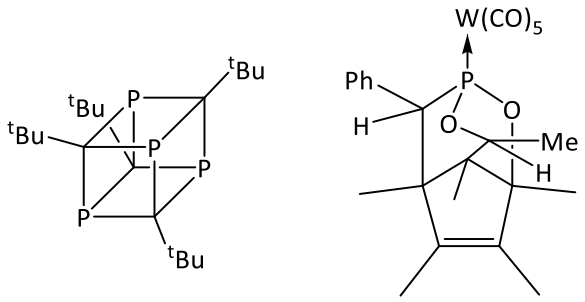

XL[63] **XLI**[64]

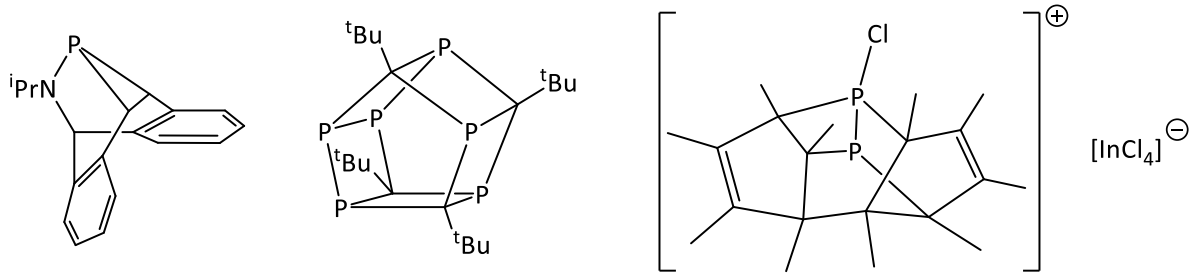

XLII[71] **XLIII**[69] **XLIV**[74,75]

Scheme 3.1.1. Tetra-*tert*-butyltetraphosphacubane[63] (**XL**) and examples of oxygen (**XLI**),[64] nitrogen (**XLII**)[71] and phosphorus (**XLIII**)[69] containing phosphorus cage-type molecules and an example of a cationic cage (**XLIV**).[74,75]

3.2. N,P,C-Cage complexes *via* reaction of a *P*-Cp* substituted Li/Cl phosphinidenoid complex with carbaldimines

In continuation of earlier efforts to develop azaphosphiridine complex chemistry,[50] and because a main group element-bound Cp* group has offered interesting reactivity in the past,[74] a *P*-Cp* substituted azaphosphiridine complex was targeted first. Therefore, the reaction of Li/Cl phosphinidenoid complex **2**,[39] prepared from **1**[77] and observed at 280.2 ppm ($^1J_{W,P}$ = 76.5 Hz) in the $^{31}P\{^1H\}$ NMR spectrum,[39] with carbaldimines **3a-f**[78,79] was investigated. With **3a,b** formation of the novel N,P,C-cage complexes **4a,b** occurred in 60 and 95% conversion according to ^{31}P NMR integration (THF), displaying $^{31}P\{^1H\}$ NMR resonances at -34.1 ppm ($^1J_{W,P}$ = 268.3 Hz) and -34.5 ppm ($^1J_{W,P}$ = 272.0 Hz), respectively. Reaction of **2** with **3c** and **3f** yielded **4c,f** in negligible amounts along with mixtures of unidentified products. No evidence for **4d** was observed when **2** was reacted with **3d**. Reaction of **2** with **3e** yielded selectively a complex **5** showing a $^{31}P\{^1H\}$ NMR resonance at 173.0 ppm ($^1J_{W,P}$ = 260.6 Hz in THF) presumably with a bicyclic azaphospholene ligand structure[51] (Scheme 3.2.1, Table 3.2.1).[80]

Table 3.2.1. ^{31}P NMR resonances [ppm] and $^{1}J_{W,P}$ [Hz] for **4a-f** in the reaction of **2** with **3a-f** (THF).[80]

Aryl	δ ^{31}P	$^{1}J_{W,P}$	**4a-f** [%] (^{31}P NMR int.)
Phenyl (**a**)	-34.1	268.3	60
2-Furyl (**b**)	-34.5	272.0	95
2-Thienyl (**c**)	-34.8	274.9	3
3-Furyl (**d**)	-	-	0
3-Thienyl (**e**)	-	-	0
p-CF_3-Phenyl (**f**)	-29.6	272.0	15

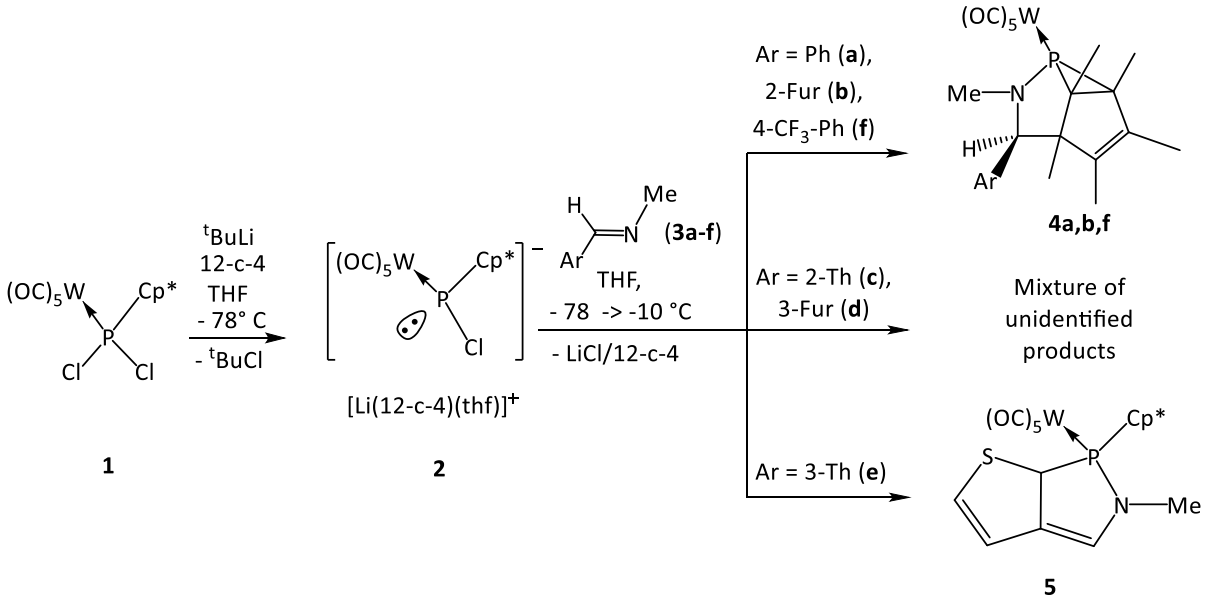

Ar = Phenyl (**a**), 2-furyl (**b**), 2-thienyl (c), 3-furyl (**d**), 3-thienyl (**e**), 4-CF_3-phenyl (**f**)

Scheme 3.2.1. Reaction of Li/Cl phosphinidenoid complex **2** with carbaldimines **3a-f**.[80]

3.2.1. Low temperature rearrangement of azaphosphiridine complexes to N,P,C-cage complexes

In case of **4b**, low temperature $^{31}P\{^{1}H\}$ NMR monitoring (THF) (Figure 3.2.1) revealed the formation of three intermediates which rapidly transformed into the final product. Compared to data of known azaphosphiridine complexes,[50] intermediates observed at -42.8 ppm ($^{1}J_{W,P}$ = 277.8 Hz) and at -38.5 ppm ($^{1}J_{W,P}$ = 271.0 Hz) were assigned to two stereoisomers of transient azaphosphiridine complexes **7b** and **7b'** (Scheme 3.2.1.1) for which a *trans* configuration of

the NMe and the 2-furyl groups is assumed. The intermediate displaying a $^{31}P\{^{1}H\}$ NMR resonance at -28.7 ppm ($^{1}J_{W,P}$ = 259.0 Hz) was assigned to the N,P,C-cage complex **4b'** which isomerizes to **4b**. Complex **4b** was isolated in 70% yield and fully characterized and its molecular structure was confirmed by X-ray crystallography.[81]

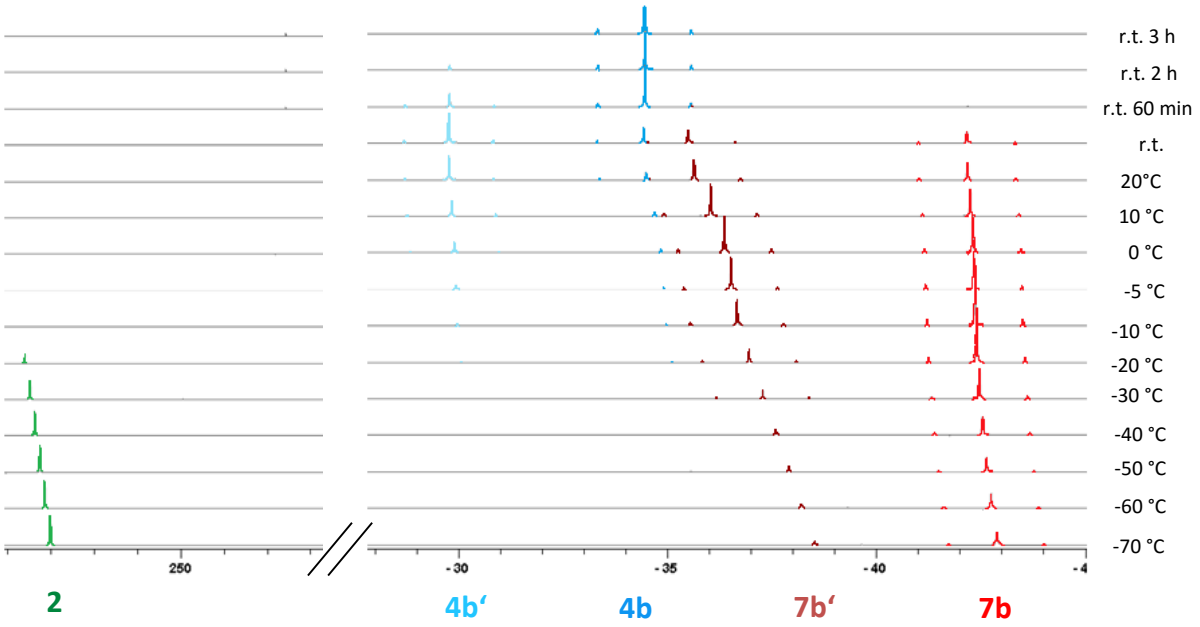

Figure 3.2.1.1 Low temperature $^{31}P\{^{1}H\}$ NMR monitoring (THF) of the reaction of *P*-Cp* phosphinidenoid tungsten(0) complex **2** and *C*-furyl-*N*-methyl carbaldimine **3b**. Time interval between each measurement was 10 minutes.[81]

The molecular structure of **4b** crystallized in the triclinic crystal system, space group $P\bar{1}$ and displays an almost planar geometry at nitrogen ($\Sigma°\angle N$ = 357.97), and a P–C(3) bond of 1.881(2) Å which is slightly elongated compared to the standard P,C bond distance (of about 1.80 Å)[82] (Figure 3.2.1.2).

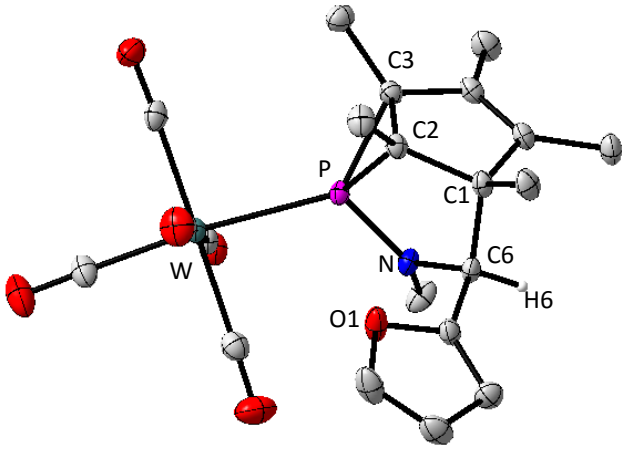

Figure 3.2.1.2. Molecular structure of complex **4b** (50% probability level, hydrogen atoms except H6 are omitted for clarity). Selected bond lengths [Å] and angles [°]: P-W 2.4907(6), P-C2 1.810(2), P-N 1.6723(18), P-C3 1.881(2), C3-P-C2 49.23(10).[81]

Espinosa performed DFT calculations (B3LYP-D3/def2-TZVP) on the reaction pathway using chromium as metal and H instead of the methyl group at nitrogen, starting from model azaphosphiridine complex **7g** with the furyl and Cp* groups in *trans* (Scheme 3.2.1.1); the epimer at N (**7g'**) was found to be less stable.[81] An intermediate iminium phosphane-ylid complex[83] **8g** is predicted to be initially formed by P–C bond cleavage through a low-lying TS (Figure 3.2.1.3) and displays the P–N–C plane almost perpendicular to the Cp* ring due to T-stacking of the model NH group with the p-system. In the real system **8b** the larger N-substituent presumably favors the conformer locating the side-chain parallel to the Cp* ring. Despite the low energy barrier for the transformation of **7g** into **8g**, this conversion constitutes the rate-determining step for the overall transformation into the final N,P,C-cages **4g,g'**. This species can undergo thermal aza-phospha-Cope [3,3] sigmatropic rearrangement affording phosphinidene complex **9g**^{conf} in a kinetically favored process. To the best of our knowledge only one example of a related aza-phospha-Cope reaction has been reported.[84] This reactive species **9g**^{conf} features the P atom lying almost antiperiplanar to the furyl substituent and far away from the dienic moiety.[1] Rotation of the C–N bond can furnish the thermodynamically favored conformer **9g**. Final addition of the phosphinidene complex to a C=C double bond[84] of the Cp* group would lead to the reaction product **4g**[2] (Scheme 3.2.1.1, Figure 3.2.1.3).

[1] A O···H–N interaction (d = 2.437 Å) is formed.

[2] TS(**9g** → **4g**) could not be properly located due to geometry convergence problems in a rather flat area of the hypersurface.

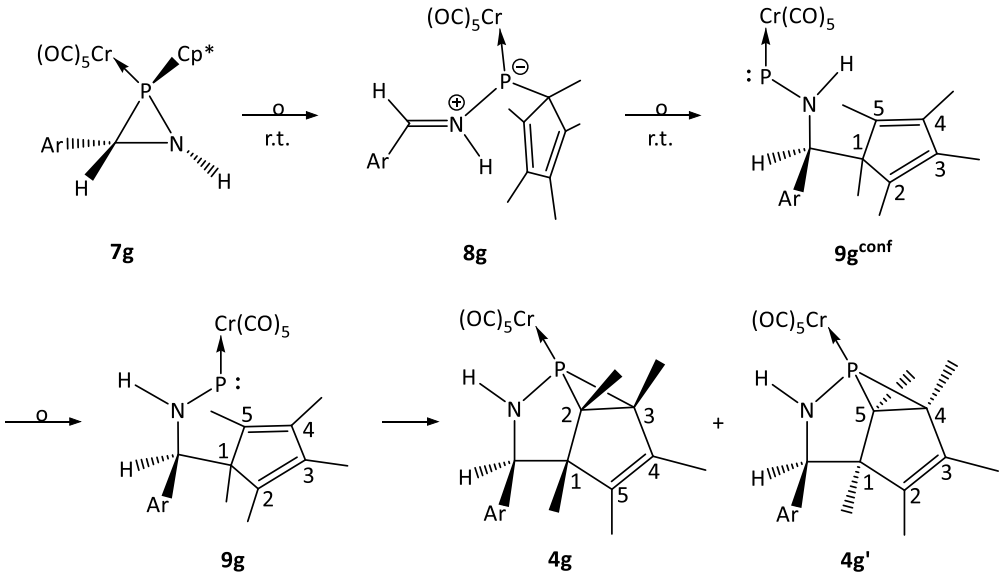

Scheme 3.2.1.1. Proposed mechanism for the isomerization of azaphosphiridine model complex **7g** into final complex **4g** (Ar: 2-furyl).[81]

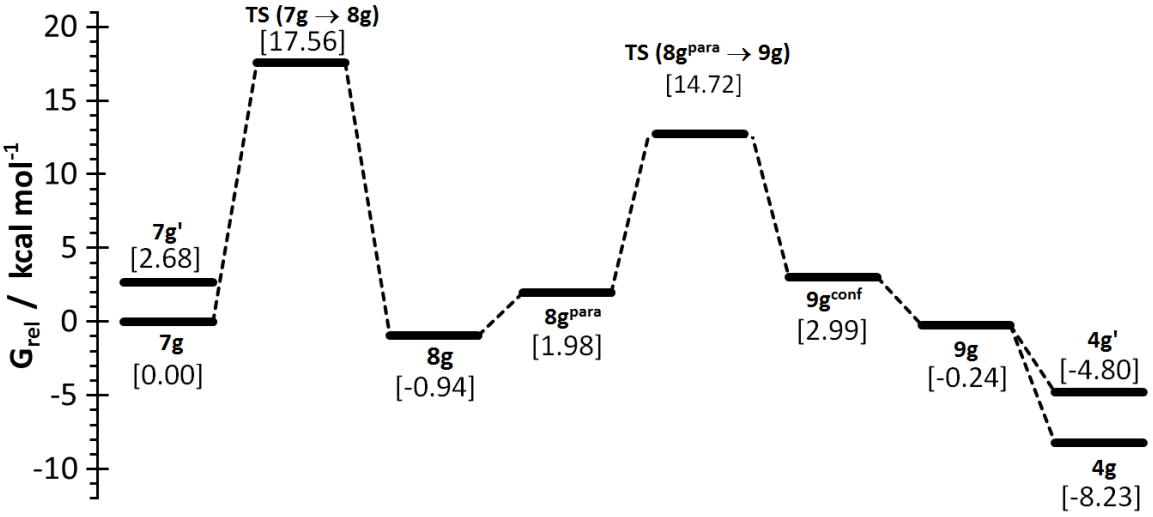

Figure. 3.2.1.3. Computed (B3LYP-D3/def2-TZVPP) minimum energy profile for the transformation **7g→4g**.[81]

The relatively low energy of **9g** can be explained as arising from electron density donation into the formally vacant p orbital of phosphorus, either (i) *directly* from the lone pair of the adjacent N atom and (ii) *through-space* from two different electron sources, namely the O atom of the 2-furyl substituent and a terminal carbon of the Cp* dienic unit. DFT calculations performed by Espinosa for the location of the BCPs (bond critical points) corresponding to

these two NCIs[3] fully supports these assumptions. These NCIs are conveniently visualized by color-coded RDG (reduced density gradient) isosurfaces (Figure 3.2.1.4). A rough estimation of the sum of NCIs, amounting to 3.2 kcal mol^{-1}, can be obtained from comparison between both conformers. When *C*-phenyl *N*-methyl carbaldimine (**3a**) was used instead of **3b**, a significant selectivity decrease (from 95% conv. to 60%, by ^{31}P NMR integration) was observed. This might be explained in terms of an increased electrophilicity at phosphorus and a decreased stability in the corresponding phosphinidene complex intermediate by loss of one of the "through-space" NCIs.

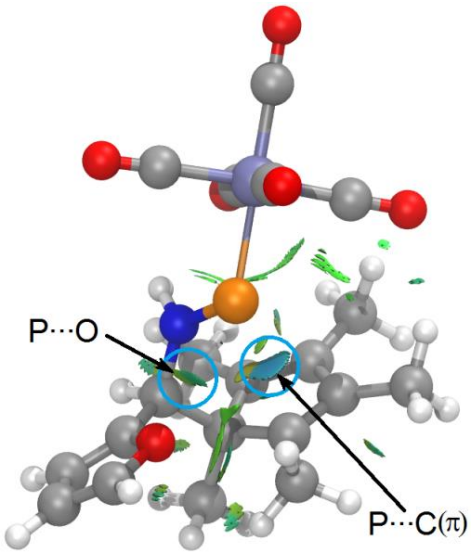

Figure 3.2.1.4. Computed (B3LYP-D3/def2-TZVP) structure for complex **9g** highlighting key NCIs.[81]

[3] P···C, d 3.110 Å, WBI 0.052, ρ(r) = 1.52x10^{-2} e/a_o^3; P···O, d 3.324 Å, WBI 0.007, ρ(r) = 0.84x10^{-2} e/a_o^3.

3.2.2. Trapping reaction with phenyl acetylene

The hypothesis of a transient terminal phosphinidene complex was further examined by studying trapping reactions. When phenyl acetylene was added to the reaction mixture of **7b,b'** at -30 °C, **4b** and **12** (δ ^{31}P = -3.9, $^{1}J_{WP}$ = 277.6 Hz) were obtained in a 1 : 4 ratio (Figure 3.2.2.1, Scheme 3.2.2.1).

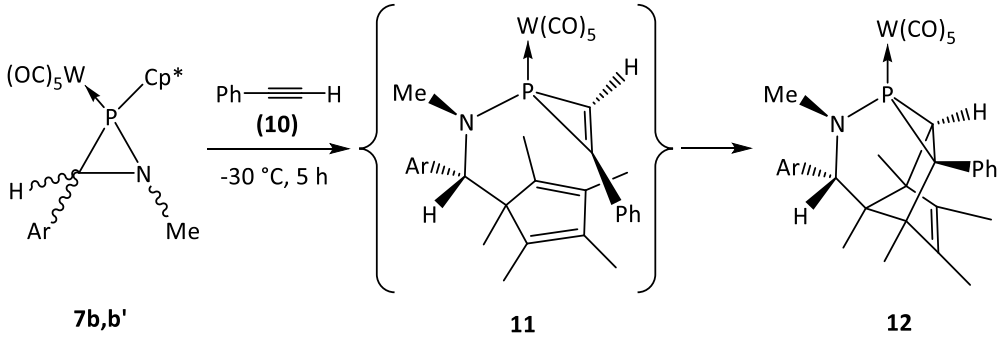

Scheme 3.2.2.1. Synthesis of complex **12** (Ar: 2-furyl).

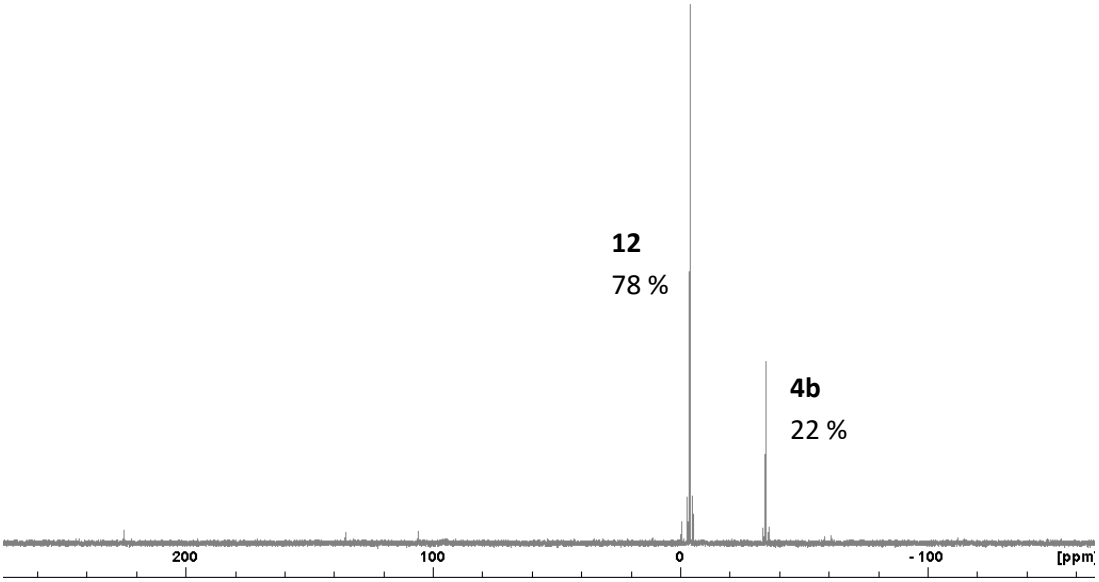

Figure 3.2.2.1. ^{31}P{^{1}H} NMR spectra with signal integrals (in %) of a mixture of complexes **4b** and **12**.[81]

Complex **12** was isolated in 60% yield and X-ray structure analysis (crystal system monoclinic, space group P21/n) (Figure 3.2.2.2) confirmed the formation of a new N,P,C-cage complex **12,** which can be explained by a [2+1] cycloaddition of the transient terminal

phosphinidene complex **9b** leading to **11**, followed by an intramolecular Diels-Alder reaction to give **12**.

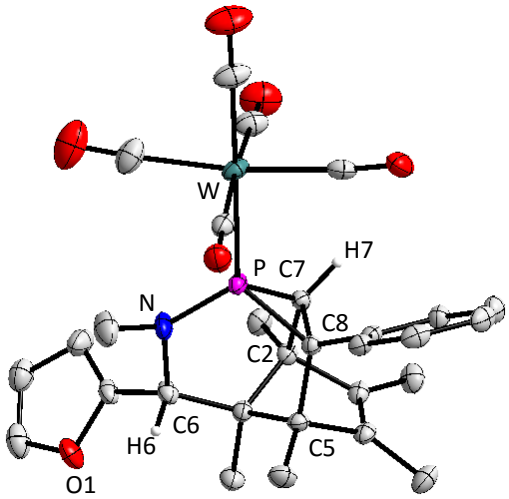

Figure 3.2.2.2. Molecular structure of complex **12** (50% probability level, hydrogen atoms except H6 are omitted for clarity). Selected bond lengths [Å] and angles [°]: P-W 2.4978(8), P-C8 1.803(3), P-N 1.666(3), P-C7 1.824(3), C7-P-C8 50.60(63).[81]

3.3. N,P,C-Cage complexes *via* reaction of a *P*-Cp* substituted terminal electrophilic phosphinidene complex with aldimines

When *P*-Cp* substituted phosphinidene complex **14**, generated thermally from 2*H*-azaphosphirene complex **13**[86] in toluene, reacted in *situ* with *C*-aryl-*N*-methyl carbaldimines **3a-f**,[78,79] complexes **4a-f** and **15a-f** were obtained in different ratios. Complexes **15a-f** exhibit resonances in the range of 226 to 231 ppm with tungsten-phosphorus coupling constants of about 230 Hz in the $^{31}P\{^{1}H\}$ NMR spectra and **4a-f** possesses ^{31}P resonances between -27 and -36 ppm with tungsten-phosphorus coupling constants of about 274 Hz (Scheme 3.3.1, Table 3.3.1, Figure 3.3.1). In analogy to previously reported reactions of complex **14** with nitriles,[68] an ylidic structure of transiently formed complexes **8a-f** was initially proposed to explain the formation of **4a-f** and **15a-f**. [80]

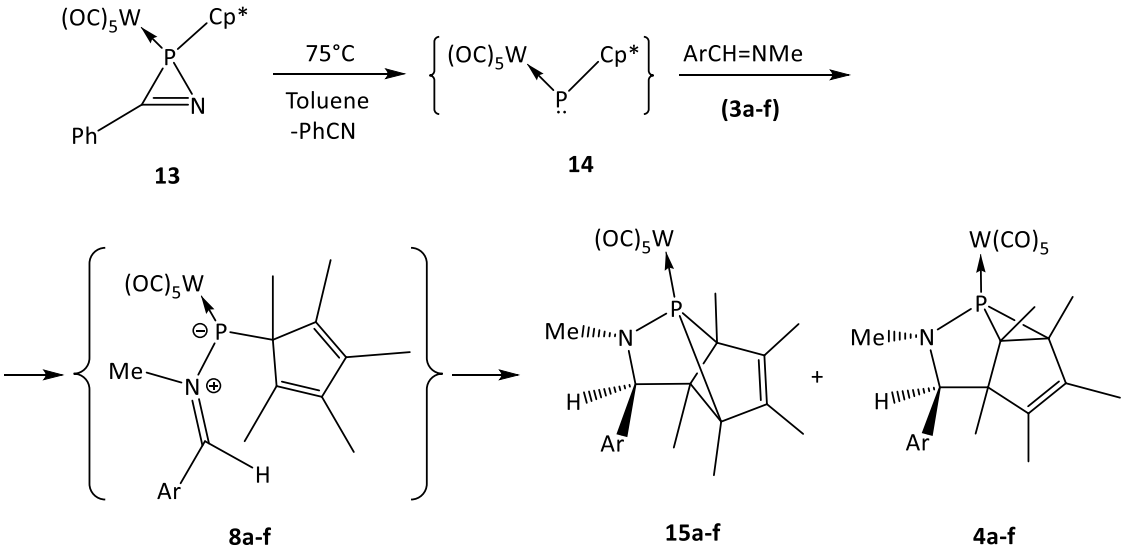

Ar = Ph (**a**), 2-furyl (**b**), 2-thienyl (**c**), 3-furyl (**d**), 3-thienyl (**e**), 4-CF_3-Ph (**f**)

Scheme 3.3.1. Synthesis of complexes **15a-f** and **4a-f**.[80]

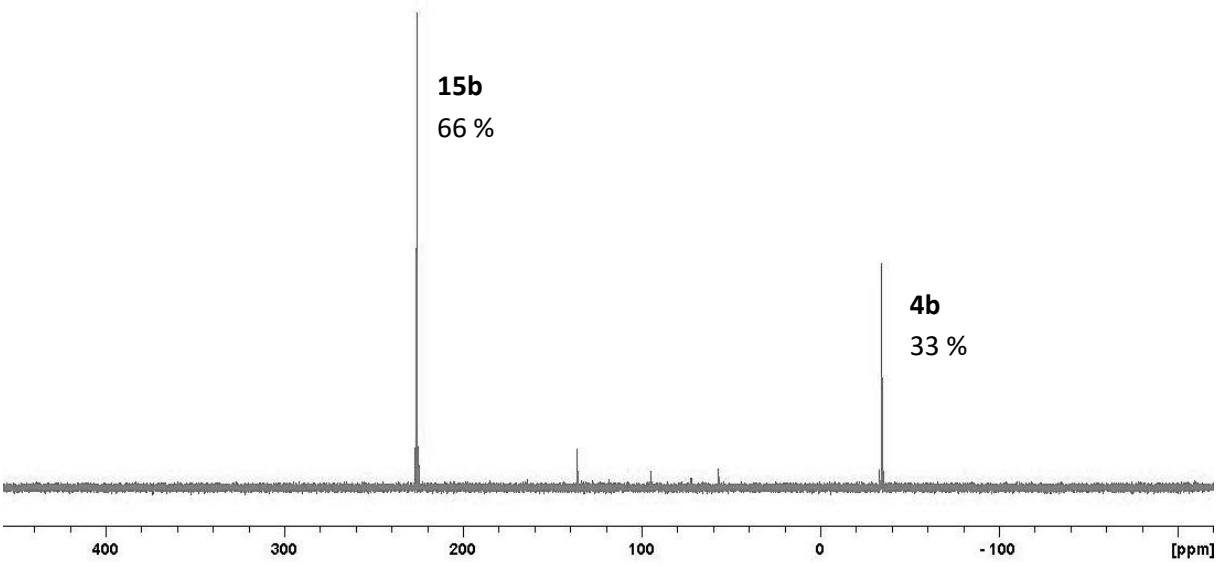

Figure 3.3.1. Spectrum of the reaction mixture of **14** and **3b** showing signals corresponding to **4b** and **15b**.

Table 3.3.1. ^{31}P NMR resonances [ppm] ($^{1}J_{W,P}$ [Hz]) and ratios for **5a-f** and **15a-f** in the reaction of **14** with **3a-f** (in toluene).[80]

Aryl	δ ^{31}P ($^{1}J_{W,P}$) **15a-f**	δ ^{31}P ($^{1}J_{W,P}$) **4a-f**	Ratio (**15:4**)
Phenyl (**a**)	228.4 (228.4)	-27.7 (273.4)	3:1
2-Furyl (**b**)	225.9 (228.4)	-34.1 (272.0)	2:1
2-Thienyl (**c**)	226.1 (228.8)	-34.2 (272)	2:1
3-Furyl (**d**)	226.3 (228.7)	-33.1	5:1
3-Thienyl (**e**)	226.2 (228.8)	-35.6	4:1
p-CF_3-Phenyl (**f**)	226.9 (230.8)	-27.0 (275.8)	6:1

From these mixtures, only complex **15f** could be isolated (36 % yield) and characterized by ^{1}H, ^{13}C NMR and IR spectroscopy. Additionally, its molecular structure was confirmed by X-ray crystallography (crystal system monoclinic, space group P21/c)(Figure 3.3.2). The unusual downfield shift of the ^{31}P NMR resonances of complexes **15a-f** is of particular interest, especially because polycyclic P(III) ligands with low ring strain usually possess resonances close to their acyclic relatives. Similar observations have been made before, *e.g.* for 2,3-bis(methoxycarbonyl)-5,6-dimethyl-7-phenyl-7-phosphanorborna-diene(pentacarbonyl)-tungsten complex and tetra-*tert*-butyl tetraphosphacubane, which show resonances at 208.0[21] and 257.4[67,68] ppm, respectively. Although the ^{13}C NMR chemical shift of 63.4 and 66.2 ppm of C^2 and C^5 atoms and their $^{1}J_{P,C}$ coupling constants of 33.3 and 20.1 Hz are in the expected range for this type of compounds , the fact that both P-C bonds (P-C2 = 1.881(6) Å and P-C5 = 1.867(7) Å) are elongated compared with standard P-C single bonds[82] (P-C = 1.80-1.82 Å), suggests unusual bonding in **15f** (*vide infra*).

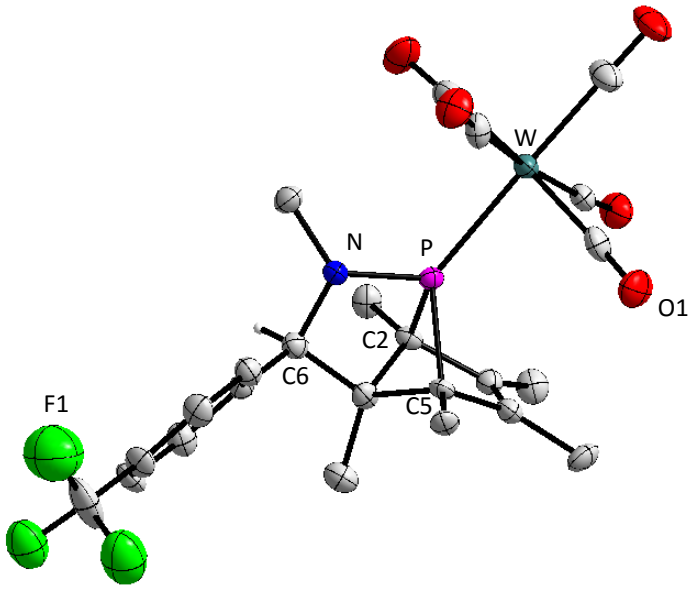

Figure 3.3.2. Molecular structure of complex **15f** (50% probability level, hydrogen atoms except at C6 are omitted for clarity). Selected X-ray crystal structure data (distances [Å] and angles [°]): P-W 2.462(18), P-C2 1.881(6), P-C5 1.867(7), P-N 1.683(5), C2-P-N 97.1(3), C5-P-N 94.6(3), C2-P-C5 71.5(3).[80]

As NMR and structural characteristics of complexes **15** and **4** had created further interest, the stability and reactivity of these two types of N,P,C-cage ligands was studied and, for this, the isolated complexes **4b** and **15f** were chosen as good case in point. It was found that both ligands interconverted rapidly at room temperature, but only to a certain extent. In case of **4b** and after 48 h, 70 % of complex **4b** was converted into **15b** (**15b** was detected by ^{31}P NMR spectroscopy after 1 h), whereas in case of **15f**, 15 % of complex **15f** converted into **4f** after the same time. No further conversion could be achieved by means of heating the reaction mixtures. Especially the latter observation was a great surprise because three-membered rings usually possess much larger ring strain energies than five-membered rings, thus being expected to be thermodynamically unfavored. The rearrangement is explained as to be a dynamic process in which transient phosphinidene complexes **9a-f** are generated, which serve as common intermediates for both interconversions (**4a-f** ↔ **15a-f**) (Scheme 3.3.2).

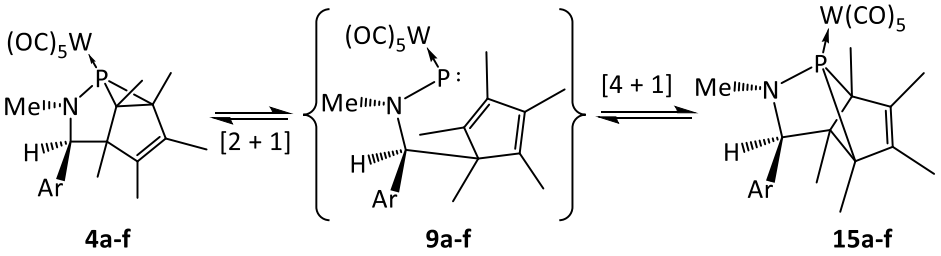

Ar = Ph (**a**), 2-furyl (**b**), 2-thienyl (**c**), 3-furyl (**d**), 3-thienyl (**e**), 4-CF_3-Ph (**f**)

Scheme 3.3.2. Equilibrium between **4a-f** and **15a-f** *via* proposed intermediates **9a-f**.[80]

To study the plausibility of the proposed key intermediates **9** (Scheme 3.3.2) as well as the possible occurrence of the initial intermediate **8**, DFT calculations ($COSMO_{toluene}$/ B3LYP-D3/def2-QZVPP//B3LYP-D3/def2-TZVP) were performed by Espinosa using Cr (instead of W) model complexes (subscript "Cr" is used for naming the corresponding structures), with H as N-substituent and 2-furyl (**b**) and 4-trifluoromethylphenyl (**f**) as aryl (Ar) substituents. As previously proposed (Scheme 3.3.1), complex $\mathbf{8_{Cr}f}$ is also the intermediate resulting upon nucleophilic attack of the N atom of the corresponding model imine Ar-CH=NH (**3'**) to the model electrophilic phosphinidene complex $\mathbf{14_{Cr}}$. The dipolar nature of this iminium phosphane-ylid ligand is evidenced by the large C=N bond (1.305 Å in $\mathbf{8_{Cr}f}$) in comparison to typical imine bonds (1.268 Å in model imine **3'f**) as reported for related structures.[87] According to the recent report for the reaction of phosphinidene complexes with carbon monoxide studied theoretically,[88] the approach of both reagents leading to phosphaketene complexes, proceeds very exergonically (ΔE_{ZPE} = -24.42 kcalmol^{-1} for reaction $\mathbf{14_{Cr}}$ + **3'f**$\rightarrow\mathbf{8_{Cr}f}$) and in a barrierless fashion, as no van der Waals complex could be located at the current level of theory. Recently, transient formation of methylphosphaketene complexes which kann act as precorsurs of non-hindered phosphinidene complexes upon loss of CO under UV irradiation at room temperature was reported.[89] This privileged conformation undergoes a kinetically and thermodynamically favoured transformation into phosphinidene complex $\mathbf{9_{Cr}f}$ by means of an azaphospha-Cope [3.3] shift [84] as explained beforehand.

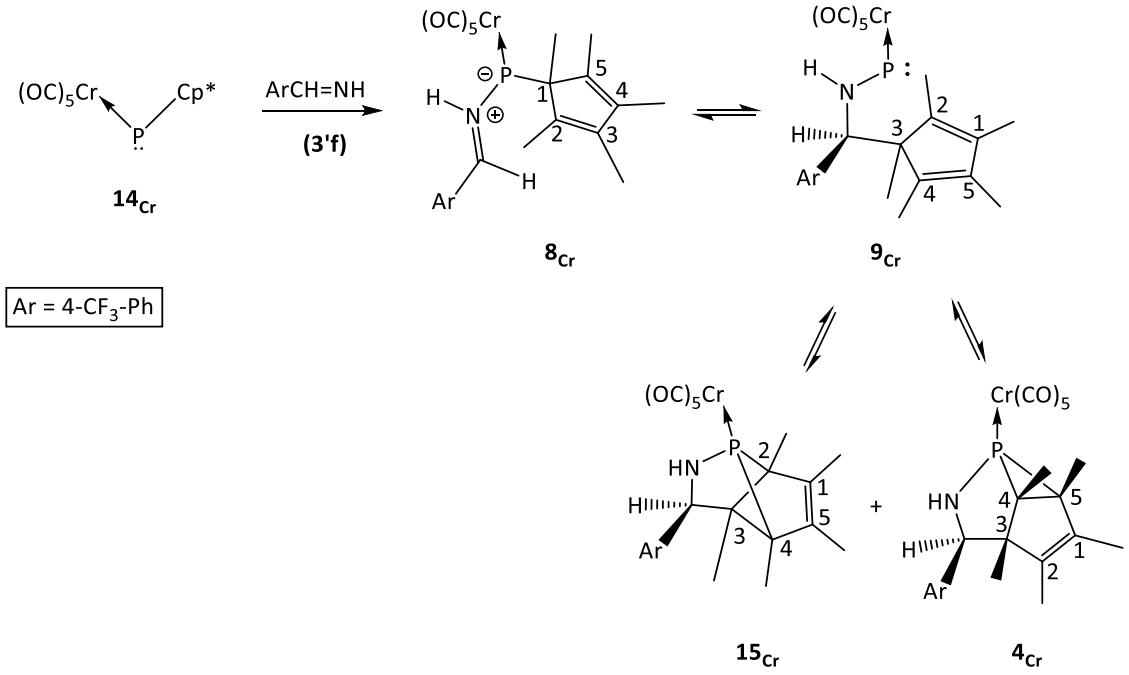

Scheme 3.3.3. Proposed mechanism for the reaction of model phosphinidene chromium complex **14$_{Cr}$** and carbaldimine **3'f** yielding final complexes **4$_{Cr}$** and **15$_{Cr}$**.[80]

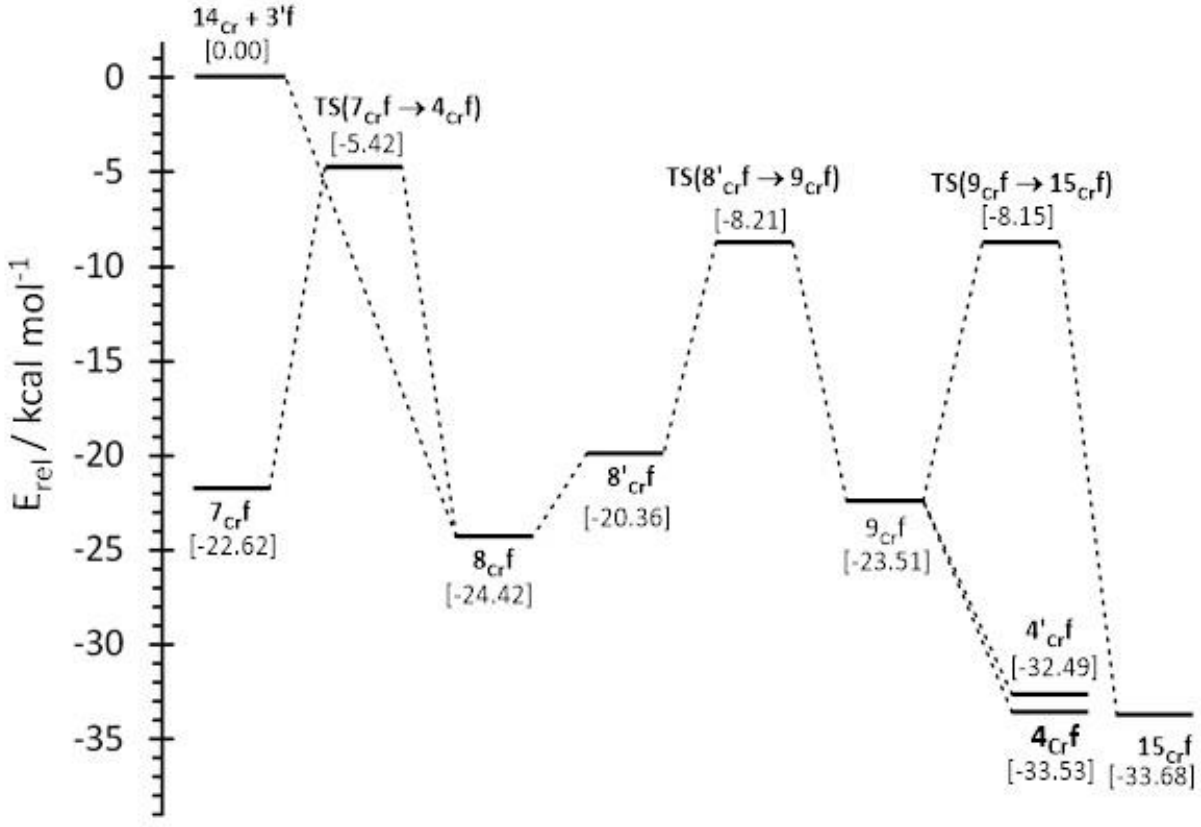

Figure 3.3.2. Computed (COSMO$_{toluene}$/B3LYP-D3/def2-QZVPP) minimum energy profile for the transformation of **7$_{Cr}$f** and **14$_{Cr}$ + 3'f** into **4$_{Cr}$f** and **15$_{Cr}$f**.[80]

Usually electrophilic terminal phosphinidenes complexes with π-acidic co-ligands[31,66,90] belong to a well-known class of highly reactive intermediates and, therefore, it is worth to mention the surprisingly low energy of complexes **9$_{Cr}$**. This is even more impressive when compared to the energy of the azaphosphiridine **7$_{Cr}$** which are usually stable, easily manipulated and storable compounds. In this case, **9$_{Cr}$** receives strong stabilization using several *through-bond* (classical electronic inductive and mesomeric effects) and *through-space* (noncovalent interactions, NCIs) pathways that can be analysed with the aid of the NBO (natural bond orbital) theory.[91] According to the results of Espinosa, the most prominent interaction is the *through-bond* electron density donation from the N lone pair into the (formally) vacant orbital of phosphorus. Using the NBO analysis, this corresponds to a $p_N \rightarrow p_P$ electron transfer with an associated stabilization of 69.93 kcal/mol in the second order perturbation theory (SOPT) analysis of the Fock matrix in NBO basis and entails strengthening of the N-P bond. This is evidenced by the rather short bond distance ($d_{N\text{-}P}$ = 1.657 Å) and quantified by the WBI (Wiberg bond index),[92] MBO (Mayer bond order),[93] LBO (Löwdin bond order)[94] and electron density at the BCP (bond critical point) using the topological analysis of the electron density in the context of Bader's AIM (atoms-in-molecules) methodology[95,96] (WBI = 1.090; MBO = 1.303; LBO = 1.659; ρ(r) = $17.33 \cdot 10^{-2}$ e/a_0^3). A second weaker yet important interaction is a *through-bond* back-donation from the electron enriched phosphorus atom, using both its filled *p* orbital and the formally vacant but partially populated *p* orbital (populations 1.937 and 0.530 *e*, respectively, according to NBO analysis) into the adjacent amino group (*through-bond* back-donation) by using a σ*(P-N) orbital as acceptor, with little SOPT energy of stabilization amounting to 0.62 and 0.70 kcal/mol, respectively. The formally vacant *p* orbital at P is the major contribution at LUMO, whereas the filled *p* orbital at P predominates at HOMO (Figure 3.3.3). Three other significant *through-space* interactions are evidenced by location of the corresponding BCPs. The strongest one consist of an electron donation from one of the π(C=C) orbitals at the Cp* unit to the formally vacant *p* orbital at P ($d_{P\cdots C(1)}$ = 3.027 Å; ρ(r) = $1.79 \cdot 10^{-2}$ e/a_0^3; ellipticity ε = 0.364; ΣWBI = 0.118; ΣLBO = 0.209; stabilization E_{SOPT} = 8.92 kcal/mol) as represented in HOMO-1 (Figure 3.3.3c). The other two are weaker and constitute channels for alleviating the excess of electron density at the otherwise too electron enriched P atom into i) the corresponding π*(C=C) orbital at Cp* (stabilization E_{SOPT} = 0.67 kcal/mol) (see HOMO-4 in Figure 3d) and ii) the σ*(C-H) orbital of one of the *ortho*-positions of the aryl substituent by formation of a P···H-C hydrogen bond

($d_{P\cdots H}$ = 2.661 Å; ρ(r) = $1.38\cdot10^{-2}$ e/a_0^3; WBI = 0.012; LBO = 0.071; angle P···H-C 126.6°; stabilization E_{SOPT} = 1.42 kcal/mol). Furthermore, NBO deletion calculations[39,97] provide an additional approach for the quantification of the above mentioned main stabilizing interactions whose associated binding energies are in good agreement with the reported E_{SOPT}: *through-bond* N→P donation, 67.4 kcal/mol; *through-bond* N←P back-donation, 0.4 kcal/mol; *through-space* P←$\pi_{(C=C)}$ transfer, 8.0 kcal/mol; *through-space* P→$\pi^*_{(C=C)}$ transfer, 1.3 kcal/mol; *through-space* P→$\sigma^*_{(P\cdots HC)}$ transfer, 5.1 kcal/mol.[80]

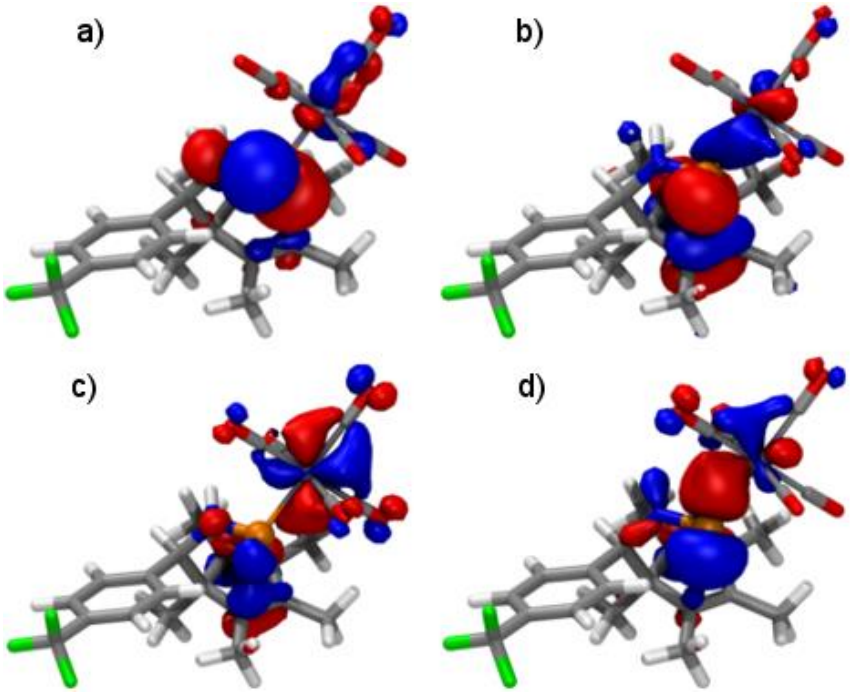

Figure 3.3.3. Computed (B3LYP-D3/def2-QZVPP) Kohn-Sham isosurfaces (0.04 au isovalue) for representative frontier molecular orbitals in complex 10_{Cr}f: a) LUMO, b) HOMO, c) HOMO-1 and d) HOMO-4.[80]

These two ways of *non-covalent interactions* are conveniently visualized by colour-coded RDG (reduced density gradient) isosurfaces using the NCIplot technique (Figure 3.3.4).

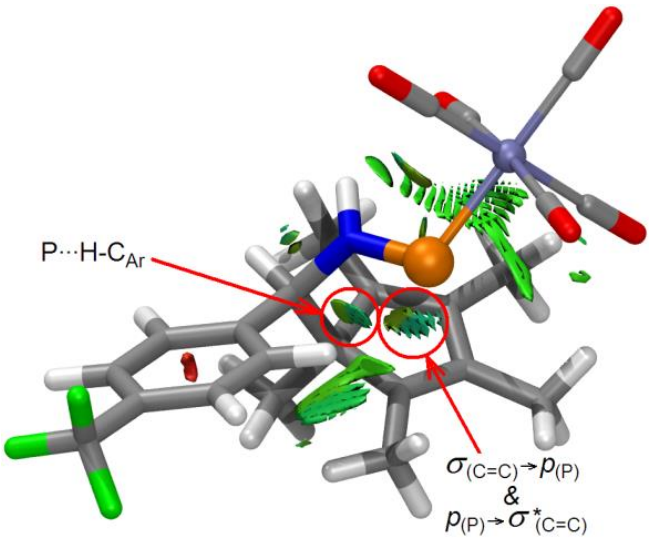

Figure 3.3.4. Computed (B3LYP-D3/def2-TZVP) most stable structure for complex **9$_{Cr}$f** with NCIplot highlighting key stabilizing NCIs; the two most significant ones explicitly indicated in green. The RDG *s* = 0.2 au isosurface is coloured over the range -0.1 < sign(λ_2)·ρ < 0.1 au: blue denotes strong attraction, green stands for moderate interaction, and red indicates strong repulsion.[80]

Here it is worth mentioning that the low electrophilic character of the phosphinidene complex intermediate **9$_{Cr}$f,** according to its high value of HOMO-LUMO gap (3.054 eV), can be used as diagnostic criterion in agreement with the comparative study, recently reported.[66]

Finally, the phosphinidene complex can undergo [4+1] cycloaddition through a low-lying transition state affording **15$_{Cr}$f** or a [2+1] cycloaddition with either the C^4=C^5 or the C^2=C^1 Cp* units giving rise to the diastereomeric pairs **4$_{Cr}$f** or **4'$_{Cr}$f**, respectively (Scheme 3.3.3). For the last type of cycloaddition reactions the corresponding TS could not be located. Nevertheless, as both transformations **9$_{Cr}$f→15$_{Cr}$f** and **9$_{Cr}$f→4$_{Cr}$f** start from the same compound and lead to products of similar energy via reactions of the same type, we assume that the energy content for the TS of both transformations should be rather similar. The higher stability of **15$_{Cr}$f** in comparison to **4$_{Cr}$f** (and **4'$_{Cr}$f**) (Figure 3.3.2) agrees with the experimental ratio in which complexes **15f**/**4f** are obtained (Table 3.3.1).

As previously mentioned, the P-C bond distances in **15f** were found to be larger than expected in the solid state structure (Figure 3.3.1), which deserves a closer inspection by computational means. Metrics obtained for the computed model species **15$_{Cr}$f** ($d_{P\text{-}C}$ = 1.903 and 1.904 Å) agree well with the experimental data and points to weaker covalent P-C bonds

($WBI_{aver.}$ = 0.772; $MBO_{aver.}$ = 0.746; $LBO_{aver.}$ = 0.818) when compared to isomer **4$_{Cr}$f** (d_{P-C} = 1.819 and 1.864 Å; $WBI_{aver.}$ = 0.812; $MBO_{aver.}$ = 0.826; $LBO_{aver.}$ = 0.986) or even the strained intermediate **7$_{Cr}$f** (d_{P-C} = 1.823 Å; WBI = 0.848; MBO = 0.827; LBO = 1.088). Therefore, the N,P,C-cage complexes **15** can be formally viewed, to some extent, as an amino phosphinidene species with a moderate interaction of the P atom with the termini of the dienic moiety of a Cp* group, as additionally shown by the rough coplanarity of the methyl groups at C2 and C4 (see numbering in Scheme 3.3.3) with the C2-C1-C5-C4 plane (dihedrals in **15$_{Cr}$f**: Me-C2-C1-C5 -173.7°; Me-C4-C5-C1 174.5°). This is in line with the behaviour shown by the genuine phosphinidene complex **9**. Nevertheless, to a smaller extent, the P-N bond in **15$_{Cr}$f** is strengthened (dP-N = 1.691 Å; WBI = 0.982; MBO = 1.014; LBO = 1.276) in relation to **4$_{Cr}$f** (dP-N = 1.697 Å; WBI = 0.859; MBO = 0.942; LBO = 1.272) which, in turn, shows a stronger P–N bond than the strained complex **7$_{Cr}$f** (dP-N = 1.738 Å; WBI = 0.828; MBO = 0.984; LBO = 1.266).[80]

3.4. Ring-ring interconversion of N,P,C-cage ligands

To confirm the proposed intermediacy of **9a,f**, trapping experiments were performed using reagents that have been shown before to react selectively with electrophilic terminal phosphinidene complexes.[51,81] Here, the former were employed as solvents: complex **4b** was dissolved in phenyl acetylene (**10**) or *C*-phenyl *N*-methyl carbaldimine (**3a**) at ambient temperature. Both reactions where monitored by $^{31}P\{^{1}H\}$ NMR spectroscopy and in both cases the formation of a mixture of complexes **4b** and **15b** was observed, showing that the intramolecular conversion is kinetically favoured. In the first case (Scheme 3.4.1), first evidence for a mixture of two structural isomers **12b,**[81] (major isomer, 80%, δ ^{31}P = -3.9, $^{1}J_{WP}$ = 277.6 Hz) and **12b'** (minor isomer, 20%, δ ^{31}P = -0.4 ppm, $^{1}J_{WP}$ = 279.4 Hz) was observed after 16 h. To increase the reaction progression, the reaction mixture was heated at 90 °C until the reaction was completed after 20 hours. The major isomer was isolated in 40% yield and fully characterized. Formally, an insertion of the C-C triple bond unit of phenyl acetylene (**10**) into the P-C4 and P-C5 or P-C2 and P-C4 bonds of **9b** occurred (using the numbering depicted in Scheme 5), forming **11b,b'** followed by an intramolecular Diels-Alder reaction, strongly suggesting the presence of the transient phosphinidene complex **9b**. When the same experiment was performed using **15f**, a mixture of **12f** (major isomer, δ ^{31}P = -2.4 ppm, $^{1}J_{WP}$ = 275.2 Hz) and **12f'** (δ ^{31}P = 1.7 ppm, $^{1}J_{WP}$ = 278.3 Hz) in a ratio of 1:2 was obtained, thus

providing further evidence for the existence of **9** as common intermediates in the proposed interconversion of **15** and **4** (Schemes 3.3.3 and 3.4.1).[80]

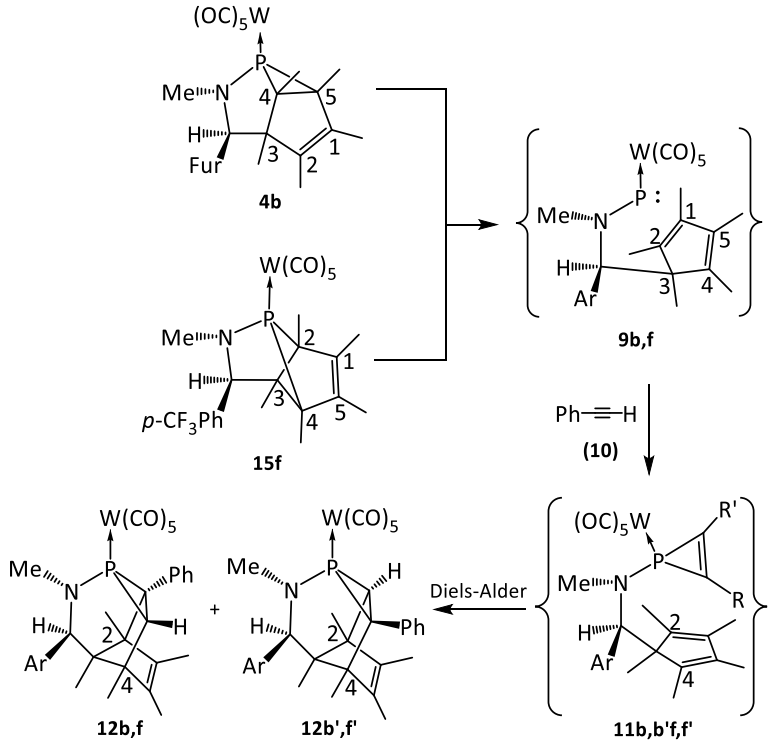

Scheme 3.4.1. Synthesis of complexes **12b,b',f,f'** (numbering corresponds to that used in Scheme 3.3.3). Ar = 2-furyl (b), p-CF_3Ph (f); R,R'' = Ph, H.[80]

In the second case, when **3a** was used as trapping reagent, about 90 % of the starting material was converted into product **17** at 90 °C after 20 hours; 10 % of not identified species were formed. Complex **17** was isolated in 50 %, yield and fully characterized, *e.g.* it displayed a ^{31}P NMR resonance at 145.1 ppm ($^{1}J_{WP}$ = 186.2 Hz). The formation of **17** suggests a nucleophilic attack of the nitrogen atom of **3a** to the phosphorus atom of **9b** leading to the iminium phosphane-ylide complex **16**, which upon [3+2] cycloaddition yielded the final product **17** (Scheme 3.4.2). The intermediacy of **16** could also rationalize the observed high regioselectivity, which could not be explained if the imine undergoes initial [4+2] cycloaddition with the Cp* unit. DFT calculations performed by Espinosa demonstrates that a model complex similar to **16** but replacing the 2-furyl and N-methyl groups by hydrogen atoms (**16'**) exists as a minimum at the working level of theory and possess the required 1,3-dipolar

electronic structure similar to that of **8$_{Cr}$** (Scheme 3.3.3). It undergoes an intramolecular exergonic (-21.82 kcal/mol) 1,3-dipolar cycloaddition to model tricyclic complex **17'** via a low-lying TS.

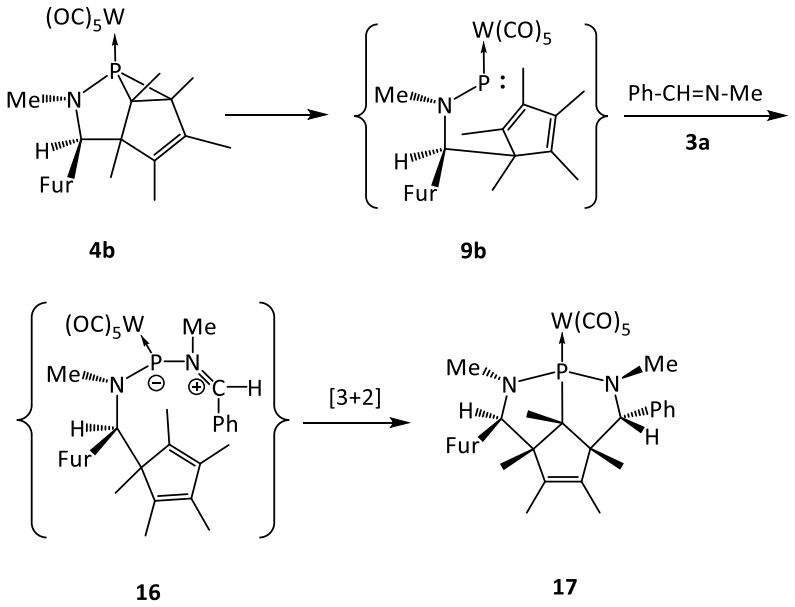

Scheme 3.4.2. Proposed pathway for the formation of complex **17**.[80]

The X-ray diffraction study of **17** confirmed the proposed structure (Figure 3.4.1). **17** crystallized in a triclinic crystal system, and $P\bar{1}$ space group. The P-N(1) and P-N(2) bond length are 1.694(7) and 1.698(8) Å, respectively, which is in accordance with other examples of bicyclic azaphospholane complexes found in the literature.[98] The sum of bond angles around the N atoms are 346.82° (N1) and 344.16° (N2), thus suggesting a geometry getting close to trigonal planar.

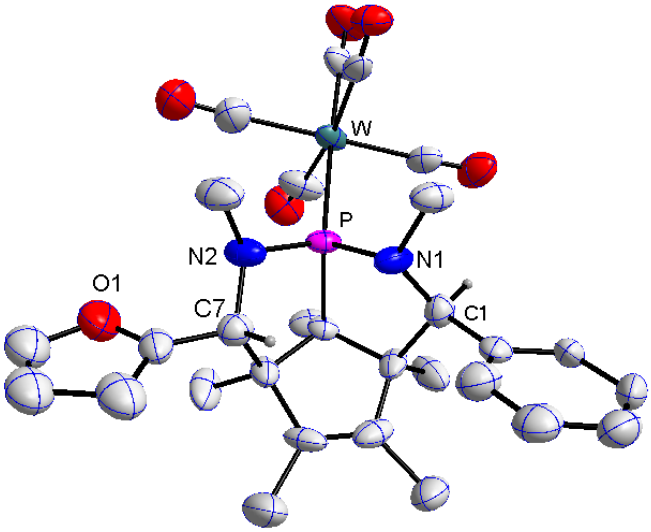

Figure 3.4.1. Molecular structure of complex **17** (50% probability level, hydrogen atoms except at C6, C7, and at the furyl substituent are omitted for clarity). Selected X-ray crystal structure data (distances [Å] and angles [°]): P-W 2.524(2), P-N2 1.698(8), P-N1 1.694(7), P-C2 1.845(8), N1-P-N2 106.5(4), C2-P-N2 94.4(4), C2-P-N1 92.8(4).[80]

4. 3-Imino-azaphosphiridine complexes

4.1. Introduction

4.1.1. Ring strain energy in three-membered rings

The ring strain energy (RSE) is defined as the difference between the observed heat of formation and that expected for a strain-free molecule with the same number of atoms and type of bonds.[99] It represents a useful tool for explaining reactivities and thermodynamics of cyclic compounds. It combines bond lengths and angles distortions, reflecting deviations from the ideal 109.5° for angles around carbon atoms in the ring, torsional interaction strain, which takes into account the bond rotational barriers, transannular interaction strain that reflects interactions of group in opposite sides of the ring, and the energy changes due to rehybridization. In the case of cyclopropanes, angle strain dominates the RSE, because the deviation of ring angles of 60 ° from the ideal value of 109.5 ° is severe, whereas the three-membered ring geometry minimizes torsional and transannular interactions.[100] The question of an addition of sp^2 centers in the cycloprapane ring was studied, among others,[101] by Wiberg and co-workers,[102] Borden and co-workers[103] and Bach and co-workers.[14] The increase of ring strain of about 12-14 kcal/mol per trigonal center is attributed to two main factors namely the hybridization strain associated with the sp^2 center[102] and, specially, the loss of a very strong tertiary C-H bond (Scheme 4.1.1).[103]

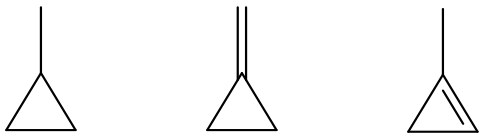

27.5 41.0 53.1

XLV **XLVI** **XLVII**

Scheme 4.1.1. Strain energies (kcal/mol) of methylcylopropane (**XLV**) and methylenecyclopropane (**XLVI**) and 1-methylcyclopropene (**XLVII**).[102]

Lammertsma and Würthwein studied ring strain energies in three-membered heterocycles having one or two heteroatoms and performed a thorough analysis on the preferences of an endo- or exocyclic unsaturation in these derivatives. As shown in Scheme

4.1.2, substitution of a carbon for a nitrogen atom in the cyclopropane ring does not have a large influence in the ring strain. To the contrary, substitution for a phosphorus atom implies a reduction of the ring strain of about 25%. As one might expect, substitution of a second carbon atom in the phosphirane or aziridine rings for a nitrogen or a phosphorus atom respectively, leads to a ring strain value that merges in between of that of the mono-substituted cycles. When it comes to endo- or exocyclic unsaturations, in contrast to that observed in cyclopropanes, aziridines and phosphiranes prefer a E–C (E = N, P) endocyclic double bond rather than an C–C exocyclic one, being this effect smoother in the case of phosphiranes. In case of azaphosphiridines an unsaturation in the N–C bond is preferred compared with a P–N bond single, a C–C exocyclic double bond, and a P–C bond unsaturation (Figure 4.1.2).[105]

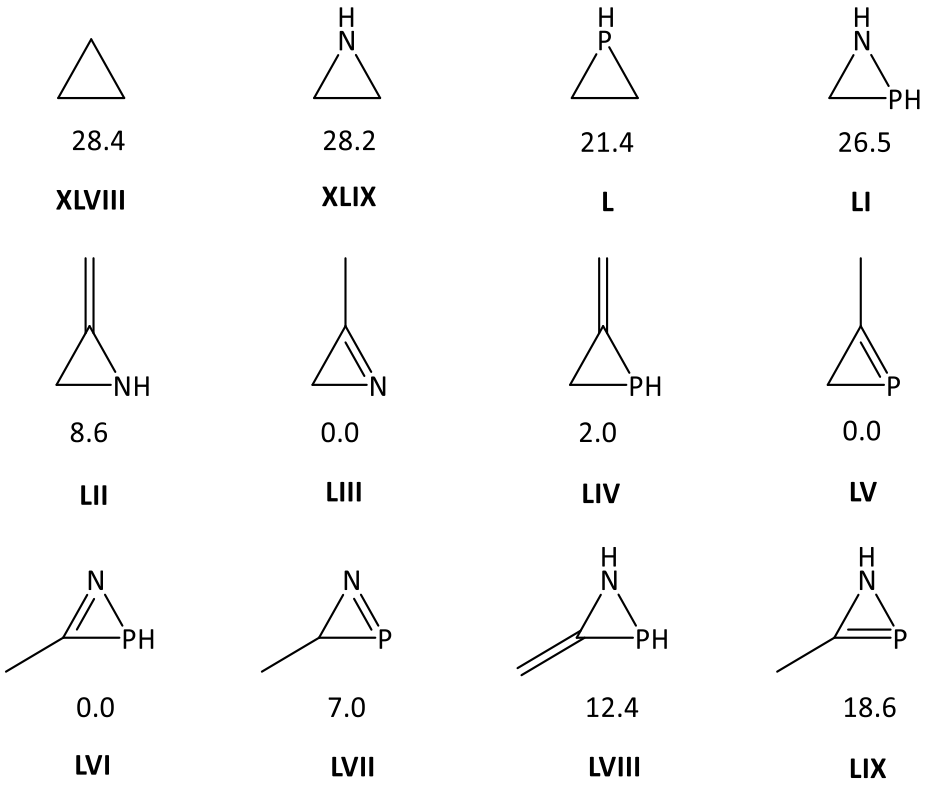

Scheme 4.1.2. Calculated ring strain energies (kcal/mol) for cyclopropane and heterocycles **XLVIII-LIX**. RSE of **LII**, **LIV** and **LVII**, **LVIII**, **LIX** are referred to RSE of **LIII**, **LIV** and **LVI** respectively.[105]

4.1.2. 3-Imino substituted 3-membered heterocycles

3-Iminoaziridines (**LX**),[106] which were first obtained by Quast in 1970 by treating α-bromoamidine with potassium *tert*-butoxide,[107] belong to the group of highly strained three-membered heterocycles and, hence, enable a wide range of interesting synthetic transformations. In contrast and to the best of our knowledge, 3-imino-phosphiranes (**LXI**) are unknown, but transition metal complexes (**LXII**) were recently described.[108] Including a second heteroatom such as a group 15 element leads to the series **LXIII**–**LXVI**. Iminodiaziridine (**LXIII**)[109] was synthesized first from two moles of N,N',N''-tri-*tert*-butylguanidine and one mole of *tert*-butyl hypochlorite by Quast.[110] The first example of a iminodiphosphirane[111,112] (**LXIV**) was prepared by Baudler *via* reaction of dimetallo-diphosphanes and isocyanide dichlorides ($ArN{=}CCl_2$). Here, only those species with a bulky substituent at the imino-aryl ring proved to be stable at room temperature, whereas the derivatives with less demanding substitution patterns were subject to slow decomposition with the formation 2,4-diimino-1,3-diphosphetanes.[111] Complexed iminodiphosphiranes (**LXV**) were prepared by Weber by the reaction of metallodiphosphenes and isocyanides.[113] Iminoazaphosphiridine (**LXVI**) was proposed as a reactive intermediate only,[114] and azaphosphiridine complexes **LXVII** remained unknown until the beginning of this work (Scheme 4.2.1).

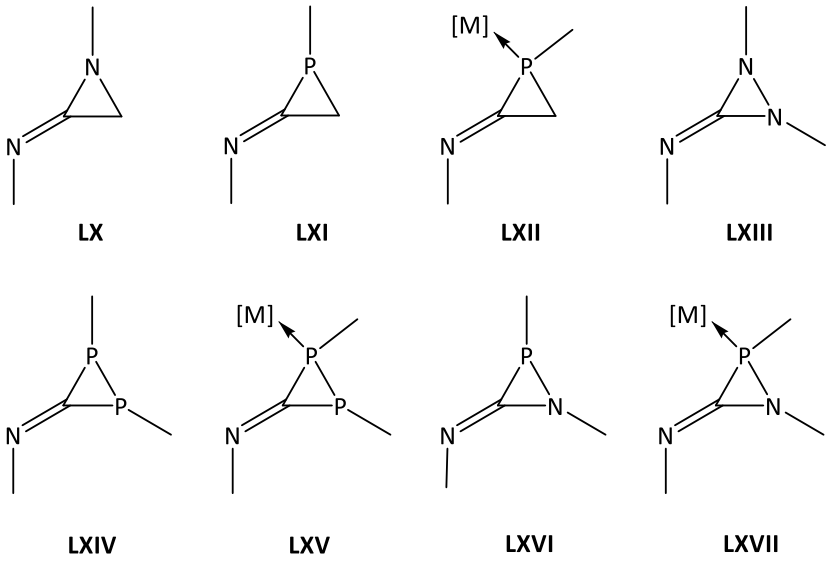

Scheme 4.2.1. 3-Imino-aziridines (**LX**), and related heterocycles **LXI-LXVII** including some transition metal complexes (**LXII**, **LXV**, **LXVII**) (exocyclic lines denote organic substituents).

4.1.3. Frustrated Lewis pairs and small molecule activation

Frustrated Lewis pairs (FLPs) are compounds having a Lewis acid (LA) and a Lewis base (LB) functional group within the same molecule which because of steric and/or electronic factors cannot form a bond.[115] Stephan and co-workers in 2006 discovered that the intramolecular Lewis acid/Lewis base pair could reversibly heterolytically cleave the dihydrogen molecule under ambient conditions (Scheme 4.1.3.1).[116] This ability, which was attributed before to d orbitals in transition metal complexes as to be an exclusive feature, marked the starting point for the development of this new chemistry.

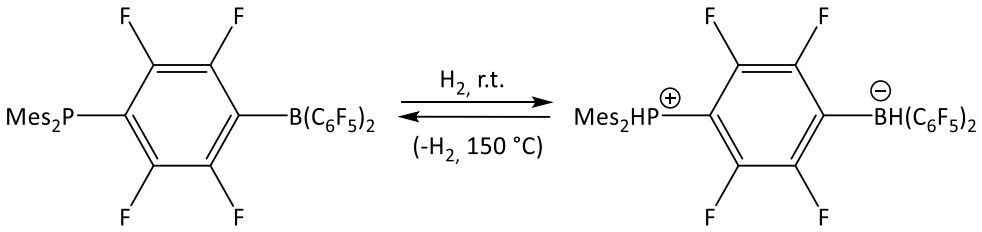

LXVIII **LXIX**

Scheme 4.1.3.1. First example of FLP activation of dihydrogen.[116]

Since the discovery of the reversible splitting of dihydrogen by FLPs, a variety of methods for metal-free catalytic hydrogenation processes of various organic unsaturated substrates such as imines,[117] enamines,[118] silyl enols ethers,[119] non functionalized alkenes[120] and alkynes[121] or electron-poor alkenes[122] and alkynes[123] and arenes[124] as well as asymmetric hydrogenations[125] were developed using different kinds of LB/LA systems such as P/B, N/B or even C/B combinations.

Reversible CO_2 capture by inter- or intramolecular P/B FLPs was first shown by Stephan and Erker in 2009 (Scheme 4.1.3.2).[126] Later on, different studies on the capture of CO_2 by modified P/B FLPs systems have been reported.[127] Substitution of the phosphane base by a primary or secondary amine[128] or by a carbene[129] has been also shown to be an affective system for CO_2 sequestration as well as FLPs having aluminum as a Lewis acid and phosphane as base, which were reported by Uhl and Lammertsma[130] among other authors.[131]

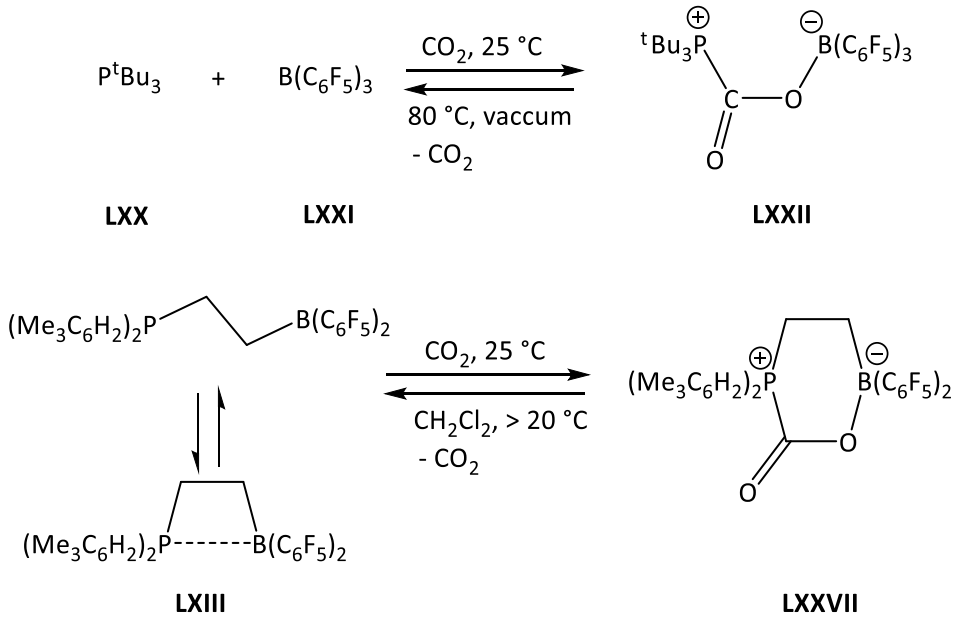

Scheme 4.1.3.2. Reversible CO_2 uptake and release by intermolecular- **LXX·LXXI** and intramolecular **LXIII** frustrated phosphane/borane Lewis pairs.[126]

The donor/acceptor properties of FLPs suggest a potential metal center-analogous behavior towards small molecules such as isocyanides or carbon monoxide (CO). For example, Erker showed that conjugated phosphane/borane FLPs undergo 1,1-addition reaction to *n*-butyl isocyanide forming new P–C and B–C bonds. Use of *tert*-butyl isocyanide led to a dynamic behavior between the isocyanide–[B] adduct and the 1,1-addition product in solution.[132] Some saturated vicinal P/B (Scheme 4.1.3.3)[133] or N/B[134] FLP exhibit a similar behavior towards CO.[4]

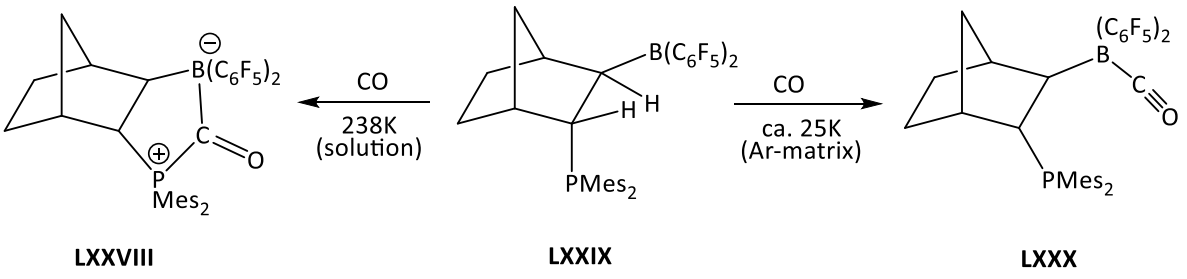

Scheme 4.1.3.3. Cooperative (left) and *end*-on behavior of FLPs towards carbon monoxide.[133]

In a similar fashion, FLPs have been shown to undergo addition reactions of small molecules such as sulfur dioxide (SO_2),[136] nitrous oxide (N_2O),[137] or nitric oxide (NO).[138]

[4] Recently, it was shown by Schulz that five-membered biradicaloids can also add carbon monoxide.[135]

4.2. Synthesis of 3-imino-azaphosphiridine complexes

Recently, it has been achieved to solve the challenge of building up an array of three atoms in a molecular compound two of which have no bonding interactions and being opponents in terms of the Lewis acid and base concept; this has been termed frustrated Lewis pair (FLP). Due to this, a wide range of new chemical structures such as **LXXXI** were discovered in recent years (**LXXXI,LXXXI'**: LB1 = CR_2; Scheme 1); evidence for **LXXXI'** was not obtained, so far. Among the many interesting transformations, enabled by **LXXXI**, is the activation of quite unreactive substrates such as H_2 and CO_2 through interactions of LA/LB centers such as B/P and Al/P (for references, see above).

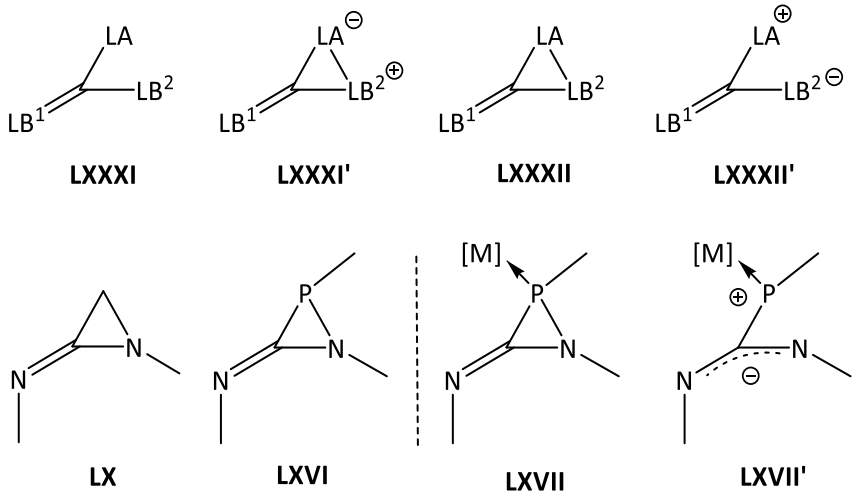

Scheme 4.2.1. 1,1'-Vinyl-derived frustrated Lewis pairs **LXXXI**, closed isomers **LXXXI'** and neutral rings with polar bonds **LXXXII** and zwitterions thereof **LXXXII'** (LB^1 = CR_2); 3-imino-aziridines **LX**, 3-imino-azaphosphiridines **LXVI** and their complexes **LXVII**/**LXVII'** (lines denote organic substituents and [M] a transition metal complex).

In order to approach the FLP concept from a different angle, we contemplated about the necessities to enhance reactivity of three-membered heterocycles having three different, strongly polarized ring bonds (i),[81,139–141] high ring strain (ii) being combined with an *exo* nucleophilic centre LB^1.[142] It is well known that implementation of an sp^2-hybridized centre increases ring strain and bond strain in the distal bond in three-membered P-heterocycles.[61,105] Due to our longstanding interest in the chemistry of complexes possessing strained heterocyclic ligands having polar ring bonds such as 2*H*-azaphosphirenes,[24] oxaphosphiranes[38,48,140] and azaphosphiridines,[50,51,81] we contemplated about reactions of

Li/Cl phosphinidenoid complexes and cumulenes in order to obtain structures such as **LXVII**, **LXVII'**. Until recently, only 3-imino-aziridines **LX**[107] were at hand and **LXVI** were claimed as reactive intermediate.[114] Complexes **LXVII**, appear as particularly interesting targets as they may feature a masked (crypto) FLP-type character, ready to be unveiled upon cleavage of a markedly weakened endocyclic P-N bond (**LXVII'**).

The first example of this will be reported in this chapter, together with theoretical calculations performed by Espinosa on the ring strain energy of the hitherto unknown complexes **LXVII**.

When Li/Cl phosphinidenoid complexes **2**[39] and **19**,[40] prepared from complexes **1**[77] and **18**[40] respectively, were reacted in situ with diisopropyl- and dicyclohexyl carbodiimides **20a,b** formation of the novel 3-iminoazaphosphiridine complexes **21a,b,22a,b** was observed (Scheme 4.2.1); low temperature ^{31}P NMR spectroscopic monitoring for the reaction of **2** and **20a** didn't reveal any further evidence for intermediates. A fast work-up by exchanging the solvent to *n*-pentane and filtration of lithium chloride is required in order to obtain **21a,b,22a,b** in pure form and avoid decomposition. Compared to data of known azaphosphiridine complex derivatives,[50,51,81] the complexes **21a,b,22a,b**, possess $^{31}P\{^1H\}$ NMR resonances significantly downfield-shifted (Table 4.2.1). The imino carbon atoms of **21a,22a,b** exhibit $^{13}C\{^1H\}$ NMR resonances at 137.0 ppm, 139.7 ppm and 139.9 ppm, respectively, displaying relatively small sum of scalar coupling constants (**21a**: $J_{C,P}$ = 7.2 Hz; **22a**: $J_{C,P}$ = 5.5 Hz and **22b**: $J_{C,P}$ = 5.2 Hz).

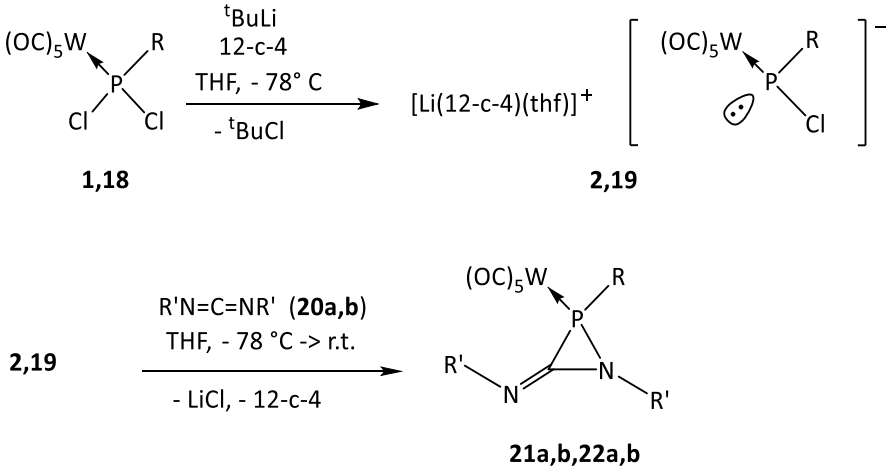

Scheme 4.2.1. Synthesis of 3-imino-azaphosphiridine complexes **21a,b,22a,b**.[143,144]

Table 4.2.1. $^{31}P\{^{1}H\}$ NMR resonances (ppm) [$^{1}J_{W,P}$ (Hz)] for **21a,b,22a,b** in the reaction of **2,19** with **20a,b** ($CDCl_3$).

R' \ R	[143]CPh_3 (**21**)	[144]Cp* (**22**)
^{i}Propyl (**a**)	2.1 [257.4]	4.0 [265.6]
Cyclohexyl (**b**)	0.0 [257.2]	1.5 [265.9]

The structure of 3-imino-azaphosphiridine complexes **21a** and **22a** were confirmed by X-ray diffraction analysis (Figure 4.2.1). **21a** Crystallized in the monoclinic crystal system, space group P2/a and **22a** in the triclinic crystal system, $P\bar{1}$ space group. Although they were severely disordered (79:21 (**21a**) and 67:33 (**22a**), they were solved appropriately. **21a** And **22a** show a pyramidal geometry at the N1 atom (sum of bond angles: 150.4° (**21a**) and 342.7° (**22a**)) and, interestingly, the N1–C1 bond lengths of 1.369(7) and 1.366(8) Å respectively, are shortened compared with 1.48-1.47 Å as reported for azaphosphiridine complexes not possessing the 3-imino group[50] and elongated compared to an 3-amino-2*H*-azaphosphirene complex derivative of 1.297(5) Å.[37] The P–N1 bond lengths of 1.767(4) Å (**21a**) and 1.795(5) Å (**22a**) are slightly elongated compared with the values of 1.72-1.73 Å reported for azaphosphiridine complexes.[50] The N2–C1 bond lengths of 1.258(7) Å (**21a**) and 1.249(6) Å (**22a**) are similar to the corresponding C–N bond length of the imino group in the *N*-phenyl-2-iminophosphirane iron complex (1.273(7) Å),[108] and shorter than in the the same 3-amino-2*H*-azaphosphirene complex (1.326(5) Å)[37] suggesting considerable C=N double bond character. Despite contribution of canonical structure **21,22^{res}** which is less important than **21,22**, these compounds might be best depicted by resonance hybrid structures **21,22^{hyb}** (Scheme 4.2.2).

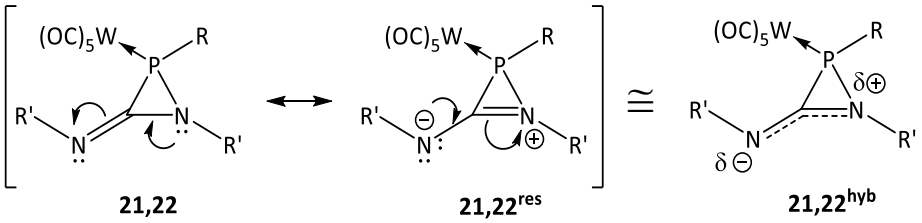

Scheme 4.2.2. Resonance structures of 3-imino-azaphosphiridine complexes **21,22**.

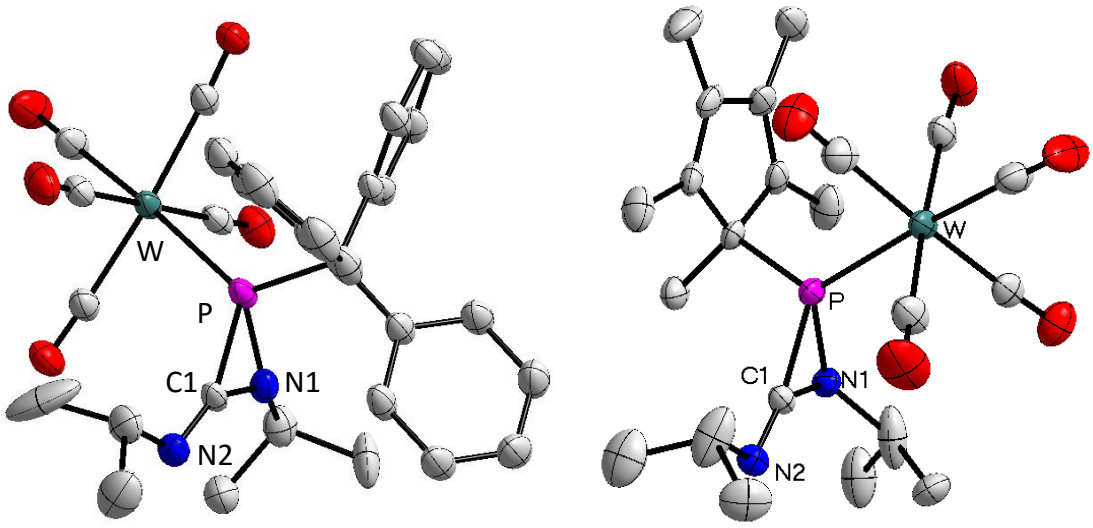

Figure 4.2.1. Molecular structure 3-imino-azaphosphiridine complex **21a** (left). (50% probability level, hydrogen atoms, except at N atoms, are omitted for clarity; only the main part of the disordered moiety is shown here). Selected X-ray crystal structure data (distances [Å] and angles [°]): P-W 2.5062(9), P-C(1) 1.824(6), P-N(1) 1.767(4), C(1)-N(1) 1.369(7), C(1)-N(2) 1.258(7), N(1)-C(1)-N(2) 141.1(7), N(1)-C(1)-P 65.4(3), N(2)-C(1)-P 153.0(6). Molecular structure of 3-imino-azaphosphiridine complex **22a** (right). (50 % probability level, hydrogen atoms are omitted for clarity; only the main part of the disordered moiety is shown here. Selected structural parameters (distances [Å] and angles [°]): P-W 2.4779(9), P-C(1) 1.840(6), C(1)-N(1) 1.366(8), C(1)-N(2) 1.249(6), P-N(1) 1.795(5), C(1)-P-N(1) 44.1(3), N(1)-C(1)-P 66.2(3), P-N(1)-C(1) 69.7(4), P-C(1)-N(2) 154.4(9), N1-C1-N2 138.9(9).

3-Imino-zaphosphiridine complexes were also studied computationally by Espinosa at the DFT level (B3LYP-D3/def2-TZVP). First, the *E*/*Z* isomerism of the exocyclic C=N bond was inspected using model complexes bearing either H (**23**) or methyl groups (**24**) as P- and N-substituents. The *Z*-isomer is the most stable diastereomer by 1.57 and 2.97 kcal/mol for complexes **23** and **24**, respectively. A very important feature of these complexes is their remarkably large ring strain energy (RSE) of 50.58 and 52.26 kcal mol^{-1} computed for both diastereomers **23*Z*** and **23*E***, using homodesmotic reactions, like those employed previously for related systems.[57] This is almost twice as much as the value for the parent azaphosphiridine complex (23.9 kcal mol^{-1}).[57] Moreover, the Lagrange kinetic energy at the ring critical point (RCP), *G*(r), was recently shown to correlate with RSEs within related systems,[107] at much lower computational cost, and also successfully employed within a related oxaphosphirane series.[48,145] This computationally inexpensive *G*(r) quantity suggests that the ring strain

slightly increases with trimethyl substitution on going from **23** (0.1311 au) to **24** (0.1362 au).

A small but significant contribution of resonance structures **21,22^{res}** (Scheme 4.2.2) is supported by the inspection of typical bond-strength related parameters such as the Wiberg bond index (WBI)[92] and the electron density ρ(r) at bond critical points (BCP) within the atoms-in-molecules (AIM) framework in the model complexes **23,24**.[95,96] The slightly larger than single bond order found for the endocyclic C-N bond in **23,24** (WBI = 1.176 (**23**) and 1.169 (**24**); ρ(r) = 32.69x10^2 (**23**) and 32.73x10^2 *e/a$_o^3$* (**24**)) and smaller than double bond for the exocyclic one (WBI = 1.886 and 1.816; ρ(r) = 41.31x10^2 and 41.12x10^2 *e/a$_o^3$*). The weakest endocyclic bond in **23,24** was found to be the P-N bond (WBI = 0.778 and 0.748; ρ(r) = 14.77x10^2 and 15.07x10^2 *e/a$_o^3$* respectively), which is responsible for ring opening reactions (*vide infra*).

As one might expect due to the large ring strain energy of complexes 3-imino-azaphosphiridine complexes, this kind of structures are unstable in solution in standard organic solvents and present difficulties when it comes to their handling. For example, **22b** decomposed upon low temperature column chromatography (-20 °C, Al_2O_3, petrol ether (40/60) / Et_2O = 70 /30) into several products, one of which could be identified by X-ray crystallographic analysis (crystal system triclinic, space group $P\bar{1}$)(Figure 4.2.3). The zwitterionic bicyclic complex **25** (Scheme 4.2.3) displayed a ^{31}P NMR resonance of -23.6 ppm ($^1J_{W,P}$ = 230.5 Hz, $^1J_{P,H}$ = 230.5 Hz) resulted from the formal addition of a H_2 (or a proton plus a hydride, or two H atoms) molecule to **22b**. Unfortunately, the origins of the H^+ and the H^- (or the two H atoms) as well as the formation of **25** remain still unknown.

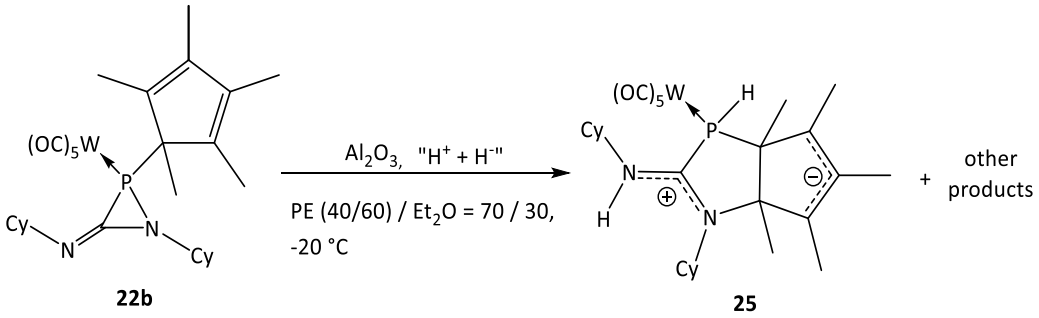

Scheme 4.2.3. Decomposition reaction of **22b** upon column chromatography to form **25**.

The P-C15 bond length of 1.874(3) was found to be slightly elongated from its standard value of 1.80-1.82 Å.[82] The C16-C17 and C17-C18 are 1.381(4) and 1.425(4) respectively suggesting intermediate situation between single and double bonds, circumstance that repeats for the C1-N1 and C1-N2 bonds which lengths are 1.333(3) and 1.339(3) respectively.

The folding angle between the best mean planes defined by C14-C15-C16-C7-C18 and C14-C15-P-C1-N1 is 69.2 °. The sum of angles around C16, C17, C18, N1, C1 and N2 is in all cases almost to 360 °, thus suggesting trigonal planar environment and an overall zwitterionic structure.

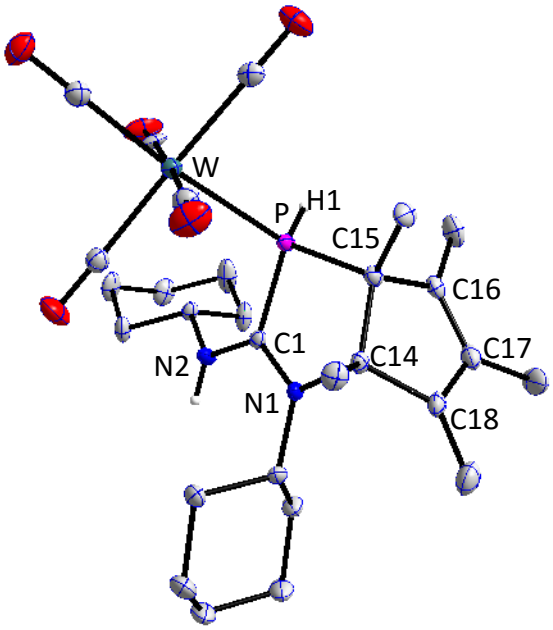

Figure 4.2.3. Molecular structure of zwitterionic bicyclic complex **25** (50 % probability level, hydrogen atoms, except for HX are omitted for clarity). Selected structural parameters (distances [Å]): P-W 2.6253(7), P-C(1) 1.810(3), P-C(15) 1.874(3), C(15)-C(16) 1.527(4), C(16)-C(17) 1.381(4), C(17)-C(18) 1.425(4), C(18)-C(14) 1.533(4), C(1)-N(1) 1.333(3), C(1)-N(2) 1.339, (3), N(1)-C(14) 1.509(3).

4.3. Studies on the decomposition pattern of 3-imino-azaphosphiridine complexes in solution

After leaving an ethereal (Et_2O or THF) solution of **21a** at ambient temperature, two new products displaying ^{31}P NMR resonance of -50.7 ppm ($^1J_{W,P}$ = 119.6 Hz) **26a** and 150.8 ppm ($^1J_{W,P}$ = 288.3 Hz) **27** (Et_2O) appeared after two hours. Upon warming the reaction solution till 60 °C the reaction was accelerated and no other products were observed (Scheme 4.3.1). The nature of **26a** was assigned by comparison with the isolated and characterized product **26b**, obtained from the reaction of **21a** with isonitrile **52b** (see chapter 4.4.2.4). 1,3,2-Diazaphosphetidine complex **27** was identified by single crystal X-ray analysis (crystal system triclinic, space group $P\bar{1}$) (Figure 4.3.1). Here, a P–N and C–N bond cleavage in **21a** occurred leading to the formation of the isonitrile-phosphinidene complex adduct **23a** (see also chapter

4.4.2.4) and transfer of a nitrene unit being inserted into the P–C bond of a second molecule of **21a**.

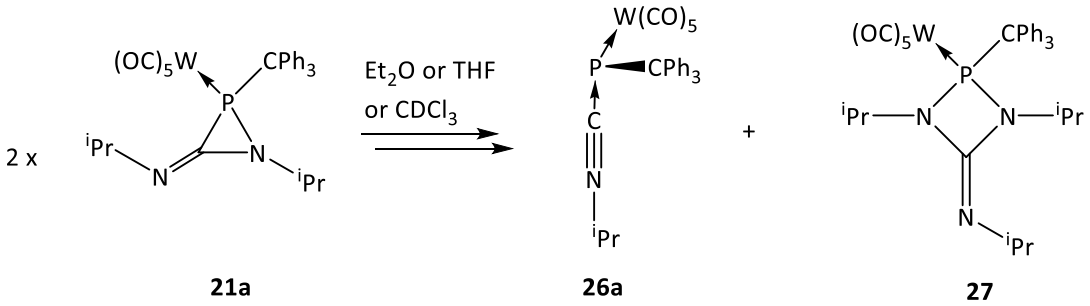

21a **26a** **27**

Scheme 4.3.1. Decomposition reaction of **21a** to form **26a** and **27**.

In complex **27**, the P-N1 and P-N2 bond lengths were found to be similar, 1.704(4) Å and 1.713(4) Å respectively, and the C1-N1 bond length of 1.400(6) shorter than the C1-N2 bond length of 1.442(5). The folding angle between the planes defined by N1-C1-N2 and N1-P-N2 atoms is 6.2 ° thereford showing an almost planar ring structure (Figure 4.3.1).

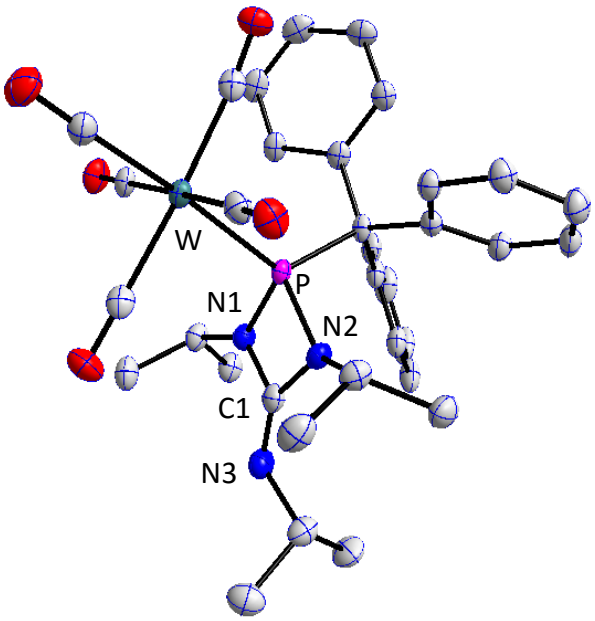

Figure 4.3.1. Molecular structure of 1,3,2 diazaphosphetidine complex **27**. (50 % probability level, hydrogen atoms are omitted for clarity. Selected structural parameters (distances [Å] and angles [°]): P-W 2.5094(10), P-N(1) 1.704(4), P-N(2) 1.713(4), N(1)-C(1) 1.400(6), C(1)-N(2) 1.442(5), N(1)-P-N(2) 76.38(17), P-N(2)-C(1) 92.7(3), N(2)-C(1)-N(1) 96.0(3), C(1)-N(1)-P 94.6(3).

4.4. Reactivity of 3-Imino-azaphosphiridine complexes

4.4.1. Examples for a substrate stimuli-responsive masked FLP-type reactivity

In the presence of certain substrates such as water, heterocumulenes like phenylisocyanate or carbon dioxide or pentafluorobenzaldehyde 3-imino-azaphosphiridine complexes show a stimuli-responsive masked FLP-type reactivity. In the present chapter, the synthesis and characterization of the products obtained upon reaction of 3-imino-azaphosphiridine complexes and the above mentioned substrates are described. Reaction mechanisms of representative reactions based on DFT calculations performed by Espinosa are also discussed.

4.4.1.1. Ring opening reaction with water

When THF, Et_2O or toluene solutions of complexes **21a,b** and **22,a,b w**ere treated with 1 eq. of water at ambient temperature, the formation of complexes **28a,b** and **29a,b** occurred selectively (Scheme 4.4.1.1.1) which were obtained in pure form and good yields via crystallization from diethyl ether solutions (Table 4.4.1.1.1). The resonances of the carbon nuclei, directly bound to two nitrogens, appear as doublets in the $^{13}C\{^1H\}$ NMR spectra (**28a**: 172.5 ppm, $^1J_{P,C}$ = 32.5 Hz, **29a**: 171.9 ppm, $^1J_{P,C}$ = 14.4 Hz and **29b**: 170.8 ppm, $^1J_{P,C}$ = 14.1 Hz).

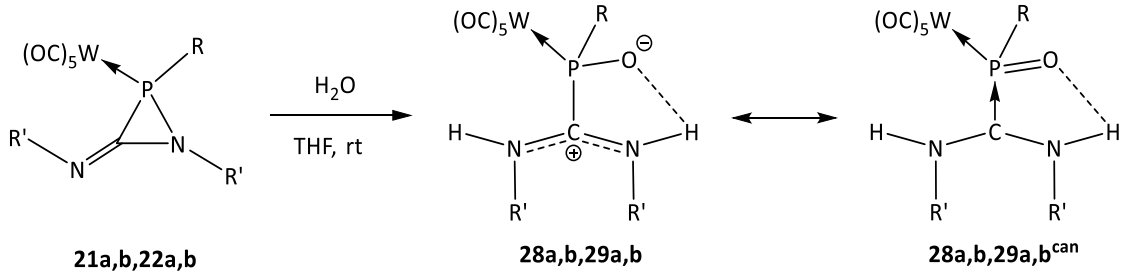

21a,b,22a,b **28a,b,29a,b** **28a,b,29a,b^{can}**

21,28: R = CPh_3; **22,29**: R = Cp*
a: R' = ^{i}Pr; **b**: R' = Cy

Scheme 4.4.1.1.1 Synthesis of **28a,b** and **29a,b**.

Table 4.4.1.1.1. ^{31}P NMR resonances (ppm) [$^1J_{W,P}$ (Hz)] for **28a,b,29a,b** in the reaction of **21a,b,22a,b** with water ($CDCl_3$).

R' \ R	$^{[143]}CPh_3$ (**28**)	$^{[144]}Cp^*$ (**29**)
^{i}Propyl (a)	92.4 [285.6]	84.3 [269.0]
Cyclohexyl (b)	91.2 [284.2]	85.0 [269.8]

Interestingly, the ^{1}H NMR spectra ($CDCl_3$) of **29a** showed a broad singlet at 6.7 ppm for the N-*H* protons at ambient temperature which, upon cooling to –70 °C, splits into two doublets ($^{3}J_{H,H}$ = 6.5 Hz) at 5.1 and 8.0 ppm ($^{4}J_{P,C}$ = 8.0 Hz) revealing that rotation around the P–C^{N} bond is hampered due to an PO···H–N hydrogen bonding. According to the Gutowsky–Holms equation ($K_c = \pi\nabla/\sqrt{2}$),[146] and the Eyring equation {$\Delta G^{\neq}_c = 4.58T_c[10.32 + \log(T_c/K_c)]$}[147] the free energy activation at coalescence temperature for this process was calculated to be between 10.9 and 11.4 kcal mol^{-1} (Figure 4.4.1.1.1).

$K_c = \pi\Delta\nu_o/\sqrt{2} = \pi\ 861/\sqrt{2} = 1912.7$

$\Delta G^{\neq}_c = 4.58 \times 264\ [10.32 + \log(264/1912.7)] = 11.4$ kcal mol^{-1}

$K_c' = \pi\Delta\nu_o'/\sqrt{2} = \pi\ 33/\sqrt{2} = 73.3$

$\Delta G^{\neq}_c' = 4.58 \times 221\ [10.32 + \log(221/73.3)] = 10.9$ kcal mol^{-1}

Where K_c stands for the rate constant for the process at coalescence temperature (T_c) and ∇ stands for the chemical shift difference of the signals in hertz.

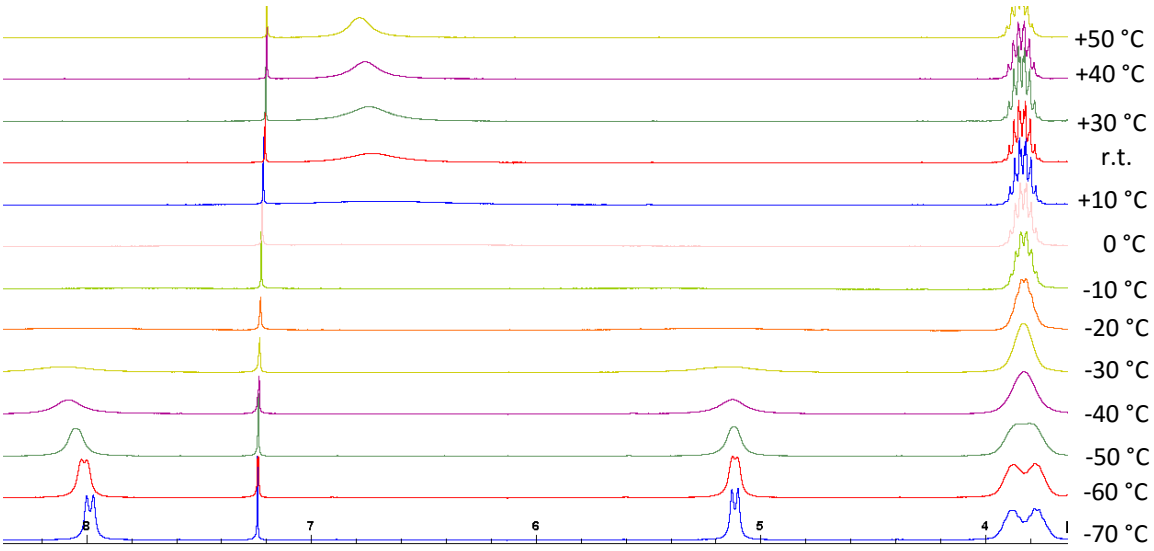

Figure 4.4.1.1.1. Low temperature ^{1}H NMR monitoring of **29a**. Time interval between each measurement was 10 minutes.[144]

Complexes **28a** and **29a,b** were also structurally confirmed (crystal system monoclinic, space group $P2_1/n$ in all three cases) (Figures 4.4.1.1.2 and 4.4.1.1.3) revealing a unique bonding of a zwitterion ligand possessing a delocalized cationic moiety where the sum of the bond angles around C1 atom are 359.5 ° (**28a**), 359.8° (**29a**) and 359.7° (**29b**), almost identical C–N distances, an elongated P–C (1.921(8) Å (**28a**), 1.897(2) Å (**29a**) and 1.902(4) Å (**29b**)) and shortened P-O bond (1.518(6) Å (**28a**), 1.5201(16) Å (**29a**) and 1.521(3) Å (**29b**)). This situation bears also features of a carbene donor adduct to a terminal phosphinidene oxide complex as expressed by the formulae **28,29^{can}** (BDE for model complex **30** (methyl substituent at P and N atoms) was computed to be 53.69 Kcal·mol^{-1}, see below) (Figure 4.4.1.1.1). Albeit having a O1–C1 distance of 2.64 Å (**29a**), which is shorter than the sum of van der Waals radii (3.22 Å),[148] it is clearly the first example of a valence isomer of an oxaphosphirane complex. Furthermore, there is a O1···H-N2 hydrogen bond (O1-H 2.06, O1-N2 2.639(2) Å), which reflects the situation in solution at low temperature.

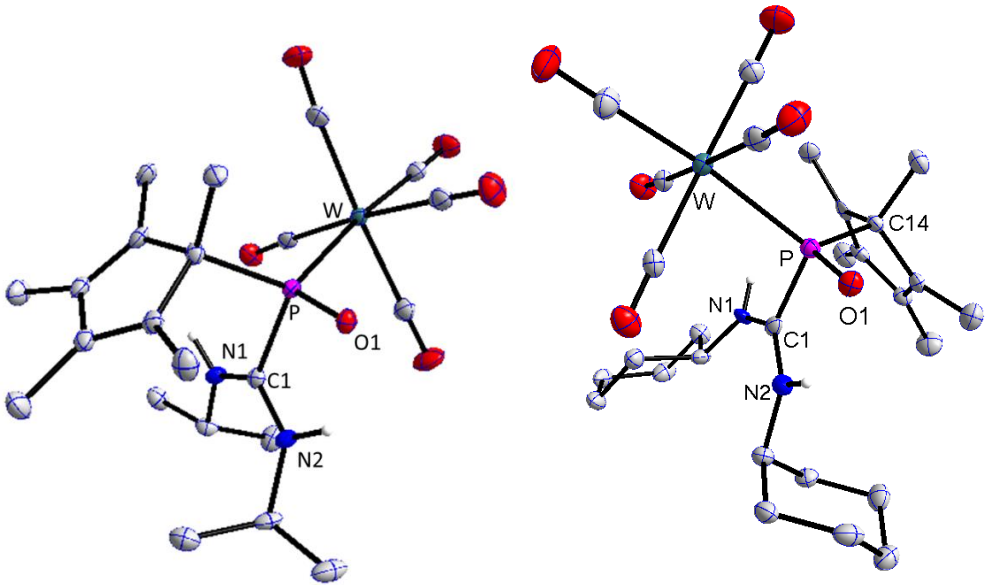

Figure 4.4.1.1.2. Molecular structure of **29a** (left) and **29b** (right). (50 % probability level, hydrogen atoms (except at nitrogen atoms) are omitted for clarity. Selected structural parameters (distances [Å] and angles [°]) for **29a**: P-W 2.5384(6), P-C(1) 1.897(2), C(1)-N(1) 1.319(3), C(1)-N(2) 1.311(3), P-O 1.5201(16), C(1)-P-O 100.61(10), N(1)-C(C1)-N(2) 127.1(2), N(1)-C(1)-P 122.71(17), N(2)-C(1)-P 110.03(16); **29b**: P-W 2.5440(11), P-C(1) 1.902(4), C(1)-N(1) 1.317(5), C(1)-N(2) 1.305(5), P-O1 1.521(3), C(1)-P-O 101.76(19), N(1)-C(C1)-N(2) 128.0(4), N(1)-C(1)-P 121.3(3), N(2)-C(1)-P 110.5(3).[144]

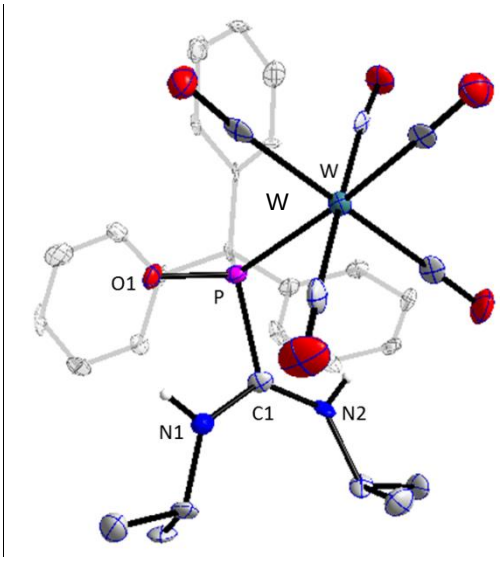

Figure 4.4.1.1.3. Molecular structure of **28a**. (50% probability level, hydrogen atoms, except at N atoms, are omitted and CPh_3 group shown in grey for clarity). Selected X-ray crystal structure data (distances [Å] and angles [°]): P-W 2.541(2), P-C(1) 1.921(8), P-O(1) 1.518(6), C(1)-N(1) 1.334(11), C(1)-N(2) 1.317(9), N(1)-C(1)-N(2) 126.1(7), N(1)-C(1)-P 108.5(5), N(2)-C(1)-P 124.9(6).[143]

Studies by Espinosa on the reaction mechanism support that the basic character of the exocyclic N atom in model complex **24** enables initial hydrogen bond (HB) formation leading to the van der Waals complex **24·H₂O**, which promotes weakening of the exocyclic C=N bond (lower double bond character) thus allowing rotation of this bond to afford the slightly less stable isomer **24^{E}·H₂O** (Figure 4.4.1.1.4).

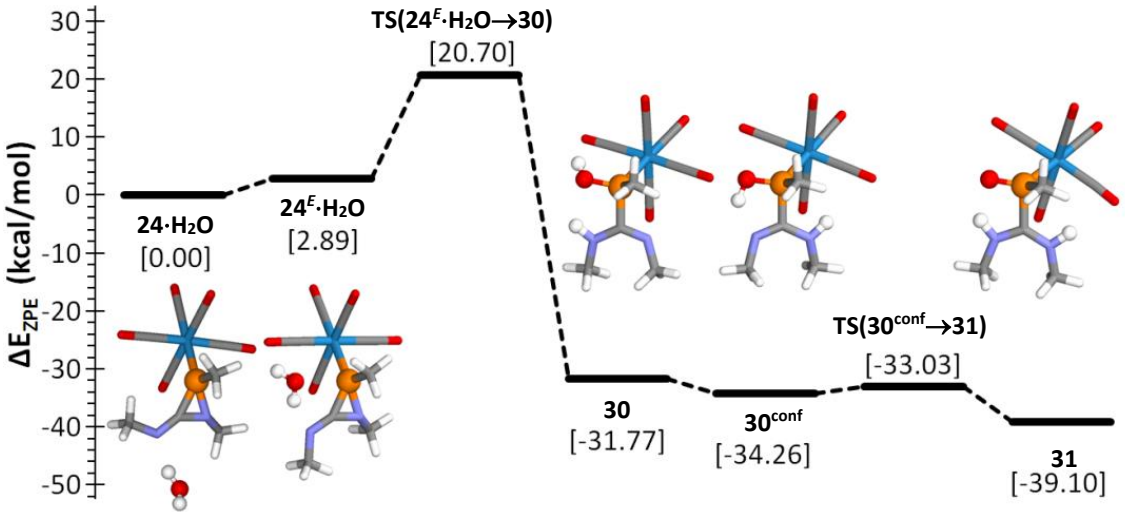

Figure 4.4.1.1.4. Calculated energy profile ($COSMO_{THF}$/LPNO-NCEPA1/def2-TZVPP//B3LYP-D3/def2-TZVP) for the hydrolysis of model complex **24** (see text) to **31**.[144]

This *E*-configured van der Waals complex displays a two-point anchoring of the water molecule to **24**^{E} by means of a OH···N HB (d = 2.025 Å; WBI = 0.030) and a weak secondary O···P interaction (d = 3.1985 Å; WBI = 0.020), as visualized in a NCI (noncovalent interactions) plot[91,149] (Figure 4.4.1.1.5). This in turn entails an important change in **24**^{E} as it remarkably increases the ring strain (*G*(r) = 0.1566 au) and weakens the P-N bond (WBI = 0.726; ρ(r) = 14.55x10^{2} e/a_o^3), thus giving rise to a cascade set of reactions.

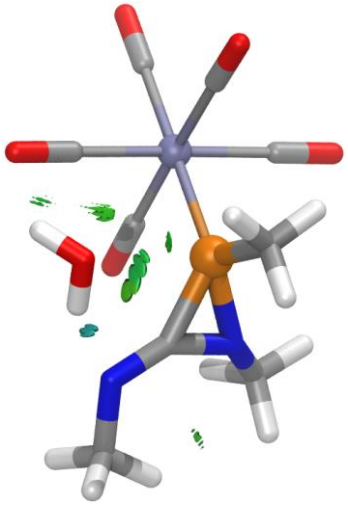

Figure 4.4.1.1.5. Computed (B3LYP-D3/def2-TZVP-f) structure for **24**^{E}·H_2O with NCIplot highlighting key stabilizing NCIs. The RDG *s* = 0.25 au isosurface is coloured over the range -0.07 < sign(λ_2)·ρ < 0.07 au: blue denotes strong attraction, green stands for moderate interaction, and red indicates strong repulsion.[144]

The proposed reaction sequence starts with a low barrier (20.7 kcal mol^{-1}), exergonic, unusual pericyclic [2σ+(2π+2σ)] process corresponding to the formal addition of water across the P–C=N termini and leading to the open-chain intermediate **30** that displays intramolecular NH···O(H)P HB-stabilization. Rotation around the C–P bond affords conformer **30**^{conf} that is stabilized by a different (and stronger) intramolecular hydrogen bond of POH···N type and enables the final slightly exergonic and very low barrier O-to-N proton transfer leading to **31**.

In order to inspect further the bonding in **31**, the heterolytic P-C bond dissociation energy (BDE) was computed to 53.69 Kcal·mol^{-1}, which is rather low for a not heavily substituted system (as in **28a,29a**) in comparison to the reported mean value of *ca.* 123 kcal/mol.[150] Furthermore, descriptors for bond strength points to a weak P-C bond in **31** (WBI = 0.726; ρ(r) = 13.92x10^{2} e/a_o^3) in comparison to the closely related precursor **30**^{conf} (WBI = 0.828; ρ(r) = 15.99x10^{2} e/a_o^3) and even the strained P-C bond in **24** (WBI = 0.809; ρ(r) = 15.47x10^{2} e/a_o^3), thus providing some additional support for the formulation as a

diaminocarbene-stabilized phosphinidene oxide complex **28,29**^{can} (Scheme 4.4.1.1.1). Rotation around the C-P bond in **31** requires to surpass a transition state barrier of 7.62 kcal/mol ($CHCl_3$ solution), which is in quite good agreement with the experimental value obtained for **29a**, especially if taking the larger substituents at both N and P into account.

4.4.1.1.1. Reaction of complex 28a with tritylium tetrafluoroborate

The unusual 1,3-zwitterionic P-ligand structure of **28,29** raised our particular interest, and the option of single electron transfer oxidation reactions was contemplated. Such reactions could lead to interesting radical cationis as stable products, or intermediates. When the zwitterionic complex **28a** was reacted with tritylium tetrafluoroborate (**32**), known to be a strong SET oxidant,[151] in Et_2O or THF at room temperature for twenty hours, complex **33** displaying ^{31}P NMR resonance of 110.6 ppm ($^1J_{W,P}$ = 294.3 Hz)($CDCl_3$) was obtained selectively (Scheme 4.4.1.1.1.1). In contrast to the precursor **28a**, the ^1H NMR spectrum of the new product showed a broad singlet at 6.5 ppm at room temperature corresponding to the two N-*H* hydrogen atoms. This finding reveals a free rotation around the P-C1 bond and the loss of the hydrogen bonding between the P-O atom and the hydrogen atom at the nitrogen atom. The $^{13}C\{^1H\}$ NMR spectrum showed a doublet for the C1 atom at 169.0 ppm ($^1J_{P,C}$ = 11.5 Hz) which in comparison with 172.5 ppm ($^1J_{P,C}$ = 32.5 Hz) observed in the precursor **28a**, suggests a similar environment at the P-C^{N2} carbon atom, and a weakening of this phosphorus-carbon bond might be concluded. The ^{11}B NMR spectrum showed a broad singlet at -1.1 ppm and the ^{19}F NMR spectrum a broad doublet at -139.9 ppm ($^1J_{F,B}$ = 2.7 Hz).

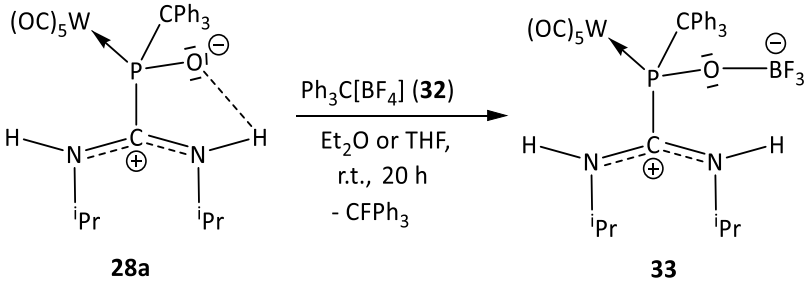

28a **33**

Scheme 4.4.1.1.1.1. Reaction of **28a** with tritylium tetrafluoroborate to give **33**.

The P-ligand in complex **33** can be described as a carbene donor adduct to a terminal phosphinidene oxide complex which, in turn, coordinates to boron trifluoride via a lone pair at the oxygen atom (**33**^{can} (can = canonical structure))(Scheme 4.4.1.1.1.2).

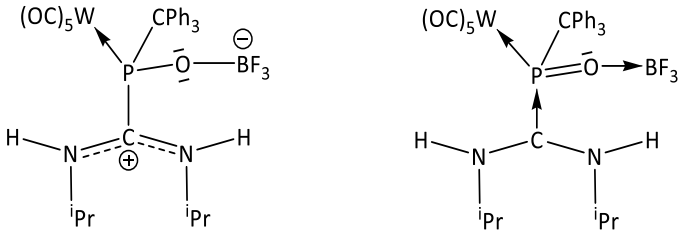

33 **33^{can}**

Scheme 4.4.1.1.1.2. Two canonical structures of complex **33**.

Compared to the metrics of the starting material **28a**, the P–C1 bond length of 1.9191(1) Å remains almost unchanged (1.921(8) Å for **28a**), while the P–O1 bond length of 1.543(7) Å is, as expected, significantly elongated compared with 1.518(6) Å in **28a**, due to the coordination to boron trifluoride (Figure 4.4.1.1.1.1). Compared with literature values for related compounds, the O1–B bond length of 1.5146(1) Å is almost equal to the one observed for the triphenylphosphine oxide trifluoroborane adduct (**LXXXIII**)[152] (d_{O-B} = 1.516(6) Å) and slightly elongated with respect to **LXXXIV**[153] and **LXXXV**[154] of 1.487 and 1.488(6) Å, respectively (Scheme 4.4.1.1.1.3).

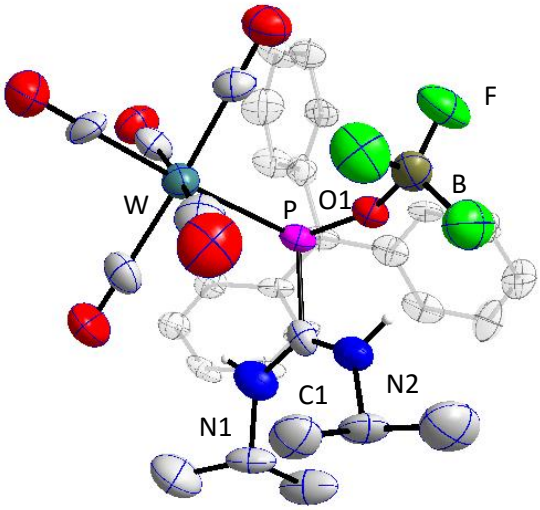

Figure 4.4.1.1.1.1. Molecular structure of **33**. (50% probability level, hydrogen atoms, except at N atoms, are omitted and CPh_3 group shown in grey for clarity). Selected X-ray crystal structure data (distances [Å] and angles [°]): P-W 2.533(1), P-C(1) 1.9191(1), P-O(1) 1.543(7), O(1)-B 1.5146(1) , C(1)-N(1) 1.327(1), C(1)-N(2) 1.301(1), N(1)-C(1)-N(2) 128.57, N(1)-C(1)-P 112.54, N(2)-C(1)-P 118.68.[5]

[5] The structure as obtained by X-ray analysis is not yet refined.

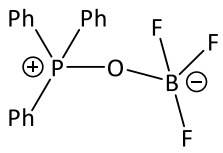

LXXXIII[152]

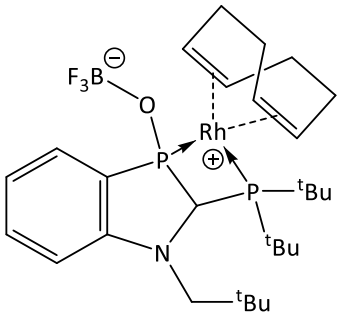

LXXXIV[153]

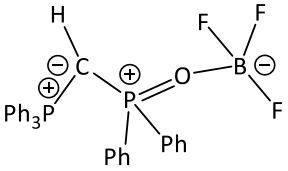

LXXXV[154]

Scheme 4.4.1.1.1.3**.** Some examples of literature known compounds having the P–O–BF_3 unit.

4.4.1.2. Reaction with isocyanates and bis-isocyanates

When 3-imino-azaphosphiridine complex **21a** was treated with 1 eq. of phenyl isocyanate (**34a**) in THF, Et_2O or toluene at ambient temperature (Scheme 4.4.1.2.1), 1,3,5-oxazaphospholane complex **35** was obtained. Interestingly, no reaction was observed when isopropyl isocyanate (**34b**) was used under the same conditions. Complex **35** displayed a $^{31}P\{^1H\}$ resonance at 131.7 ppm ($^1J_{W,P}$ = 277.7 Hz); this was accompanied by the formation of a complex (~4%; $^{31}P\{^1H\}$ = 103.4 ppm, $^1J_{W,P}$ = 288.0 Hz) which could not be identified. In case of **35**, a formal insertion of the carbonyl group of the phenyl isocyanate into the P-N bond of complex **21a** had occurred. Product **35** was isolated in 65% yield and its molecular structure was confirmed by X-ray analysis (crystal system monoclinic, space group $P2_1/c$) (Figure 4.4.1.2.1). The $^{13}C\{^1H\}$ NMR spectra of **35** revealed resonances for the imino carbon atoms at 143.5 ppm ($^{2+3}J_{P,C}$ = 12.4 Hz) and 150.7 ppm ($^{1+4}J_{P,C}$ = 10.2 Hz). For a mechanistic proposal see chapter 4.4.1.3.

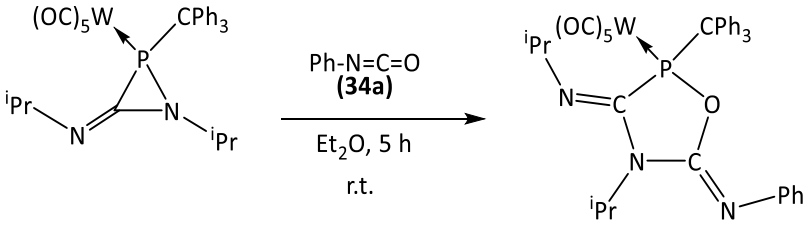

21a **35**

Scheme 4.4.1.2.1. Reaction of 3-imino-azaphosphiridine complex **21a** with phenyl isocyanate (**34a**) to give 1,3,5-oxazaphospholane complex **35**.

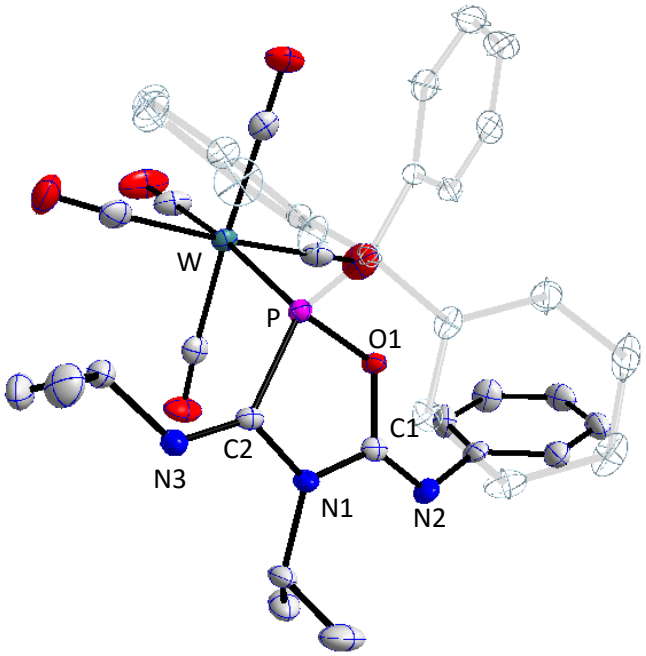

Figure 4.4.1.2.1. Molecular structure of 1,3,5-oxazaphospholane complex **35**. (50% probability level, hydrogen atoms are omitted and CPh_3 group in gray for clarity). Selected structural parameters (distances [Å] and angles [°]): P-W 2.5011(6), P-C(2) 1.885(2), P-O(1) 1.6562(15), O(1)-C(1) 1.386(2) C(1)-N(1) 1.370(3), N(1)-C(2) 1.406(3), C(2)-P-O(1) 89.98(9), O(1)-C(1)-N(1) 111.20(19), N(1)-C(2)-P 105.21(15).[143]

Interestingly, when a large excess of ca. 100 eq. of **34a** was added to the reaction mixture of freshly prepared **21a**, formation of a crystalline, trimeric structure of the phenyl isocyanate $(PhNCO)_3$ (**36**)[155] occurred (Scheme 4.4.1.2.2). Simple hand-touching of the reaction vessel revealed an exothermic reaction. The trimerization was not observed when a large excess of **34a** was added neither to solutions of isolated **21a** nor to lithium chloride. The product, which co-crystallized together with a THF molecule, was identified by X-ray crystallographic analysis (crystal system triclinic, space group $P\bar{1}$) (Figure 4.4.1.2.2). A nucleophilic attack of the lone pair at imino nitrogen atom to the allenic carbon of the isocyanate (see chapter 4.4.1.3), in which lithium chloride might be somehow involved, and which does not allow for a fast ring closure might be the explanation. But the overall mechanism of the trimerization requires further theoretical studies.

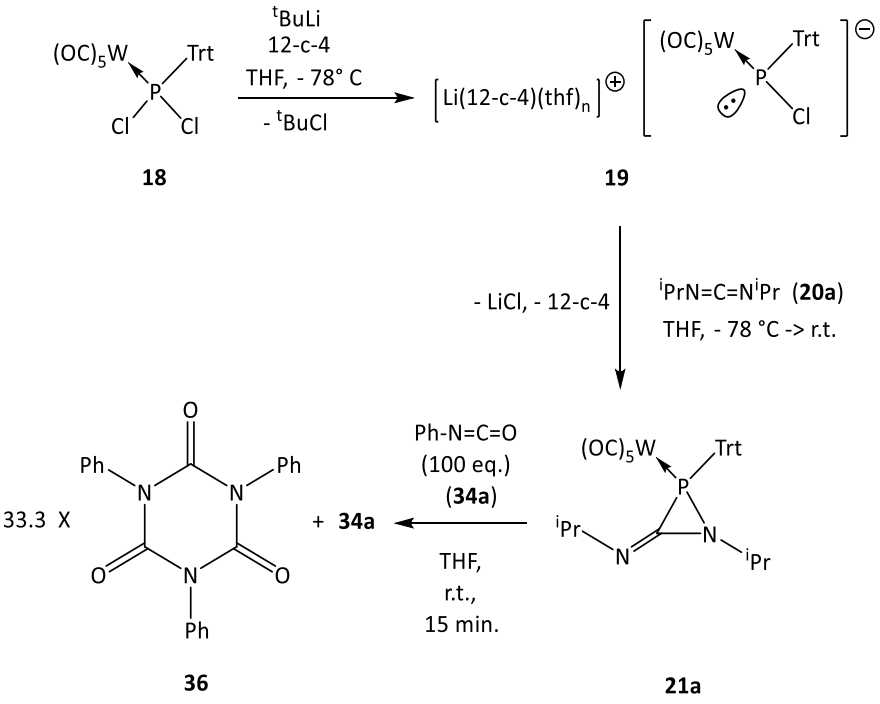

Scheme 4.4.1.2.2. Formation of 1,3,5-triphenyl-1,3,5-triazinane-2,4,6-trione **36**.

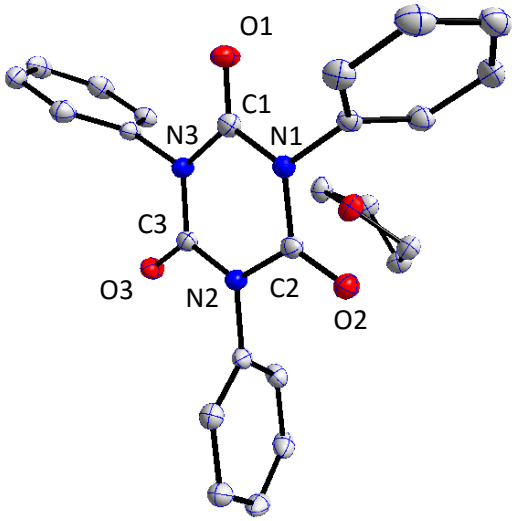

Figure 4.4.1.2.2. Molecular structure of **36**. (50% probability level, hydrogen atoms are omitted for clarity). Selected structural parameters (distances [Å]): C(1)-N(1) 1.3897(16), N(1)-C(2) 1.3905(16), C(2)-N(2) 1.3932(15), N(2)-C(3) 1.3881(16), C(3)-N(3) 1.3926(16), N(3)-C(1) 1.3928(16), C(1)-O(1) 1.2059(15), C(2)-O(2) 1.2078(15), C(3)-O(3) 1.2101(15).

The selectivity observed for the reaction **21a** with phenyl isocyanate (**34a**) extends to bis-isocyanates. Reaction of 1,4-phenylene diisocyanate (**37**) with two equivalents of 3-iminoazaphosphiridine complex **22a** led selectively to the formation of 1,4-phenylene-bis-

1,3,5-oxazaphopholane complex **38**. The $^{31}P\{^{1}H\}$ NMR spectrum showed three broad signals at 132.1 ppm, 132.6 ppm and 134.3 ppm with $^{1}J_{W,P}$ = 276 Hz probably due to diastereoism at the phosphorus atom (Scheme 4.4.1.2.3). Complex **38** was isolated in 50 % yield by low temperature column chromatography and both ^{1}H and ^{13}C NMR spectra displayed broad signals as it was expected for this kind of "bis-structures" (see experimental part).

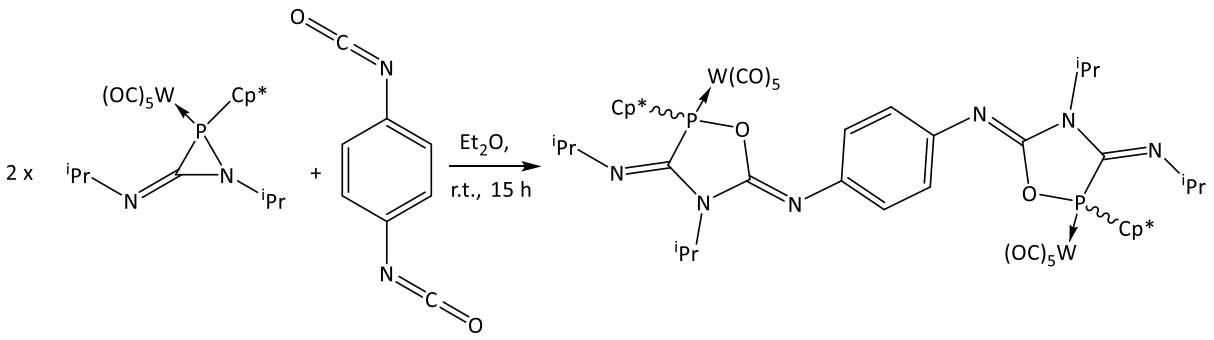

Scheme 4.4.1.2.3. Reaction of 3-imino-azaphosphiridine complex **21b** with 1,4-phenylene diisocyanate (**37**) to give complex **38**.

The structure of **38** was further confirmed by X-ray analysis (crystal system monoclinic, space group $P2_1/n$)(Figure 4.4.1.2.3). In general, all bonding parameters in the 1,3,5-oxazaphospholane rings in **35** and **38** are in the same range, except of the P-C(2) bond length of 1.859(4) Å in **38** which is shortened in comparison with the P-C(2) bond length of 1.885(2) in **35**.

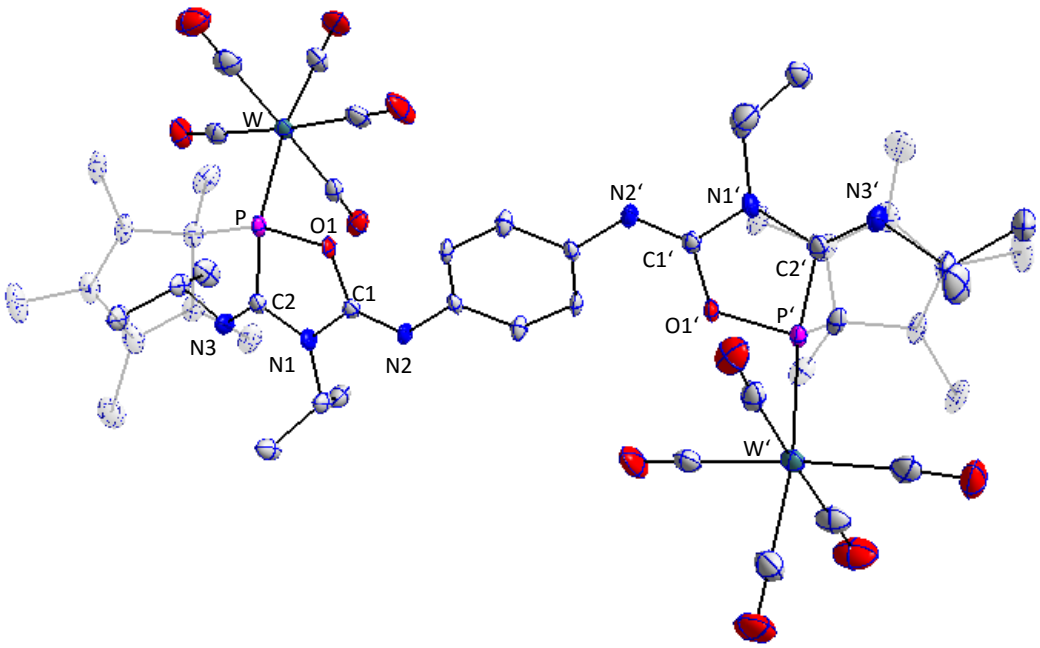

Figure 4.4.1.2.3. Molecular structure of 1,4-phenylene-bis-1,3,5-oxazaphospholane complex **38**. (50% probability level, hydrogen atoms are omitted and Cp* groups in grey for clarity). Selected structural parameters (distances [Å] and angles [°]): P-W 2.4966(10), P-C(2) 1.859(4), P-O(1) 1.678(3), O(1)-C(1) 1.376(4) C(1)-N(1) 1.385(5), N(1)-C(2) 1.406(5), C(2)-P-O(1) 90.19(16), O(1)-C(1)-N(1) 110.7(3), N(1)-C(2)-P 105.6(3).

4.4.1.3. Reaction with carbon dioxide

In order to test its reactivity further, **21a** was treated with carbon dioxide, first in THF (1 bar, r.t.), to give readily 1,3,5-oxazaphospholane complex **39** *via* ring expansion. Under these conditions ~15% of an unknown complex was observed (δ $^{31}P\{^1H\}$ = 71.6, $^1J_{W,P}$ = 288.0 Hz, $^1J_{P,H}$ = 358.5 Hz) which could not be isolated. This by-product formation was suppressed, if the reaction was carried out in Et_2O at 20 bar of CO_2 and ambient temperature (Scheme 4.4.1.3.1). Product **39** (δ $^{31}P\{^1H\}$ = 128.0, $^1J_{W,P}$ = 272.4 Hz) was fully characterized including X-ray structure analysis (crystal system triclinic, space group $P\bar{1}$) (Figure 4.4.1.3.1) and displayed $^{13}C\{^1H\}$ NMR resonances of 151.0 ppm ($^{1+4}J_{P,C}$ = 8.1 Hz) and 149.5 ($^{2+3}J_{P,C}$ = 12.1 Hz) for the imino and carbonylic carbon atoms, respectively.

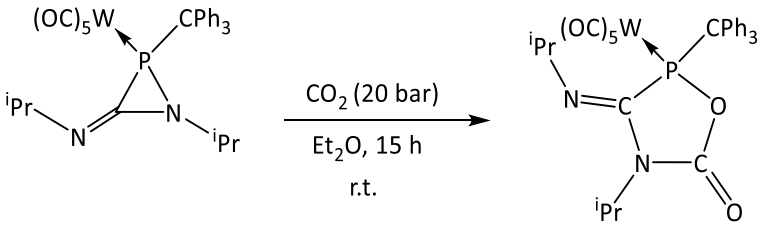

21a **39**

Scheme 4.4.1.3.1. Reaction of 3-imino-azaphosphiridine complex **21a** with CO_2 to give complex **33**.

The 1,3,5-oxazaphospholane rings in **35**, **38** and **39** are planar, showing in all cases a largest distance of a ring atom with respect to the best mean plane formed by all ring atoms below 0.04 Å and a sum of bond angles at the N1 atom of **35**: 359.9 °; **33**: 359.6 °; **39**: 360.0 °, showing a planar environment (Figures 4.4.1.2.1, 4.4.1.2.3 and 4.4.1.3.1).

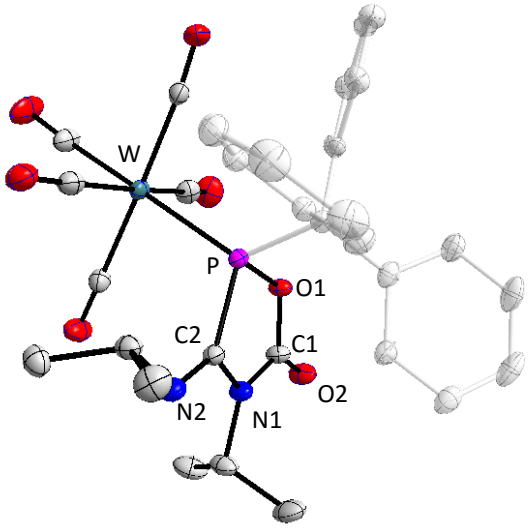

Figure 4.4.1.3.1. Molecular structure of 1,3,5-oxazaphospholane complex **39**. (50% probability level, hydrogen atoms are omitted and trityl group in grey for clarity). Selected structural parameters (distances [Å] and angles [°]):P-W 2.4935(8), P-C(2) 1.885(3), P-O(1) 1.671(3), O(1)-C(1) 1.377(4), C(1)-N(1) 1.370(5), N(1)-C(2) 1.407(4), C(2)-P-O(1) 89.82(14), O(1)-C(1)-N(1) 111.2(3), N(1)-C(2)-P 104.9(2).[143]

To understand the formal P–N bond-selective ring expansion process, Espinosa performed quantum chemical calculations ($COSMO_{toluene}$/DLPNO-CCSD(T)/def2-TZVPPecp//$COSMO_{toluene}$/B3LYP-D3/def2-TZVP ecp) to elucidate the reaction pathway. Here,

the *in silico* reaction with carbon dioxide of model complex **24** (methyl groups at both P and N atoms were used for the sake of computational efficiency) was explored. Initially, the basic exocyclic N atom of the most stable *Z*-configured initial model complex **24** interacts with the electrophilic centre of carbon dioxide leading to **24·CO₂** that undergoes rotation of the weakened exocyclic C-N bond to afford the van der Waals complex **24^{E}·CO₂** bound by weak non-covalent interactions (NCIs) (Scheme 4.4.1.3.2).

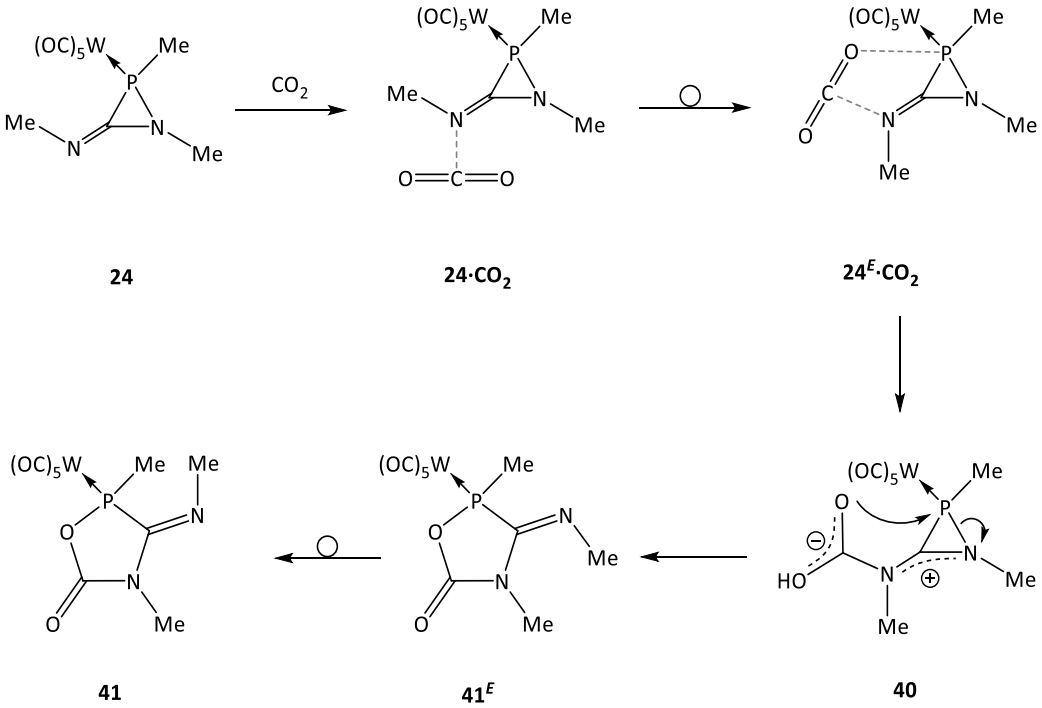

Scheme 4.4.1.3.2. Proposed mechanism for the formation of model complex **41**.[143]

The van der Waals complex **24^{E}·CO₂** is easily visualized by the NCIplot technique of colour-coded reduced density gradient (RDG) isosurfaces (Figure 4.4.1.3.2).[156] The most significant NCIs are those linking the exocyclic N atom with the CO_2 carbon (d = 2.858 Å; WBI = 0.010; ρ(r) = 1.15x10^{-2} e/a_o^3) and one CO_2 oxygen atom with the P atom (d = 3.330 Å; WBI = 0.003; ρ(r) = 0.68x10^{-2} e/a_o^3) and a carbonyl ligand (d = 3.205 Å; WBI = 0.002; ρ(r) = 0.51x10^{-2} e/a_o^3).

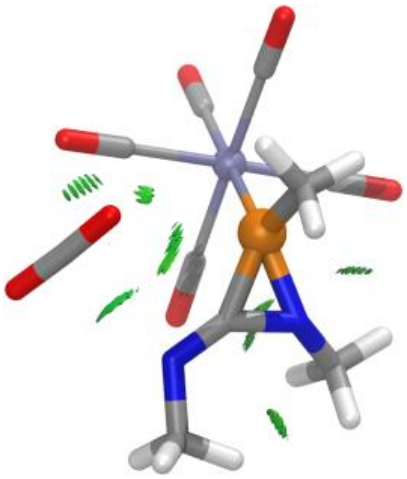

Figure 4.4.1.3.2. Computed (B3LYP-D3/def2-TZVPecp) most stable structure for van der Waals complex **24^{E}·CO$_2$** with NCIplot highlighting key stabilizing NCIs. The RDG *s* = 0.28 au isosurface is coloured over the range -0.05 < sign(λ_2)·ρ < 0.05 au: blue denotes strong attraction, green stands for moderate interaction, and red indicates strong repulsion.

Strengthening of the N···C interaction in the van der Waals complex leads to zwitterionic intermediate **40** that undergoes ring opening by attack of the negatively charged O atom to phosphorus thus forming a new 5-membered 1,3,5-oxazaphospholane ring **41^{E}** in a highly exergonic low barrier process (Figure 4.4.1.3.3). Finally the exocyclic *E*-configured C=N bond rotates to give the most stable *Z*-configuration of the final product **41**.[143]

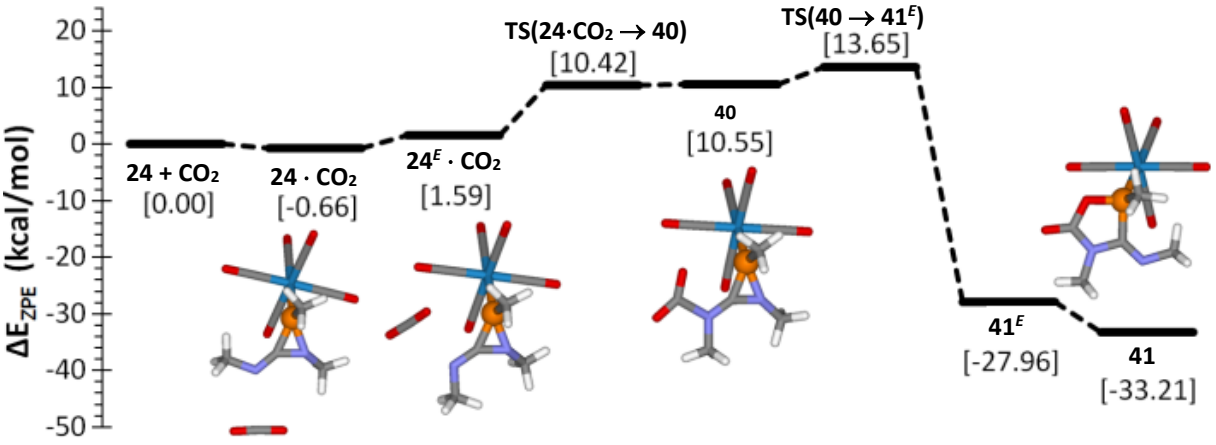

Figure 4.4.1.3.3**.** Computed (COSMO$_{toluene}$/DLPNO-CCSD(T)/def2-TZVPPecp) minimum energy path for the transformation **24** + CO_2 → **41**.[143]

The driving force for the overall transformation **24** + CO_2 → **41** must be mainly related to the release of the remarkably high ring strain (50.58 kcal/mol was calculated for the parent

complex).[152] In this line, the computationally inexpensive *G(r)* (Lagrangian of the kinetic energy density at ring critical points)[101] values reveal a dramatic increase of ring strain on moving from **24** to **24^{E}**·CO_2 (8.9%) and to **40** (19.0%) (Table 4.4.1.3.1), which parallels a significant weakening of the P-N bond. This situation approaches a bonding described by formula **LXXXII'** (or more specifically **LXVII'**) as result of an external substrate stimulus. Some commonly used bond strength related parameters support this view (Table 4.4.1.3.1).

Table 4.4.1.3.1**.** Ring strain and P-N bond strength related parameters for selected computed species. [143]

Entry	$G(r)_{RCP}$[a]	$d_{P\text{-}N}$[b]	$WBI_{P\text{-}N}$	$\rho(r)_{P\text{-}N}$[c]
24	0.1362	1.747	0.748	0.1507
24^{E}·CO_2	0.1483	1.750	0.739	0.1493
40	0.1621	1.768	0.673	0.1389

[a] In au. [b] In Å. [c] In e/a_o^3.

4.4.1.4. Reaction with pentafluorobenzaldehyde

To extend the reactivity studies on 3-imino-azaphosphiridine complexes towards the class of carbonylic compounds, complex **21a** was reacted with benzaldehyde (**42**) and pentafluorobenzaldehyde (**43**). Since both reactions have different outcomes, we focus first in this chapter on the reactivity of **21a** with **43**. Reaction of **21a** with **42** will be discussed in chapter 4.4.2.2.

When **21a** was reacted with 1 eq. of pentafluorobenzaldehyde (**43**) in Et_2O at room temperature, complex **44** showing $^{31}P\{^1H\}$ NMR resonance of 138.3 ppm ($^1J_{W,P}$ = 274.6 Hz) was obtained together with 18 % (according to $^{31}P\{^1H\}$ NMR integration) of a minor product **45** displaying $^{31}P\{^1H\}$ NMR resonance of 9.3 ppm ($^1J_{W,P}$ = 316.6 Hz). The assignment of the minor product **45** as oxaphosphirane tungsten(0) complex bearing pentafluorophenyl substituent at the ring carbon atom, is supported by a recent report of this complex and the similarity of their ^{31}P NMR spectral data[139] (see chapter 4.4.2.2). Interestingly, the amount of **45** in the reaction mixture could be reduced to 3 % by doubling the concentration of **21a** and **43** and keeping other reaction conditions constant (Scheme 4.4.1.4.1). Complex **44**, showing a 1,3,5-

oxazaphospholane structure formed in a diastereoselective manner upon a P–N bond ring expansion reaction with the carbonylic moiety of **43**, was isolated in 50 % yield and completely characterized and its molecular structure was confirmed by X-ray crystallographic analysis (Figure 4.4.1.4.2). The ^{1}H NMR spectrum displayed a singlet for the C1-H hydrogen atom at 4.4 ppm ($CDCl_3$). In the $^{13}C\{^{1}H\}$ NMR spectrum, the C1 carbon atom shows a resonance of 83.6 ppm ($CDCl_3$) and a multiplicity of a triplet ($^{3}J_{F,C}$ = 10.5 Hz) due to coupling with the *ortho*-fluorine atoms of the pentafluorophenyl group. Interestingly, the ^{13}C NMR resonance for the *cis*-carbonyl carbon atoms at tungsten appeared as a doublet of doublets at 196.5 ppm ($^{2}J_{P,C}$ = 6.5 Hz, $J_{F\text{-}C}$ = 3.6 Hz). In order to clarify if the splitting of the common multiplicity of the *cis*-carbonyl carbon atoms (doublet) is caused by a hampered rotation around the P–W bond, a ^{13}C NMR spectrum was measured in chloroform-*d*8 at 60 °C. Here, the *cis*-carbonyl carbon atoms continue to show a doublet of doublet multiplicity. This observation together with the similar values of through space coupling constants between the fluorine and carbonyl carbon nuclei of 5.5 Hz as reported for related compounds such as **LXXXVI** (Figure 4.4.1.4.1),[157] suggests a through space coupling as the origin of the observed multiplicity. Accordingly, the ^{19}F NMR spectrum showed five different resonances for the five different fluorine nuclei at the phenyl ring (see experimental part).

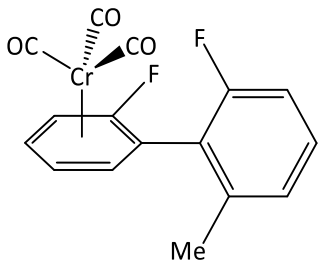

LXXXVI[157]

Figure 4.4.1.4.1. Example of a complex having a trough-space interaction between carbonyl carbon atoms and a fluorine substituent ($J_{F\text{-}C}$ = 5.5 Hz).

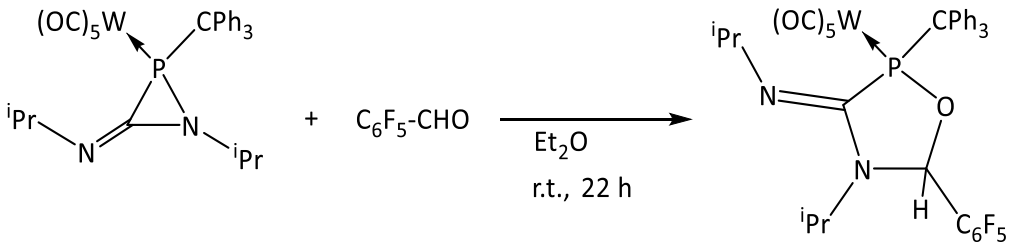

21a **43** **44**

Scheme 4.4.1.4.1. Reaction of **21a** and **43** to give complex **44**.

1,3,5-Oxazaphospholane complex **44** crystallized in a monoclinic crystal system and a C2/c space group and displayed shortening of P-C2, P-O1 and N1-C2 bond lengths of 1.82(2) Å, 1.654(14) Å and 1.37(2) Å, respectively, compared with 1.885(3) Å, 1.671(3) Å and 1.407(4) Å shown by **39**. To the contrary, O1-C1 and C1-N1 bond lengths of 1.47(2) Å and 1.45(3) Å are elongated compared with 1.377(4) Å and 1.370(5) Å of **39**. The 1,3,5-oxazaphospholane ring shows a non-planar structure showing the C1 atom the greatest distance (d(C1-best plane) = 0.128 Å) from the best mean plane defined by all five ring atoms (Figure 4.4.1.4.2).

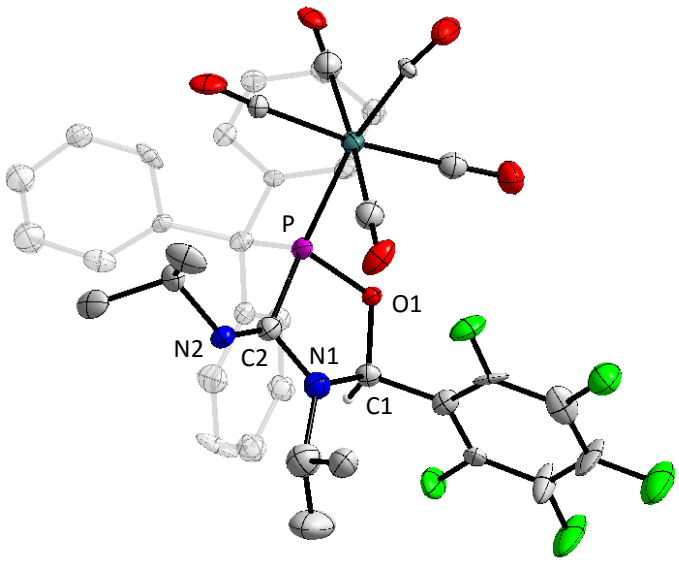

Figure 4.4.1.4.2. Molecular structure of 1,3,5-oxazaphospholane complex **44**. (50% probability level, hydrogen atoms are omitted and trityl group in grey for clarity). Selected structural parameters (distances [Å] and angles [°]): P-W 2.528(6), P-C(2) 1.82(2), P-O(1) 1.654(14), O(1)-C(1) 1.47(2), C(1)-N(1) 1.45(3), N(1)-C(2) 1.37(2), C(2)-P-O(1) 89.7(9), O(1)-C(1)-N(1) 104.1(16), N(1)-C(2)-P 109.7(16).

In a similar fashion of what was proposed for the reaction of **21a** with CO_2, we can assume an initial van der Waals complex **21a·F_5C_6(H)C=O** formation which upon nucleophilic attack of the imino N atom to the electrophilic centre of carbonyl carbon of the aldehyde then leads to a subsequent P–O bond formation and ring closure (Scheme 4.4.1.4.2).

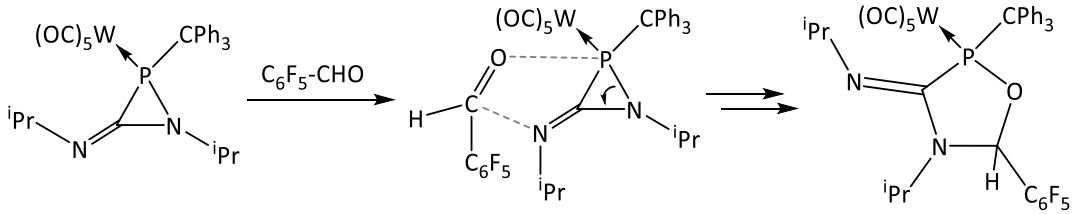

Scheme 4.4.1.4.2. Proposed mechanism for the formation of **44**.

4.4.2. Examples as electrophilic phosphinidene complex transfer reagent

Unexpectedly, 3-imino-azaphosphiridine complexes **21,22** were observed to react in a different manner towards certain substrates. In contrast to the behavior observed towards water, heterocumulenes such as isocyanates or carbon dioxide and pentafluorobenzaldehyde, reaction of **21a** with carbon monoxide, with benzaldehyde, with cyclohexyl carbodiimide and with ^{n}butyl- and ^{t}butyl isocyanides yielded a phosphinidene complex transfer reaction, thus revealing a surprising dichotomy of the reactivity of 3-imino-azaphosphiridine complexes.

4.4.2.1. Reaction with carbon monoxide

When a Et_2O solution of 3-imino-azaphosphiridine complex **21a** was stirred under CO (20 bar) atmosphere, selective formation of 1,3-azaphosphetidinone complex **45** was observed at ambient temperature (Scheme 4.4.2.1.1). Complex **45** was isolated in 70 % yield and its molecular structure confirmed by X-ray analysis (Figure 4.4.2.1.1). **45** displayed a $^{31}P\{^{1}H\}$ resonance at 94.9 ppm ($^{1}J_{W,P}$ = 226.5 Hz); $^{13}C\{^{1}H\}$ NMR resonances of the carbon nuclei of the imino and carbonyl groups were observed at 148.9 ppm ($^{1+3}J_{P,C}$ = 13.2 Hz) and 169.6 ppm ($^{1+3}J_{P,C}$ = 52.1 Hz), respectively. An unligated 1,3-azaphosphetidinone derivative having *tert*-butyl groups at phosphorus and nitrogen atoms showing a $^{31}P\{^{1}H\}$ NMR resonance of 60.5

ppm was prepared by reaction of a phospha-carbodiimide and an isocyanate, reported in 1982 by Kolodyazhnyi.[158]

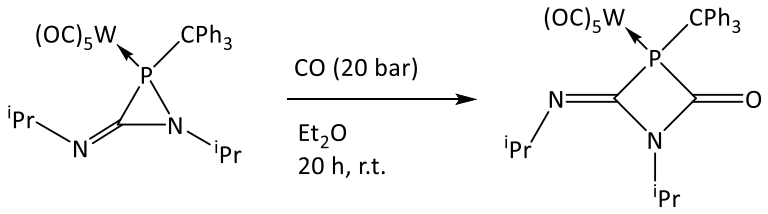

21a **45**

Scheme 4.4.2.1.1. Synthesis of 1,3-azaphosphetidinone complex **45**.

Complex **45** crystallized in a triclinic crystal system and a $P\bar{1}$ space group. The P-C1 and P–C2 bond lengths of 1.916(10) and 1.887(9) are significantly elongated compared to standard P–C single bond lengths of 1.80-1.82 Å.[82] Interestingly, the two endocyclic N-C bonds differ significantly (N1-C1 1.326(11) and N1-C2 1.455(12) Å) thus pointing to a strong π-electron interaction between the lone pair at the N1 atom and the C=O moiety, thus the resonance structure **45res** should have a considerable contribution (Scheme 4.4.2.1.2). The azaphosphetidinone ring is almost planar showing a folding angle between the planes defined by the C1-N1-C2 and N1-P-C2 of 5.2 ° (Figure 4.4.2.1.1).

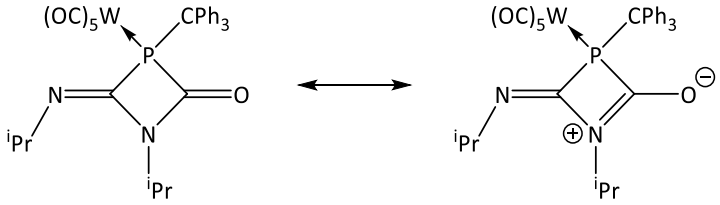

45 **45res**

Scheme 4.4.2.1.2. Two resonance structures of 1,3-azaphosphetidinone complex **45**.

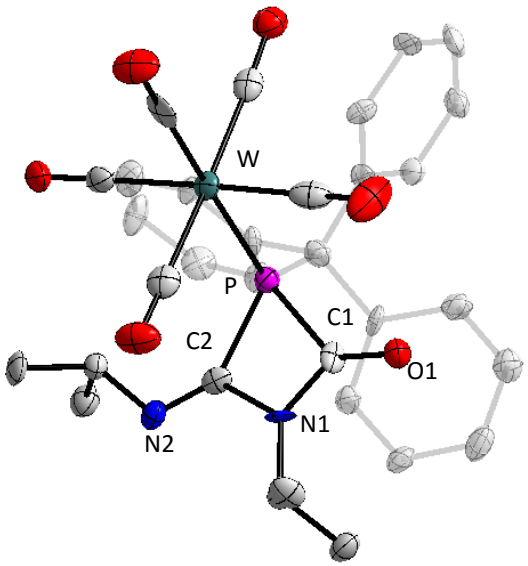

Figure 4.4.2.1.1. Molecular structure of 1,3-azaphosphetidinone complex **45** (50% probability level, hydrogen atoms are omitted and CPh_3 group in grey for clarity). Selected structural parameters (distances [Å] and angles [°]): P-W 2.510(3), P-C(1) 1.916(10), P-C(2) 1.887(9), N(1)-C(1) 1.326(11), N(1)-C(2) 1.455(12), C(2)-N(2) 1.255(11), C(2)-P-C(1) 69.9(4), P-C(1)-N(1) 94.8(6), P-C(2)-N(1) 91.9(6).

DFT calculations were performed by Espinosa ($COSMO_{toluene}$/DLPNO-CCSD(T)/def2-TZVPP(ecp), ZPE-corrected) on the reaction mechanism using model azaphosphiridine complex **24** having methyl groups at P and N atoms. The result was not a mechanistic pathway corresponding to the initial activation of the endocyclic P-N bond. Instead, a fast equilibrium of **24** with an *end-on* carbodiimide N→P complex **46** seems to initiate the overall process. This is followed by a CO / MeNCNMe ligand exchange reaction *via* the TS **46·CO→20c·47** (Scheme 4.4.2.1.3) giving rise to a phosphaketene complex **47**[89,159] and carbodiimide **20c**. Subsequent stepwise nucleophilic attack of the carbodiimide N atom to the C atom in **47** and of the P centre to the highly electrophilic carbodiimidium C atom in **48** yields complex **49**, finally.

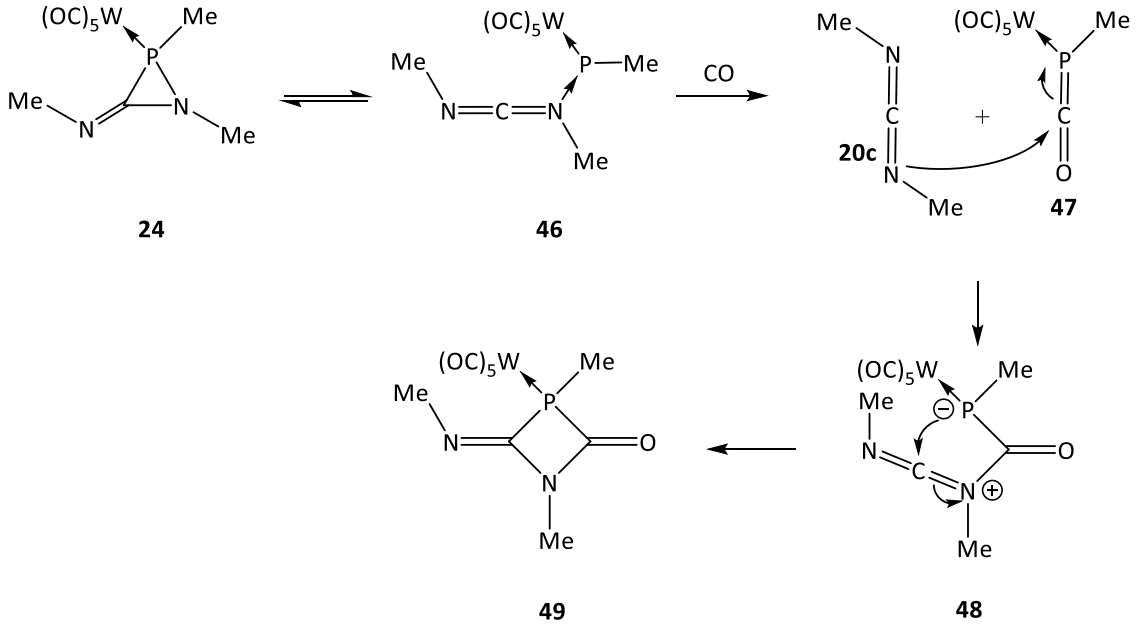

Scheme 4.4.2.1.3. Proposed mechanistic path for the transformation **24** + CO → **49**.

According to the calculations, the rate determining step should be the initial isomerization of the ring in **24** resulted in the formation of carbodiimide *end-on* complex **46** (ΔE_{ZPE} = 13.88 kcal/mol) through a relatively low energetic barrier ($\Delta E^{\neq}_{ZPE}$ = 17.92 kcal/mol). Ligand displacement at phosphorus exhibits an even lower barrier of 7.51 kcal/mol (Figure 4.4.2.1.2). Indeed, the very low bond dissociation energy (BDE) of 18.65 kcal/mol computed for the P-N bond in **46** at 25 °C supports its representation as dative bonding from the carbodiimide (ligand) to the P center thus underlining the metal-like bonding behavior. The two subsequent cyclization steps (**47**·**20c** → **48** → **49**) are almost barrierless processes ($\Delta E^{\neq}_{ZPE}$ = 3.28 kcal/mol and 0.91 kcal/mol respectively), although in the real system the steric hinderance of the substituent should raise these values, the last one being remarkably exergonic (ΔE_{ZPE} = 41.27 kcal/mol) due to the high stability of **49**. The long endocyclic P-C2 (WBI = 0.814; ρ(r) = $15.50 \cdot 10^{-2}$ e/a_0^3) and P-C1 (WBI = 0.800; ρ(r) = $15.43 \cdot 10^{-2}$ e/a_0^3) bonds calculated for **49** ($d_{P\text{-}C2}$ = 1.878 Å and $d_{P\text{-}C1}$ = 1.898 Å) are in good agreement with experimental values for **45** ($d_{P\text{-}C2}$ = 1.887(9) Å and $d_{P\text{-}C1}$ = 1.916(10) Å).

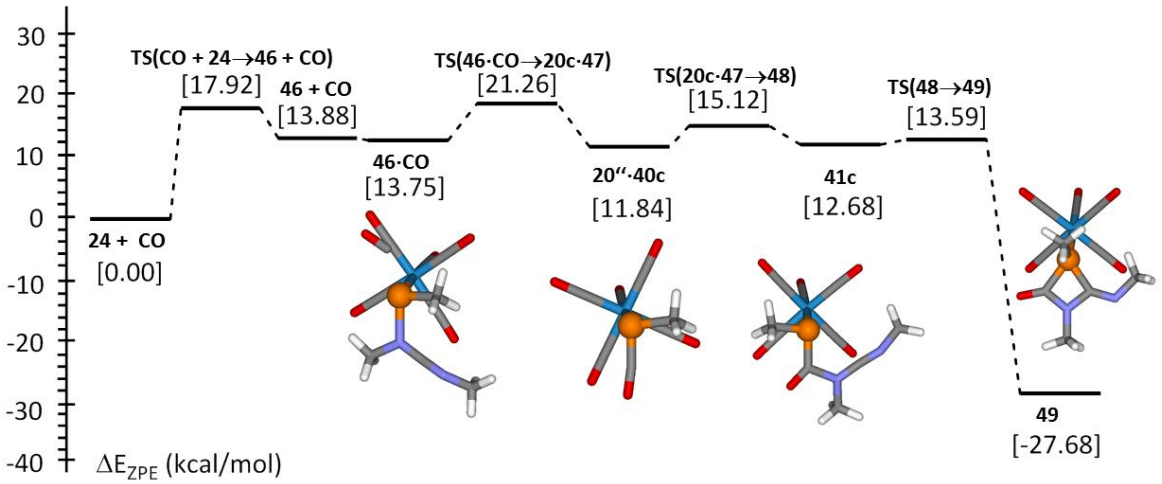

Figure 4.4.2.1.2. Computed ($COSMO_{toluene}$/DLPNO-CCSD(T)/def2-TZVPP(ecp), ZPE-corrected) relative energy profile for the transformation **24 + CO** to **49**.

4.4.2.2. Reaction with benzaldehyde

In contrast to the observed reaction of **21a** with pentafluorobenzaldehyde, the reaction with benzaldehyde (**42**) led to complex **50** displaying a $^{31}P\{^{1}H\}$ NMR resonance of 16.2 ppm ($^{1}J_{W,P}$ = 312.2 Hz) (Et_2O) (Scheme 4.4.2.2.1). Approximately 30 % of another complex was observed showing a $^{31}P\{^{1}H\}$ NMR resonance of 145.8 ppm ($^{1}J_{W,P}$ = 280.0 Hz) (Et_2O), probably having a 1,3,5-oxazaphospholane structure obtained *via* P–N bond ring expansion reaction of **21a** with **42** as in the formation of **44**. The amount of the minor-product could be reduced to 4 % by reducing the concentration of the reagents to a 50 % value. The identity of the product **50** was assigned to be the *P*-trityl oxaphosphirane complex **50**, which was obtained before by reaction of Li/Cl phosphinidenoid complex **19** and benzaldehyde.[40]

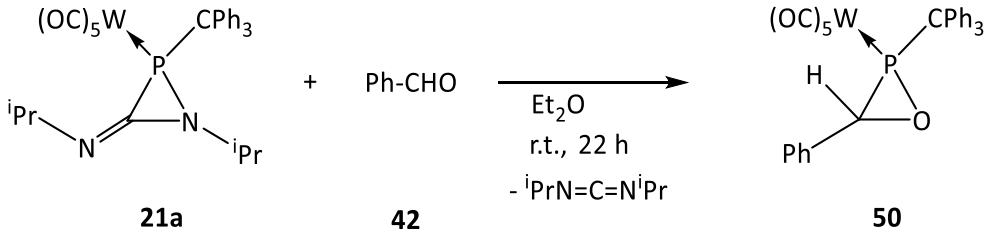

21a **42** **50**

Scheme 4.4.2.2.1. Reaction of 3-imino-azaphosphiridine complex **21a** with benzaldehyde to give oxaphosphirane complex **50.**

In this case, again, a terminal phosphinidene complex transfer via the carbodiimide *side-on* intermediate species **51** thus yielding a formal [2+1] cycloaddition product seems to be a plausible mechanism for the formation of **50** (Scheme 4.4.2.2.2). In the case of pentafluorobenzaldehyde the carbonylic carbon of the aldehyde is much more electrophilic due to the electron-withdrawing effect of the C_6F_5 group, thus making it more reactive towards the nucleophilic attack of the imino N atom. As this would also create a comparatively stronger N-C bond, so that an intramolecular follow-up reaction is more likely to occur than in case of the benzaldehyde.

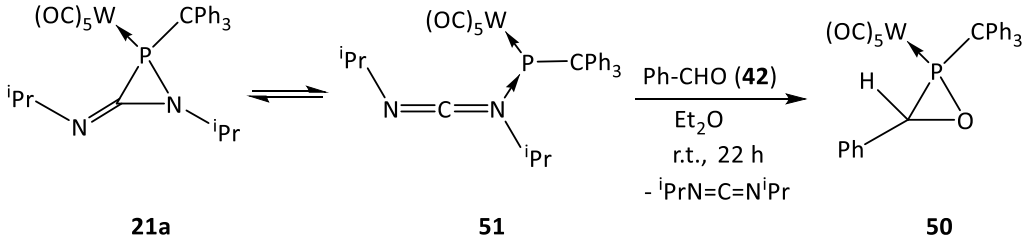

21a **51** **50**

Scheme 4.4.3.2.2. Proposed mechanism for the formation of **50** *via end-on* carbodiimide N→P complex **51**.

At this point two aspects shall be emphasized. In the reaction of 3-imino-azaphosphiridine complex **21a** with benzaldehyde and pentafluorobenzaldehyde, two competitive reactions namely i) P–N bond ring expansion reaction with the carbonyl moiety of the aldehyde and ii) generation of a short-lived *end-on* carbodiimide N→P complex **51** intermediate, reacting as a source for a terminal phosphinidene complex, occurred. Depending on the electronic properties of the aldehyde a substrate-depending reaction path was favored, i.e. a remarkable substrate stimulated response of complex **21a** resulted. This might be also described as new example of an aldehyde sensor.

4.4.2.3. Reaction with dicyclohexyl carbodiimide

When the 3-imino-azaphosphiridine complex **21a** was allowed to react with 1 eq. of dicyclohexyl carbodiimide (**20b**) in THF at ambient temperature, a mixture of **21a** and **21b** (ratio 1:1) was obtained after 3 h (Figure 4.4.2.3.1); this ratio remained constant over time. Here, again, an unusual substitution reaction at the phosphorus center had occurred in which the diisopropyl carbodiimide moiety in **21a** was exchanged by the dicyclohexyl carbodiimide to form **21b** (Scheme 4.4.2.3.1). As in the reaction of **21a** with benzaldehyde, the phosphinidene complex transfer reaction is favored, maybe caused by steric repulsion of the N-substituent. To examine this exchange further the alternative reaction of **21b** with carbodiimide **20a** was performed, and again a 1:1 mixture was formed.[143]

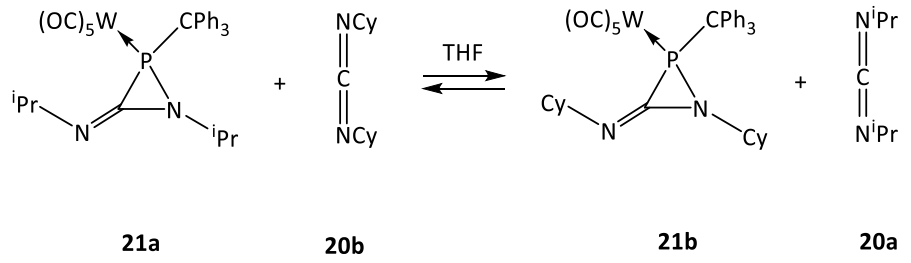

Scheme 4.4.2.3.1. Carbodiimide exchange reactions of 3-imino-azaphosphiridine complex **21a,b**.[151]

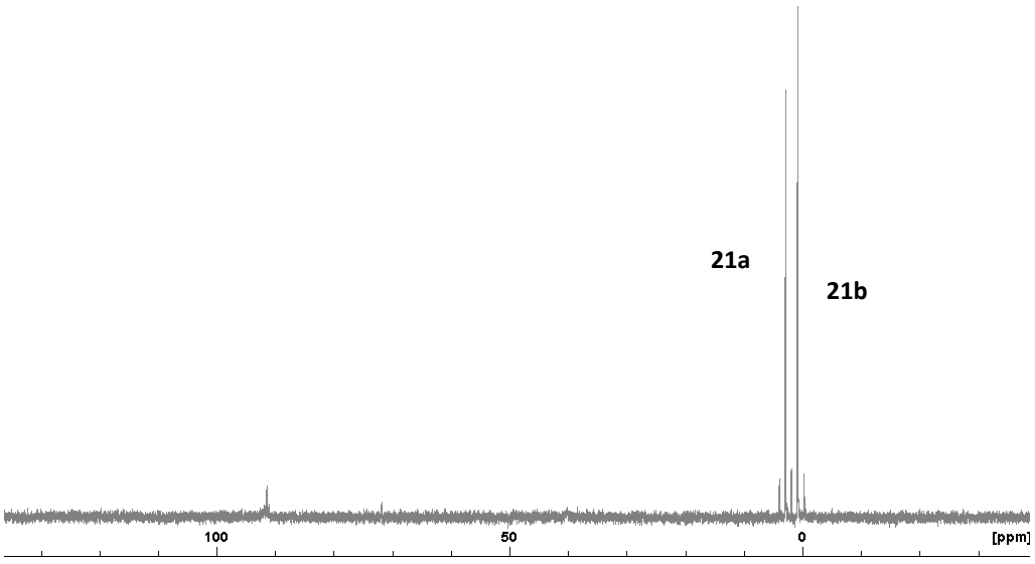

Figure 4.4.2.3.1. $^{31}P\{^{1}H\}$ NMR spectrum of the reaction mixture of **21a** and dicyclohexyl carbodiimide **20b** in Et_2O.

Besides the evidence obtained from the $^{31}P\{^{1}H\}$ NMR spectra, the nature of the newly formed product as **21a'** was confirmed additionally through formation of a 1:1 mixture of their hydrolysis products **25a,a'** occurring upon reaction of **21a,a'** with water (Scheme 4.4.2.3.2) (Figure 4.4.2.3.2).[143]

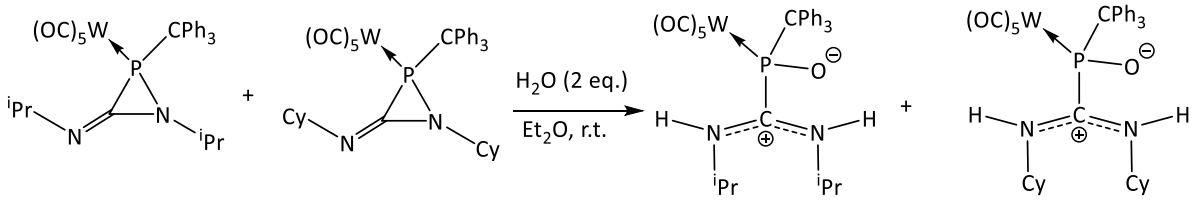

21a **21b** **28a** **28b**

Scheme 4.4.2.3.2. Hydrolysis reaction of 3-imino-azaphosphiridine complexes **21a** and **21b**.

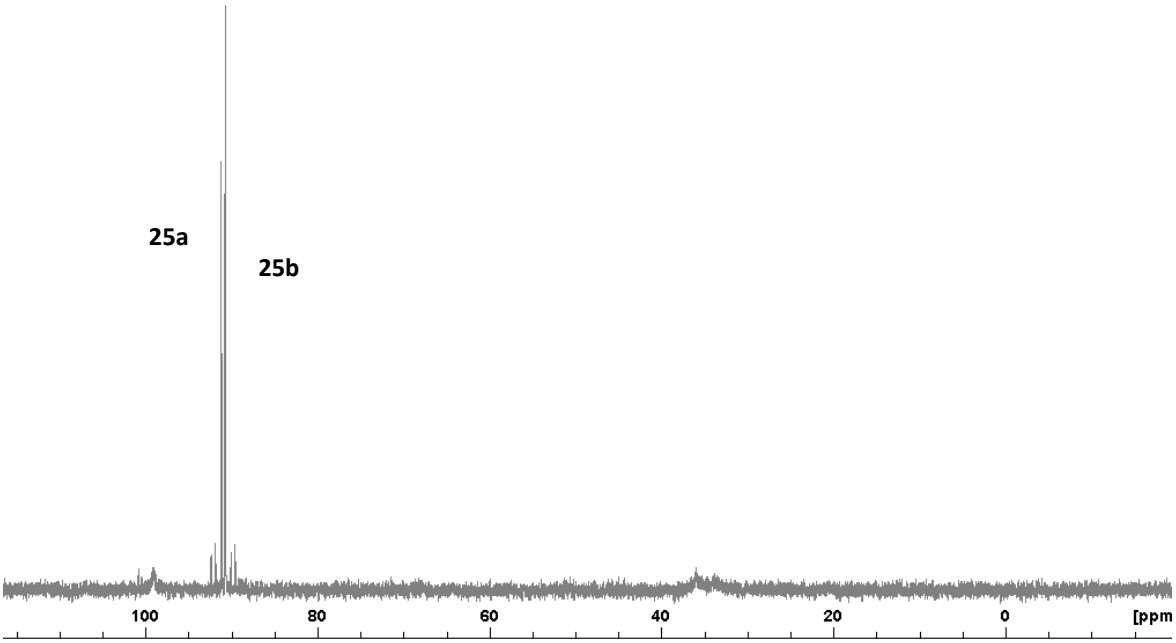

Scheme 4.4.2.3.2. $^{31}P\{^{1}H\}$ NMR spectrum of the reaction mixture of **21a,b** with water to give **28a,b**.

4.4.2.4. Reaction with isonitriles

In order to examine if a "bulkier CO analogue" would change the reaction course, we turned to isonitriles as they are closely related to CO with respect to their coordination behavior towards transition-metals. Here, the reaction of **21a** with isonitriles **52b,c** did not yield 1,3-azaphosphetidine complexes. Instead, the isonitrile-to-phosphinidene complex adducts **26b,c** were obtained selectively (Scheme 4.4.2.4.1).

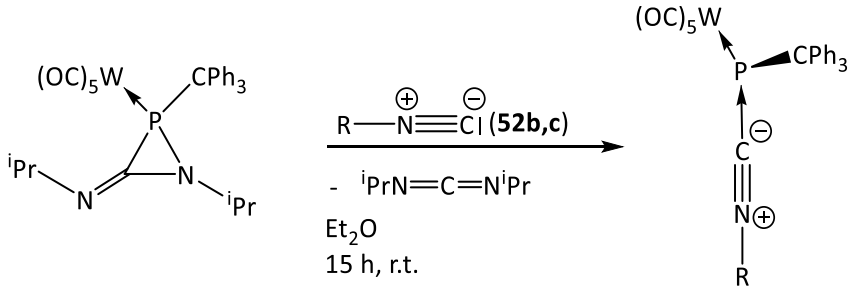

21a **26b,c**

R = ^{t}Bu (**b**), ^{n}Bu (**c**)

Scheme 4.4.2.4.1. Reaction of 3-imino-azaphosphiridine complex **21a** with isonitriles **52b,c** to give isonitrile-to-phosphinidene complex adducts **26b,c**.

$^{31}P\{^{1}H\}$ NMR spectra ($CDCl_3$) of complexes **26b,c** displayed resonances of -49.8 ppm and -51.8 ppm, respectively and surprisingly small phosphorus-tungsten coupling constant magnitudes of 118.5 Hz (**26b**) and 118.2 Hz (**26c**). The $^{13}C\{^{1}H\}$ NMR spectra showed resonances for the isonitrile carbon atoms at 146.9 ppm (**26b**) and 146.6 ppm (**26c**) and small phosphorus-carbon coupling constant magnitudes of 6.8 Hz (**26a**) and 6.6 Hz (**26b**). A comparison with the values of 209.4 ppm (**LXXXVIIa**) and 192.2 (**LXXXVIIb**) reported by Yoshifuji for phosphacarbodiimide structures,[160] of 195.5 ppm by Streubel for phosphacarbodiimide complex **LXXXVIII**[161] and 140.0 ppm by Scheer for the isocyanide-to-phosphinidene dinuclear complex **LXXXIX**[162] (Figure 4.4.2.4.1), it can be concluded that the adduct description of **26b,c** has a large contribution to the canonical structures (Figure 4.4.2.4.2).

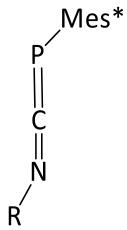

LXXXVIIa,b[160]

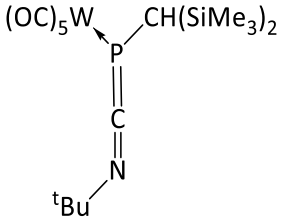

LXXXVIII[161]

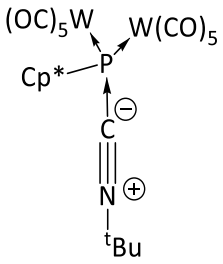

LXXXIX[162]

R = Ph (a), ^{t}Bu (b);
Mes* = 2,4,6-tri-*t*-butylphenyl

Figure 4.4.2.4.1. Phosphacarbodiimide **LXXXVIIa,b**,[160] phosphacarbodiimide complex **LXXXVIII**[161] and isocyanide-to--phosphinidene dinuclear complex **LXXXIX**.[162]

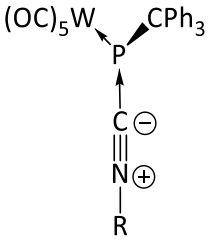

26a-c

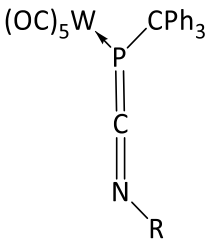

26a^{can}-c^{can}

R = ^{i}Pr (**a**), ^{t}Bu (**b**), ^{n}Bu (**c**)

Figure 4.4.2.4.2. Two canonical structures of complexes **26**.

X-ray structure analysis of **26b** (crystal system monoclinic, space group $P2_1/n$) showed P-C1 and C1-N bond distances of 1.747(3) Å and 1.156(3) Å, respectively (Figures 4.4.3.4.3). Together with a unique set of bond angles (C6-P-W 124.25(7)°, C6-P-C1 98.57(11)° and C1-P-W 101.06(8)°) it supports the adduct geometry and bonding (Figure 4.4.3.4.2). This becomes even more apparent if compared to **LXXXVIIa**, which showed P–C and C–N bond distances of 1.651(3) and 1.209(4) Å, respectively.[160] Nevertheless, the not strictly linear C1-N-C2 bond angle of 165.5(3) indicates some contribution of the valence isomer structure of **26^{can}** (Figure 4.4.3.4.2). A similar situation was observed by Scheer in **LXXXIX**. In this case, respective P–C and C–N bond distances of 1.796(6) and 1.140(7) Å where reported,[162] thus revealing a slightly less disturbed C-N bonding in this case.

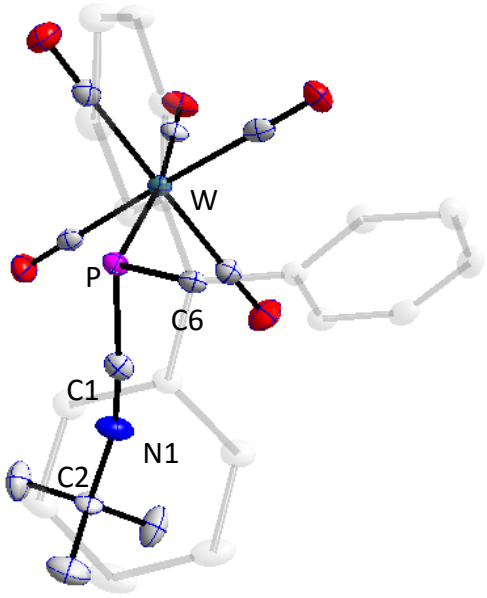

Figure 4.4.2.4.3**.** Molecular structure complex **26b**. (50% probability level, hydrogen atoms are omitted and CPh_3 group in grey for clarity). Selected structural parameters (distances [Å] and angles [°]): P-W 2.5908(7), P-C(1) 1.747(3), P-C(6) 1.952(2), C(1)-N 1.156(3), N-C(2) 1.462(3), C(6)-P-W 124.25(7), C(6)-P-C(1) 98.57(11), C(1)-P-W 101.06(8), C(1)-N-C(2) 165.5(3).

Mechanistically, this reaction is similar to that effected by carbon monoxide and proceeds by a nucleophilic displacement of the carbodiimide by the isonitrile at phosphorus in **51**, which for model systems (**46** + Me-N=C: (**52d**)) is a very low barrier process ($\Delta E^{\neq}_{ZPE}$ = 2.68 kcal/mol) and slightly exergonic (ΔE_{ZPE} = -13.59 kcal/mol) starting from the **46**·CNMe van der Waals complex (Scheme 4.4.2.4.2).

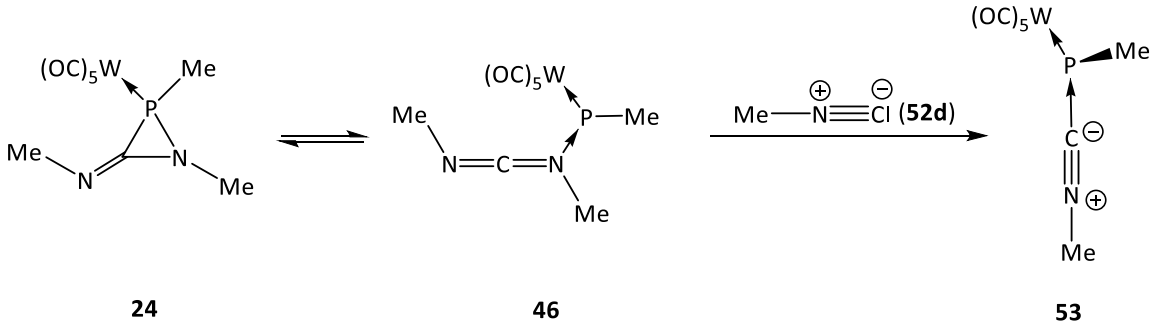

24 **46** **53**

Scheme 4.4.2.4.2. Proposed mechanism for the formation of the methyl model isocyanide-to-phosphinidene complex adduct **53**.

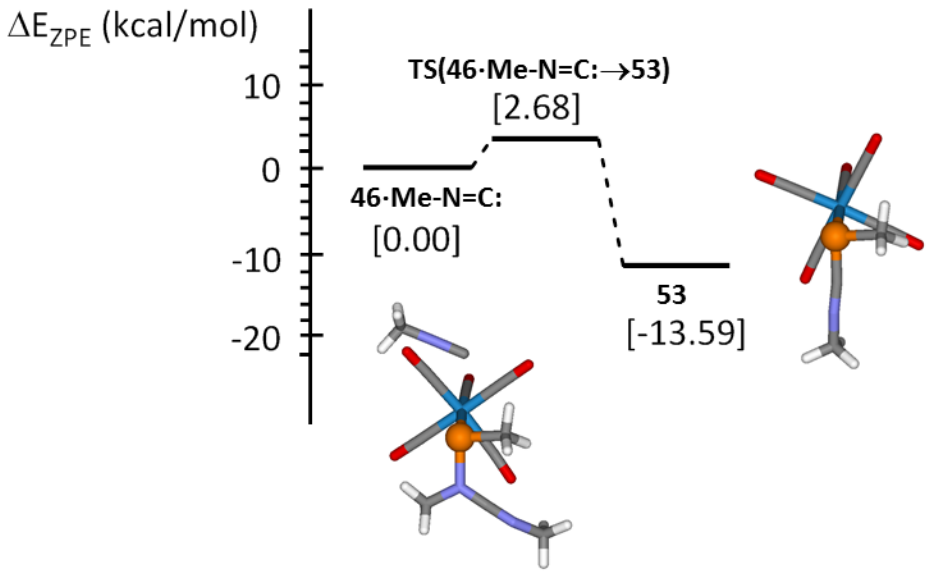

Figure 4.4.2.4.4. Computed ($COSMO_{toluene}$/DLPNO-CCSD(T)/def2 -TZVPP(ecp), ZPE-corrected) relative energy profile for the transformation **46c·Me-N=C:** to **53**.

Model complex **53** features a strong multiple N-C bond (d = 1.162 Å; WBI = 2.282; ρ(r) = $45.86 \cdot 10^{-2}$ e/a_0^3) together with a moderately strong P-C bond (d = 1.742 Å; WBI = 1.237; ρ(r) = $15.11 \cdot 10^{-2}$ e/a_0^3) in very good agreement with the experimental values found for **26b** (Figure 4.4.2.4.3). This can be explained in the light of the second order perturbation theory analysis of Fock matrix in NBO (natural bond orbital)[91,149] basis as resulting from extensive back-donation of electron density from a *3p* atomic orbital at P to two (N-C)π orbitals, amounting to a 61.98 kcal/mol stabilization, which would support a formulation as **26^{can}**. The computed BDE of 31.22 kcal/mol for the P-C bond in **53** lies halfway between that of the above mentioned carbodiimide-to-phosphinidene- complex (18.65 kcal/mol, see chapter 4.4.2.1) and the strong P-C bond (50.71 kcal/mol) in the recently reported NHC-to-phosphinidene adduct (NHC = 1,3-dimethyl-imidazole-2-ylidene).[163] Frequency calculation in **53** shows the expected uncorrected vibration of the C-N bond at 2258.0 cm^{-1}, together with five coupled stretching modes for the carbonyl groups at 2117.5, 2025.4, 1982.3, 1973.8 and 1966.6 cm^{-1}, in reasonable agreement with the experimentally observed absorption bands.

4.4.3. Chalcogen atom insertion reactions into the endo P–C bond

In order to test further the reactivity of the 3-imino-azaphosphiridine ligands and examine their ability and utility in forming new heterocyclic structures, chalcogen (i.e. sulfur and selenium) atom insertions were targeted.

4.4.3.1. Sulfur insertion

Complex **21a** was reacted with sulfur in toluene. Here, a formal insertion of a sulfur atom into the P-C ring bond was observed, thus forming 1,2,3-thiazaphosphetidine complex **54** that displays a $^{31}P\{^{1}H\}$ NMR resonance of 122.6 ppm ($^{1}J_{W,P}$ = 280.5 Hz) ($CDCl_3$); 10 % of an unidentified compound ($\delta\,^{31}P$ = 96.6) was observed too (Scheme 4.4.3.1.1). Complex **54** was isolated and completely characterized and its molecular structure was confirmed by X-ray analysis (Figure 4.4.3.1.1). The ^{13}C NMR resonance of the imino carbon atom was found in the expected range at 139.1 ppm having a small $^{2+2}J_{P,C}$ coupling constant of 6.8 Hz. An unligated 1,2,3-thiazaphosphetidine derivative, synthesized *via* reaction of an *P*-amino iminophosphane derivative and carbon disulfide,[164] reported by Niecke in 1986, showed a ^{31}P NMR resonance of 100.9 ppm.

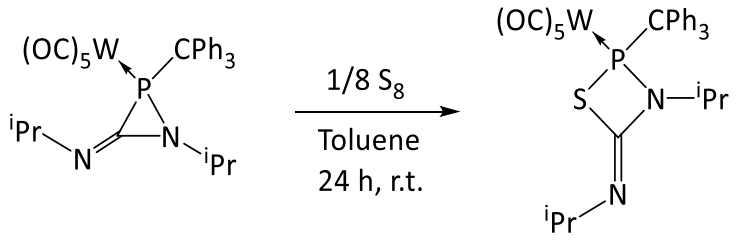

21a **54**

Scheme 4.4.3.1.1**.** Reaction of **21a** with sulfur to form 1,3,2-thiazaphosphetidine complex **54**.

The X-ray crystallographic analysis showed that **54** crystallized in a triclinic crystal system and a $P\bar{1}$ space group revealing a planar structure of the four-membered ring with a small folding angle between the planes defined by the N1-C1-S and N1-P-S of 0.6 °. The endocyclic N atom is very slightly pyramidalized as shown by the sum of bond angles of 357.4°. The phosphorus-sulfur bond length of 2.132(3) Å, was found to be in the expected range for a P–S single bonds, as in **XC** (d_{P-S} = 2.136(1)[165] or **XCI** (d_{P-S} = 2.1348(13)[166] and slightly

elongated with respect to literature known P–S single bounds being part of a cyclic structure and in which a phosphorus center is coordinated to pentacarbonyltungsten as in **XCII**.[167]

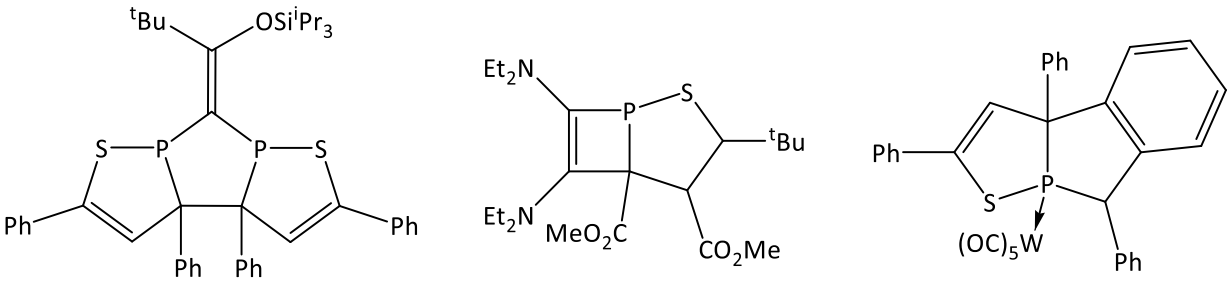

XC[165] **XCI**[166] **XCII**[167]

Scheme 4.4.3.1.2**.** Examples of literature known five-membered ringss having a P-S single bond.

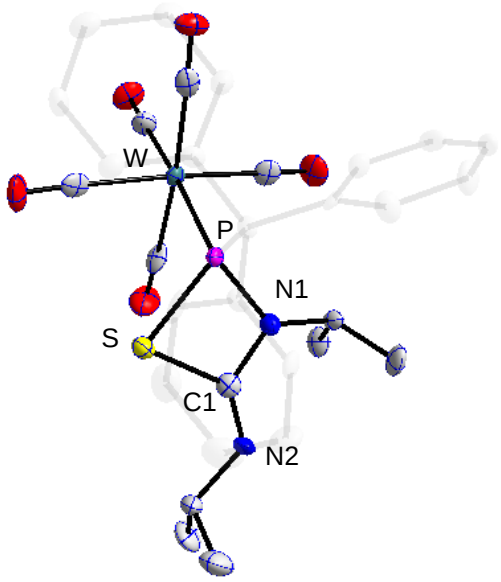

Figure 4.4.3.1.1**.** Molecular structure of 1,3,2-thiazaphosphetidine complex **54**. (50% probability level, hydrogen atoms are omitted and CPh_3 group in grey for clarity). Selected structural parameters (distances [Å] and angles [°]): P-W 2.506(2), P-N(1) 1.707(6), P-S 2.132(3), N(1)-C(1) 1.388(9) C(1)-S 1.841(7), C(1)-N(2) 1.237(10), S-P-N(1) 80.2(2), C(1)-S-P 75.6(3), P-N(1)-C(1) 103.9(4).

Preliminary theoretical studies of Espinosa on the reaction of model 3-imino-azaphosphiridine complex **24** with sulfur leading to 4-imino-1,3,2-thiazaphosphetidine complex **55** were performed. Here, the (likely) intermediacy of the carbodiimide *end-on* adduct to a terminal phosphinidene-sulfide complex **56** was assumed. This intermediate results from direct oxidation of the phosphorus centre to the P-sulfide of the open-chain derivative **46** and quickly cyclizes to give **55** in an exergonic (ΔE_{ZPE} = -18.80 kcal/mol) and almost barrierless process ($\Delta E^{\neq}_{ZPE}$ = 1.70 kcal/mol).

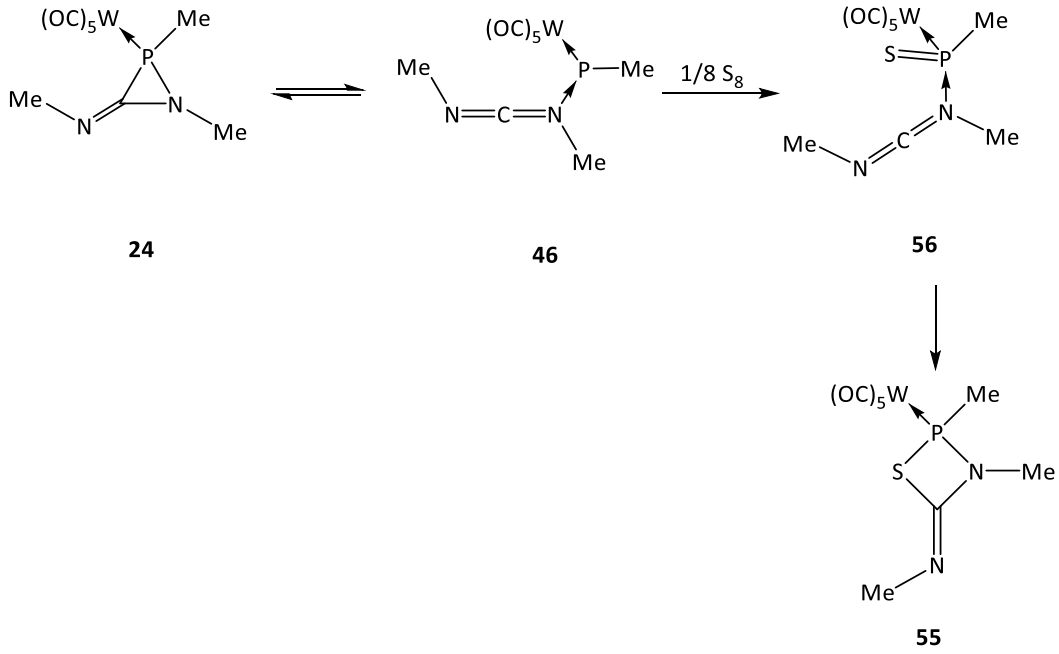

Scheme 4.4.3.1.3. Proposed mechanism for the formation of the model imino-1,3,2-thiazaphosphetidine complex **55**.

4.4.3.2. Selenium insertion

With the purpose to extend this reactivity to other chalcogens, we tried the same experiment with elemental selenium instead of sulfur. Despite many efforts by means of changing reaction conditions, no reaction could be found between elemental selenium and **21a**. At this point, we thought about using compounds that have served effectively as selenium transfer reagents in the past. In this regard, tris(dimethylamino)phosphane selenide[168] (**57**) was reported to transfer a selenium atom onto a distibene to form a selenadistibirane derivative.[169] Reaction of **57** with **21a** in Et_2O led to a mixture in which the main product, having incorporated a selenium atom bound to phosphorus as judged from the ^{31}P NMR spectrum, was rapidly decomposing presumably due to the presence of the liberated

tris(dimethylamino)phosphane. To avoid this, **21a** was reacted with 0.05 eq. of **57** in the presence of 1 eq. of elemental selenium in Et_2O (Scheme 4.4.4.2.1). In this way, the liberated tris(dimethylamino)phosphane reacted with elemental selenium and the newly in *situ* generated **57**, served as selenium atom transfer reagent to give selectively **58** together with 0.05 eq. of **57**. As expected, the $^{31}P\{^1H\}$ NMR resonance of 111.6 ppm ($^1J_{W,P}$ = 275.3 Hz, $^1J_{Se,P}$ = 148.0 Hz) of **58** is slightly highfield-shifted with respect of that of the sulfur derivative **54** ($^{31}P\{^1H\}$ = 122.6 ppm). The compound was isolated and completely characterized and its molecular structure was confirmed by X-ray analysis (Figure 4.4.4.2.1).The ^{13}C NMR resonance of the imino carbon atom of 132.0 ppm ($^{2+2}J_{P,C}$ = 8.5 Hz) was found slightly highfield-shifted compared to its sulfur analogue **54** and displayed a ^{77}Se NMR resonance of 649.2 ppm ($^1J_{Se,P}$ = 148.0 Hz) ($CDCl_3$), lowfield-shifted as compared with the value of 501.0 ppm reported for **XCIV**.[170]

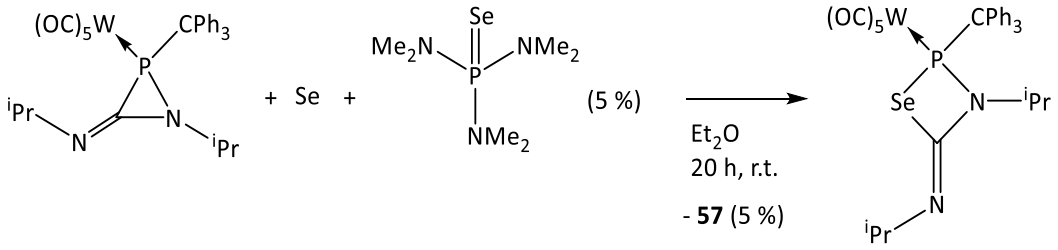

21a **57** **58**

Scheme 4.4.3.2.1. Formation of 1,3,2-selenazaphosphetidine complex **47**.

The X-ray crystallographic analysis (crystal system triclinic, space group $P\bar{1}$) showed, as well as in the case of **54**, a planar ring structure with a small folding angle between the planes defined by the N1-C1-Se and N1-P-Se of 0.5 °. The endocyclic N atom is slightly more pyramidalized than that in **54** with a sum of bond angles at nitrogen of 352.1°. The phosphorus-selenium bond length of 2.2719(6) Å is in the expected range as compared with literature known P-Se single bonds of heterocycles as in **XCIII** (d_{P-Se} = 2.242(3) Å)[171] or **XCIV** (d_{P-Se} = 2.253(2) Å)[170].

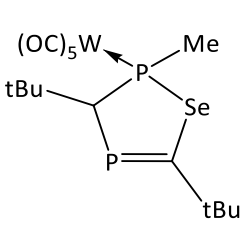

XCIII[171]

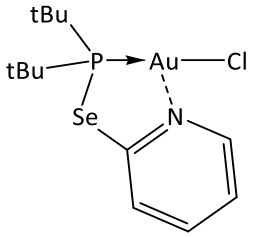

XCIV[170]

Scheme 4.4.3.2.2**.** Examples of literature know compounds having P–Se single bond.

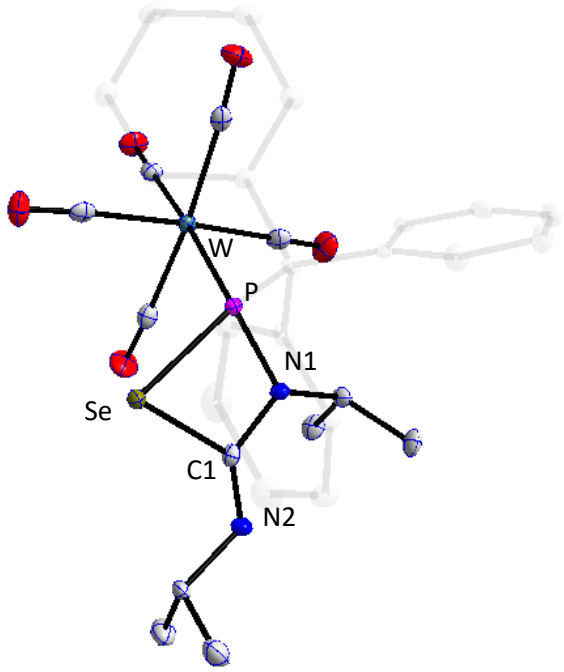

Figure 4.4.3.2.1. Molecular structure of 1,3,2-selenazaphosphetidine complex **58**. (50% probability level, hydrogen atoms are omitted and CPh_3 group in grey for clarity). Selected structural parameters (distances [Å] and angles [°]): P-W 2.5103(5), P-N(1) 1.7125(17), P-Se 2.2719(6), N(1)-C(1) 1.386(3), C(1)-Se 1.987(2), C(1)-N(2) 1.245(3), Se-P-N(1) 81.26(6), C(1)-Se-P 71.27(6), P-N(1)-C(1) 106.60(13).

5. Summary

As a first objective of this PhD work, synthesis of a *P*-Cp* substituted azaphosphiridine complex was attempted. To reach this objective, two routes were explored, namely i) reaction of *P*-Cp* substituted Li/Cl phosphinidenoid complex with a series of carbaldimines and ii) reaction of thermally generated *P*-Cp* substituted transient terminal electrophilic phosphinidene complex with the same substrates. In chapter 3.2 attempts using route i) are described. Reaction of **2** with furan-2-carbaldimine (**3b**) yielded selectively the novel N,P,C-cage complex **4b** which was isolated and completely characterized. The observed selectivity decreased to ca. 60 % when *N*-benzylidenemethylamine (**3a**) was used instead. Reaction of **2** with **3f** yielded **4f** in negligible ammounts only and no sign of **4c,d** was observed in the reaction of **2** and **3c,d**. The bicyclic azaphospholane complex **5** was selectively obtained upon reaction of **2** with thiophen-3-carbaldimine (**3e**).

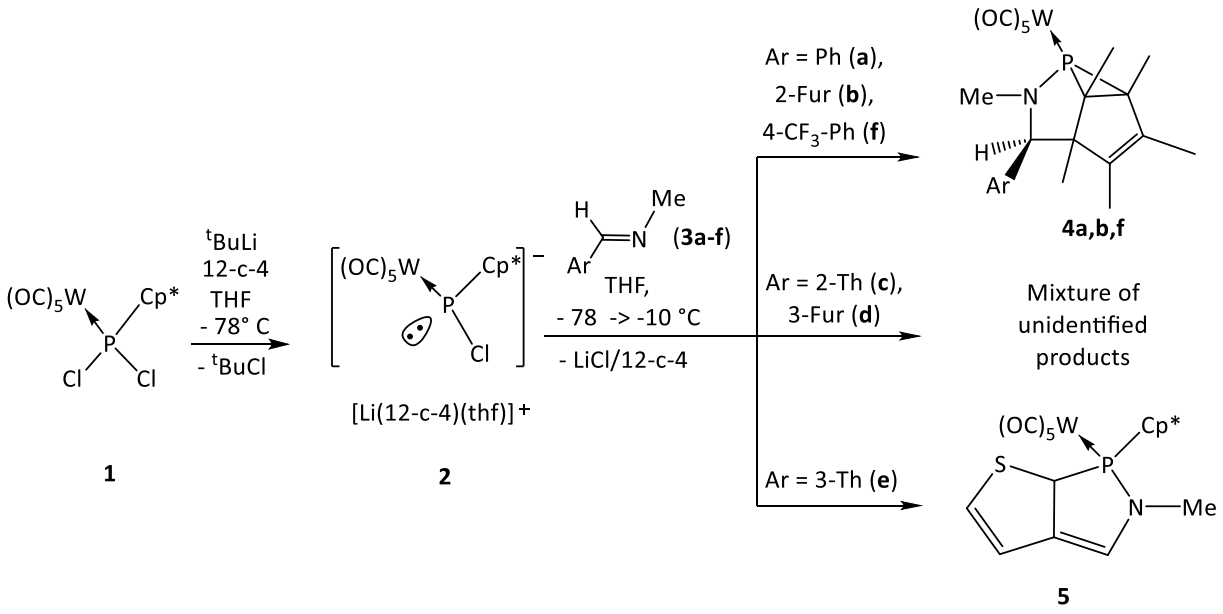

Ar = Phenyl (**a**), 2-furyl (**b**), 2-thienyl (c), 3-furyl (**d**), 3-thienyl (**e**), 4-CF_3-phenyl (**f**)

Scheme 5.1. Reaction of Li/Cl phosphinidenoid complex **2** with carbaldimines **3a-f**.

In order to verify the presence or absence of the expected azaphosphiridine complex as the first intermediate in the formation of the N,P,C-cage complex **4b**, or to be the first product in the reaction of **2** with **3b**, low temperature ^{31}P NMR monitoring (THF) was performed. The experiment revealed the formation of three intermediates which rapidly

transformed into the final product. Two of them were assigned to two stereoisomers of transient azaphosphiridine complexes **7b** and **7b'** and the remaining one to the N,P,C-cage complex **4b'** which isomerizes to **4b**.

DFT calculations (B3LYP-D3/def2-TZVP) performed by Espinosa using a model complex supported the hypothesis that an intermediate iminium phosphane-ylid complex **8g** is initially formed which undergoes thermal aza-phospha-Cope [3,3] sigmatropic rearrangement leading to the phosphinidene complex **9g.** Final addition of the phosphinidene complex to a C=C double bond of the Cp* group would lead to the reaction product **4g** (Figure 3.2.1.3). The relatively low energy of **9g** arises from electron density donation into the formally vacant p orbital of phosphorus, either (i) *directly* from the lone pair of the adjacent N atom and (ii) *through-space* (non-covalent interactions) from two different electron sources, namely the O atom of the 2-furyl substituent and a terminal carbon of the Cp* dienic unit.

The intermediacy of the terminal amino phosphinidene comlex **9b** in the formation of **4b** was proven *via* a trapping experiment with phenylacetylene at -30 °C which led to the formation of the N,P,C-cage complex **12**; the latter was also structurally confirmed by X-ray diffraction studies.

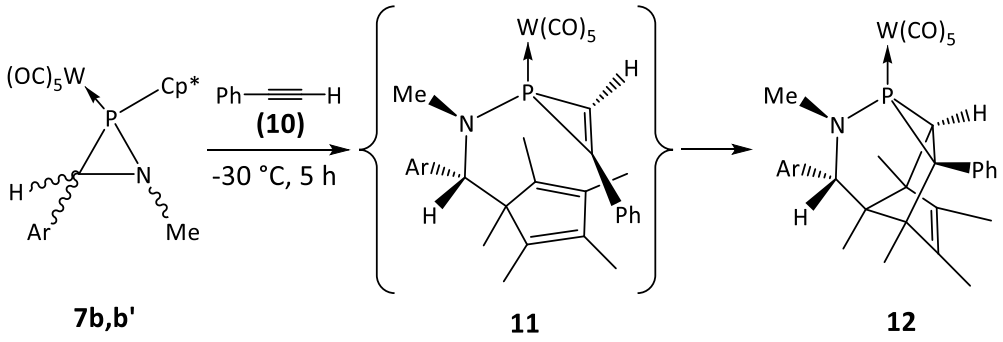

Scheme 5.2. Synthesis of complex **12** (Ar: 2-furyl).

In chapter 3.3 attempts to synthesize *P*-Cp* azaphosphiridine complex using route ii) are described. When *P*-Cp* substituted electrophilic terminal phosphinidene complex **14** reacted with carbaldimines **3a-f** complexes **4a-f** and **15a-f** were obtained in different ratios, **15** being always the predominant species. From these mixtures, complex **15f** could be isolated and characterized by NMR spectroscopy and X-ray diffraction.

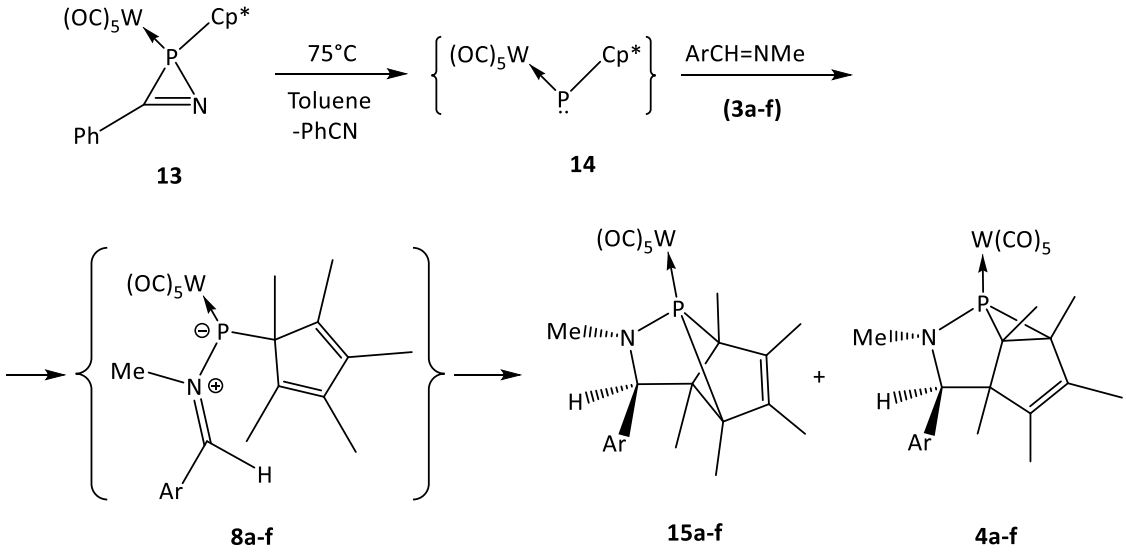

Ar = Ph (**a**), 2-furyl (**b**), 2-thienyl (**c**), 3-furyl (**d**), 3-thienyl (**e**), 4-CF_3-Ph (**f**)

Scheme 5.3. Synthesis of complexes **15a-f** and **4a-f**.

Interestingly, it was found that both polycyclic ligands interconvert rapidly and to a certain extent at room temperature. The rearrangement is explained as a dynamic process in which transient terminal phosphinidene complexes **9a-f** are generated, serving as common intermediates for both interconversions (**4a-f** ↔ **15a-f**). On the basis of DFT calculations, performed by Espinosa, complexes **9** get stabilized by through-bond ($p_N \rightarrow p_P$) and through-space non-covalent interactions.

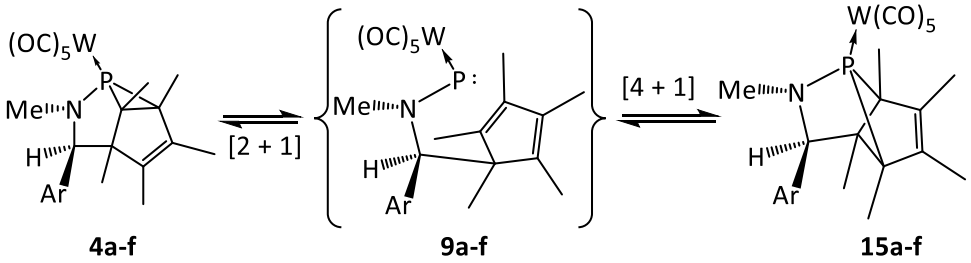

Ar = Ph (**a**), 2-furyl (**b**), 2-thienyl (**c**), 3-furyl (**d**), 3-thienyl (**e**), 4-CF_3-Ph (**f**)

Scheme 5.4. Equilibrium between **4a-f** and **15a-f** *via* proposed intermediates **9a-f**.

To obtain proof for the intermediacy of complexes **9a-f** trapping reactions with phenyl acetylene and *N*-benzylidenemethylamine were performed using **4b** and **15f** as starting point. In the first case, an addition of the phosphinidene complex to the triple bond of phenylacetylene occurred, which was followed by an intramollecular Diels-Alder reaction

yielding N,P,C-complexes **12b,b',f,f'**. In the second case, a nucleophilic attack of the nitrogen atom of **3a** to the phosphorus atom of **9b** leading to the iminium phosphane-ylide complex **16**, which upon [3+2] cycloaddition yielded the final product **17** which was characterized by NMR spectroscopy and X-ray diffraction studies.

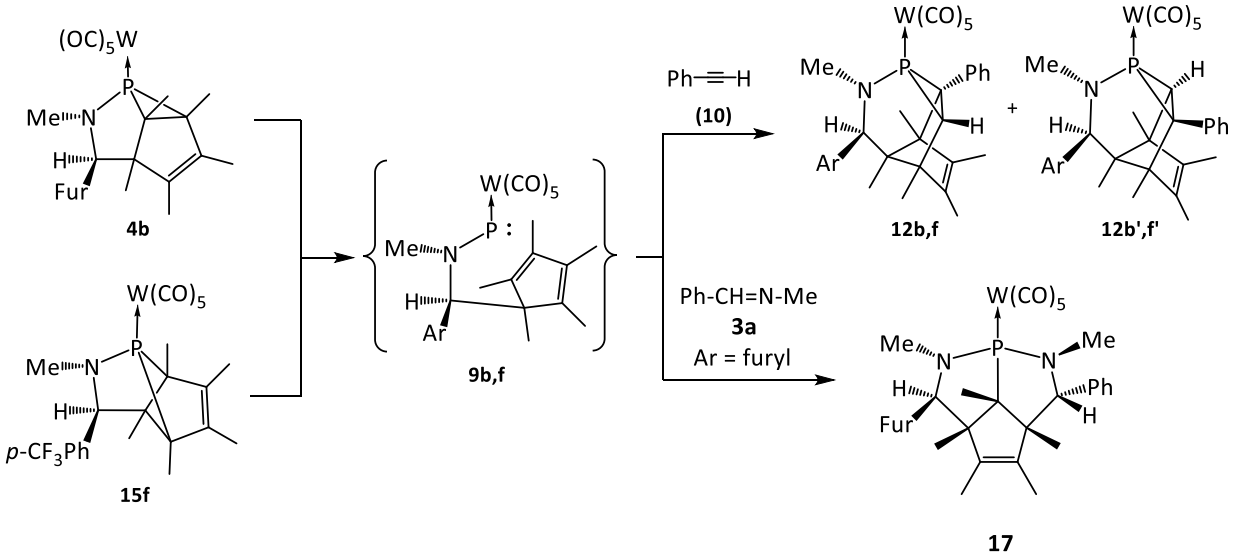

Scheme 5.5. Synthesis of complexes **12b,b',f,f'** (Ar = 2-furyl (b), p-CF_3Ph (f); R,R'' = Ph, H) and **17** (Ar = furyl).

As a second objective of this work, the concept of increasing ring strain via an exocyclic *C*-imino bond in azaphosphiridine complexes was examined. In chapter 4.2 the synthesis of the first examples of 3-imino-azaphosphiridine complexes **21a,b,22a,b** is described. Reaction of Li/Cl phosphinidenoid complexes **2,19** and carbodiimides **20a,b** was again key to success, and low temperature ^{31}P NMR spectroscopic monitoring did not show any evidence for the presence of intermediates (Scheme 5.6).

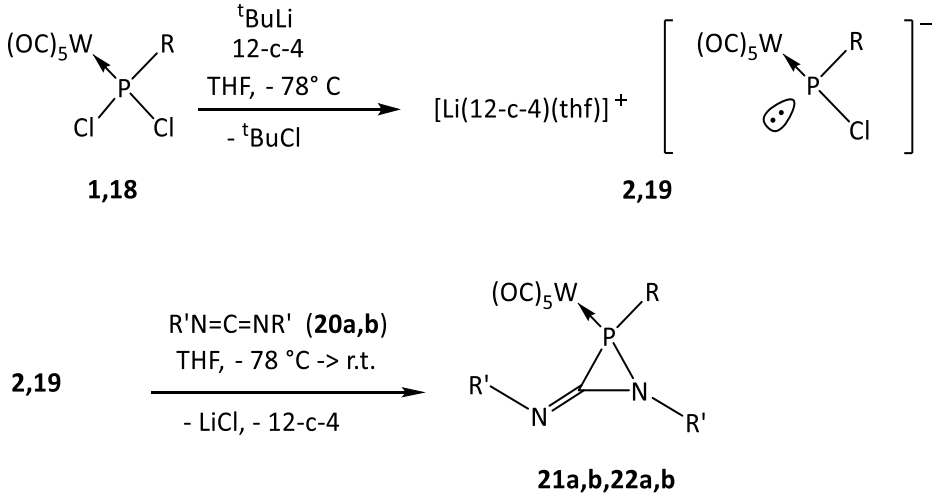

Scheme 5.6. Synthesis of 3-imino-azaphosphiridine complexes **21a,b,22a,b**.

Complexes **21,22** were studied computationally by Espinosa at the DFT level (B3LYP-D3/def2-TZVP). A very important feature of these complexes is their remarkably large ring strain energy (RSE): 50.58 and 52.26 kcal mol^{-1} was computed for both diastereomers **24*Z*** and **24*E***. Due to the large ring strain energy, complexes **21,22** are unstable and highly reactive in solution. For example, **22b** decomposed during low temperature column chromatography (-20 °C, Al_2O_3, petrol ether (40/60) / Et_2O = 70 /30) to give several products, one of which, the zwitterionic bicyclic complex **25,** could be identified by X-ray crystallographic analysis.

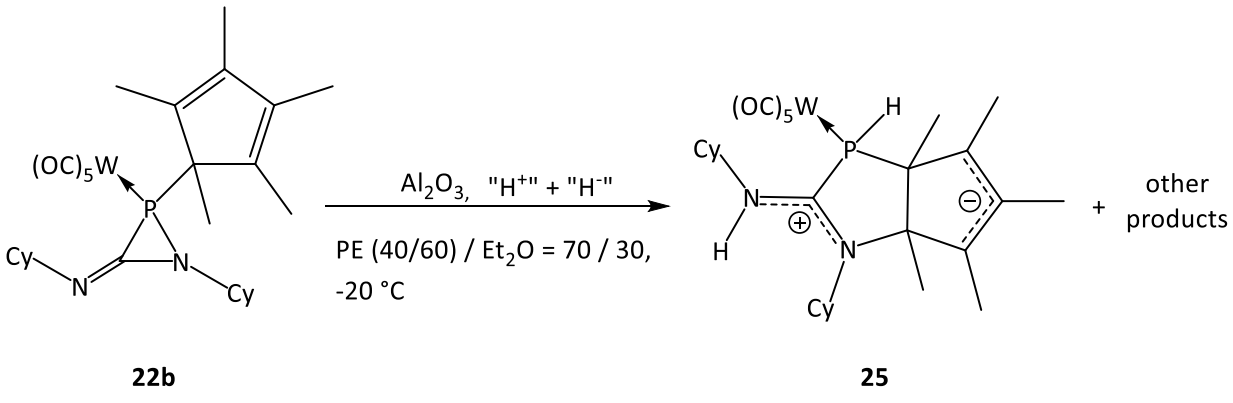

Scheme 5.7. Decomposition reaction of **22b** during column chromatography to form **25** and other products.

In chapter 4.3 studies on the decomposition of 3-imino-azaphosphiridine complexes in solution are presented. Leaving an ethereal (Et_2O or THF) solution of **21a** at ambient temperature for 12 hours, led to the formation of two new products. The nature of **26a** was assigned by comparison with the isolated and characterized product as to be the isonitrile-to-phosphinidene complex adduct **26b**, obtained from the reaction of **21a** with isonitrile **52b** (see chapter 4.4.2.4). The other product resulted formally from a nitrene transfer being inserted into the P-C ring bond of **21a** which was isolated and identified by single-crystal X-ray diffractometry as 1,3,2-diazaphosphetidine complex **27**.

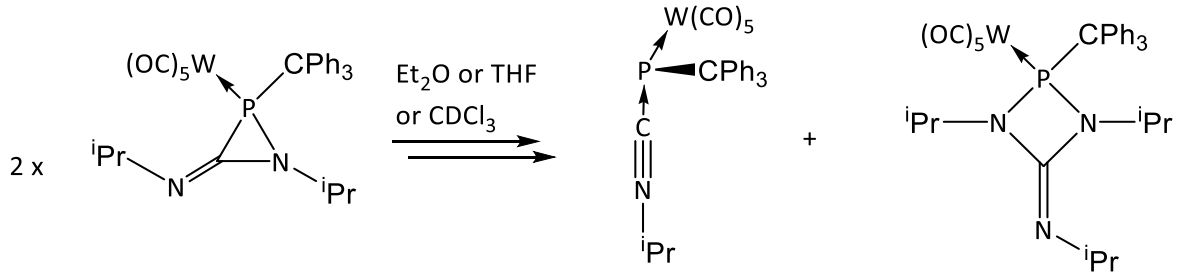

21a **26a** **27**

Scheme 5.8. Decomposition reaction of **21a** in solution to form **26a** and **27**.

In chapter 4.4 three other reactivity aspects of 3-imino-azaphosphiridine complexes are described. In chapter 4.4.1 examples of the reactivity of complexes **21,22** acting as masked frustrated Lewis pairs are presented. Here, initial van der Waals contact of the exocyclic imino nitrogen atom with the substrate led to a ring activation and weakening of the P–N bond seems to be the common starting point for this class of reactions.

Ring opening reaction of **21,22** with water leading to the first valence isomer of an oxaphosphirane complex **28,29** are shown in chapter 4.4.1.1. These complexes **28,29** have a 1,3-zwitterionic P-ligand with a delocalized cationic moiety and a negative charge located at the P-oxygen atom. Alternatively, this can be described as a diaminocarbene-stabilized terminal phosphinidene oxide complex which is further backed by the comparatively low BDE value (53.69 Kcal·mol^{-1}) of this P-C bond.

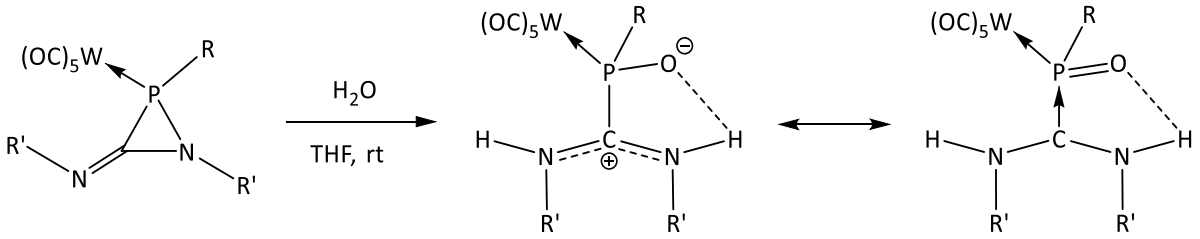

21a,b,22a,b **28a,b,29a,b** **28a,b,29a,b^{can}**

21,28: R = CPh_3; **22,29**: R = Cp*
a: R' = ^{i}Pr; **b**: R' = Cy

Scheme 5.9. Synthesis of **28a,b,29a,b**.

DFT studies ($COSMO_{THF}$/LPNO-NCEPA1/def2-TZVPP//B3LYP-D3/def2-TZVP) performed by Espinosa on the reaction mechanism support that the basic character of the exocyclic N atom in model complex **24** (methyl substituent at P and N atoms) enables the initial [2σ+(2π+2σ)] process corresponding to the formal addition of water across the P–C=N moiety. Rotation of the P–C bond and subsequent O-to-N proton transfer would lead to the final complex **30**. The zwitterionic complex **28a** was reacted with tritylium tetrafluoroborate (**26**) which resulted in a fluoride substitution reaction and the formation of the 1,4-zwitterionic complex **27**.

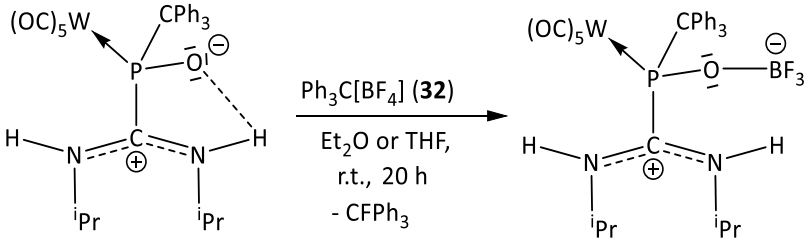

28a **33**

Scheme 5.10. Reaction of **28a** with tritylium tetrafluoroborate to give **33**.

When **21a** reacted with 1 eq. of phenyl isocyanate and **22a** with half eq. of 1,4-phenylene diisocyanate, ring expansion reactions occurred, leading to 1,3,5-oxazaphospholane ligand structures **35** and **38**. Analogously, **21a** reacted with CO_2 and with pentafluorobenzaldehyde to give 1,3,5-oxazaphospholane complexes **39** and **44** (Chapter 4.4.1.2, 4.4.1.3 and 4.4.1.4).

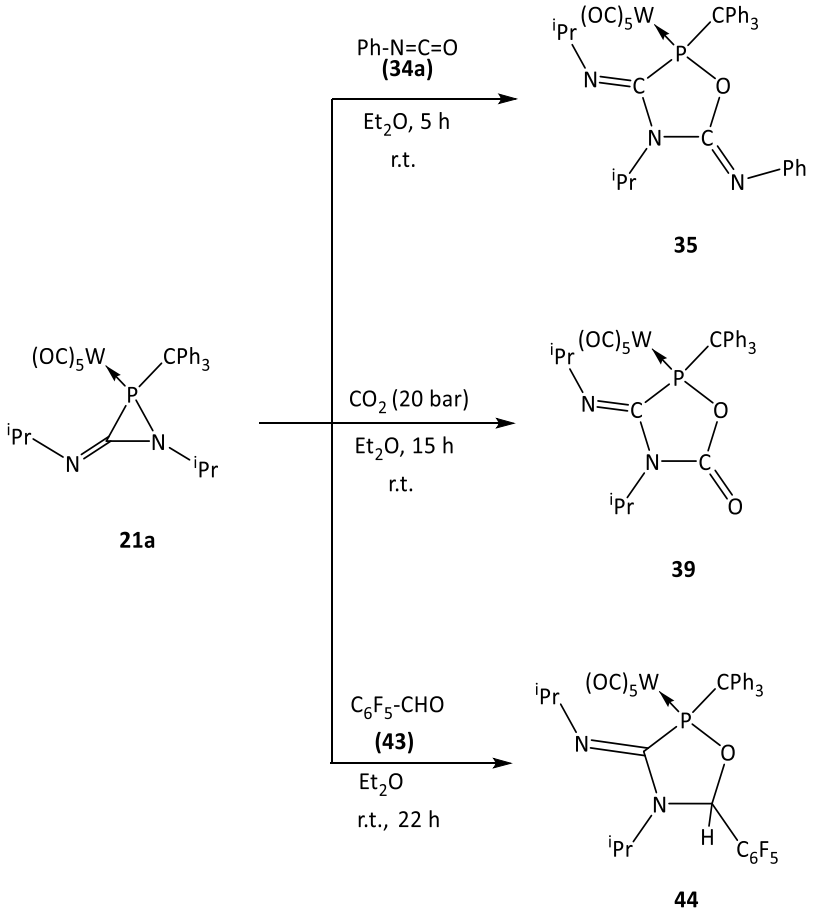

Scheme 5.11. Reactions of **21a** with phenyl isocyanate, carbon dioxide and pentafluoro-benzaldehyde to give 1,3,5-oxazaphospholane complexes **35**, **39** and **44,** respectively.

The reaction mechanism of the reaction of 3-imino-azaphosphiridine complex **21a** with CO_2 was studied computationally by Espinosa ($COSMO_{toluene}$/DLPNO-CCSD(T)/def2-TZVPPecp//$COSMO_{toluene}$/B3LYP-D3/def2-TZVP ecp) using the model comlex **24**. They support an initial nucleophilic atack of the basic exocyclic N atom of **24** to the electrophilic centre of CO_2 leading to **24·CO_2**. Subsequent attack of the negatively charged O atom to phosphorus then forms the model 1,3,5-oxazaphospholane ring **41** (Scheme 4.4.1.3.2, Figure 4.4.1.3.3).

Chapter 4.4.2 describes examples of 3-imino-azaphosphiridine complex **21a** behaving as a terminal phosphinidene complex transfer reagent. In this case, a ligand substitution reaction of the *end-on* carbodiimide N→Pcomplex **51** seems to be the crucial step for this class of reactions.

Reaction of 3-imino-azaphosphiridine complex **21a** with CO, where the carbon atom of CO inserted into the P–N bond leading to 1,3-azaphosphetidinone complex **45** is described in chapter 4.4.2.1.

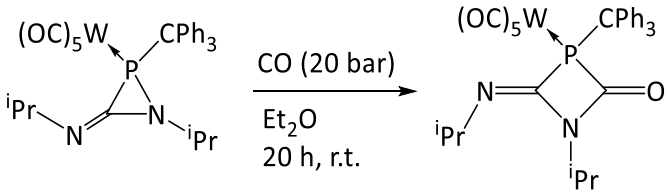

21a **45**

Scheme 5.12. Synthesis of 1,3-azaphosphetidinone complex **45** by reaction of **21a** and CO.

DFT calculations performed by Espinosa ($COSMO_{toluene}$/DLPNO-CCSD(T)/def2-TZVPP(ecp)) ZPE-corrected on the reaction mechanism using model azaphosphiridine complex **24.** Here, the formation of the *end-on* carbodiimide N→Pcomplex **46** is the rate limiting step and initiate the overall process. This is followed by a CO / MeNCNMe ligand exchange reaction *via* the TS **46·CO→20c·e** (Scheme 4.4.2.1.3) leading to phosphaketene complex **47** and carbodiimide **20c**. Subsequent stepwise nucleophilic attack of the carbodiimide nitrogen atom to the carbon atom in **47** and of the phosphorus centre to the carbodiimidium carbon atom in **48** yields final model complex **45**.

Reaction with benzaldehyde (**42**) led to the (known) oxaphosphirane complex **50** (Chapter 4.4.2.2).

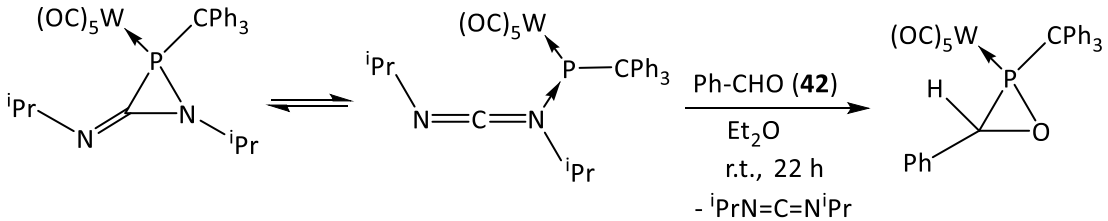

21a **51** **50**

Scheme 5.13. Reaction of 3-imino-azaphosphiridine complex **21a** with benzaldehyde to give oxaphosphirane complex **50.**

In reaction with dicyclohexyl carbodiimide (**20b**), a mixture of **21a** and **21b** (ratio 1:1) was obtained, suggesting again that a substitution reaction had occurred in which the

diisopropyl carbodiimide moiety in **21a** was exchanged by the dicyclohexyl carbodiimide to form **21b** (Chapter 4.4.2.3).

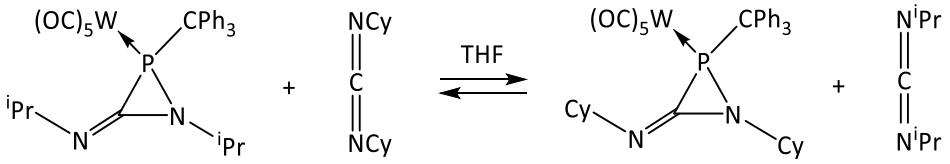

21a **20b** **21b** **20a**

Scheme 5.14. Carbodiimide exchange reactions between 3-imino-azaphosphiridine complexes **21a** and **21b**.

The nature of the newly formed product as **21b** was confirmed additionally through formation of a 1:1 mixture of their hydrolysis products **28a,b** upon reaction of **21a,b** with H_2O.

In chapter 4.4.2.4 reaction of 3-imino-azaphosphiridine complex **21a** with isocyanides **52b,c** is described. Here, in contrast to the previously observed reaction of **21a** with CO, isonitrile-to-phosphinidene complex adducts **26b,c** were obtained selectively.

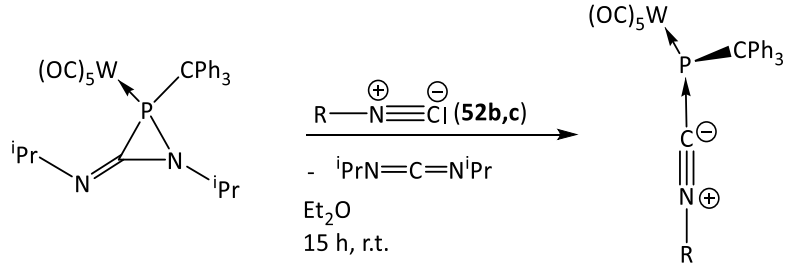

21a **26b,c**

R = ^{t}Bu (**b**), ^{n}Bu (**c**)

Scheme 5.15. Reaction of 3-imino-azaphosphiridine complex **21a** with isonitriles **52b,c** to give isonitrile-to-phosphinidene complex adducts **26b,c**.

Chapter 4.4.3 decribes P-C ring bond chalcogen insertion reactions of 3-imino-azaphosphiridine complex **21a**. In case of sulfur, the reaction of **21a** yielded 1,2,3-

thiazaphosphetidine complex **54** almost selectively. In contrast, reaction of **21a** with selenium afforded no reaction, but sub-stoichiometric amounts of an *in situ* generated selenium transfer reagent such as tris(dimethylamino)phosphane *P*-selenide yielded selectively 1,3,2-selenazaphosphetidine complex **58**.

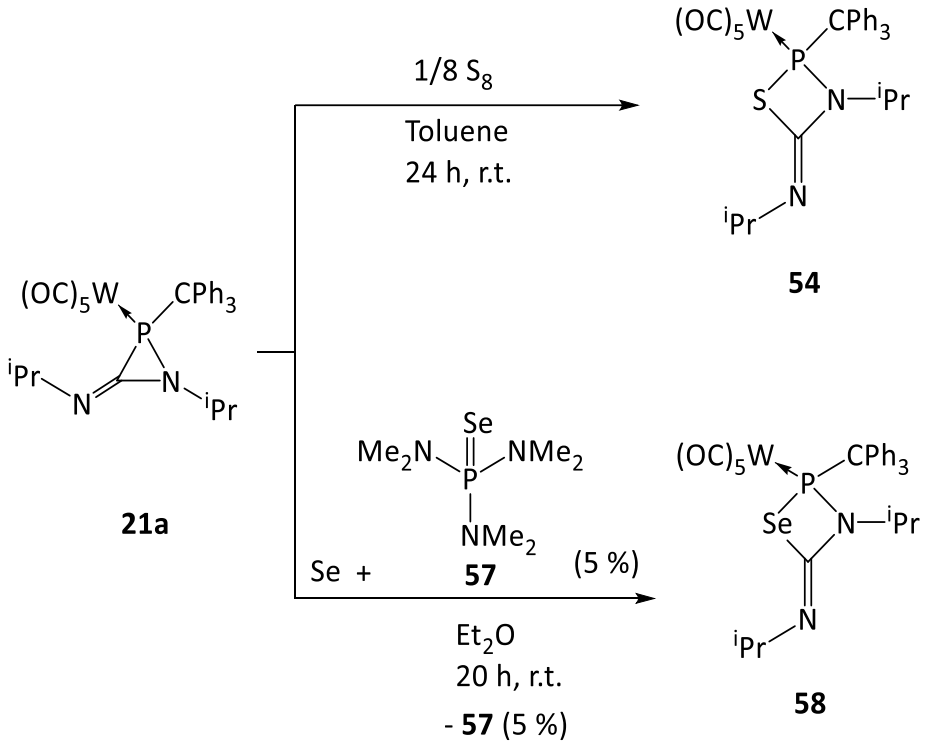

Scheme 5.16**.** Sulfur and selenium insertion into te iminoazaphosphiridine ligand P–C bond to form 1,3,2-thiazaphosphetidine complex **54** and 1,3,2-selenazaphosphetidine complex **58** respectively.

6. Experimental part

6.1. General procedures

All operations were performed in an atmosphere of deoxygenated and dried argon (BTS catalyst (Merck) heated at 100 to 130 °C, phosphorus pentoxide, and silica gel) using standard Schlenk techniques or glove-box with conventional glassware, which was evacuated, heated in vacuo, and filled with inert gas before usage. Solvents (petrol ether (40/60)) were dried over sodium, sodium/benzophenone (THF and diethyl ether) or calcium hydride (dichloromethane) according to procedures described in the literature[172] and stored in brown-glass bottles under inert atmosphere over sodium wire or molecular sieves. Deuterated solvents (cloroform-*d*3, benzende-*d*6, THF-*d*8, and toluene-*d*8) were stored under inert atmosphere over molecular sieves. High temperature reactions were carried out in an oil bath. In the case of low temperature reactions, ethanol and liquid nitrogen were employed as coolant. Cannulas with whatman glass microfiber filters (GF/B, d = 25 mm) connected to one end with Teflon band were used for filtrations with pressure gradient of the argon gas. Most products were purified by low-temperature column chromatography using chromatographic columns equipped with integrated cooling mantles cooled with a connected cryostat (cooling medium: ethanol, technical grade); in most cases retention factors were previously estimated by thin layer chromatography. In the description of experimental procedures the applied temperatures, the column dimensions (length × diameter), the solvent mixtures that were used as eluents, and the materials of the employed stationary phase are specified (i.e., silica gel 60, 60-200 mesh (Merck) or neutral aluminum oxide (Merck)).

6.1.1. Analytical methods

Melting points (or decomposition temperatures) were determined with a Büchi apparatus Type S; the values are not corrected.

NMR data were recorded on a Bruker Advance 300 spectrometer (^{1}H: 300.13 MHz; ^{13}C: 75.5 MHz; ^{19}F: 282.4 MHz; ^{31}P: 121.5 MHz) or a Bruker Avance 400 spectrometer (1H: 400.13 MHz; ^{13}C: 100.6 MHz; ^{31}P: 161.9 MHz) at room temperature (if not otherwise denoted) using C_6D_6, $CDCl_3$, CD_2Cl_2, toluene-d_8 or THF-d_8 as solvent and internal secondary standard; chemical shifts (δ) are referenced to external standards: tetramethylsilane (^{1}H, ^{13}C), trichlorofluoromethane (^{19}F), boron trifluoride diethyl etherate in $CDCl_3$ (^{11}B) and 85% H_3PO_4 (^{31}P). The assignment of NMR signals was supported by ^{1}H gsCOSY as well as ^{1}H detected, pfg-selected 2D ^{1}H,X (X = ^{13}C,

^{31}P) gsHSQC, gsHMQC, or gsHMBC measurements, ^{31}P{^{1}H} NMR (and in some cases ^{1}H NMR) spectroscopic reaction monitoring was carried out to follow reaction progressions, and signal integration was used to estimate product shares (%) of reaction mixtures. Magnitudes of coupling constants are abbreviated as $^{x}J_{A,B}$, where A and B denote the coupling nuclei (nuclear number omitted; ordered by decreasing atomic number), and x denotes the number of bonds that separate A and B (for further abbreviations see Appendix A); only absolute values were determined.

EI-Mass spectra were recorded on aMAT 95 XL Finnigan (70 eV) spectrometer. ESI-mass spectra (positive mode) and ESI tandem mass spectra were recorded on a Bruker APEX IV Fourier transform ion cyclotron resonance (FT-ICR) mass spectrometer equipped with an Apollo ESI source (selected data given).

Elemental analyses were performed using an elementary vario EL analytical gas chromatograph. The mean valuesof two or three independent measurements are given in each case.

IR spectra were recorded on a Thermo Nicolet 380 FT-IR spectrometer using KBr for samples preparation or on a ATR diamond plate.

Reflection data for the X-ray crystallographic analysis were on a STOE IPDS-2T diffractometer (STOE&Cie GmbH, Darmstadt, Germany), using graphite monochromated Mo-K_α radiation (λ = 0.71073 Å). The diffractometer was equipped with a low-temperature device (Cryostream 700er series, Oxford Cryosystems, 123K). Intensities were measured by fine-slicing ω-scans at different ϕ-angels and corrected for background, polarization and Lorentz effects or collected at the BL38B1 beamline of the SPring-8 (JASRI, 2014B1556) using Rayonix/MX225HE CCD detector and Si(111)-monochromated X-ray radiation (λ = 0.80000 Å). The structures were solved by Patterson methods or Direct Methods (SHELXS-97) and refined by full-matrix least squares on F^2 (SHELXL-97). All non-hydrogens were refined anisotropically. Hydrogen atoms were included isotropically using the riding model on the bound atoms; in some (denoted) cases hydrogen atoms were located in the Fourier difference electron density. Absorption corrections were carried out analytically or semi-empirically from equivalents. Additionally, some calculation of bond lengths and angles were obtained using the Ortep32 program.

6.1.2. Purchased reagents and solvents

The following reagents and solvents were purchased and in some cases purified before usage: Acetic acid (Merck); acetone (Biesterfeld); acetonitrile (Merck); [D3]acetonitrile (Euriso-Top); aluminum oxide neutral (Merck); ammonia (PraxAir); benyaldehzde (Aldrich); [D6]benzene (Euriso-Top); *N*-benzylidenemethylamine (Aldrich); *N*-(4-trifluoromethzl)benzylidenemethylamine (Aldrich); benzonitrile (Merck); 1,2-bis(diphenylphosphino)ethane (Aldrich); n-butyllithium, 1.6 M in n-hexane, (Aldrich); tert-butyllithium, 1.7 M in n-pentane (Aldrich); iso-butyl isocyanide (Acros); tert-butyl isocyanide (Acros), calcium chloride (KMF); calcium hydride (Acros); carbon dioxide (Air Liquide); carbon monoxide (Air Liquide); [D]chloroform (Merck); chromium hexacarbonyl (Acros); 12-crown-4 (Acros); cyclohexyl isocyanide (Merck); dichloromethane (Biesterfeld); [D2]dichloromethane (Euriso-Top); dicyclohexylcarbodiimide (Fluka), diethyl ether (Prolabo); ethanol, technical grade (Hofmann); diisopropylcarbodiimide (Aldrich), ferrocene (Acros); furan-2-carbaldehyde (Acros); furan-3-carbaldehyde (Acros); hexamethyphosphorustriamide (Alfa Aesar); hydrochloric acid 37 % (Riedel-de Haën); magnesium sulfate (Riedel-de Haën); mineral oil (Fluka); molecular sieves 3 and 4 Å (Merck); molybdenum hexacarbonyl (Acros); n-pentane (Grüssing); naphtalene (Alfa Aesar); pentafluorobenzaldehyde (Aldrich); petroleum ether 40/60 (Biesterfeld); phenyl acetylene (Alfa Aesar); phenyl isocyanate (Acros); phosphorus pentoxide (Riedel-de Haën); phosphorus trichloride (Aldrich); selenium powder (Alfa Aesar); silica gel 60, 60-200 mesh (Merck); silica gel silanized 60, 60-200 mesh (Merck); sodium (Riedel-de Haën); Sodium hyposphosphite (Aldrich), sodium hydroxide (Grüssing), stirene (acros); sulfur (KMF); sulfuric acid, 98% (Merck); tetrabutylammonium fluoride (Acros); tetrabutylammonium hexafluorophosphate (Fluka); tetrabutylammonium tetraphenylborate (Aldrich); tetrahydrofuran (Aldrich); thiophen-2-carbaldehyde (Aldrich); thiophen-3-carbaldehyde (Aldrich); tris(4-bromophenyl)ammoniumyl hexachloroantimonate (Aldrich); 4-(trifluoromethyl)benzaldehyde (Aldrich); toluene (Acros); triphenylmethanol (Aldrich); tungsten hexacarbonyl (Acros).

6.1.3. Reactants synthesized according to published procedures

- [Amino(phenyl)carbene]pentacarbonyltungsten(0) [173]
- [2-(1,2,3,4,5-Pentamethylcyclopenta-2,4-dien-1-yl)-3-phenyl-2*H*-azaphosphirene-κP]pentacarbonyltungsten(0) [86]

- Dichloro(1,2,3,4,5-pentamethylcyclopenta-2,4-dien-1-yl)phosphan[119]
- [Dichloro(1,2,3,4,5-pentamethylcyclopenta-2,4-dien-1-yl)phosphan-κP]pentacarbonyltungsten(0)[77]
- Dichloro(triphenylmethyl)phosphan[174]
- [Dichloro(triphenylmethyl)phosphan-κP]pentacarbonyltungsten(0)[40]
- Acetonitrilpentacarbonyltungsten(0)[175]
- *N*-[(thiophen-2-yl)methylen]methanamin[88,89]
- *N*-[(thiophen-3-yl)methylen]methanamin[88,89]
- *N*-[(furane-2-yl)methylen]methanamin[88,89]
- *N*-[(furane-2-yl)methylen]methanamin[88,89]
- 4-trifluoromethyl *N*-benzylidenemethylamine[88,89]

6.1.4. Working procedure and chemical waste

The working with the chemicals was accomplished using fume hoods and/or a glove box according to the valid legislation (in agreement with the dangerous material regulation). All work resulting in this sense took place in appropriate protective clothing available in the laboratory. The already used solvents were collected in the canisters and properly removed according to the institutes waste disposal policy. The used silica gel was likewise supplied to the solid wastes.

6.2. Reaction of *P*-Cp* substituted Li/Cl phosphinidenoid complex 2 with aldimines 3a-f

6.2.1. General procedure for the reaction of Li/Cl phosphinidenoid complex with aldimines

To a THF solution of dichlorophosphane tungsten complex **1** and 1 eq. of 12-crown-4, 1.1 eq. of *tert*-butyl lithium (1.5 M in *n*-hexane) were slowly added at -78 ℃. After 15 min. 1.5 eq. of the corresponding aldimine (**3a-f**) was slowly added at -78 °C. The reaction mixtures were then allowed to warm up slowly to room temperature.

6.2.2. Synthesis of pentacarbonyl[6-(furan-2-yl)-2,3,4,5,7,8-hexamethyl-7-aza-1-phosphatricyclo[3.2.1.$0^{2,8}$]oct-3-ene-κP]tungsten(0) complex (4b)

To a solution of 506 mg (0.9 mmol) of dichlorophosphane complex **1** and 156 mg (1 eq.) of 12-crown-4, dissolved in THF, 1.1 eq. of *tert.*-butyl lithium (1.5 M in *n*-hexane) were slowly added at -78 ℃. After 15 min. 145 mg (1.5 eq.) of furan-2-carbaldimine (**3b**) was slowly added at -78

°C. The reaction mixture was warmed up slowly to room temperature. Lithium chloride was filtrated via filter paper (Schleicher & Schuell S&S 598) and evaporation of all volatile components (ca. 10^{-2} mbar); the residue was subjected to column chromatography (h = 8 cm, d = 3 cm, silica gel, -20 °C, petroleum ether / Et_2O: 5 / 1) and the product, a light yellow solid, was obtained via subsequent crystallization from Et_2O at -70°C.

Yield: 380 mg (0.63 mmol, 70 %); m. p. = 104 – 105 °C. ^{1}H NMR (C_6D_6): δ = 0.62 (s, 3H, C^1-CH_3), 1.03 (d, 3H, $^3J_{P,H}$ = 17.4 Hz, P-C^3-CH_3), 1.27 (d, 3H, $^3J_{P,H}$ = 16.3 Hz, P-C^2-CH_3), 1.32 (dq, 3H, $^5J_{H,H}$ = 1.0 Hz, $^4J_{P,H}$ = 4.5 Hz, CH_3-C^4=C^5), 1.45 (dq, 3H, $^5J_{H,H}$ = 1.0 Hz, $^5J_{P,H}$ = 1.8 Hz, CH_3-C^5=C^4), 2.27 (d, 3H, $^3J_{P,H}$ = 11.2 Hz, N-CH_3), 3.64 (d, 1H, $^3J_{P,H}$ = 12.2 Hz, N-C*H*-Fu), 5.92 (dd, 1H, $^3J_{H3,H2}$ = 3.2 Hz, $^4J_{H3,H1}$ = 0.8 Hz, Fu*H*^{3}), 6.03 (dd, 1H, $^3J_{H2,H3}$ = 3.2 Hz, $^3J_{H2,H1}$ = 1.9 Hz, Fu*H*^{2}), 7.15 (dd, 1H, $^3J_{H1,H2}$ = 1.9 Hz, $^4J_{H1,H3}$ = 0.8 Hz, Fu*H*^{1}). ^{13}C{^{1}H} NMR (C_6D_6): δ = 10.6 (d, $^3J_{C,P}$ = 1.9 Hz, P-C^1-*C*H$_3$), 10.83 (d, $^1J_{C,P}$ = 1.8 Hz, P-C^2-*C*H$_3$), 12.05 (s, P-C^5-*C*H$_3$), 14.12 (d, $^1J_{C,P}$ = 9.3 Hz, P-C^3-*C*H$_3$), 15.31 (d, $^3J_{C,P}$ = 2.8 Hz, P-C^4-*C*H$_3$), 35.12 (d, $^2J_{C,P}$ = 8.2 Hz, N-*C*H$_3$), 46.37 (s, *C*^{1}), 59.10 (d, $^1J_{C,P}$ = 32.0 Hz, *C*^{3}), 65.93 (d, $^1J_{C,P}$ = 2.7 Hz, *C*^{3}), 78.00 (d, $^2J_{C,P}$ = 1.8, Fu-*C*H-N), 107.70 (s, *C*^{3}Fu), 109.57 (s, *C*^{2}Fu), 131.03 (d, $^3J_{C,P}$ = 4.8 Hz, -*C*^{3}=C), 134.93 (d, $^2J_{C,P}$ = 9.3 Hz, -C=*C*^{2}), 141.96 (s, -*C*^{1}Fu), 153.40 (s, *C*^{4}Fu), 195.63 (dSat, $^2J_{P,C}$ = 8.3 Hz, $^1J_{W,C}$ = 125.7, *cis-C*O), 198.00 (d, $^2J_{P,C}$ = 32.1 Hz). ^{31}P{^{1}H} NMR (C_6D_6): -34,1 ppm, $^1J_{W,P}$ = 272.8 Hz. MS (EI, 70 eV, ^{184}W): *m/z* (%): MS (EI, ^{184}W): m/z (%): 599.1 [M]$^+$ (40); 543.1 [M-2xCO]$^+$ (5); 459.1 [M-5xCO]$^+$ (10); 444.1 [M-5xCO-Me]$^+$ (10); 406.0 [M-4CO-Me-C_4H_3O]$^+$ (100); 378.0 [M-5xCO-Me-C_4H_3O]$^+$ (40). IR (KBr): ũ = 2967 (b, ν-CH), 2725 (b, ν-CH), 2072 (s, ν-CO), 1944, (s, ν-CO), 1462 (s, ν-C-C/Ar) cm^{-1}.

Elemental analysis (%) for $C_{21}H_{22}NO_6PW$ calcd.: C 42.09, H 3.70, N 2.34; found: C 42.09, H3.77, N 2.30.

6.3. Synthesis pentacarbonyl[5-(furan-2-yl)-1,4,6,7,8,9-hexamethyl-2-phenyl-4-aza-3-phosphatetracyclo[4.3.0.1^{3,9}.0^{2,10}]dec-8-ene-κP]tungsten(0) complex (12b) (route a)

To a solution of 580 mg (1.03 mmol) of dichlorophosphane complex **1** and 179 mg (1 eq.) of 12-crown-4, dissolved in 20 mL THF, 1.1 eq. of *tert.*-butyl lithium (1.5 M in *n*-hexane) were slowly added at -78 °C. After 15 min. 113 mg (1 eq.) of furan-2-carbaldimine (**3b**) was slowly added at -78 °C. The reaction mixture was warmed slowly until -30 °C. Around 75 % of the solvent was removed under *vacuo* and 10 mL phenyl acetylene was added at -30 °C. The reaction mixture was stirred between -30 and -20 °C during 5 hours. The excess of phenyl

acetylene and the remaining solvent was removed under *vacuo* (ca. 10^{-2} mbar) and the product was purified by column chromatography (SiO_2, d = 3 cm, h = 6 cm, pure petrol ether (40/60)) and then crystallized from a mixture of *n*-pentane and diethyl ether (3/1) at -60 °C. A white solid was thus obtained.

Yield: 430 mg (0.62 mmol, 60 %); m. p. = 151 – 152 °C. ^{1}H NMR(C_6D_6): δ = 0.73 (s, 3H, C-C*H*$_3$), 0.85 (quint, 3H, $^{5}J_{H,H}$ = 1.33 Hz + $^{5}J_{P,H}$ = 1.33 Hz, C=C-C*H*$_3$), 1.00 (s, 3H, Fu-CH-C-C*H*$_3$), 1.19 (s, 3H, C-C*H*$_3$), 1.36 (q, 3H, $^{5}J_{H,H}$ = 1.33 Hz, C=C-C*H*$_3$), 1.99 (d, 1H, $^{2}J_{P,H}$ = 13.11 Hz, P-C*H*), 2.51 (d, 3H, $^{3}J_{P,H}$ = 14.70 Hz, N-C*H*$_3$), 3.7 (d, 1H, $^{4}J_{H,H}$ = 0.8 Hz, Fu-C*H*-N), 6.00 (dd, 1H, $^{3}J_{H2,H3}$ = 3.24 Hz, $^{4}J_{H2,H1}$ = 1.85 Hz, Fu*H*^{2}), 6.1 (dt, 1H, $^{3}J_{H3,H2}$ = 3.42 Hz, $^{3}J_{H3,H1}$ = 0.8 Hz, $^{4}J_{H3,CH-N}$ = 0.8 Hz, Fu*H*^{3}), 6.97 (dd, 1H, $^{3}J_{H1,H2}$ = 1.85 Hz, $^{4}J_{H1,H3}$ = 0.8 Hz, Fu*H*^{1}), 7.01 (m, 5H, C-*Ph*). ^{13}C{^{1}H} NMR (C_6D_6): δ = 9.7 (s, C^{10}), 10.7 (s, C^{6}), 12.1 (s, *C*^{9}), 12.8 (s, *C*^{7}), 16.8 (s, *C*^{8}), 40.5 (d, $^{2}J_{C,P}$ = 13.8 Hz, N-*C*H$_3$), 43.5 (d, $^{1}J_{C,P}$ = 6.0 Hz, P-*C*H), 52.5 (d, $^{1}J_{C,P}$ = 21.0 Hz, P-*C*-Ph), 55.1 (d, $^{3}J_{C,P}$ = 4.8 Hz, *C*^{1}), 59.1 (d, $^{2}J_{C,P}$ = 2.0 Hz, *C*^{5}), 64.0 (d, $^{2}J_{C,P}$ = 5.1 Hz, N-*C*H), 64.7 (d, $^{2}J_{C,P}$ = 3.1 Hz, *C*^{2}), 109.3 (s, *C*^{3}Fu), 110.5 (s, *C*^{2}Fu), 127.2 (d, $^{3}J_{C,P}$ = 1.5 Hz, *ipso*Ph), 127.6 (s, *p*-Ph), 127.9 (s, *o*-Ph), 128.2 (s, *m*-Ph), 138.3 (d, $^{3}J_{C,P}$ = 4.0 Hz, -*C*=C), 139.2 (d, $^{3}J_{C,P}$ = 4.8 Hz, -C=*C*), 140.1 (d, $^{2}J_{C,P}$ = 6.6 Hz), 141.4 (s, *C*^{1}Fu), 154.1 (d, $^{3}J_{C,P}$ = 4.1 Hz, *C*^{4}Fu), 195.9 (dSat, $^{2}J_{P,C}$ = 8.7 Hz, $^{1}J_{W,C}$ = 125.6, *cis*-*C*O), 198.6 (d, $^{2}J_{P,C}$ = 31.6 Hz, *trans*-*C*O). ^{31}P δ = -3.7 ppm, quintSat, $^{1}J_{W,P}$ = 277.6 Hz, $J_{H,P}$= 14.1 Hz. MS (EI, 70 eV, ^{184}W): *m*/*z* (%): 701.1 [M]$^{+}$ (30); 673.1 [M-CO]$^{+}$ (10); 617.1 [M-3xCO]$^{+}$ (30); 561.1, [M-4xCO]$^{+}$, (30); 534.1 [M-5x CO]$^{+}$ (5). IR (KBr): ũ = 2976 (b, ν-CH), 2073 (s, ν-CO), 1992 (s, ν-CO), 1918 (s, ν-CO),1496 (s, ν-C-C/Ar) cm^{-1}.

Elemental analysis (%): Calcd for $C_{29}H_{28}NO_6PW$: C 49.66, H 4.02, N 2.00, found: C 49.64, H 4.83, N 2.07.

6.4. Formation of complexes 15a–f

6.4.1 General procedure for the formation of complexes 15a–f

To yellow solutions of 2*H*-azaphosphirene pentacarbonyl tungsten complex **13**, 1.5 equivalent of aldimines **3a-f** were added at room temperature. The solutions were then heated at 70 °C during 1.5 hours

6.4.2 Synthesis of pentacarbonyl[7-(4-trifluoromethylphenyl)-2,3,4,5,6,8-hexamethyl-8-aza-1-phosphatricyclo[3,3,0,$0^{2,6}$]oct-3-ene-κP]tungsten(0) complex (15f)

The solvent was removed under *vacuo* (ca. 10^{-2} mbar) and the product recrystallized from diethyl ether at -70 °C to give a pale yellow solid.

Yield: 280 mg (36 %), m.p. 135-134 °C; ^{1}H NMR (C_6D_6) δ = 0.55 (d, 3H, $^{3}J_{P,H}$ = 16.9 Hz, P-C-C*H*$_3$), 0.61 (d, 3H, $^{4}J_{P,H}$ = 1.6 Hz, C-C-C*H*$_3$), 0.66 (d, 3H, $^{3}J_{P,H}$ = 16.1 Hz, P-C-C*H*$_3$), 1.56 (dq, 3H, $^{5}J_{H,H}$ = 1.3 Hz, $^{4}J_{P,H}$ = 2.6 Hz, C*H*$_3$-C=C), 1.63 (dq, 3H, $^{5}J_{H,H}$ = 1.3 Hz, $^{4}J_{P,H}$ = 5.3 Hz, C*H*$_3$-C=C), 2.75 (d, 3H, $^{3}J_{P,H}$ = 9.4 Hz, N-C*H*$_3$), 3.83 (s, 1H, N-C*H*-Ph), 7.15 (d, 1H, $^{3}J_{H,H}$ = 8.2 Hz, *m*-Ph*H*), 7.33 (d, 1H, $^{3}J_{H,H}$ = 8.2 Hz, *o*-Ph*H*). ^{13}C NMR (C_6D_6): δ = 6.8 (d, $J_{C,P}$ = 1.2 Hz, -*C*H$_3$), 8.0 (s, -*C*H$_3$), 10.25 (d, $J_{C,P}$ = 10.7 Hz, -*C*H$_3$), 10.45 (d, $J_{C,P}$ = 1.2 Hz, -*C*H$_3$), 10.69 (d, $J_{C,P}$ = 2.4 Hz, -*C*H$_3$), 34.77 (s, N-*C*H$_3$), 63.39 (d, $^{1}J_{C,P}$ = 33.3 Hz, P-*C*), 66.18(d, $^{1}J_{C,P}$ = 20.1 Hz, P-*C*), 73.04 (s, N-*C*-Ph), 85,08 (s, C-*C*-C), 124.53 (q, $^{1}J_{C,F}$ = 271.8 Hz, Ph-*C*F$_3$), 124.68 (q, $^{3}J_{C,F}$ = 3.6 Hz, *m*-Ph), 128.8 (s, *o*-Ph), 129.3 (q, $^{2}J_{C,F}$ = 32,2 Hz, *p*-Ph), 130.4 (d, $^{2}J_{C,P}$ = 10.1 Hz, *C*=C), 130.9 (d, $^{2}J_{C,P}$ = 10.1 Hz, C=*C*), 141.08 (s, Ph*C*^{1}) 195,3 (dSat, $^{2}J_{P,C}$ = 6.6 Hz, $^{1}J_{W,C}$ = 123.8, *cis*-*C*O), 197.43 (dSat, $^{2}J_{P,C}$ = 27.4 Hz, $^{1}J_{W,C}$ = 143.1, *trans*-*C*O). ^{19}F NMR (C_6D_6): δ = -62.36 (s, C*F*$_3$). ^{31}P{^{1}H} NMR (C_6D_6): δ = 226.8 ppm, $^{1}J_{W,P}$ = 229.8 Hz. MS (EI, ^{184}W) : m/z (%): 677.0 [M]$^+$ (40); 608.0 [M-CF$_3$]$^+$ (10); 580.0 [M-CF$_3$-CO]$^+$ (10); 535.0 [M-CF$_3$-2xCO-Me]$^+$ (10); 490.0 [M-PhCF$_3$-CO-Me]$^+$ (20); 406.0 [M-PhCF$_3$-4xCO-Me]$^+$ (100). IR (KBr pellet): ũ = 2921 (b, ν-CH), 2071 (s, ν-CO), 1983 (s, ν-CO), 1944 (s, ν-CO), 1616 (w, ν-C=C), 1462 (s, ν-C-C/Ar) cm^{-1}. UV/Vis (CH_2Cl_2): λ_{max}/nm 233.5 (ε/dm^3 mol^{-1} cm^{-1} 102 047), 290.0 (10 709).

Elemental analysis (%) Calcd for $C_{24}H_{23}F_3NO_5PW$: C 41.65, H 3.19, N 2.11, found: C 42.29, H 3.53, N 2.07.

6.5. Synthesis pentacarbonyl[5-(furan-2-yl)-1,4,6,7,8,9-hexamethyl-2-phenyl-4-aza-3-phosphatetracyclo[4.3.0.1^{3,9}.0^{2,10}]dec-8-ene-κP]tungsten(0) complex (12b) (route b)

To a THF solution of 935 mg (1.67 mmol) of *P*-Cp*dichlorophosphane tungsten complex **(1)** and 1 eq. of 12-crown-4, 1.1 eq. of *t*-butyl lithium (1.5 M in *n*-hexane) were slowly added at -78 °C. After 15 minutes 1.5 eq. of 2-furyl-*N*-methyl aldimine (**3a**) was slowly added at -78 °C. The reaction mixture was warmed up slowly until room temperature. After 2 h stirring at room temperature, LiCl was filtered off and the solvent was removed in *vacuo* (~10^{-2} mbar). The remaining red oil was dissolved in 6 mL phenyl acetylene and the solution was stirred during

20 h at 90 °C. After completion (^{31}P NMR), the excess of phenyl acetylene was removed in *vacuo* (~10^{-2} mbar) and recovered and a red oil was obtained. **12b,b'** was separated from the crude mixture by column chromatography (SiO_2, d = 3 cm, h = 6 cm, pure petrol ether (40/60)) and **12b** was crystallized from a mixture of n-pentane and diethyl ether (3:1) at -60 °C.
Yield 470 mg (40 %), m.p. = 151-152 °C, ^{1}H NMR (C_6D_6): δ = 0.73 (s, 3H, C-CH_3), 0.85 (quint, 3H, $^{5}J_{H,H}$ = 1.33 Hz + $^{5}J_{P,H}$ = 1.33 Hz, C=C-CH_3), 1.00 (s, 3H, Fu-CH-C-CH_3), 1.19 (s, 3H, C-CH_3), 1.36 (q, 3H, $^{5}J_{H,H}$ = 1.33 Hz, C=C-CH_3), 1.99 (d, 1H, $^{2}J_{P,H}$ = 13.11 Hz, P-C*H*), 2.51 (d, 3H, $^{3}J_{P,H}$ = 14.70 Hz, N-CH_3), 3.7 (d, 1H, $^{4}J_{H,H}$ = 0.8 Hz, Fu-C*H*-N), 6.00 (dd, 1H, $^{3}J_{H2,H3}$ = 3.24 Hz, $^{4}J_{H2,H1}$ = 1.85 Hz, FuH^2), 6.1 (dt, 1H, $^{3}J_{H3,H2}$ = 3.42 Hz, $^{3}J_{H3,H1}$ = 0.8 Hz, $^{4}J_{H3,CH-N}$ = 0.8 Hz, FuH^3), 6.97 (dd, 1H, $^{3}J_{H1,H2}$ = 1.85 Hz, $^{4}J_{H1,H3}$ = 0.8 Hz, FuH^1), 7.01 (m, 5H, C-*Ph*). ^{13}C NMR (C_6D_6): δ = 9.7 (s, C^{10}), 10.7 (s, C^6), 12.1 (s, C^9), 12.8 (s, C^7), 16.8 (s, C^8), 40.5 (d, $^{2}J_{C,P}$ = 13.8 Hz, N-*C*H$_3$), 43.5 (d, $^{1}J_{C,P}$ = 6.0 Hz, P-*C*H), 52.5 (d, $^{1}J_{C,P}$ = 21.0 Hz, P-*C*-Ph), 55.1 (d, $^{3}J_{C,P}$ = 4.8 Hz, C^1), 59.1 (d, $^{2}J_{C,P}$ = 2.0 Hz, C^5), 64.0 (d, $^{2}J_{C,P}$ = 5.1 Hz, N-*C*H), 64.7 (d, $^{2}J_{C,P}$ = 3.1 Hz, C^2), 109.3 (s, C^3Fu), 110.5 (s, C^2Fu), 127.2 (d, $^{3}J_{C,P}$ = 1.5 Hz, ^{ipso}Ph), 127.6 (s, *p*-Ph), 127.9 (s, *o*-Ph), 128.2 (s, *m*-Ph), 138.3 (d, $^{3}J_{C,P}$ = 4.0 Hz, -*C*=C), 139.2 (d, $^{3}J_{C,P}$ = 4.8 Hz, -C=*C*), 140.1 (d, $^{2}J_{C,P}$ = 6.6 Hz), 141.4 (s, C^1Fu), 154.1 (d, $^{3}J_{C,P}$ = 4.1 Hz, C^4Fu), 195.9 (dSat, $^{2}J_{P,C}$ = 8.7 Hz, $^{1}J_{W,C}$ = 125.6, *cis*-*C*O), 198.6 (d, $^{2}J_{P,C}$ = 31.6 Hz, *trans*-*C*O). ^{31}P {^{1}H} NMR (C_6D_6): δ = -3.72 ppm, $^{1}J_{W,P}$ = 278.9 Hz, ^{31}P NMR (C_6D_6): δ = -3.72 ppm (quintSat, $^{1}J_{W,P}$ = 278.9 Hz, $J_{P,H}$ = 14.3 Hz. MS (EI, ^{184}W) : m/z (%): 701.1, $[M]^+$, (30); 673.1 $[M-CO]^+$, (10); 617.1 $[M-3xCO]^+$ (30); 561.1 $[M-4xCO]^+$ (30); 534.1 $[M-5x\ CO]^+$ (5). IR (KBr pellet): ũ = 2976 (b, ν-CH), 2073 (s, ν-CO), 1992 (s, ν-CO), 1918 (s, ν-CO),1496 (s, ν-C-C/Ar) cm^{-1}.

6.6. Synthesis pentacarbonyl[1,4,6,7,8,9-hexamethyl-2-phenyl-5-(4-trifluoromethylphenyl)-4-aza-3-phosphatetracyclo[4.3.0.1^{3,9}.0^{2,10}]dec-8-ene-κP]tungsten(0) complex (12f,f')

20 mg of complex **5f** was dissolved in 0.5 mL of phenyl acetylene and the solution was stirred during 20 h at 90 °C. After completion (^{31}P{^{1}H} NMR) the crude mixture was analysed without further purification. A mixture of **13f** (major isomer, δ ^{31}P = -2.4 ppm, $^{1}J_{WP}$ = 275.2 Hz) and **13f'** (δ ^{31}P = 1.7 ppm, $^{1}J_{WP}$ = 278.3 Hz) in a ratio of 1:2 was obtained.

6.7. Synthesis of pentacarbonyl[3-(furan-2-yl)-2,4,5,6,7,9-hexamethyl-8-phenyl-2,9-diaza-phosphatricyclo[5.2.1.0^{4,10}]dec-5-ene-κP]tungsten(0) complex (17)

490 mg (0.81 mmol) of complex **4b** were dissolved in 5 mL of *N*-benzylidenemethylamine (**3a**) and the yellow solution was stirred during 20 h at 90 °C. When the reaction was completed

($^{31}P\{^1H\}$ NMR), the excess of imine was removed and a yellow oil was obtained. The product, a white solid, was then purified by column chromatography (SiO_2, d = 3 cm, h = 8 cm, -20 °C, petrol ether 40/60) and recrystallized from *n*-pentane at -60 °C.

Yield: 300 mg (50 %), m.p. = 132-133 °C; ^1H NMR (C_6D_6): δ = 0.33 (q, 3H, $^5J_{H,H}$ = 0.84 Hz, C=C-CH_3), 0.67 (s, 3H, C^3-CH_3), 0.87 (s, 3H, C^1-CH_3), 1.24 (q, 3H, $^5J_{H,H}$ = 0.84 Hz, C=C-CH_3), 1.28 (d, 3H, $^3J_{P,H}$ = 21.8 Hz, P-C^2-CH_3), 2.13 (d, 3H, $^3J_{P,H}$ = 10.17 Hz, Ph-CH-N-CH_3), 2.40 (d, 3H, $^3J_{P,H}$ = 13.31 Hz, Fu-CH-N-CH_3), 3.46 (s, 1H, N-C*H*-Ph), 4.58 (d, $^3J_{P,H}$ = 5.63 Hz, 1H, N-C*H*-Fu), 5.93 (dd, 1H, $^3J_{H3,H2}$ = 3.20 Hz, $^4J_{H3,H1}$ = 0.7 Hz, FuH^3), 5.98 (dd, 1H, $^3J_{H2,H3}$ = 3.2 Hz, $^3J_{H2,H1}$ = 1.80 Hz, FuH^2), 6.96 (dd, 1H, $^3J_{H1,H2}$ = 1.8 Hz, $^4J_{H1,H3}$ = 0.7 Hz, FuH^1), 7.01 (m, 5H, N-C-*Ph*).^{13}C NMR (C_6D_6): δ = 10.0 (s, *C*H_3-C-P), 10.1 (s, 10.2), 17.2 (s, C^{10}), 19.9 (s, C^8), 21.3 (s, C^9), 32.50 (d, $^2J_{C,P}$ = 3.2 Hz, Fu-CH-N-*C*H_3), 36.42 (d, $^2J_{C,P}$ = 9.5 Hz, Ph-CH-N-*C*H_3), 60.0 (d, $^1J_{C,P}$ = 39.8 Hz, P-C^1), 60.0 (d, $^2J_{C,P}$ = 1.8 Hz, P-C^5), 62.0 (d, $^2J_{C,P}$ = 2.6 Hz P-C^4), 46.37 (s, C^4), 59.10 (d, $^1J_{C,P}$ = 32.0 Hz, C^1), 65.93 (d, $^1J_{C,P}$ = 2.7 Hz, C^5), 70.68 (d, $^2J_{C,P}$ = 1.8, Fu-*C*H-N), 77.50 (d, $^2J_{C,P}$ = 11.6, Ph-*C*H-N), 109.2 (s, C^3Fu), 109.2 (s, C^2Fu), 126.7 (s, *p*-Ph), 127.1 (s, *o*-Ph), 127.5 (s, *m*-Ph), 132.65 (d, $^3J_{C,P}$ = 3.2 Hz, -C^3=C), 136.76 (d, $^3J_{C,P}$ = 3.2 Hz, -C=C^2), 138.2 (d, $^3J_{C,P}$ = 5.6 Hz, ^{ipso}Ph), 140.7 (s, C^1Fu), 152.05 (d, $^3J_{C,P}$ = 11.95 Hz, C^4Fu), 196.72 (dSat, $^2J_{P,C}$ = 8.3 Hz, $^1J_{W,C}$ = 125.0, *cis*-*C*O), 198.00 (d, $^2J_{P,C}$ = 25.71 Hz, *trans*-*C*O). $^{31}P\{^1H\}$ NMR (C_6D_6): δ = 145.1 ppm, $^1J_{W,P}$ = 286.1 Hz. MS (EI, 184W) : m/z (%): 718.0 $[M]^+$(30); 662.0, $[M\text{-}2xCO]^+$ (30); 599.0 $[M\text{-}PhC(H)NMe]^+$ (100); 578.1 $[M\text{-}5xCO]^+$ (20). IR (KBr pellet): ũ = 2923 (b, ν-CH), 2068 (s, ν-CO), 1980 (s, ν-CO), 1905 (s, ν-CO), 1443 (s, ν-C-C/Ar) cm^{-1}.

Elemental analysis (%) for $C_{29}H_{31}N_2O_6PW$ Calc: C 48.49, H 4.35, N 3.90, found (%): C 49.60 , H 4.86, N 3.68.

6.8. Synthesis of imino azaphosphiridine complexes 21a,b,22a,b

6.8.1. General procedure for the synthesis of imino azaphosphiridine complexes 21a,b,22a,b

To a THF solution of dichloro(pentamethylcyclo-pentadienyl) or phosphane dichloro(triphenylmethyl)phosphane tungsten complex (**1,18**) and 1 eq. of 12-crown-4, 1.1 eq. of tert-butyl lithium (1.7 M in n-hexane) were slowly added at -78 °C. After 15 min. 1 eq. of diisopropyl- and dicyclohexyl carbodiimides (**20a,b**) was slowly added at -78 °C. In case of **21a,b** the reaction mixture was stirred and warmed up slowly to +4 °C and then kept at 4°C

during 15h. In case of **22a,b** the reaction mixture was stirred and warmed up slowly (4 h) to room temperature. The solvent was then removed *in vacuo* (~10^{-2} mbar) and LiCl filtered from a pentane solution.

6.8.2. Synthesis of [pentacarbonyl{(1-isopropyl-3-isopropylimino-2-(triphenylmethyl)-1,2-azaphosphiridine-κP}tungsten(0)] (21a)

Yellow solid, yield: 900 mg (1.24 mmol, 87%), m. p. = 120-121 °C, ^{1}H NMR ($CDCl_3$): 0.80 (d, 3H, P-N-CH-C*H*$_3$, $^{3}J_{H,H}$ = 6.5 Hz), 0.80 (d, 3H, C=N-CH-C*H*$_3$, $^{3}J_{H,H}$ = 6.2 Hz), 1.17 (d, 3H, P-N-CH-C*H*$_3$, $^{3}J_{H,H}$ = 6.5 Hz), 1.29 (d, 3H, C=N-CH-C*H*$_3$, $^{3}J_{H,H}$ = 6.3 Hz), 3.35 (dsep, 1H, N-C*H*(CH_3)$_2$, $^{3}J_{H,H}$ = 6.5 Hz, $^{3}J_{P,H}$ = 3.8 Hz), 3.44 (sep, 1H, N-C*H*(CH_3)$_2$, $^{3}J_{H,H}$ = 6.3 Hz); ^{13}C NMR ($CDCl_3$): 19.6 (d, P-N-CH-*C*H$_3$, $^{3}J_{P,C}$ = 2.7 Hz), 20.3 (d, P-N-C-*C*H$_3$, $^{3}J_{P,C}$ = 1.7 Hz), 23.1 (s, C=N-C-*C*H$_3$), 24.1(s, C=N-C-*C*H$_3$), 50.6 (s, P-N-*C*H-CH$_3$), 56.9 (d, N-*C*H-CH$_3$, $^{3}J_{P,C}$ = 14.3 Hz), 65.6 (d, P-*C*-Ph$_3$, $^{1}J_{P,C}$ = 15.8 Hz), 125.1 (s, Ph), 127.2 (s, Ph), 128.5 (s, Ph) 130.0 (d, ^{ipso}Ph, $^{2}J_{P,C}$ = 9.8 Hz), 137.0 (d, N=*C*, $^{1}J_{P,C}$ = 7.2 Hz), 140.4 (d, Ph, $J_{P,C}$ = 3.0 Hz), 143.0 (s, Ph), 194.6 (dSat, $^{2}J_{P,C}$ = 6.5 Hz, $^{1}J_{W,C}$ = 126.3 Hz, *cis*-*C*O), 196.1 (d, $^{2}J_{P,C}$ = 35.9 Hz, *trans*-*C*O); ^{31}P NMR ($CDCl_3$): 2.1 ppm, $^{1}J_{W,P}$ = 257.4 Hz. MS (EI, ^{184}W) : m/z (%): 724.1, $[M]^+$, (0.3); 598.0, $[M\text{-}^{i}PrN{=}C{=}N^{i}Pr]^+$ (0.3); 570.0, $[M\text{-}^{i}PrN{=}C{=}N^{i}Pr\text{-}CO]^+$ (0.03); 542.0 $[M\text{-}^{i}PrN{=}C{=}N^{i}Pr$ -2xCO$]^+$ (0.1); 514.0$[M\text{-}^{i}PrN{=}C{=}N^{i}Pr$ 3xCO$]^+$, (0.5); 483.0 $[M]^+$-$^{i}PrN{=}C{=}N^{i}Pr$ -4xCO$]^+$ (0.03); 458.0 $[M\text{-}^{i}PrN{=}C{=}N^{i}Pr$-5xCO$]^+$ (1.2); 243.1 $[CPh_3]^+$ (70), 69.1, $[^{i}PrN{=}C]^+$ (100); IR (ATR): ũ = 2969 (b, ν-CH_2), 2072 (s, ν-CO), 1980 (s, ν-CO), 1917 (s, ν-CO), 1740 (s, ν-CO), 1597 (b, ν-C=N) cm^{-1}.

Elemental analysis for $C_{31}H_{29}N_2O_5PW$ Calc (%): C 51.40, H 4.04, N 3.87; found (%): C 53.21 , H 4.63 , N 3.59.

6.8.3 Synthesis of [pentacarbonyl{(1-isopropyl-3-isopropylimino-2-(1,2,3,4,5-pentamethylcyclopentadienyl)-1,2-azaphosphiridine-κP}tungsten(0)] (22a)

Yellow solid, yield 412 mg (75 %), m. p. = 153-154 °C, ^{1}H NMR ($CDCl_3$): δ = 1.14 (d, 3H, P-C-C*H*$_3$, $^{3}J_{P,H}$ = 14.1 Hz), 1.24 (d, 3H, C-N-CH-C*H*$_3$, $^{3}J_{H,H}$ = 6.5 Hz), 1.27 (d, 3H, C-N-CH-C*H*$_3$, $^{3}J_{H,H}$ = 6.5 Hz), 1.44 (d, 3H, C=N-CH-C*H*$_3$, $^{3}J_{H,H}$ = 6.6 Hz), 1.47 (d, 3H, C=N-CH-C*H*$_3$, $^{3}J_{H,H}$ = 6.5 Hz), 1.84 (d, 6H, Cp*-C*H*$_3$, $^{4}J_{P,H}$ = 4.9 Hz), 1.89 (s, 3H, Cp*-C*H*$_3$), 1.97 (s, 3H, Cp*-C*H*$_3$), 3.65 (sep, 1H, N-C*H*(CH_3)$_2$, $^{3}J_{H,H}$ = 6.5 Hz), 3.65 (dsep, 1H, N-C*H*(CH_3)$_2$, $^{3}J_{H,H}$ = 6.5 Hz, $^{4}J_{P,H}$ = 2.3 Hz), ^{13}C NMR : δ = 11.0 (d, Cp*-*C*H$_3$, $^{4}J_{P,C}$ = 3.3 Hz), 11.5 (d, Cp*-*C*H$_3$, $^{4}J_{P,C}$ = 1.6 Hz), 12.00 (d, Cp*-*C*H$_3$, $^{3}J_{P,C}$ = 5.7 Hz), 12.00 (d, Cp*-*C*H$_3$, $^{3}J_{P,C}$ = 5.7 Hz), 16.56 (d, P-*C*-C*H*$_3$, $^{2}J_{P,C}$ = 4.3 Hz), 21.78 (d, C-N-C-*C*H$_3$, $^{2}J_{P,C}$ = 1.9 Hz),

22.41 (d, C-N-C-*C*H$_3$, $^2J_{P,C}$ = 1.6 Hz), 25.14 (s, C=N-C-*C*H$_3$), 25.30 (s, C=N-C-*C*H$_3$), 51.62 (s, C=N-*C*H-CH$_3$), 57.71 (d, N-*C*H-CH3, $^2J_{P,C}$ = 13.5 Hz), 64.64 (d, P-*C*(Cp*), $^1J_{P,C}$ = 15.5 Hz), 133.33 (d, C=*C*, $J_{P,C}$ = 7.1 Hz), 135.55 (s, C=*C*,), 139.7 (d, N=*C*, $^1J_{P,C}$ = 5.5 Hz), 142.71 (d, C=*C*, $J_{P,C}$ = 6.0 Hz), 144.12 (d, C=*C*, $J_{P,C}$ = 7.8 Hz), 195.02 (dsat, $^2J_{P,C}$ = 7.6 Hz, $^1J_{W,C}$ = 125.1, *cis*-*C*O), 196.45 (d, $^2J_{P,C}$ = 33.3 Hz, *trans*-*C*O), ^{31}P NMR ($CDCl_3$): δ = 4.03 (ssat, $^1J_{W,P}$ = 265.8 Hz), MS (EI, ^{184}W) : m/z (%): 618.1 $[M]^+$ (4); 588.1 $[M\text{-}CO]^+$ (5); 560.1 $[M\text{-}2xCO]^+$ (2); 532.1 $[M\text{-}3xCO]^+$ (2); 504.1 $[M\text{-}4xCO]^+$ (2); 476.1 $[M\text{-}5xCO]^+$ (2), IR (ATR): ũ = 2969 (b, ν-CH$_2$), 2924 (b, ν-CH$_2$), 2071 (s, ν-CO), 2074 (s, ν-CO), 1995 (s, ν-CO), 1895 (b, ν-CO), 1609 (b, ν-C=N) cm^{-1}.

Elemental analysis for $C_{22}H_{29}N_2O_5PW$ Calc (%): C 42.88, H 4.74, N 2.55, found (%): C 42.72, H 5,06, N 4.28.

6.8.4. Synthesis of [pentacarbonyl{(1-cyclohexyl-3-cyclohexylimino-2-(1,2,3,4,5-pentamethylcyclopentadienyl)-1,2-azaphosphiridine-κP}tungsten(0)] (22b)

Yellow oil, yield 250 mg (63 %), ^{1}H NMR ($CDCl_3$): δ =1.06 (d, 3H, $^3J_{P,H}$ = 14.2 Hz, Cp*-C^1*H*$_3$), 1.10-1.33 (br m, 10H, Cy-C*H*$_2$), 1.42-1.90 (br m, 10H, Cy-C*H*$_2$), 1.77 (s, 3H, Cp*-C*H*$_3$), 1.78 (s, 3H, Cp*-C*H*$_3$), 1.83 (s, 3H, Cp*-C*H*$_3$), 1.90 (s, 3H, Cp*-C*H*$_3$), 3.15 (br m, 2H, 2 x NC*H*), ^{13}C NMR : δ = 10.5 (d, Cp*-*C*H$_3$, $^3J_{P,C}$ = 2.7 Hz), 11.3 (s, Cp*-*C*H$_3$), 11.7 (s, Cp*-*C*H$_3$), 11,9 (s, Cp*-*C*H$_3$), 16.3 (d, Cp*-*C*H$_3$, $^2J_{P,C}$ = 3.7 Hz), 24.7 (s, Cy*C*H$_2$), 24.9 (s, Cy*C*H$_2$), 25.1 (d, Cy*C*H$_2$, $^3J_{P,C}$ = 18.2 Hz), 25.1 (d, Cy*C*H$_2$, $^3J_{P,C}$ = 17.6 Hz), 25.4 (s, Cy*C*H$_2$), 25.5 (s, Cy*C*H$_2$), 34.9 (s, Cy*C*H$_2$), 34.9 (s, Cy*C*H$_2$), 35.2 (s, Cy*C*H$_2$), 35.5 (s, Cy*C*H$_2$), 55.7 (s, N-*C*H), 58.8 (s, N-*C*H), 64.64 (d, P-*C*(Cp*), $^1J_{P,C}$ = 13.5 Hz), 133.15 (d, C=*C*, $J_{P,C}$ = 6.9 Hz), 135.45 (d, C=*C*, $J_{P,C}$ = 1.5 Hz), 139.95 (d, N=*C*, $^1J_{P,C}$ = 5.2 Hz), 142.33 (d, C=*C*, $J_{P,C}$ = 6.0 Hz), 143.87 (d, C=*C*, $J_{P,C}$ = 78.6 Hz), 194.85 (dSat, $^2J_{P,C}$ = 7.5 Hz, $^1J_{W,C}$ = 125.5, *cis*-*C*O), 196.28 (d, $^2J_{P,C}$ = 33.1 Hz, *trans*-*C*O), ^{31}P NMR ($CDCl_3$): δ = 1.47 (s, $^1J_{W,P}$ = 265.8 Hz), IR (ATR): ũ = 2971 (b, ν-CH$_2$), 2922 (b, ν-CH$_2$), 2070 (s, ν-CO), 2069 (s, ν-CO), 1993 (s, ν-CO), 1890 (b, ν-CO), 1613 (b, ν-C=N) cm^{-1}.

6.9. Synthesis of complexes 28a,b,29a,b

6.9.1. General procedure for the synthesis of complexes 28a,b,29a,b

To a THF solution of **21a,b,22a,b** 1 eq. of water was added at room temperature. The reaction mixture was stirred during 5 minutes. The solvent was removed in *vacuo* (~10^{-2} mbar) and a yellow oil was obtained. The compound was then crystallized from pure Et_2O at -20 °C.

6.9.2. Synthesis of [pentacarbonyl{(isopropylamino)(isopropyliminio)methyl (triphenylmethyl)phosphinite-κP}tungsten(0)] (28a)

White solid, yield = 250 mg (0.34 mmol, 70%), m. p. = 162-163 °C, ^{1}H NMR ($CDCl_3$): 1.0-1.4 (m, 12H, $^{i\text{-}Pr}CH_3$), 3.9 (bs, 2H, , $^{i\text{-}Pr}CH$), 6.7-7.7 (m, 3 x Ph), N-*H* are in coalescence process at room temperature; ^{13}C NMR ($CDCl_3$): 22.8 (s, ^{i}Pr-*C*H3), 22.9 (s, ^{i}Pr-*C*H3), 47.0 (s, 2 x $^{i\text{-}Pr}CH$), 69.0 (d, $^{1}J_{C,P}$ = 2.6 Hz, P-*C*Ph_3), 126.0 (d, $J_{C,P}$ = 1.0 Hz, *C*-Ph), 127.0 (d, $J_{C,P}$ = 1.7 Hz, *C*-Ph), 127.1 (d, $J_{C,P}$ = 1.0 Hz, *C*-Ph), 127.4 (d, $J_{C,P}$ = 2.3 Hz, *C*-Ph), 128.0 (s, *C*-Ph), 128.5 (s, *C*-Ph), 130.0 (d, $J_{C,P}$ = 6.4 Hz, *C*-Ph), 130.5 (d, $J_{C,P}$ = 2.3 Hz, *C*-Ph), 131.1 (d, $J_{C,P}$ = 7.4 Hz, *C*-Ph), 140.3 (d, $^{2}J_{C,P}$ = 5.13 Hz, C^{ipso}-Ph), 141.4 (d, $^{2}J_{C,P}$ = 2.3 Hz, C^{ipso}-Ph), 144.7 (d, $^{2}J_{C,P}$ = 10.7 Hz, C^{ipso}-Ph), 172.5 (d, N-*C*-N, $^{1}J_{P,C}$ = 32.5 Hz), 197.7 (dSat, $^{2}J_{P,C}$ = 8.4 Hz, $^{1}J_{W,C}$ = 127.5, *cis*-*C*O), 200.4 (d, $^{2}J_{P,C}$ = 27.5 Hz, *trans*-*C*O, $^{1}J_{W,C}$ = 144.2, *trans*-*C*O); ^{31}P NMR ($CDCl_3$): 92.4 ppm, qSat, $^{1}J_{W,P}$ = 285.6 Hz, $J_{P,H}$ = 16. Hz; MS (EI, ^{184}W): m/z (%): m/z (%): 743.1 $[M]^+$, (1); 658.1 $[M- 3xCO]^+$ (2); 630 $[M-4xCO]^+$ (1); 243.1, $[CPh_3]^+$ (100); IR (ATR): ũ = 3347 (b, N-H), 2967 (b, ν-CH_2), 2068 (s, ν-CO), 1986 (s, ν-CO), 1933 (s, ν-CO), 1915 (s, ν-CO), 1899 (s, ν-CO), 1607 (b, ν–C=N) cm^{-1}.

Elemental analysis for $C_{31}H_{31}N_2O_6PW$ Calc (%): C 50.15, H 4.21, N 3.77, found (%): C 49.99 , H 4.37 , N 3.79.

6.9.3. Synthesis of [pentacarbonyl{(isopropylamino)(isopropyliminio)methyl (1,2,3,4,5-pentamethylcyclopentadienyl)phosphinite-κP}tungsten(0)] (29a)

White solid, yield 250 mg (80 %), m. p. 164-165 °C, ^{1}H NMR ($CDCl_3$): δ = 1.24-1.30 (m, 12H, $^{i\text{-}Pr}CH_3$), 1.43 (d, 3H, Cp*-CH_3, $^{3}J_{P,H}$ = 16.7 Hz), 1.73 (bs, 3H, Cp*-CH_3), 1.82 (dd, 3H, Cp*-CH_3, $J_{P,H}$ = 3.3 Hz, $J_{H,H}$ = 1.1 Hz), 1.86 (bs, 3H, Cp*-CH_3), 2.05 (bs, 3H, Cp*-CH_3), 3.89 (m, 2H, , $^{i\text{-}Pr}CH$), 6.79 (bs, 2H, N-*H*); ^{13}C NMR : δ = 10.9 (s, Cp*-*C*H_3), 11.7 (d, Cp*-*C*H_3, $J_{C,P}$ = 1.0 Hz), 12.9 (s, Cp*-*C*H_3), 13.0 (s, Cp*-*C*H_3), 16.0 (d, P-C-*C*H_3, $^{2}J_{C,P}$ = 5.8 Hz), 23.6 (s, 2 x ^{i}Pr-*C*H3), 23.7 (s, 2 x ^{i}Pr-*C*H3), 47.1 (s, 2 x $^{i\text{-}Pr}CH$), 66.2 (d, $^{1}J_{C,P}$ = 2.7 Hz, P-Cp*-*C1*), 135.0 (d, $J_{C,P}$ = 2.7 Hz, C=C), 135.2 (d, $J_{C,P}$ = 4.7 Hz, C=C), 139.9 (d, $J_{C,P}$ = 6.7 Hz, C=C), 143.4 (d, $J_{C,P}$ = 3.7 Hz, C=C), 65.3 (d, Cp*$C^{1,}$ $^{1}J_{C,P}$ = 2.7 Hz), 134.2 (d, C=*C*, $^{3}J_{C,P}$ = 2.7 Hz), 134.3 (d, *C*=C, $^{2}J_{C,P}$ = 4.5 Hz), 171.9 (d, N-*C*-N, $^{1}J_{P,C}$ = 14.4 Hz), 198.6 (dsat, $^{2}J_{P,C}$ = 8.4 Hz, $^{1}J_{W,C}$ = 126.4, *cis*-*C*O), 200.7 (d, $^{2}J_{P,C}$ = 23.6 Hz, *trans*-*C*O, $^{1}J_{W,C}$ = 143.4, *trans*-*C*O), ^{31}P NMR ($CDCl_3$): δ = 84.3 (qsat, $^{1}J_{W,P}$ = 269.0 Hz, $J_{P,H}$ = 16.0 Hz); MS (EI, ^{184}W) : m/z (%): 634.1 $[M]^+$ (10); 606.1 $[M-CO]^+$ (1); 578.1 $[M-2xCO]^+$ (1); 550.1 $[M-3xCO]^+$ (5); 499.0 $[M-Cp^*]^+$ (100); 471.0 $[M-Cp^*-CO]^+$, (60); 443.0 $[M-Cp^*-2xCO]^+$ (80); 415.0 $[M-Cp^*-3xCO]^+$ (85); 387.0 $[M-Cp^*-4xCO]^+$ (40); 359.0 $[M-Cp^*-5xCO]^+$ (20); 175.1 $[M-Cp^*-W(CO)5]^+$ (15); 58.0

$[CHMe_2NH]^+$ (20); IR (ATR): ũ = 3387 (b, NH) 2977 (b, ν-CH_2), 2918 (b, ν-CH_2), 2065 (s, ν-CO), 1978 (s, ν-CO), 1910 (s, ν-CO), 1888 (s, ν-CO), 1609 (b, ν-C=N) cm^{-1}.

Elemental analysis for $C_{22}H_{31}N_2O_6PW$ Calc (%): C 41.66, H 4.93, N 4.42, found (%): C 41.52, H 5.104 , N 4.29.

6.9.4. Synthesis of [pentacarbonyl{(cyclohexylamino)(cyclohexyliminio)methyl(1,2,3,4,5-pentamethylcyclopentadienyl)phosphinite-κP}tungsten(0)] (29b)

White solid, yield 215 mg (70 %), m.p. 174-175 °C, ^{1}H NMR ($CDCl_3$): δ = 1.19-1.37 (br m, 10H, Cy-C*H*$_2$), 1.43 (d, 3H, $^3J_{P,H}$ = 16.8 Hz, Cp*-C^1*H*$_3$), 1.65-1.69 (br m, 2H, Cy), 1.73 (s, 3H, Cp*-C*H*$_3$), 1.82 (d, 3H, $J_{P,H}$ = 3.4 Hz, Cp*-C*H*$_3$), 1.83-1.90 (broad m, 8H, CyC*H*$_2$), 1.86 (s, 3H, Cp*-C*H*$_3$), 3.42 (br m, 2H, 2 x NC*H*), 6.8 (br s, 2 x N*H*); ^{13}C NMR : δ = 9.9 (s, Cy*C*), 10.7 (d, Cy*C*, $J_{C,P}$ = 0.6 Hz), 11.97 (d, Cy*C*, $J_{C,P}$ = 2.8 Hz), 12.01 (s, Cy*C*), 14.91 (s, Cy*C*), 23.49 (s, Cp*-*C*H$_3$), 23.64 (s, Cp*-*C*H$_3$), 23.8 (s, Cp*-*C*H$_3$), 32.95 (s, Cp*-*C*H$_3$), 32.99 (s, Cp*-*C*H$_3$), 53.4 (s, Cy*C*), 65.3 (d, Cp**C*^{1,} $^1J_{C,P}$ = 2.7 Hz), 134.2 (d, C=*C*, $^3J_{C,P}$ = 2.7 Hz), 134.3 (d, *C*=C, $^2J_{C,P}$ = 4.5 Hz), 138.8 (d, *C*=C, $^2J_{C,P}$ = 6.7 Hz), 142.2 (d, *C*=C, $^3J_{C,P}$ = 4.0 Hz), 170.8 (d, N-*C*-N, $^1J_{C,P}$ = 14.5 Hz), 197.6 (dsat, $^2J_{P,C}$ = 8.6 Hz, $^1J_{W,C}$ = 126.0, *cis*-*C*O), 199.7 (d, $^2J_{P,C}$ = 23.5 Hz, *trans*-*C*O), ^{31}P NMR ($CDCl_3$): δ = 85.0 (qsat, $^1J_{W,P}$ = 269.8 Hz, $J_{P,H}$ = 16.8 Hz), MS (EI, ^{184}W): m/z (%): 714.1 $[M]^+$ (5); 579.0 $[M\text{-}Cp^*]^+$ (80); 551.0 $[M\text{-}Cp^*\text{-}CO]^+$ (60); 523.0 $[M\text{-}Cp^*\text{-}2xCO]^+$ (90); 495.2 $[M\text{-}Cp^*\text{-}3xCO]^+$ (90); 467.2 $[M\text{-}Cp^*\text{-}4xCO]^+$ (50), IR (ATR): ũ = 3390 (b, NH), 2932 (b, ν-CH_2), 2857 (b, ν-CH_2), 2062 (s, ν-CO), 1971 (s, ν-CO), 1912 (s, ν-CO), 1892 (s, ν-CO), 1618 (b, ν-C=N) cm^{-1}.

Elemental analysis for $C_{28}H_{39}N_2O_6PW$ Calc (%): C 47.07, H 5.50, N 3.92, found (%): C 47.27, H 5.83 , N 3.74.

6.10. Synthesis of [pentacarbonyl{trifluoro(((isopropylamino)(isopropyliminio)-methyl)(trityl)phosphinooxy)borate-κP}tungsten(0)] (33)

To a suspension of 465.0 mg (0.6263 mmol) of complex **28a** in 40 mL Et_2O, a suspension of 206.8 mg (0.6263 mmol, 1 eq.) of tritylium tetrafluoroborate in 40 mL Et_2O was added at room temperature. After 1 hour the color of the solution of the reaction mixture changed from colorless to pale yellow. After 20 hours stirring at room temperature, a white precipitate was observed and the color of the solution turned again to colorless. The precipitate was filtered and washed three times with 5 mL of *n*-pentane.

White solid, yield 385 mg (83 %), m. p. = 173-174 °C, ^{1}H NMR ($CDCl_3$): 1.02 (d, 6H, $^{i\text{-}Pr}CH_3$, $^{3}J_{H,H}$ = 6.4 Hz), 1.20 (d, 6H, $^{i\text{-}Pr}CH_3$, $^{3}J_{H,H}$ = 6.4 Hz), 3.91 (m, 2H, $^{i\text{-}Pr}CH$), 6.50 (bs, 2H, N*H*), 6.8-7.5 (m, 3 x Ph), ^{13}C NMR ($CDCl_3$): 22.7 (s, 2 x ^{i}Pr-CH_3), 22.8 (s, 2 x ^{i}Pr-CH_3), 48.9 (s, 2 x $^{i\text{-}Pr}CH$), 70.0 (d, P-CPh_3, $^{1}J_{C,P}$ = 15.3 Hz), 128.9 (d, $J_{C,P}$ = 0.5 Hz, *C*-Ph), 129.0 (d, $J_{C,P}$ = 3.0 Hz, *C*-Ph), 129.5 (d, $J_{C,P}$ = 1.2 Hz, *C*-Ph), 130.6 (d, $J_{C,P}$ = 3.0 Hz, *C*-Ph), 131.0 (s, *C*-Ph), 131.1 (s, *C*-Ph), 131.2 (s, *C*-Ph), 138.9 (d, $^{2}J_{C,P}$ = 6.8 Hz, C^{ipso}-Ph), 139.8 (d, $^{2}J_{C,P}$ = 4.5 Hz, C^{ipso}-Ph), 142.7 (d, $^{2}J_{C,P}$ = 8.7 Hz, C^{ipso}-Ph), 169.1 (dd, N-*C*-N, $^{1}J_{P,C}$ = 11.6 Hz, *J* = 1.6 Hz), 196.2 (dSat, $^{2}J_{P,C}$ = 7.2 Hz, $^{1}J_{W,C}$ = 127.1, 2 x *cis*-*C*O), 197.7 (d, $^{2}J_{P,C}$ = 33.4 Hz, 2 x *trans*-*C*O, $^{1}J_{W,C}$ = 144.2, *trans*-*C*O); ^{31}P NMR ($CDCl_3$): 110.6 ppm, qSat, $^{1}J_{W,P}$ = 293.4 Hz, $J_{P,H}$ = 2.0 Hz; IR (ATR): ũ = 3344 (b, N-H), 3281 (b, N-H), 2970 (b, ν-CH_2), 2077 (s, ν-CO), 2003 (s, ν-CO), 1940 (s, ν-CO), 1907 (s, ν-CO), 1778 (s, ν-CO), 1621 (b, ν–C=N) cm^{-1}.

Elemental analysis for $C_{31}H_{31}BF_3N_2O_6PW$ Calc (%): C 45.96, H 3.86, N 3.46, found (%): C 45.52, H 4.14 , N 3.30.

6.11 Synthesis of [pentacarbonyl{4-isopropyl-3-isopropylimino-5-phenylimino-2-triphenylmethyl-1,3,5-oxazaphospholidine-κP}tungsten(0)] (35)

To a solution of 500 mg (0.69 mmol) of imino-azaphosphiridine complex **21a** in Et_2O, 82.2 mg (1 eq.) of phenyl isocyanate (**35**) were added at room temperature and stirred for 5 hours. The solvent was removed in *vacuo* (~10^{-2} mbar) and a dark yellow oil was obtained. The product was then crystallized from Et_2O at -20 °C and obtained as white solid.

Yield: 380 mg (0.45 mmol, 65%), m. p. = 148-149 °C; ^{1}H NMR ($CDCl_3$): δ = 0.46 (d, 3H, C=N-CH-C*H*$_3$, $^{3}J_{H,H}$ = 5.9 Hz), 1.12 (d, 3H, C=N-CH-C*H*$_3$, $^{3}J_{H,H}$ = 5.8 Hz), 1.46 (d, 3H, C-N-CH-C*H*$_3$, $^{3}J_{H,H}$ = 6.9 Hz), 1.56 (d, 3H, C-N-CH-C*H*$_3$, $^{3}J_{H,H}$ = 7.0 Hz), 3.48 (sep, 1H, C=N-C*H*$(CH_3)_2$, $^{3}J_{H,H}$ = 5.8 Hz), 4.89 (sep, 1H, C-N-C*H*$(CH_3)_2$, $^{3}J_{H,H}$ = 6.9 Hz), 6.5-7.7 (m, 15H, 3 x C_6H_5); ^{13}C NMR ($CDCl_3$): δ = 17.5 (s, C-N-CH-*C*H_3), 18.5 (s, C-N-CH-*C*H_3), 23.4 (s, C=N-CH-*C*H_3), 24.7 (s, C=N-CH-*C*H_3) 48.7 (s, C-N-*C*H), 56.2 (d, $^{3}J_{P,C}$ = 12.5 Hz C=N-*C*H), 71.2 (d, *C*Ph_3, $^{1}J_{P,C}$ = 4.1 Hz), 122.8 (s, C-C^{Ph}), 122.9 (s, C-C^{Ph}), 128.0 (s, C-C^{Ph}), 128.1(d, $J_{P,C}$ = 1.7 Hz C-C^{Ph}), 128.4(d, $J_{P,C}$ = 1.5 Hz C-C^{Ph}), 128.4 (s, C-C^{Ph}), 128.7 (s, C-C^{Ph}), 130.9 (d, $J_{P,C}$ = 2.3 Hz C-C^{Ph}), 131.2 (d, $J_{P,C}$ = 8.6 Hz C-C^{Ph}), 131.7 (d, $J_{P,C}$ = 6.3 Hz C-C^{Ph}), 137.6 (d, $^{2}J_{P,C}$ = 6.5 Hz C-$C^{ipso\text{-}Ph}$), 138.9 (d, $^{2}J_{P,C}$ = 6.7 Hz C-$C^{ipso\text{-}Ph}$), 141.9 (d, $^{2}J_{P,C}$ = 8.1 Hz C-$C^{ipso\text{-}Ph}$), 143.5 (d, $^{2}J_{P,C}$ = 12.4 Hz, *C*=N-Ph), 145.6 (s, N-$C^{ipso\text{-}Ph}$), 150.7 (d, $^{1}J_{P,C}$ = 10.2 Hz, ^{i}Pr-N=*C*), 195.2 (dSat, $^{2}J_{P,C}$ = 6.2 Hz, $^{1}J_{W,C}$ = 127.1, *cis*-*C*O), 197.5 (d, $^{2}J_{P,C}$ = 34.1 Hz, *trans*-*C*O); ^{31}P NMR

($CDCl_3$): 125.06 ppm, $^1J_{W,P}$ = 273.8 Hz; MS (EI, ^{184}W) : m/z (%): 843.1 $[M]^+$, (0.12); 787.2 [M- 2 x CO]$^+$ (0.1); 759.2 [M- 3 x CO]$^+$ (0.1); 559.0 [M-CPh_3 - 3 x CO]$^+$ (0.1); 488.9 [M- CPh_3 - 3 x CO]$^+$ (0.12); 243.1 $[CPh_3]^+$; IR (ATR): ũ = 2971 (b, ν-CH_2), 2928 (b, ν-CH_2), 2077 (s, ν-CO), 1997 (s, ν-CO), 1933 (s, ν-CO), 1697 (s, ν-CO), 1630 (b, ν-C=N), 1594 (b, ν-C=N) cm^{-1}.

Elemental analysis for $C_{38}H_{34}N_3O_6PW$ Calcd (%): C 54.11, H 4.06, N 4.98, found (%): C 53.97 , H 4.11 , N 4.98.

6.12 Synthesis of 1,3,5-triphenyl-1,3,5-triazinane-2,4,6-trione (36)

To a 1 mL THF solution of 40 mg (0.055 mmol) of dichloro(triphenylmethyl)phosphane tungsten complex (**18**) and 1 eq. of 12-crown-4, 1.1 eq. of *tert*-butyl lithium (1.7 M in n-hexane) were slowly added at -78 °C. After 15 min. 1 eq. of diisopropyl carbodiimide (**20a**) was slowly added at -78 °C. The reaction mixture was stirred and warmed up slowly (4 h) to room temperature. Then, 65.8 mg (60 μL, 100 eq.) of phenyl isocyanate (**34a**) were added at room temperature. After 30 minutes of gentle stirring, the reaction vessel was found to be full of a crystallinic material (**37**) together with lithium chloride. X-ray diffraction analysis of the single crystalls revealed the nature of **37** as a trimer of phenyl isocyanate.

6.13. Synthesis of [N^1,N^4-bis{pentacarbonyl[4-isopropyl-3-isopropylimino-2-triphenylmethyl-1,4,2-oxazaphospholidine-5-yl]-κP}tungsten(0)]benzene-1,4-diimine] (38)

To a 5 mL Et_2O solution of 333 mg (0.54 mmol) of *P*-Cp* 3-imino-azaphosphiridine tungsten **22a**, 43 mg (0.5 eq.) of 1,4-phenylen diisocyanate (**38**) suspended in 5 mL Et_2O were added at room temperature reaction mixture was stirred for 20 h at this temperature. The solvent was removed in *vacuo* (~10^{-2} mbar) and a yellow oil was obtained. The product was then purified by column chromatography (-10 °C, Al_2O_3, d = 3 cm, h = 6 cm, PE (40/60) / Et_2O = 95 / 5) and crystallized from pure Et_2O at -20 °C. White powder, yield: 190 mg (0.14 mmol, 50 %), m. p. = 110-111 °C; ^{1}H NMR ($CDCl_3$): δ = 1.00-2.00 (m, 54H, 18 x -CH_3), 3.40 (bs, 2H, 2 x -C*H*(CH_3)$_2$), 4.91 (bs, 2H, 2 x -C*H*(CH_3)$_2$), 6.97 (bs, 2H, N-*Ph*-N), 7.01 (bs, 2H, N-*Ph*-N); ^{13}C NMR ($CDCl_3$): δ = 11.5 (s, C-*C*H_3), 11.9 (s, C-*C*H_3), 12.2 (s, C-*C*H_3), 12.6 (s, C-*C*H_3), 14.2 (s, C-*C*H_3), 16.2 (s, C-*C*H_3), 18.1 (s, C-*C*H_3), 18.5 (s, C-*C*H_3), 22.5 (s, C-*C*H_3), 25.3 (s, C-*C*H_3), 25.4 (s, C-*C*H_3), 29.8 (s, C-*C*H_3), 34.2 (s, C-*C*H_3), 48.4 (bs, 2 x C-N-*C*H-CH_3), 55.1 (bd, 2 x C=N-*C*H-CH3, $^3J_{P,C}$ = 13.2 Hz), 64.6 (bs, 2 x P-C^{Cp*}), 127.7 (d, $J_{C,P}$ = 1.9 Hz, *C*-Ph), 123.4 (s, 2 x N-*Ph*-N), 123.6 (s, 2 x N-*Ph*-N), 133.3 (bs,

2 x *C*=C), 138.0 (bs, 2 x *C*=C), 140.9 (bs, 2 x C=*C*), 142.4 (bs, 2 x *C*=C), 144.3 (bs, 2 x *C*=N-Ph), 148.6 (bs, 2 x *C*=N-^{i}Pr), 195.7 (bdSat, $^{2}J_{P,C}$ = 5.9 Hz, $^{1}J_{W,C}$ = 124.5, *cis*-*C*O), 197.5 (d, $^{2}J_{P,C}$ = 31.7 Hz, *trans*-*C*O); ^{31}P NMR ($CDCl_3$): δ = 132.8 (sSat, $^{1}J_{W,P}$ = 270.5 Hz), 133.1 (sSat, $^{1}J_{W,P}$ = 270.5 Hz); MS (EI, ^{184}W): m/z (%): 1392.3 $[M]^+$, (25); 1258.1 $[M - C_{10}H_{14}]^+$ (35); 1201.1 [M - Cp* - 2 x CO]$^+$, (35); 1122.1 [M - 2 x Cp*]$^+$ (70); IR (ATR): ũ = 29765 (b, ν-CH_2), 2076 (s, ν-CO), 1991 (s, ν-CO), 1921 (s, ν-CO), 1684 (s, ν-CO), 1627 (w, ν-C=N) cm^{-1}.

Elemental analysis for $C_{52}H_{62}N_6O_{12}P_2W_2$ Calcd (%): C 44.61, H 4.98, N 5.70, found (%): C 44.84, H 4.49 , N 6.03.

6.14. Synthesis of [pentacarbonyl{4-isopropyl-3-isopropylimino-5-one-2-triphenylmethyl-1,3,5-oxazaphospholidine-κP}tungsten(0)] (39)

(route a): To a solution of freshly prepared **21a** (295 mg (0.44 mmol) of dichloro(triphenyl-methyl)phosphane tungsten complex, 69.4 μL (1 eq.) of 12-crown-4 and 0.30 mL (1.1 eq.) of *tert*-butyl lithium (1.6 M in *n*-hexane) being slowly added at -78 ℃. Then 69.5 mL (1 eq.) of *N,N'*-diisopropyl carbodiimide **20a** was slowly added at -78 °C after 15 min. The reaction solution was stirred and warmed up slowly to +4 °C and then kept at 4°C during 15h) CO_2 was bubbled through the solution during 30 min and then LiCl was filtered off (Al_2O_3) from a 1 to 1 mixture of petrol ether (40/60) and Et_2O at 25 °C and the main impurity extracted with *n*-pentane at room temperature. The product was then crystallized from Et_2O at -20 °C and obtained as light yellow solid; yield: 100 mg (0.14 mmol, 30%); (route b): a 100 mg (0.14 mmol) 5 mL Et_2O solution of 3-imino-azaphosphiridine complex **21a** was stirred under a CO_2 (20 bar) atmosphere for 15 hours. The solvent was removed in *vacuo* (~10^{-2} mbar) and a yellow oil was obtained. The product was then crystallized from Et_2O at -20 °C and obtained as white solid; yield: 75 mg (0.98 mmol, 70%); m. p. = 155-156 °C; ^{1}H NMR (C_6D_6): δ = 0.27 (d, 3H, C=N-CH-C*H*$_3$, $^{3}J_{H,H}$ = 5.8 Hz), 0.94 (d, 3H, C=N-CH-C*H*$_3$, $^{3}J_{H,H}$ = 5.8 Hz), 1.04 (d, 3H, C-N-CH-C*H*$_3$, $^{3}J_{H,H}$ = 7.0 Hz), 1.11 (d, 3H, C-N-CH-C*H*$_3$, $^{3}J_{H,H}$ = 7.0 Hz), 3.48 (sep, 1H, C=N-C*H*$(CH_3)_2$, $^{3}J_{H,H}$ = 5.8 Hz), 4.52 (sep, 1H, C-N-C*H*$(CH_3)_2$, $^{3}J_{H,H}$ = 7.0 Hz), 6.8-7.8 (m, 15H, 3 x C_6H_5); ^{13}C NMR (C_6D_6): δ = 18.2 (s, C-N-CH-*C*H$_3$), 18.5 (s, C-N-CH-*C*H$_3$), 23.4 (s, C=N-CH-*C*H$_3$), 24.8 (s, C=N-CH-*C*H$_3$), 48.0 (s, C-N-CH), 55.6 (d, $^{1}J_{P,C}$ = 11.7 Hz, C=N-*C*H), 71.2 (d, *C*Ph$_3$, $^{1}J_{P,C}$ = 2.2 Hz), 128.5 (d, $J_{P,C}$ = 2.0 Hz C-*C*^{Ph}), 128.6 (d, $J_{P,C}$ = 2.7, Hz C-*C*^{Ph}), 128.9 (s, C-*C*^{Ph}), 129.2 (s, C-*C*^{Ph}), 129.8 (s, C-*C*^{Ph}), 131.1 (d, $J_{P,C}$ = 2.7, Hz C-*C*^{Ph}), 131.6 (d, $J_{P,C}$ = 9.2, Hz C-*C*^{Ph}), 132.0 (d, $J_{P,C}$ = 7.0, Hz C-*C*^{Ph}), 136.9 (d, $^{2}J_{P,C}$ = 6.4 Hz C-*C*$^{ipso\text{-}Ph}$), 139.3 (d, $^{2}J_{P,C}$ = 6.4 Hz, C-*C*$^{ipso\text{-}Ph}$), 141.9 (d, $^{2}J_{P,C}$ = 8.5 Hz C-*C*$^{ipso\text{-}Ph}$), 149.5 (d, O-

C=O, $^{2}J_{P,C}$ = 12.1 Hz), 151.0 (d, P-*C*=N, $^{1}J_{P,C}$ = 8.1 Hz), 195.6 (dSat, $^{2}J_{P,C}$ = 6.2 Hz, $^{1}J_{W,C}$ = 126.8, *cis*-*C*O), 197.4 (d, $^{2}J_{P,C}$ = 34.1 Hz, *trans*-*C*O); ^{31}P NMR (C_6D_6): δ = 128.07 ppm, $^{1}J_{W,P}$ = 274.6 Hz. MS (EI, ^{184}W) : m/z (%): 768.1 $[M]^+$ (5); 740.1 $[M\text{-}CO]^+$ (2); 712.1 $[M\text{-}2xCO]^+$ (10); 684.1 $[M\text{-}3xCO]^+$ (1); 712.1 $[M\text{-}2xCO]^+$ (10); 684.1 $[M\text{-}3xCO]^+$ (2); 640.1 $[M\text{-}CO_2\text{-}3xCO]^+$ (10); 584.1 $[M\text{-}CO_2\text{-}5xCO]^+$ (25); 243 [CPh3 (100)]$^+$; IR (ATR): ũ = 2929 (b, ν-CH_2), 2076 (s, ν-CO), 1997 (s, ν-CO), 1919 (s, ν-CO), 1767 (s, ν-C=O), 1661 (b, ν-C=N) cm^{-1}.

Elemental analysis for $C_{32}H_{29}N_2O_7PW$ Calc (%): C 50.02, H 3.80, N 3.65, found (%): C 49.80, H 4.17, N 3.50.

6.15. Synthesis of [pentacarbonyl{4-isopropyl-3-isopropylimino-5-pentafluoro-phenyl-2-triphenylmethyl-1,4,2-oxazaphospholidine-κP}tungsten(0)] (44)

To a 20 mL Et_2O solution of 375 mg (0.52 mmol) of 3-imino-azaphosphiridine tungsten **21a**, 64 μ (1 eq.) of pentafluorobenzaldehyde (**43**) were added at room temperature. The reaction mixture was stirred for 22 h at this temperature. The solvent was removed in *vacuo* (~10^{-2} mbar) and an orange oil was obtained. The product was then crystallized from pure Et_2O at -30 °C. White powder, yield: 240 mg (0.26 mmol, 50 %), m. p. = 180-181 °C; ^{1}H NMR ($CDCl_3$): δ = 0.42 (d, 3H, C=NH-CH-C*H*$_3$, $^{3}J_{H,H}$ = 5.8 Hz), 0.99 (d, 3H, C-N-CH-C*H*$_3$, $^{3}J_{H,H}$ = 7.2 Hz), 1.10 (d, 3H, C-N-CH-C*H*$_3$, $^{3}J_{H,H}$ = 6.5 Hz), 1.13 (d, 3H, C=N-CH-C*H*$_3$, $^{3}J_{H,H}$ = 5.8 Hz), 3.53 (dsep, 1H, C=N-C*H*$(CH_3)_2$, $^{3}J_{H,H}$ = 5.8 Hz, $^{4}J_{P,H}$ = 1.6 Hz), 3.92 (sep, 1H, C-N-C*H*$(CH_3)_2$, $^{3}J_{H,H}$ = 6.9 Hz), 4.42 (s, N-C(C_6F_5)*H*-O), 7.2-7.9 (m, 15H, C-C^{Ph}); ^{13}C NMR ($CDCl_3$): δ = 18.2 (s, C-N-CH-*C*H_3), 19.7 (s, C-N-CH-*C*H_3), 24.1 (s, C=N-C-*C*H_3), 24.9 (s, C=N-C-*C*H_3), 48.0 (d, $^{3}J_{P,C}$ = 2.2 Hz, C-N-*C*H-CH_3) 56.8 (d, $^{3}J_{P,C}$ = 14.6 Hz, C=N-*C*H-CH_3), 70.2 (d, P-*C*Ph_3, $^{1}J_{P,C}$ = 6.1 Hz), 83.7 (t, $^{4}J_{F,H}$ = 10.2 Hz), 128.3 (s, *C*-C^{Ph}), 128.4 (s, *C*-C^{Ph}), 128.5 (s, *C*-C^{Ph}), 128.7 (s, *C*-C^{Ph}), 128.8 (s, *C*-C^{Ph}), 131.6 (d, $J_{C,P}$ = 8.3 Hz, *C*-C^{Ph}), 131.8 (d, $J_{C,P}$ = 2.2 Hz, *C*-C^{Ph}), 132.1 (d, $J_{C,P}$ = 6.1 Hz, *C*-C^{Ph}), 135.6 (C^{C6F5}), 136.5 (C^{C6F5}), 139.0 (d, $^{2}J_{C,P}$ = 5.8 Hz, *C*^{ipso}-Ph), 139.9 (C^{C6F5}), 140.2 (d, $^{2}J_{C,P}$ = 6.0 Hz, *C*^{ipso}-Ph), 141.0 (C^{C6F5}), 143.1 (d, $^{2}J_{C,P}$ = 8.0 Hz, *C*^{ipso}-Ph), 144.2 (C^{C6F5}), 147.3 (C^{C6F5}), 151.8 (d, $^{2}J_{C,P}$ = 4.0 Hz, *C*=N-^{i}Pr), 196.5 (ddSat, $^{2}J_{P,C}$ = 6.5 Hz, $J_{F\text{-}C}$ = 3.6 Hz, $^{1}J_{W,C}$ = 127.6, *cis*-*C*O), 198.7 (d, $^{2}J_{P,C}$ = 33.3 Hz, *trans*-*C*O, $^{1}J_{W,C}$ = 141.5, *trans*-*C*O).; ^{31}P NMR ($CDCl_3$): δ = 137.7 (sSat, $^{1}J_{W,P}$ = 273.1 Hz); MS (EI, ^{184}W): m/z (%): 780.1 $[M - 5xCO]^+$ (1); 243, $[CPh_3]^+$ (100); IR (ATR): ũ = 2981 (b, ν-CH_2), 2074 (s, ν-CO), 2008 (s, ν-CO), 1941 (s, ν-CO), 1925 (s, ν-CO), 1627 (w, ν-C=N) cm^{-1}.

Elemental analysis for $C_{38}H_{30}F_5N_2O_6PW$ Calcd (%): C 49.58, H 3.29, N 3.04, found (%): C 49.68, H 3.65, N 2.84.

6.16. Synthesis of [pentacarbonyl{1-isopropyl-4-(isopropylimino)-3-triphenylmethyl-1,3-azaphosphetidin-2-one-κP}tungsten(0)] (45)

A 180 mg (0.25 mmol) 5 mL Et_2O solution of 3-imino-azaphosphiridine complex **21a** was stirred under a CO (20 bar) atmosphere for 20 hours at room temperature. The solvent was removed in *vacuo* (~10^{-2} mbar) and a yellow oil was obtained. The product was then crystallized from Et_2O at -20 °C and obtained as white solid.

Yield: 130 mg (0.175 mmol, 70%), m. p. = 162-163 °C; ^{1}H NMR (C_6D_6): δ = 0.63 (d, 3H, C=N-CH-C*H*$_3$, $^3J_{H,H}$ = 6.0 Hz), 1.11 (d, 3H, C=N-CH-C*H*$_3$, $^3J_{H,H}$ = 6.0 Hz), 1.13 (d, 3H, C-N-CH-C*H*$_3$, $^3J_{H,H}$ = 7.0 Hz), 1.29 (d, 3H, C-N-CH-C*H*$_3$, $^3J_{H,H}$ = 7.0 Hz), 3.20 (sep, 1H, C=N-C*H*$(CH_3)_2$, $^3J_{H,H}$ = 6.0 Hz), 4.00 (sep, 1H, C-N-C*H*$(CH_3)_2$, $^3J_{H,H}$ = 7.0 Hz), 7.1-7.7 (m, 15H, 3 x C_6H_5); ^{13}C NMR (C_6D_6): δ = 19.6 (s, N-CH-*C*H_3), 19.9 (s, N=CH-*C*H_3), 23.0 (s, C=N-CH-*C*H_3), 24.5 (s, N-CH-*C*H_3), 47.5 (d, C-N-*C*H, $^1J_{P,C}$ = 4.2 Hz), 57.7 (d, $^1J_{P,C}$ = 9.4 Hz, C=N-*C*H), 64.8 (d, *C*Ph_3, $^1J_{P,C}$ = 2.0 Hz), 128.2 (d, $J_{P,C}$ = 2.2 Hz C-*C*^{Ph}), 128.4 (d, $J_{P,C}$ = 2.0, Hz C-*C*^{Ph}), 128.5 (d, $J_{P,C}$ = 2.4, Hz C-*C*^{Ph}), 128.6 (d, $J_{P,C}$ = 2.4, Hz C-*C*^{Ph}), 128.9 (s, C-*C*^{Ph}), 129.2 (d, $J_{P,C}$ = 0.5 Hz C-*C*^{Ph})130.1 (d, $J_{P,C}$ = 2.5, Hz C-*C*^{Ph}), 130.5 (d, $J_{P,C}$ = 8.7 Hz C-*C*^{Ph}), 132.1 (d, $J_{P,C}$ = 8.0 Hz C-*C*^{Ph}),140.1 (d, $^2J_{P,C}$ = 5.3 Hz C-*C*$^{ipso\text{-}Ph}$), 141.0 (d, $^2J_{P,C}$ = 1.5 Hz, C-*C*$^{ipso\text{-}Ph}$), 141.5 (d, $^2J_{P,C}$ = 8.5 Hz C-*C*$^{ipso\text{-}Ph}$), 148.9 (d, P-*C*=N, $^{1+3}J_{P,C}$ = 13.2 Hz), 169.6 (d, P-*C*=O, $^{1+3}J_{P,C}$ = 52.1 Hz), 195.2 (dSat, $^2J_{P,C}$ = 5.4 Hz, $^1J_{W,C}$ = 126.7, *cis*-*C*O), 197.7 (d, $^2J_{P,C}$ = 29.1 Hz, *trans*-*C*O); ^{31}P NMR (C_6D_6): δ = 94.9 (s, $^1J_{W,P}$ = 226.5 Hz); MS (EI, ^{184}W) : m/z (%): 752.0, $[M]^+$ (2); 243, $[CPh3]^+$ (100); IR (ATR): ũ = 2972 (b, ν-CH_2), 2076 (s, ν-CO), 1997 (s, ν-CO), 1919 (s, ν-CO), 1767 (s, ν-C=O), 1661 (b, ν-C=N) cm^{-1}.

Elemental analysis for $C_{38}H_{30}F_5N_2O_6PW$ Calcd (%): C 51.08, H 3.88, N 3.72, found (%): C 50.77, H 4.34, N 3.46.

6.17. Synthesis of [2-triphenylmethyl-3-phenyl-oxaphosphirane-κP]pentacarbonyltungsten(0) (50)

To a 1 mL Et_2O solution of 13.6 mg (0.019 mmol) of 3-imino-azaphosphiridine tungsten **21a**, 2 μ (1 eq.) of benzaldehyde (**42**) were added at room temperature. The reaction mixture was stirred for 22 h at this temperature; ^{31}P NMR (Et_2O): 16.2 ppm ($^1J_{W,P}$ = 312.2 Hz).

6.18. Synthesis of isocyanide-to-phosphinidene tungsten(0) complexes adduct 26b,c

6.18.1. General procedure for the synthesis of isocyanide-to-phosphinidene tungsten(0) complexes 26b,c

To Et_2O solutions of 3-imino-azaphosphiridine complex **21a**, 1 eq. of isocyanide (**52b,c**) were added at room temperature. The reaction mixtures were stirred for 15 hours. When the reactions were completed the solvent was removed in *vacuo* (~10^{-2} mbar) and yellow oils were obtained. The products were then crystallized from Et_2O at -40 °C and obtained as yellow solids.

6.18.2. Synthesis of [pentacarbonyl{(tert-butyl-isocyanide-κ*C*-to-P)(triphenylmethylphosphanylidene)-κP}tungsten(0)] (26b)

Yield: 309 mg (0.45 mmol, 60%); m. p. = 116-117 °C; ^{1}H NMR (C_6D_6): δ = 0.67 (s, 9H, C-C*H*$_3$), 6.9-7.1 (m, 9H, C_6H_5), 7.4-7.5 (m, 6H, C-C_6H_5); ^{13}C NMR (C_6D_6): δ = 28.7 (s, C-N-CH-*C*H$_3$), 58.6 (d, *C*Ph$_3$, $^1J_{P,C}$ = 25.0 Hz), 60.9 (s, N-*C*(CH$_3$)$_3$), 126.8 (d, $J_{P,C}$ = 1.8 Hz C-*C*^{Ph}), 128.1 (s, C-*C*^{Ph}), 130.4 (d, $J_{P,C}$ = 8.2, Hz C-*C*^{Ph}), 146.9 (d, N*C*→P, $^1J_{P,C}$ = 6.8 Hz), 197.9 (dSat, $^2J_{P,C}$ = 3.6 Hz, $^1J_{W,C}$ = 126.6, *cis*-*C*O), 201.0 (d, $^2J_{P,C}$ = 16.7 Hz, *trans*-*C*O); ^{31}P NMR (C_6D_6): δ = -50.0 ppm (s, $^1J_{W,P}$ = 117.7 Hz); MS (EI, ^{184}W): m/z (%): 681.0 [M]$^+$ (2.5); 598.0 [M - ^{t}BuN≡C]$^+$ (2); 514.0 [M - ^{t}BuNC - 2xCO]$^+$ (4); 243 [CPh3]$^+$ (100); IR (ATR): ũ = 2988 (b, ν-CH), 2142 (b, ν-N≡C), 2060 (s, ν-CO), 1923 (s, ν-CO), 1889 (s, ν-CO), 1847 (s, ν-CO) cm^{-1}.

Elemental analysis for $C_{29}H_{24}NO_5PW$ Calcd (%): C 51.12, H 3.55, N 2.06, found (%): C 50.90, H 3.93, N 2.61.

6.18.3. Synthesis of [pentacarbonyl{(*n*-butyl-isocyanide-κC-to-P)(triphenylmethylphosphanylidene)-κP}tungsten(0)] (26c)

^{1}H NMR ($CDCl_3$): δ = 0.80 (t, 3H, $^3J_{H,H}$ = 7.4 Hz, CH$_2$-C*H*$_3$), 1.18 (m, 2H, -C*H*$_2$-CH$_3$), 1.40 (m, 2H, -CH$_2$-C*H*$_2$-CH$_2$), 3.56 (dt, 2H, $^3J_{H,H}$ = 6.7 Hz, $^4J_{P,H}$ = 4.4 Hz, N-C*H*$_2$-CH$_2$), 7.1-7.3 (m, 15H, C_6H_5); ^{13}C NMR ($CDCl_3$): δ = 13.3 (s, CH$_2$-*C*H$_3$), 19.8 (s, -*C*H$_2$-CH$_3$), 30.8 (d, $^4J_{P,C}$ = 2.1 Hz CH$_2$-*C*H$_2$-CH2), 46.7 (s, N-*C*H$_2$-CH$_2$), 58.8 (d, *C*Ph$_3$, $^1J_{P,C}$ = 24.7 Hz), 126.9 (d, $J_{P,C}$ = 1.8 Hz C-*C*^{Ph}), 128.2 (s, C-*C*^{Ph}), 130.4 (d, $J_{P,C}$ = 8.2, Hz C-*C*^{Ph}), 146.6 (d, N≡C→P, $^1J_{P,C}$ = 6.6 Hz), 197.7 (dSat, $^2J_{P,C}$ = 3.5 Hz, ^{1}J$_{W,C}$ = 126.4, *cis*-*C*O), 201.3 (d, ^{2}J$_{P,C}$ = 17.2 Hz, *trans*-*C*O); ^{31}P NMR ($CDCl_3$): δ = -51.8 ppm (s, $^1J_{W,P}$ = 118.2 Hz).

6.19. Synthesis of [pentacarbonyl{3-isopropyl-4-(isopropylimino)-2-triphenylmethyl-1,3,2-thiazaphosphetidin-κP}tungsten(0)] (54)

To a 15 mL toluene solution of 350 mg (0.48 mmol) of 3-imino-azaphosphiridine complex **21a**, 15.5 mg (1/8 eq.) of elemental sulfur (S_8) was added at room temperature. The reaction mixture was stirred for 24 hours. When the reaction was completed the solvent was removed in *vacuo* (~10^{-2} mbar) and a yellow oil was obtained. The product was then crystallized from Et_2O at -50 °C and washed with pentane at -50 °C to obtain a white solid after drying in vacuo.

Yield: 237 mg (0.31 mmol, 65%); m. p. = 142-143 °C; ^{1}H NMR ($CDCl_3$): δ = 0.91 (d, 3H, P-N-CH-C*H*$_3$, $^3J_{H,H}$ = 6.6 Hz), 1.01 (d, 3H, C-N-CH-C*H*$_3$, $^3J_{H,H}$ = 6.2 Hz), 1.06 (d, 3H, C=N-CH-C*H*$_3$, $^3J_{H,H}$ = 6.2 Hz), 1.49 (d, 3H, C=N-CH-C*H*$_3$, $^3J_{H,H}$ = 6.6 Hz), 2.86 (dsep, 1H, C=N-C*H*$(CH_3)_2$, $^3J_{H,H}$ = 6.2 Hz, $^3J_{P,H}$ = 2.9 Hz), 2.98 (dsep, 1H, P-N-C*H*$(CH_3)_2$, $^3J_{H,H}$ = 6.6 Hz, $^3J_{P,H}$ = 11.7 Hz), 6.92-6.98 (m, 2H, C-Ph), 7.26-7.45 (m, 13H, C-Ph), 7.70-7.77 (m, 2H, C-Ph); ^{13}C NMR ($CDCl_3$): δ = 19.7 (d, P-N-CH-*C*H_3, $^2J_{P,C}$ = 1.5 Hz), 20.6 (d, P-N-C-*C*H_3, $^2J_{P,C}$ = 2.0 Hz), 24.0 (s, C=N-C-*C*H_3), 24.3 (s, C=N-C-*C*H_3), 53.7 (d, $^2J_{P,C}$ = 1.2 Hz, P-N-*C*H-CH_3), 54.0 (d, C=N-*C*H-CH3, $^2J_{P,C}$ = 1.1 Hz), 71.1 (d, P-*C*Ph_3, $^1J_{P,C}$ = 13.7 Hz), 127.9 (d, $J_{C,P}$ = 2.0 Hz, *C*-Ph), 128.0 (d, $J_{C,P}$ = 1.8 Hz, *C*-Ph), 128.3 (d, $J_{C,P}$ = 3.0 Hz, *C*-Ph), 128.5 (d, $J_{C,P}$ = 2.9 Hz, *C*-Ph) 128.8 (s, *C*-Ph), 129.0 (d, $J_{C,P}$ = 1.2 Hz, *C*-Ph), 129.4 (s, *C*-Ph), 129.7 (d, $J_{C,P}$ = 2.8 Hz, *C*-Ph), 131.3 (d, $J_{C,P}$ = 3.5 Hz, *C*-Ph), 131.4 (d, $J_{C,P}$ = 2.3 Hz, *C*-Ph), 139.1 (d, $^{2+2}J_{C,P}$ = 6.8 Hz, *C*=N-^{i}Pr), 140.4 (d, $^2J_{C,P}$ = 4.5 Hz, C^{ipso}-Ph), 141.2 (d, $^2J_{C,P}$ = 4.9 Hz, C^{ipso}-Ph), 142.5 (d, $^2J_{C,P}$ = 11.9 Hz, C^{ipso}-Ph), 196.5 (dSat, $^2J_{P,C}$ = 6.7 Hz, $^1J_{W,C}$ = 128.0, *cis*-*C*O), 198.6 (d, $^2J_{P,C}$ = 37.1 Hz, *trans*-*C*O); ^{31}P NMR ($CDCl_3$): 122.6 (dSat, $J_{P,H}$ = 10.7 Hz, $^1J_{W,P}$ = 280.5 Hz); pos-ESI-MS : m/z (%): calcd: $[M+H]^+$ = 757.1120, found: $[M+H]^+$ = 757.1123; IR (ATR): ũ = 2975 (b, ν-CH_2), 2932 (b, ν-CH_2), 2073 (s, ν-CO), 1988 (s, ν-CO), 1928 (s, ν-CO), 1677 (s, ν-CO), 1599 (b, ν-C=N) cm^{-1}.

Elemental analysis for $C_{31}H_{29}N_2O_5PSW$ calcd (%): C 49.32, H 3.86, N 3.70, S 4.24 found (%): C 49.36, H 3.98, N 3.66, S 4.28.

6.20. Synthesis of [pentacarbonyl{3-isopropyl-4-(isopropylimino)-2-triphenylmethyl-1,3,2-selenazaphosphetidin-κP}tungsten(0)] (58)

To a 7 mL Et_2O solution of 317 mg (0.44 mmol) of 3-imino-azaphosphiridine complex **21a**, 34.5 mg (1 eq.) of elemental selenium was added at room temperature. To the suspension 5.3 mg (0.022 mmol, 5 %) of tris(dimethylamino)phosphane *P*-selenide **57** was added at room temperature and the reaction mixture was stirred for 20 hours. When the reaction was

completed the solvent was removed in *vacuo* (~10^{-2} mbar) and a yellow oil was obtained. The product was then crystallized from Et_2O at -30 °C and washed with pentane at -30 °C. **58** was obtained as a white solid.

Yield: 245 mg (0.30 mmol, 70%); m. p. = 125-126 °C; ^{1}H NMR ($CDCl_3$): δ = 0.81 (d, 3H, P-N-CH-C*H*$_3$, $^3J_{H,H}$ = 6.6 Hz), 0.94 (d, 3H, C-N-CH-C*H*$_3$, $^3J_{H,H}$ = 6.2 Hz), 1.02 (d, 3H, C=N-CH-C*H*$_3$, $^3J_{H,H}$ = 6.2 Hz), 1.43 (d, 3H, C=N-CH-C*H*$_3$, $^3J_{H,H}$ = 6.6 Hz), 2.51 (dsep, 1H, C=N-C*H*$(CH_3)_2$, $^3J_{H,H}$ = 6.2 Hz, $^3J_{P,H}$ = 3.2 Hz), 2.84 (dsep, 1H, P-N-C*H*$(CH_3)_2$, $^3J_{H,H}$ = 6.6 Hz, $^3J_{P,H}$ = 10.6 Hz), 6.81-6.87 (m, 2H, C-Ph), 7.17-7.36 (m, 13H, C-Ph), 7.69-7.74 (m, 2H, C-Ph); ^{13}C NMR ($CDCl_3$): δ = 19.7 (d, P-N-CH-*C*H_3, $^2J_{P,C}$ = 1.5 Hz), 20.4 (d, P-N-C-*C*H_3, $^2J_{P,C}$ = 1.8 Hz), 23.9 (s, C=N-C-*C*H_3), 24.1(s, C=N-C-*C*H_3), 56.1 (d, $^2J_{P,C}$ = 1.6 Hz, P-N-*C*H-CH_3), 57.00 (d, C=N-*C*H-CH3, $^2J_{P,C}$ = 0.7 Hz), 70.30 (d, P-*C*Ph_3, $^1J_{P,C}$ = 17.0 Hz), 127.7 (d, $J_{C,P}$ = 1.9 Hz, *C*-Ph), 128.1 (d, $J_{C,P}$ = 3.0 Hz, *C*-Ph), 128.4 (d, $J_{C,P}$ = 2.8 Hz, *C*-Ph), 128.5 (s, *C*-Ph), 128.9 (d, $J_{C,P}$ = 0.9 Hz, *C*-Ph), 129.6 (d, $J_{C,P}$ = 2.9 Hz, *C*-Ph), 131.1 (d, $J_{C,P}$ = 9.7 Hz, *C*-Ph), 131.4 (d, $J_{C,P}$ = 7.8 Hz, *C*-Ph), 132.0 (d, $^{2+2}J_{C,P}$ = 8.5 Hz, *C*=N-^{i}Pr), 140.2 (d, $^2J_{C,P}$ = 3.5 Hz, *C*^{ipso}-Ph), 142.2 (d, $^2J_{C,P}$ = 5.0 Hz, *C*^{ipso}-Ph), 142.6 (d, $^2J_{C,P}$ = 12.8 Hz, *C*^{ipso}-Ph), 197.0 (dSat, $^2J_{P,C}$ = 6.5 Hz, $^1J_{W,C}$ = 127.0, *cis*-*C*O), 198.7 (d, $^2J_{P,C}$ = 36.5 Hz, *trans*-*C*O, $^1J_{W,C}$ = 143.2, *trans*-*C*O); ^{31}P NMR ($CDCl_3$): 111.6 (dSatSat, $^3J_{P,H}$ = 10.6 Hz, $^1J_{W,P}$ = 275.3 Hz, $^1J_{Se,P}$ = 148.0 Hz); ^{77}Se NMR ($CDCl_3$): 649.2 (d, $^1J_{Se,P}$ = 148.0 Hz). IR (ATR): ũ = 2974 (b, ν-CH_2), 2072 (s, ν-CO), 1988 (s, ν-CO), 1930 (s, ν-CO), 1692 (s, ν-CO), 1598 (w, ν-C=N) cm^{-1}.

Elemental analysis for $C_{31}H_{29}N_2O_5PSW$ Calcd (%): C 46.35, H 3.64, N 3.49, found (%): C 45.85, H 4.11, N 3.39.

7. References

[1] T. E. Gier, *J. Am. Chem. Soc.* **1961**, *83*, 1769–1770.

[2] A. B. Burg, W. Mahler, *J. Am. Chem. Soc.* **1961**, *83*, 2388–2389.

[3] M. Regitz, O. J. Scherer, R. Appel (Eds.) *Multiple bonds and low coordination in phosphorus chemistry*, G. Thieme Verlag; Thieme Medical Publishers, Stuttgart, New York, New York, **1990**.

[4] P. Floch, *Coord. chem. rev.* **2006**, *250*, 627–681.

[5] a) R. Appel, C. Casser, M. Immenkeppel, F. Knoch, *Angew. Chem. Int. Ed. Engl.* **1984**, *23*, 895–896; *Angew. Chem.* **1984**, *96*, 905–906.

[6] a) K. Dimroth, K. J. Kraft, *Angew. Chem. Int. Ed. Engl.* **1964**, *3*, 384–385; *Angew. Chem.* **1964**, *76*, 433.

[7] a) G. Märkl, *Angew. Chem. Int. Ed. Engl.* **1966**, *5*, 846–847; *Angew. Chem.* **1966**, *78*, 907–908.

[8] A. J. Ashe, *J. Am. Chem. Soc.* **1971**, *93*, 3293–3295.

[9] K. Lammertsma, *Top. Curr. Chem.* **2003**, *229*, 95–119.

[10] F. Mathey, Z. Duan, *Dalton Trans.* **2015**, DOI: 10.1039/C5DT02532J.

[11] F. Mathey, *Dalton Trans.* **2007**, 1861.

[12] a) R. Moss, *Contemporary Carbene Chemistry, Wiley Ser. React. Intermed. Chem. Biol., 7*, **2014**; b) D. J. Nelson, S. P. Nolan, *Chem. Soc. Rev.* **2013**, *42*, 6723–6753; c) S. P. Nolan (Ed.) *N-Heterocyclic Carbenes*, Wiley-VCH Verlag GmbH & Co. KGaA, Weinheim, Germany, **2014**.

[13] a) D. Falvey, *Nitrenes and Nitrenium Ions. Wiley Ser. React. Intermed. Chem. Biol., 6*, **2013**; b) A. Schulz, A. Villinger, *Angew. Chem. Int. Ed.* **2013**, *52*, 3068–3070.

[14] a) G. Frenking, R. Tonner, S. Klein, N. Takagi, T. Shimizu, A. Krapp, K. K. Pandey, P. Parameswaran, *Chem. Soc. Rev.* **2014**, *43*, 5106–5139; b) M. Driess, *Nat. chem.* **2012**, *4*, 525–526.

[15] G. Frison, F. Mathey, A. Sevin, *J. Organomet. Chem.* **1998**, *570*, 225–234.

[16] K. B. Dillon, F. Mathey, J. F. Nixon, *Phosphorus*. *The carbon copy : from organophosphorus to phospha-organic chemistry*, Wiley, Chichester, New York, **1998**.

[17] F. Mathey, N. Huy, A. Marinetti, *Helv. chim. acta* **2001**, *84*, 2938–2957.

[18] a) C. C. Cummins, R. R. Schrock, W. M. Davis, *Angew. Chem.* **1993**, *105*, 758–761; *Angew. Chem. Int. Ed. Engl.* **1993**, *32*, 756–759.

[19] a) A. Mahieu, A. Igau, J.-P. Majoral, *Phosphorus, Sulfur, and Silicon Relat. Elem.* **1995**, *104*, 235–239; b) T. L. Breen, D. W. Stephan, *Organometallics* **1996**, *15*, 4223–4227.

[20] a) B. Sterenberg, A. Carty, *J. Organomet. Chem.* **2001**, *617-618*, 696–701; b) T. L. Breen, D. W. Stephan, *J. Am. Chem. Soc.* **1996**, *118*, 4204–4205.

[21] A. Marinetti, F. Mathey, J. Fischer, A. Mitschler, *Chem. Commun.* **1982**, 667.

[22] a) A. Marinetti, F. Mathey, J. Fischer, A. Mitschler, *J. Am. Chem. Soc.* **1982**, *104*, 4484–4485; b) A. Marinetti, F. Mathey, *Organometallics* **1984**, *3*, 456–461; c) K. Lammertsma, A. W. Ehlers, M. L. McKee, *J. Am. Chem. Soc.* **2003**, *125*, 14750–14759.

[23] a) F. Mathey, *Angew. Chem. Int. Ed. Engl.* **1987**, *26*, 275–286; *Angew. Chem.* **1987**, *99*, 285–296.

[24] R. Streubel, *Coord. chem. rev.* **2002**, *227*, 175–192.

[25] a) R. Streubel, J. Jeske, P. G. Jones, R. Herbst-Irmer, *Angew. Chem.* **1994**, *106*, 115–117; *Angew. Chem. Int. Ed.* **1994**, *33*, 80–82.

[26] R. Streubel, A. Kusenberg, J. Jeske, P. G. Jones, *Angew. Chem.* **1994**, *106*, 2564–2566; *Angew. Chem. Int. Ed.* **1994**, *33*, 2427–2428.

[27] M. L. G. Borst, R. E. Bulo, C. W. Winkel, D. J. Gibney, A. W. Ehlers, M. Schakel, M. Lutz, A. L. Spek, K. Lammertsma, *J. Am. Chem. Soc.* **2005**, *127*, 5800–5801.

[28] F. Mercier, B. Deschamps, F. Mathey, *J. Am. Chem. Soc.* **1989**, *111*, 9098–9100.
[29] A. H. Cowley, R. L. Geerts, C. M. Nunn, *J. Am. Chem. Soc.* **1987**, *109*, 6523–6524.
[30] J. B. Wit, van Eijkel, Gerno T, M. Schakel, K. Lammertsma, *Tetrahedron* **2000**, *56*, 137–141.
[31] M. L. G. Borst, van der Riet, Niels, R. H. Lemmens, de Kanter, Franciscus J. J., M. Schakel, A. W. Ehlers, A. M. Mills, M. Lutz, A. L. Spek, K. Lammertsma, *Chem. Eur. J.* **2005**, *11*, 3631–3642.
[32] a) B. T. Sterenberg, K. A. Udachin, A. J. Carty, *Organometallics* **2001**, *20*, 4463–4465; b) B. Sterenberg, A. Carty, *J. Organomet. Chem.* **2001**, *617-618*, 696–701.
[33] T. W. Graham, K. A. Udachin, M. Z. Zgierski, A. J. Carty, *Organometallics* **2011**, *30*, 1382–1388.
[34] R. Melenkivitz, D. J. Mindiola, G. L. Hillhouse, *J. Am. Chem. Soc.* **2002**, *124*, 3846–3847.
[35] H. Lang, G. Mohr, O. Scheidsteger, G. Huttner, *Chem. Ber.* **1985**, *118*, 574–596.
[36] C. Compain, F. Mathey, *Z. Anorg. Allg. Chem.* **2006**, *632*, 421–424.
[37] A. Özbolat, G. von Frantzius, J. M. Pérez, M. Nieger, R. Streubel, *Angew. Chem. Int. Ed.* **2007**, *46*, 9327–9330; *Angew. Chem.* **2007**, *119*, 9488–9491.
[38] R. Streubel, M. Bode, J. Marinas Pérez, G. Schnakenburg, J. Daniels, M. Nieger, P. G. Jones, *Z. Anorg. Allg. Chem.* **2009**, *635*, 1163–1171.
[39] M. Bode, J. Daniels, R. Streubel, *Organometallics* **2009**, *28*, 4636–4638.
[40] V. Nesterov, G. Schnakenburg, A. Espinosa, R. Streubel, *Inorg. Chem.* **2012**, *51*, 12343–12349.
[41] A. Ozbolat, G. von Frantzius, W. Hoffbauer, R. Streubel, *Dalton trans.* **2008**, 2674–2676.
[42] A. Özbolat, G. von Frantzius, E. Ionescu, S. Schneider, M. Nieger, P. G. Jones, R. Streubel, *Organometallics* **2007**, *26*, 4021–4024.
[43] a) L. Duan, G. Schnakenburg, J. Daniels, R. Streubel, *Eur. J. Inorg. Chem.* **2012**, *2012*, 3490–3499; b) L. Duan, G. Schnakenburg, R. Streubel, *Organometallics* **2011**, *30*, 3246–3249.
[44] L. Duan, G. Schnakenburg, J. Daniels, R. Streubel, *Eur. J. Inorg. Chem.* **2012**, *2012*, 2314–2319.
[45] G. Boche, Lohrenz, John C. W., *Chem. Rev.* **2001**, *101*, 697–756.
[46] a) S. Bauer, A. Marinetti, L. Ricard, F. Mathey, *Angew. Chem. Int. Ed.* **1990**, *29*, 1166–1167; b) S. Bauer, A. Marinetti, L. Ricard, F. Mathey, *Angew. Chem.* **1990**, *102*, 1188–1189.
[47] R. Streubel, M. Klein, G. Schnakenburg, *Organometallics* **2012**, *31*, 4711–4715.
[48] C. Albrecht, E. Schneider, M. Engeser, G. Schnakenburg, A. Espinosa, R. Streubel, *Dalton trans.* **2013**, *42*, 8897–8906.
[49] R. Streubel, A. Ostrowski, H. Wilkens, F. Ruthe, J. Jeske, P. G. Jones, *Angew. Chem.* **1997**, *109*, 409–413; *Angew. Chem. Int. Ed.* **1997**, *36*, 378–381.
[50] S. Fankel, H. Helten, G. von Frantzius, G. Schnakenburg, J. Daniels, V. Chu, C. Müller, R. Streubel, *Dalton trans.* **2010**, *39*, 3472–3481.
[51] R. Streubel, J. M. V. Franco, G. Schnakenburg, A. E. Ferao, *Chem. Commun.* **2012**, *48*, 5986–5988.
[52] a) T. L. Gilchrist, *Heterocyclic chemistry*, Prentice Hall, **1997**; b) A. K. Yudin, *Aziridines and epoxides in organic synthesis*, John Wiley & Sons, **2006**; c) E. Rivard, *Chem. Soc. Rev.* **2015**, DOI: 10.1039/C5CS00365B.
[53] a) P. A. Bartlett, N. I. Carruthers, B. M. Winter, K. P. Long, *J. Org. Chem.* **1982**, *47*, 1284–1291; b) M. T. Boisdon, J. Barrans, *Chem. Commun.* **1988**, 615–618; c) G.-V. Röschenthaler, K. Sauerbrey, R. Schmutzler, *Chem. Ber.* **1978**, *111*, 3105–3111.
[54] a) K. Burger, J. Fehn, W. Thenn, *Angew. Chem. Int. Ed. Engl.* **1973**, *12*, 502–503; *Angew. Chem.* **1973**, *85*, 542.
[55] E. Niecke, A. Seyer, D.-A. Wildbredt, *Angew. Chem.* **1981**, *93*, 687–688; *Angew. Chem. Int. Ed.* **1981**, *20*, 675–677.
[56] O. Krahe, F. Neese, R. Streubel, *Chem. Eur. J.* **2009**, *15*, 2594–2601.
[57] A. Espinosa, R. Streubel, *Chem. Eur. J.* **2011**, *17*, 3166–3178.

[58] a) E. Niecke, K. Schwichtenhövel, H. G. Schäfer, B. Krebs, *Angew. Chem.* **1981**, *93*, 1033–1034; *Angew. Chem. Int. Ed.* **1981**, *20*, 963–964.
[59] N. Dufour, A.-M. Caminade, J.-P. Majoral, *Tetrahedron Lett.* **1989**, *30*, 4813–4814.
[60] M. J. M. Vlaar, P. Valkier, de Kanter, Frans J. J., M. Schakel, A. W. Ehlers, A. L. Spek, M. Lutz, K. Lammertsma, *Chem. Eur. J.* **2001**, *7*, 3551–3557.
[61] T. Goumans, A. W. Ehlers, M. J. Vlaar, S. J. Strand, K. Lammertsma, *J. Organomet. Chem.* **2002**, *643-644*, 369–375.
[62] N. H. Tran Huy, L. Ricard, F. Mathey, *Heteroatom Chem.* **1998**, *9*, 597–600.
[63] T. Wettling, J. Schneider, O. Wagner, C. G. Kreiter, M. Regitz, *Angew. Chem.* **1989**, *101*, 1035–1037; *Angew. Chem. Int. Ed. Engl.* **1989**, *28*, 1013–1014.
[64] M. Bode, G. Schnakenburg, P. G. Jones, R. Streubel, *Organometallics* **2008**, *27*, 2664–2667.
[65] a) U. Rohde, F. Ruthe, P. G. Jones, R. Streubel, *Angew. Chem.* **1999**, *111*, 158–160; *Angew. Chem. Int. Ed.* **1999**, *38*, 215–217.
[66] V. Nesterov, A. Espinosa, G. Schnakenburg, R. Streubel, *Chem. Eur. J.* **2014**, *20*, 7010–7016.
[67] N. Hoffmann, C. Wismach, L. Ernst, H.-M. Schiebel, P. G. Jones, R. Streubel, *Eur. J. Inorg. Chem.* **2003**, *2003*, 1815–1821.
[68] R. Streubel, U. Schiemann, N. Hoffmann, Y. Schiemann, P. G. Jones, D. Gudat, *Organometallics* **2000**, *19*, 475–481.
[69] M. Al-Ktaifani, W. Bauer, U. Bergsträßer, B. Breit, M. D. Francis, F. W. Heinemann, P. B. Hitchcock, A. Mack, J. F. Nixon, H. Pritzkow et al., *Chem. Eur. J.* **2002**, *8*, 2622–2633.
[70] R. Streubel, C. Murcia-García, G. Schnakenburg, A. Espinosa Ferao, *Organometallics* **2015**, *34*, 2676–2682.
[71] J. Liedtke, S. Loss, G. Alcaraz, V. Gramlich, H. Grützmacher, *Angew. Chem.* **1999**, *111*, 1724–1727; *Angew. Chem. Int. Ed.* **1999**, *38*, 1623–1626.
[72] a) M. M. Al-Ktaifani, D. P. Chapman, M. D. Francis, P. B. Hitchcock, J. F. Nixon, L. Nyulászi, *Angew. Chem. Int. Ed.* **2001**, *40*, 3474–3477; *Angew. Chem.* **2001**, *113*, 3582–3585.
[73] a) M. Stubenhofer, C. Kuntz, M. Bodensteiner, A. Y. Timoshkin, M. Scheer, *Organometallics* **2013**, *32*, 3521–3528; b) B. P. Johnson, G. Balázs, M. Scheer, *Coord, Chem. Rev.* **2006**, *250*, 1178–1195; c) I. Amor, M. E. García, M. A. Ruiz, D. Sáez, H. Hamidov, J. C. Jeffery, *Organometallics* **2006**, *25*, 4857–4869; d) M. E. García, V. Riera, M. A. Ruiz, D. Sáez, J. Vaissermann, J. C. Jeffery, *J. Am. Chem. Soc.* **2002**, *124*, 14304–14305; e) M. A. Alvarez, M. E. García, M. A. Ruiz, J. Suárez, *Angew. Chem. Int. Ed.* **2011**, *50*, 6383–6387; *Angew. Chem.* **2011**, *123*, 6507–6511.
[74] M. Scheer, D. Himmel, C. Kuntz, S. Zhan, E. Leiner, *Chem. Eur. J.* **2008**, *14*, 9020–9029.
[75] O. C. Presly, M. Green, J. C. Jeffery, E. Leiner, M. Murray, C. A. Russell, M. Scheer, U. Vogel, *Chem. Commun.* **2006**, 4542–4544.
[76] a) N. A. Pushkarevsky, S. N. Konchenko, A. V. Virovets, M. Scheer, *Organometallics* **2013**, *32*, 770–779; b) M. Stubenhofer, G. Lassandro, G. Balázs, A. Y. Timoshkinb, M. Scheer, *Chem. Commun.* **2012**, *48*, 7262–7264; c) O. C. Presly, T. J. Davin, M. Green, R. J. Kilby, S. M. Mansell, J. E. McGrady, C. A. Russell, *Eur. J. Inorg. Chem.* **2008**, *29*, 4511–4515; d) R. Streubel, M. Bode, G. von Frantzius, C. Hrib, P. G. Jones, A. Monsees, *Organometallics* **2007**, *26*, 1371–1375.
[77] P. Jutzi, H. Saleske, D. Nadler, *J. Organomet. Chem.* **1976**, *118*, C8-C10.
[78] M. A. Sprung, *Chem. Rev.* **1940**, *26*, 297–338.
[79] D. N. Robertson, *J. Org. Chem.* **1960**, *25*, 47–49.
[80] J. M. Villalba Franco, G. Schnakenburg, A. Espinosa Ferao, R. Streubel, *Chem. Eur. J.* **2015**, *21*, 3727–3735.

[81] J. M. Villalba Franco, A. Espinosa Ferao, G. Schnakenburg, R. Streubel, *Chem. Commun.* **2013**, *49*, 9648–9650.
[82] W. M. Haynes, D. R. Lide, *CRC handbook of chemistry and physics*. *A ready-reference book of chemical and physical data : 2012-2013*, CRC Press, Boca Raton (Fla.), London, New York, **2012**.
[83] a) X. Sava, A. Marinetti, L. Ricard, F. Mathey, *Eur. J. Inorg. Chem.*, **2002**, *2002*, 1657–1665; b) X. Sava, A. Marinetti, L. Ricard, F. Mathey, *Eur. J. Inorg. Chem.* **2002**, *2002*, 1657–1665.
[84] T. Kawashima, T. Kihara, N. Inamoto, *Chem. Lett.* **1988**, 577–580.
[85] a) M. J. M. Vlaar, A. W. Ehlers, M. Schakel, S. B. Clendenning, J. F. Nixon, M. Lutz, A. L. Spek, K. Lammertsma, *Chem-Eur. J.* **2001**, *7*, 3545–3550; b) M. J. M. Vlaar, Mark J. M. van Assema, Sander G. A. de Kanter, Frans J. J. Schakel, Marius Spek Anthony, Lutz Martin, Lammertsma Koop, *Chem-Eur. J.* **2002**, *8*, 58–65; c) R. Streubel, M. Bode, G. von Frantzius, C. Hrib, P. G. Jones, A. Monsees, *Organometallics* **2007**, *26*, 1371–1375.
[86] R. Streubel, U. Rohde, J. Jeske, F. Ruthe, P. G. Jones, *Eur. J. Inorg. Chem.* **1998**, *1998*, 2005–2012.
[87] a) M. J. M. Vlaar, P. Valkier, de Kanter, Frans J. J., M. Schakel, A. W. Ehlers, A. L. Spek, M. Lutz, K. Lammertsma, *Chem. Eur. J.* **2001**, *7*, 3551; b) M. J. M. Vlaar, P. Valkier, M. Schakel, A. W. Ehlers, M. Lutz, A. L. Spek, K. Lammertsma, *Eur. J. Org. Chem.* **2002**, *2002*, 1797–1802.
[88] G. von Frantzius, A. Espinosa Ferao, R. Streubel, *Chem. Sci.* **2013**, *4*, 4309.
[89] Y. Mao, Z. Wang, R. Ganguly, F. Mathey, *Organometallics* **2012**, *31*, 4786–4790.
[90] J. B. Wit, van Eijkel, Gerno T, M. Schakel, K. Lammertsma, *Tetrahedron* **2000**, *56*, 137–141.
[91] A. E. Reed, F. Weinhold, *J. Chem. Phys.* **1983**, *78*, 4066–4073.
[92] K. B. Wiberg, *Tetrahedron* **1968**, *24*, 1083–1096.
[93] a) I. Mayer, *Int. J. Quantum Chem.* **1984**, *26*, 151–154; b) I. Mayer, *Chem. Phys. Lett.* **1983**, *97*, 270–274; c) I. Mayer, *Theoret. Chim. Acta* **1985**, *67*, 315–322; d) A. J. Bridgeman, G. Cavigliasso, L. R. Ireland, J. Rothery, *Dalton trans.* **2001**, 2095–2108.
[94] P.-O. Löwdin (Ed.) *Advances in Quantum Chemistry*, Elsevier, **1970**.
[95] R. F. W. Bader, *Chem. Rev.* **1991**, *91*, 893–928.
[96] C. F. Matta, R. J. Boyd, *The quantum theory of atoms in molecules*. *From solid state to DNA and drug design*, Wiley-VCH, Weinheim, **2007**.
[97] E. M. Sproviero, G. Burton, *J. Phys. Chem. A* **2003**, *107*, 5544–5554.
[98] X. Sava, A. Marinetti, L. Ricard, F. Mathey, *Eur. J. Inorg. Chem.* **2002**, *2002*, 1657–1665.
[99] a) K. B. Wiberg, *Angew. Chem.* **1986**, *98*, 312–322; *Angew. Chem. Int. Ed.* **1986**, *25*, 312–322.
[100] A. M. de Lio, B. L. Durfey, A. L. Gille, T. M. Gilbert, *J Phys Chem A* **2014**, *118*, 6050–6059.
[101] A. Bauzá, D. Quiñonero, P. M. Deyà, A. Frontera, *Chem. Phys. Lett.* **2012**, *536*, 165–169.
[102] K. B. Wiberg, R. A. Fenoglio, *J. Am. Chem. Soc.* **1968**, *90*, 3395–3397.
[103] W. T. G. Johnson, W. T. Borden, *J. Am. Chem. Soc.* **1997**, *119*, 5930–5933.
[104] R. D. Bach, O. Dmitrenko, *J. Am. Chem. Soc.* **2004**, *126*, 4444–4452.
[105] T. P. M. Goumans, A. W. Ehlers, K. Lammertsma, E.-U. Würthwein, *Eur. J. Org. Chem.* **2003**, *2003*, 2941–2946.
[106] a) H. Quast, *Liebigs Ann.* **1996**, 87; b) H. Quast, A. Fuss, W. Nüdling, *Eur. J. Org. Chem.* **1998**, *1998*, 317–327; c) H. Quast, S. Aldenkortt, B. Freudenreich, P. Schäfer, M. Hagedorn, J. Lehmann, K. Banert, *J. Org. Chem.* **2007**, *72*, 1659–1666; d) H. Quast, S. Aldenkortt, *Chem. Eur. J.* **1996**, *2*, 462–469; e) H. Quast, S. Aldenkortt, E. Heller, P. Schäfer, E. Schmitt, *Chem. Ber.* **1994**, *127*, 1699–1706; f) A. J. Hubert, A. Feron, R. Warin, P. Teyssie, *Tetrahedron Letters* **1976**, *17*, 1317–1318.
[107] H. Quast, E. Schmitt, *Angew. Chem.* **1970**, *82*, 395–396; *Angew. Chem. Int. Ed.* **1970**, *9*, 381–382.

[108] 2 For 2-Phenylimino-3-bis(trimethylsilyl)phosphirane(dicarbonyl)(1,2,3,4,5-pentamethyl cyclopentadienyl)iron complex), see: Weber, Lothar, A. Ruehlicke, H. G. Stammler, B. Neumann, *Organometallics* **1993**, *12*, 4653–4656.

[109] a) H. Quast, K.-H. Ross, G. Philipp, M. Hagedorn, H. Hahn, K. Banert, *Eur. J. Org. Chem.* **2009**, *2009*, 3940–3952; b) H. Quast, L. Bieber, *Angew. Chem. Int. Ed.* **1975**, 428–429; *Angew. Chem.* **1975**, *87*, 422–423.

[110] a) H. Quast, E. Schmitt, *Angew. Chem.* **1969**, *81*, 428–429; *Angew. Chem. Int. Ed.* **1969**, *8*, 448–449.

[111] M. Baudler, J. Simon, *Chem. Ber.* **1987**, *120*, 421–424.

[112] a) D. Lentz, R. Marschall, *Z. Anorg. Allg. Chem.* **1992**, *617*, 53–58; b) J. Buschmann, D. Lentz, M. Röttger, S. Willemsen, *Z. anorg. allg. Chem.* **1999**, *625*, 1934–1939.

[113] L. Weber, S. Buchwald, D. Lentz, O. Stamm, D. Preugschat, R. Marschall, *Organometallics* **1994**, *13*, 4406–4412.

[114] W. M. Abdou, R. F. Barghash, M. S. Bekheit, *Arch. Pharm.* **2012**, *345*, 884–895.

[115] a) D. W. Stephan, G. Erker, *Angew. Chem. Int. Ed.* **2015**, *54*, 6400–6441; *Angew. Chem.* **2015**, *127*, 6498–6541b) D. W. Stephan, *Acc. Chem. Res.* **2015**, *48*, 306–316; c) D. W. Stephan, G. Erker, *Angew. Chem. Int. Ed.* **2010**, *49*, 46–76; d) D. W. Stephan, *Dalton Trans* **2009**, 3129–3136; e) D. W. Stephan, G. Erker, *Angew. Chem.* **2010**, *122*, 50–81.

[116] G. C. Welch, R. R. San Juan, J. D. Masuda, D. W. Stephan, *Science* **2006**, *314*, 1124–1126.

[117] a) P. A. Chase, D. W. Stephan, *Angew. Chem. Int. Ed. Engl.* **2008**, *47*, 7433–7437; *Angew. Chem.* **2008**, *120*, 7543–7547; b) P. A. Chase, G. C. Welch, T. Jurca, D. W. Stephan, *Angew. Chem. Int. Ed. Engl.* **2007**, *46*, 8050–8053; *Angew. Chem.* **2007**, *119*, 8196–8199.

[118] a) P. Spies, S. Schwendemann, S. Lange, G. Kehr, R. Fröhlich, G. Erker, *Angew. Chem. Int. Ed.* **2008**, *47*, 7543–7546; *Angew. Chem.* **2008**, *120*, 7654–7657.

[119] H. Wang, R. Fröhlich, G. Kehr, G. Erker, *Chem. Commun.* **2008**, 5966–5968.

[120] a) L. Greb, P. Oña-Burgos, B. Schirmer, S. Grimme, D. W. Stephan, J. Paradies, *Angew. Chem. Int. Ed.* **2012**, *51*, 10164–10168; *Angew. Chem.* **2012**, *124*, 10311–10315; b) L. Greb, S. Tussing, B. Schirmer, P. Oña-Burgos, K. Kaupmees, M. Lõkov, I. Leito, S. Grimme, J. Paradies, *Chem. Sci.* **2013**, *4*, 2788.

[121] K. Chernichenko, Á. Madarász, I. Pápai, M. Nieger, M. Leskelä, T. Repo, *Nat. chem.* **2013**, *5*, 718–723.

[122] a) B. Inés, D. Palomas, S. Holle, S. Steinberg, J. A. Nicasio, M. Alcarazo, *Angew. Chem. Int. Ed.* **2012**, *51*, 12367–12369; *Angew. Chem.* **2012**, *124*, 12533–12536; b) L. Greb, C.-G. Daniliuc, K. Bergander, J. Paradies, *Angew. Chem. Int. Ed.* **2013**, *52*, 5876–5879; *Angew. Chem.* **2013**, *125*, 5989–5992.

[123] a) B.-H. Xu, R. A. A. Yanez, H. Nakatsuka, M. Kitamura, R. Fröhlich, G. Kehr, G. Erker, *Chem. Asian. J.* **2012**, *7*, 1347–1356; b) B.-H. Xu, G. Kehr, R. Fröhlich, B. Wibbeling, B. Schirmer, S. Grimme, G. Erker, *Angew. Chem. Int. Ed.* **2011**, *50*, 7183–7186; *Angew. Chem.* **2011**, *123*, 7321–7324.

[124] a) T. Mahdi, Z. M. Heiden, S. Grimme, D. W. Stephan, *J. Am. Chem. Soc.* **2012**, *134*, 4088–4091; b) Y. Segawa, D. W. Stephan, *Chem. Commun.* **2012**, *48*, 11963–11965.

[125] a) Z. M. Heiden, D. W. Stephan, *Chem. Commun.* **2011**, *47*, 5729–5731; b) D. Chen, J. Klankermayer, *Chem. Commun.* **2008**, 2130–2131.

[126] C. M. Mömming, E. Otten, G. Kehr, R. Fröhlich, S. Grimme, D. W. Stephan, G. Erker, *Angew. Chem. Int. Ed. Engl.* **2009**, *48*, 6643–6646; *Angew. Chem.* **2009**, *121*, 6770–6773.

[127] a) R. C. Neu, G. Ménard, D. W. Stephan, *Dalton Trans* **2012**, *41*, 9016–9018; b) I. Peuser, R. C. Neu, X. Zhao, M. Ulrich, B. Schirmer, J. A. Tannert, G. Kehr, R. Fröhlich, S. Grimme, G. Erker et al., *Chem. Eur. J.* **2011**, *17*, 9640–9650; c) D. Voicu, M. Abolhasani, R. Choueiri, G. Lestari, C. Seiler, G. Menard, J. Greener, A. Guenther, D. W. Stephan, E. Kumacheva, *J. Am. Chem. Soc.* **2014**, *136*, 3875–3880; d) M. Harhausen, R. Fröhlich, G. Kehr, G. Erker, *Organometallics* **2012**, *31*, 2801–2809.

[128] T. Voss, T. Mahdi, E. Otten, R. Fröhlich, G. Kehr, D. W. Stephan, G. Erker, *Organometallics* **2012**, *31*, 2367–2378.

[129] a) M. Feroci, I. Chiarotto, S. V. Ciprioti, A. Inesi, *Electrochimica Acta* **2013**, *109*, 95–101; b) J. D. Holbrey, W. M. Reichert, I. Tkatchenko, E. Bouajila, O. Walter, I. Tommasi, R. D. Rogers, *Chem. Commun.* **2003**, 28–29; c) E. L. Kolychev, T. Bannenberg, M. Freytag, C. G. Daniliuc, P. G. Jones, M. Tamm, *Chem. Eur. J.* **2012**, *18*, 16938–16946; d) E. Theuergarten, T. Bannenberg, M. D. Walter, D. Holschumacher, M. Freytag, C. G. Daniliuc, P. G. Jones, M. Tamm, *Dalton Trans* **2014**, *43*, 1651–1662.

[130] a) C. Appelt, H. Westenberg, F. Bertini, A. W. Ehlers, J. C. Slootweg, K. Lammertsma, W. Uhl, *Angew. Chem. Int. Ed. Engl.* **2011**, *50*, 3925–3928; *Angew. Chem.* **2011**, *123*, 4011–4014.

[131] a) J. Boudreau, M.-A. Courtemanche, F.-G. Fontaine, *Chem. Commun.* **2011**, *47*, 11131–11133; b) G. Ménard, T. M. Gilbert, J. A. Hatnean, A. Kraft, I. Krossing, D. W. Stephan, *Organometallics* **2013**, *32*, 4416–4422.

[132] O. Ekkert, G. G. Miera, T. Wiegand, B. Eckert, Petersen, C. G. Daniliuc, R. Fröhlich, S. Grimme, G. Kehr, G. Erker, *Chem. Sci.* **2013**, *4*, 2657–2664.

[133] M. Sajid, A. Lawzer, W. Dong, C. Rosorius, W. Sander, B. Schirmer, S. Grimme, C. G. Daniliuc, G. Kehr, G. Erker, *J. Am. Chem. Soc.* **2013**, *135*, 18567–18574.

[134] M. A. Dureen, D. W. Stephan, *J. Am. Chem. Soc.* **2010**, *132*, 13559–13568.

[135] a) A. Hinz, A. Schulz, A. Villinger, *Angew. Chem. Int. Ed. Engl.* **2015**, *54*, 2776–2779; *Angew. Chem.* **2015**, *127*, 2815–2819.

[136] M. Sajid, A. Klose, B. Birkmann, L. Liang, B. Schirmer, T. Wiegand, H. Eckert, A. J. Lough, R. Fröhlich, C. G. Daniliuc et al., *Chem. Sci.* **2013**, *4*, 213–219.

[137] a) G. Ménard, J. A. Hatnean, H. J. Cowley, A. J. Lough, J. M. Rawson, D. W. Stephan, *J. Am. Chem. Soc.* **2013**, *135*, 6446–6449; b) E. Otten, R. C. Neu, D. W. Stephan, *J. Am. Chem. Soc.* **2009**, *131*, 9918–9919.

[138] a) A. J. P. Cardenas, B. J. Culotta, T. H. Warren, S. Grimme, A. Stute, R. Fröhlich, G. Kehr, G. Erker, *Angew. Chem. Int. Ed. Engl.* **2011**, *50*, 7567–7571; *Angew. Chem.* **2011**, *123*, 7709–7713.

[139] C. Murcia-García, A. Bauzá, G. Schnakenburg, A. Frontera, R. Streubel, *CrystEngComm* **2015**, *17*, 1769–1772.

[140] M. Klein, C. Albrecht, G. Schnakenburg, R. Streubel, *Organometallics* **2013**, *32*, 4938–4943.

[141] R. Streubel, J. Faßbender, G. Schnakenburg, A. Espinosa Ferao, *Organometallics* **2015**, 150616142707003.

[142] a) L. J. Hounjet, C. B. Caputo, D. W. Stephan, *Angew. Chem. Int. Ed. Engl.* **2012**, *51*, 4714–4717; *Angew. Chem.* **2012**, *124*, 4792–4795.

[143] J. M. Villalba Franco, G. Schnakenburg, T. Sasamori, A. Espinosa Ferao, R. Streubel, *Chem. Eur. J.* **2015**.

[144] J. M. Villalba Franco, T. Sasamori, G. Schnakenburg, A. Espinosa Ferao, R. Streubel, *Chem. Commun.* **2015**, *51*, 3878–3881.

[145] A. Espinosa, E. de las Heras, R. Streubel, *Inorg. Chem.* **2014**, *53*, 6132–6140.

[146] a) H. S. Gutowsky, C. H. Holm, *J. Chem. Phys.* **1956**, *25*, 1228–1234; b) A. Shockravi, M. Kamali, F. Sorkhei, R. Jafari, *Heteroat. chem.* **2011**, *22*, 659–668.
[147] H. Eyring, *J. Chem. Phys.* **1935**, *3*, 107–115.
[148] J. Emsley, *The elements*, Clarendon Press; Oxford University Press, Oxford, New York, **1998**.
[149] A. E. Reed, R. B. Weinstock, F. Weinhold, *J. Chem. Phys.* **1985**, *83*, 735.
[150] T. Cottrell, *The strengths of chemical bonds*, Butterworth, London, **1958**.
[151] a) N. G. Connelly, W. E. Geiger, *Chem. Rev.* **1996**, *96*, 877–910; b) A. Özbolat-Schön, M. Bode, G. Schnakenburg, A. Anoop, M. van Gastel, F. Neese, R. Streubel, *Angew. Chem.* **2010**, *122*, 7047–7051; *Angew. Chem. Int. Ed.* **2010**, *49*, 6894–6898; c) V. Nesterov, A. Özbolat-Schön, G. Schnakenburg, L. Shi, A. Cangönül, M. van Gastel, F. Neese, R. Streubel, *Chem. Asian. J.* **2012**, *7*, 1708–1712; d) V. Nesterov, Z.-W. Qu, G. Schnakenburg, S. Grimme, R. Streubel, *Chem. Commun.* **2014**, *50*, 12508–12511.
[152] N. Burford, R. E. v. H. Spence, A. Linden, T. S. Cameron, *Acta crystallogr. C* **1990**, *C46*, 92–95.
[153] M. Ghalib, P. G. Jones, G. J. Palm, J. W. Heinicke, *RSC Advances* **2013**, *3*, 17726–17731.
[154] W. Petz, F. Öxler, K. Aicher, B. Neumüller, *Z. anorg. allg. Chem.* **2010**, *636*, 1751–1759.
[155] a) A. Usanmaz, *Acta crystallogr. B* **1979**, *B35*, 1117–1119; b) Z. Guo, X. Wei, H. Tong, D. Liu, *J. Organomet. Chem.* **2015**, *776*, 136–142.
[156] E. R. Johnson, S. Keinan, P. Mori-Sánchez, J. Contreras-García, A. J. Cohen, W. Yang, *J. Am. Chem. Soc.* **2010**, *132*, 6498–6506.
[157] a) P. Szczeciński, *J. Organomet. Chem.* **1992**, *423*, 23–29; b) P. Szczeciński, K. Wiśniewski, *J. Organomet. Chem.* **1992**, *423*, C13-C15.
[158] O. Kolodyazhnyi, *Russ. J. Gen. Chem* **1982**, *52*, 2361–2362.
[159] G. von Frantzius, A. Espinosa Ferao, R. Streubel, *Chem. Sci.* **2013**, *4*, 4309.
[160] M. Yoshifuji, T. Niitsu, K. Toyota, N. Inamoto, K. Hirotsu, Y. Odagaki, T. Higuchi, S. Nagase, *Polyhedron* **1988**, *7*, 2213–2216.
[161] E. Ionescu, G. von Frantzius, P. G. Jones, R. Streubel, *Organometallics* **2005**, *24*, 2237–2240.
[162] M. Seidl, M. Schiffer, M. Bodensteiner, A. Y. Timoshkin, M. Scheer, *Chem. Eur. J.* **2013**, *19*, 13783–13791.
[163] M. Klein, G. Schnakenburg, A. Espinosa Ferao, N. Tokitoh, R. Streubel, *Eur. J. Inorg. Chem.*, submited.
[164] U. Dressler, E. Niecke, S. Pohl, W. Saak, W. W. Schoeller, H.-G. Schäfer, *Chem. Commun.* **1986**, 1086.
[165] J. Kerth, T. Jikyo, G. Maas, *Eur. J. Org. Chem.* **2003**, *2003*, 1894–1903.
[166] J. Dietz, J. Renner, U. Bergsträßer, P. Binger, M. Regitz, *Eur. J. Org. Chem.* **2003**, *2003*, 512–525.
[167] T. Jikyo, G. Maas, *Chem. Commun.* **2003**, 2794.
[168] M. D. Rudd, S. V. Lindeman, S. Husebye, O. R. Konestabo, E. J. Samuelsen, W. T. Robinson, K. Undheim, C. N. Rosendahl, M. Haugg, N. Trabesinger-Rüf et al., *Acta Chem. Scand.* **1996**, *50*, 759–774.
[169] N. Tokitoh, T. Sasamori, R. Okazaki, *Chem. Lett.* **1998**, *8*, 725–726.
[170] J. Laube, S. Jäger, C. Thöne, *Eur. J. Inorg. Chem.* **2001**, *2001*, 1983–1992.
[171] M. L. Helm, P. B. Hitchcock, J. F. Nixon, L. Nyulászi, D. Szieberth, *J. Organomet. Chem.* **2002**, *659*, 84–91.
[172] D. D. Perrin, W. L. F. Armarego, *Purification of laboratory chemicals*, Butterworth Heinemann, Oxford, Boston, **1988**.

[173] G. M. Bodner, S. B. Kahl, K. Bork, B. N. Storhoff, J. E. Wuller, L. J. Todd, *Inorg. Chem.* **1973**, *12*, 1071–1074.
[174] V. Plack, J. R. Goerlich, A. Fischer, H. Thönnessen, P. G. Jones, R. Schmutzler, *Z. Anorg. Allg. Chem.* **1995**, *621*, 1080–1092.
[175] U. Koelle, *J. Organomet. Chem.* **1977**, *133*, 53–58.

8. Appendix

8.1 Crystal data and structure refinement of **4b**

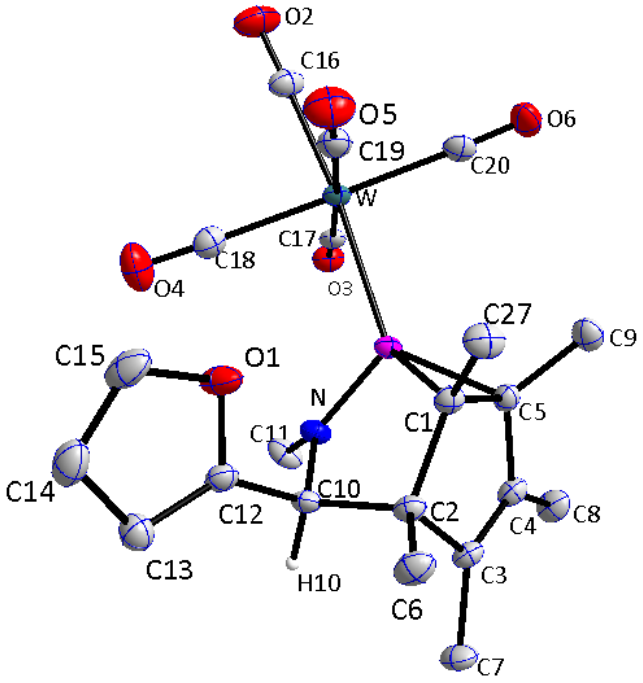

Table 8.1. Crystal data and structure refinement for **4b**.

Identification code	GSTR215, Greg1752f
Device Type	Bruker X8-KappaApexII
Empirical formula	C21 H22 N O6 P W
Moiety formula	C21 H22 N O6 P W
Formula weight	599.22
Temperature/K	100(2) K
Crystal system	Triclinic
Space group	P-1
a/Å	8.8600
b/Å	10.8854(5)
c/Å	12.8306(5)
α/°	86.595(2)
β/°	78.246(2)
γ/°	66.290(2)
Volume/Å^3	1108.89(8)
Z	2

ρ_{calc}g/cm^3	1.795
μ/mm^{-1}	5.317
F(000)	584
Crystal size/mm^3	0.50 x 0.27 x 0.26
Absorption correction	Semi-empirical from equivalents
Tmin; Tmax	0.3386; 0.1763
Radiation	MoKα (λ = 0.71073)
2Θ range for data collection/°	3.24 to 28.00°
Completeness to theta	0.996
Index ranges	-11 ≤ h ≤ 11, -174≤ k ≤ 14, -16≤ l ≤ 16
Reflections collected	13781
Independent reflections	5338 [R(int) = 0.0261]
Data/restraints/parameters	5338 / 6 / 277
Goodness-of-fit on F^2	1.034
Final R indexes [I>=2σ (I)]	R1 = 0.0174, wR2 = 0.0404
Final R indexes [all data]	R1 = 0.0184, wR2 = 0.0410
Largest diff. peak/hole / e Å^{-3}	1.121/-0.936

8.2 Crystal data and structure refinement of **12**

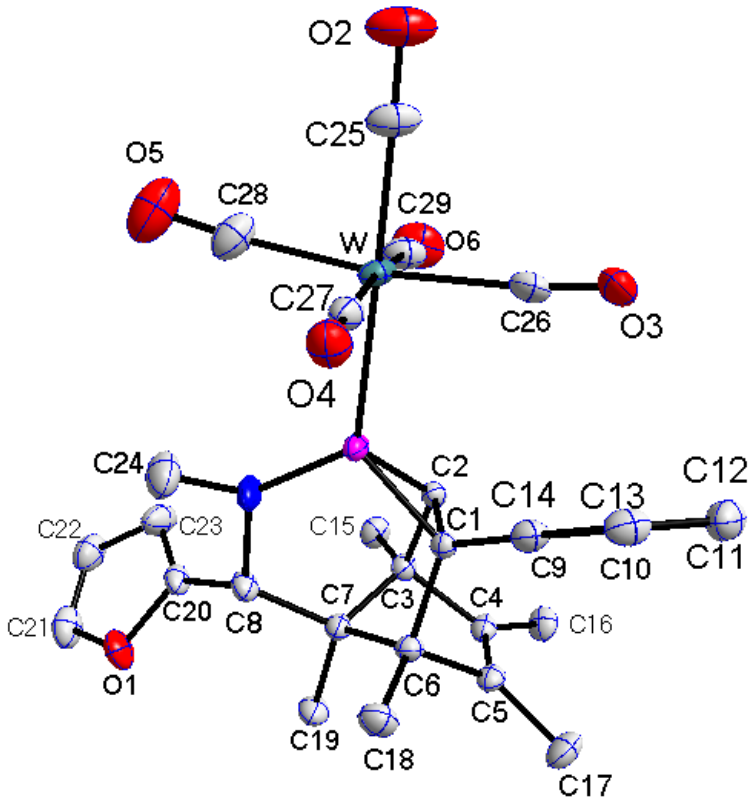

Table 8.2. Crystal data and structure refinement for **12**.

Identification code	GSTR253, Greg2252
Device Type	Nonius KappaCCD
Empirical formula	C29 H28 N O6 P W
Moiety formula	C29 H28 N O6 P W
Formula weight	701.34
Temperature/K	123(2) K
Crystal system	Monoclinic
Space group	P 21/n
a/Å	9.32930(10)
b/Å	18.8398(3)
c/Å	16.1143(2)
α/°	90
β/°	101.8670(8)
γ/°	90
Volume/Å^3	2771.75(6)
Z	4
ρ_{calc}g/cm^3	1.681

μ/mm^{-1}	4.268
F(000)	1384
Crystal size/mm^3	0.43 x 0.23 x 0.10
Absorption correction	Semi-empirical from equivalents
Tmin; Tmax	0.6749; 0.2612
Radiation	MoKα (λ = 0.71073)
2Θ range for data collection/°	3.18 to 28.00°
Completeness to theta	0.997
Index ranges	-12 ≤ h ≤ 11, -23≤ k ≤ 24, -20≤ l ≤ 21
Reflections collected	52522
Independent reflections	6681 [R(int) = 0.0494]
Data/restraints/parameters	6681 / 63 / 349
Goodness-of-fit on F^2	1.086
Final R indexes [I>=2σ (I)]	R1 = 0.0249, wR2 = 0.0576
Final R indexes [all data]	R1 = 0.0302, wR2 = 0.0594
Largest diff. peak/hole / e $Å^{-3}$	1.382/-2.255

8.3 Crystal data and structure refinment of **15f**

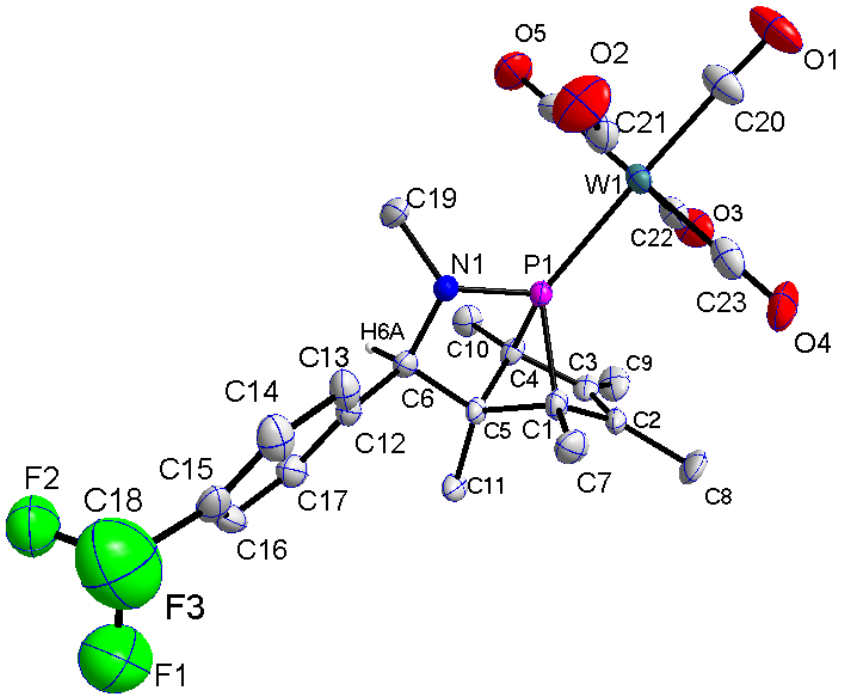

Table 8.3. Crystal data and structure refinement for **15f**.

Identification code	GSTR221, Greg1803
Device Type	Nonius KappaCCD
Empirical formula	C24 H23 F3 N O5 P W
Moiety formula	C24 H23 F3 N O5 P W
Formula weight	677.25
Temperature/K	123(2) K
Crystal system	Monoclinic
Space group	P 21/n
a/Å	12.3385(4)
b/Å	16.5060(3)
c/Å	25.2801(7)
α/°	90
β/°	92.6450(13)
γ/°	90
Volume/Å^3	5143.0(2)
Z	8
ρ_{calc}g/cm^3	1.749

μ/mm^{-1}	4.610
F(000)	2640
Crystal size/mm^3	0.27 x 0.23 x 0.10
Absorption correction	Semi-empirical from equivalents
Tmin; Tmax	0.6557; 0.3691
Radiation	MoKα (λ = 0.71073)
2Θ range for data collection/°	2.66 to 27.00°
Completeness to theta	0.992
Index ranges	-12 ≤ h ≤ 15, -18≤ k ≤ 20, -28≤ l ≤ 32
Reflections collected	33545
Independent reflections	11123 [R(int) = 0.0787]
Data/restraints/parameters	11123 / 47 / 643
Goodness-of-fit on F^2	0.970
Final R indexes [I>=2σ (I)]	R1 = 0.0452, wR2 = 0.1086
Final R indexes [all data]	R1 = 0.0706, wR2 = 0.1180
Largest diff. peak/hole / e $Å^{-3}$	2.597/-2.512

8.4 Crystal data and structure refinment of **17**

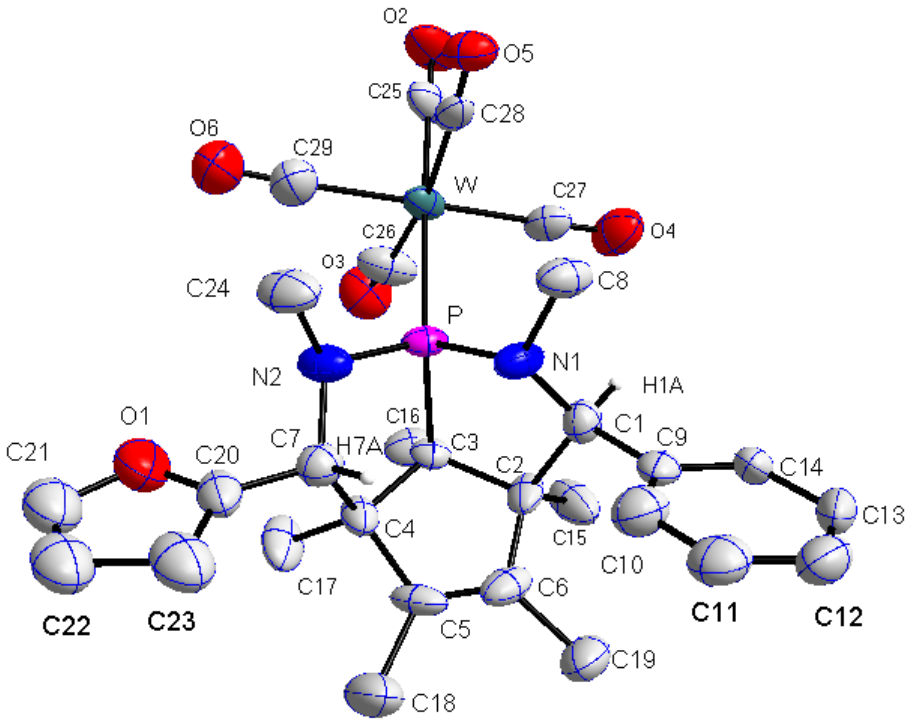

Table 8.4. Crystal data and structure refinement for **17**.

Identification code	GSTR248, 2235f
Device Type	Nonius KappaCCD
Empirical formula	C29 H31 N2 O6 P W
Moiety formula	C29 H31 N2 O6 P W
Formula weight	718.38
Temperature/K	123(2) K
Crystal system	Triclinic
Space group	P-1
a/Å	8.6782(12)
b/Å	10.8622(16)
c/Å	17.391(3)
α/°	105.044(7)
β/°	93.225(7)
γ/°	111.375(4)
Volume/Å^3	1453.4(4)
Z	2

ρ_{calc}g/cm^3	1.642
μ/mm^{-1}	4.073
F(000)	712
Crystal size/mm^3	0.22 x 0.16 x 0.08
Absorption correction	Empirical
Tmin; Tmax	0.7365; 0.4677
Radiation	MoKα (λ = 0.71073)
2Θ range for data collection/°	2.10 to 26.00°
Completeness to theta	0.999
Index ranges	-10 ≤ h ≤ 10, -13≤ k ≤ 13, -21≤ l ≤ 21
Reflections collected	38310
Independent reflections	5716 [R(int) = 0.0439]
Data/restraints/parameters	5716 / 149 / 359
Goodness-of-fit on F^2	1.148
Final R indexes [I>=2σ (I)]	R1 = 0.0544, wR2 = 0.1279
Final R indexes [all data]	R1 = 0.0650, wR2 = 0.1339
Largest diff. peak/hole / e Å^{-3}	3.117/-1.861

8.5. Crystal data and structure refinement for **21a**

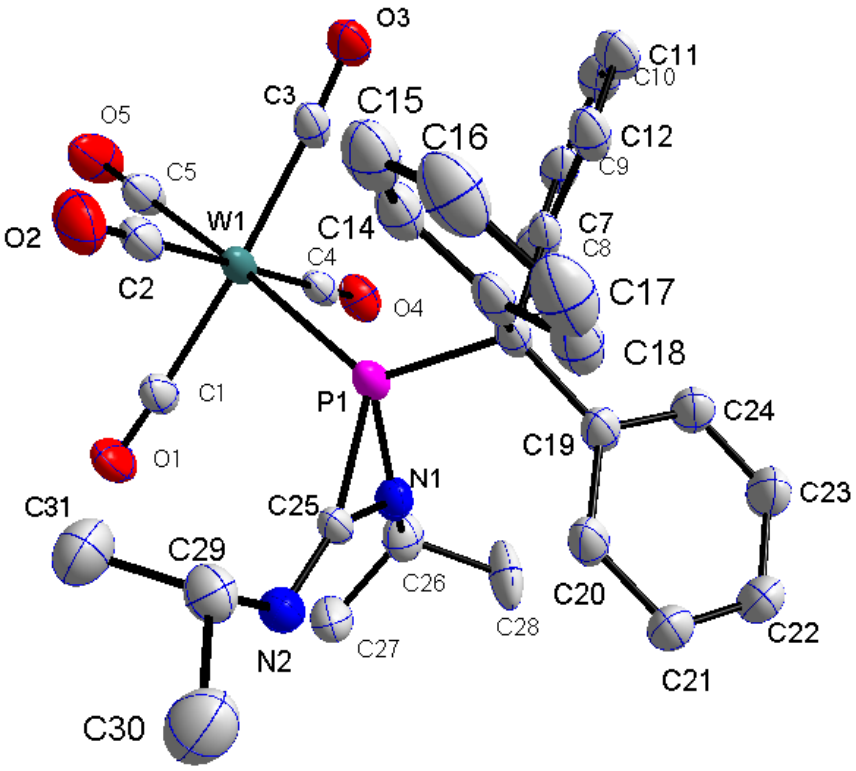

Table 8.5. Crystal data and structure refinement for **21a**.

Identification code	Jmv
Device Type	SPring-8
Empirical formula	C31 H29 N2 O5 P W
Moiety formula	C31 H29 N2 O5 P W
Formula weight	724.38
Temperature/K	93(2) K
Crystal system	Monoclinic
Space group	*P*2/a
a/Å	13.91610(10)
b/Å	13.26790(10)
c/Å	16.14500(10)
α/°	90
β/°	104.1771(4)
γ/°	90
Volume/Å^3	2890.18(4)
Z	4
ρ_{calc}g/cm^3	1.665

μ/mm^{-1}	5.518
F(000)	1432
Crystal size/mm^3	0.02 x 0.01 x 0.01
Absorption correction	Empirical
Tmin; Tmax	0.9469; 0.8976
Radiation	MoKα (λ = 0.80000)
2Θ range for data collection/°	1.46 to 29.5°
Completeness to theta	0.984
Index ranges	-10 ≤ h ≤ 10, -13≤ k ≤ 13, -21≤ l ≤ 21
Reflections collected	64704
Independent reflections	5358 [R(int) = 0.0528]
Data/restraints/parameters	5358 / 31 / 443
Goodness-of-fit on F^2	1.101
Final R indexes [I>=2σ (I)]	R1 = 0.0315, wR2 = 0.0878
Final R indexes [all data]	R1 = 0.0319, wR2 = 0.0885
Largest diff. peak/hole / e Å^{-3}	0.815/-3.198
Disorder (79:21), iPr-N=C-N-iPr moiety	

8.6. Crystal data and structure refinement for **22a**

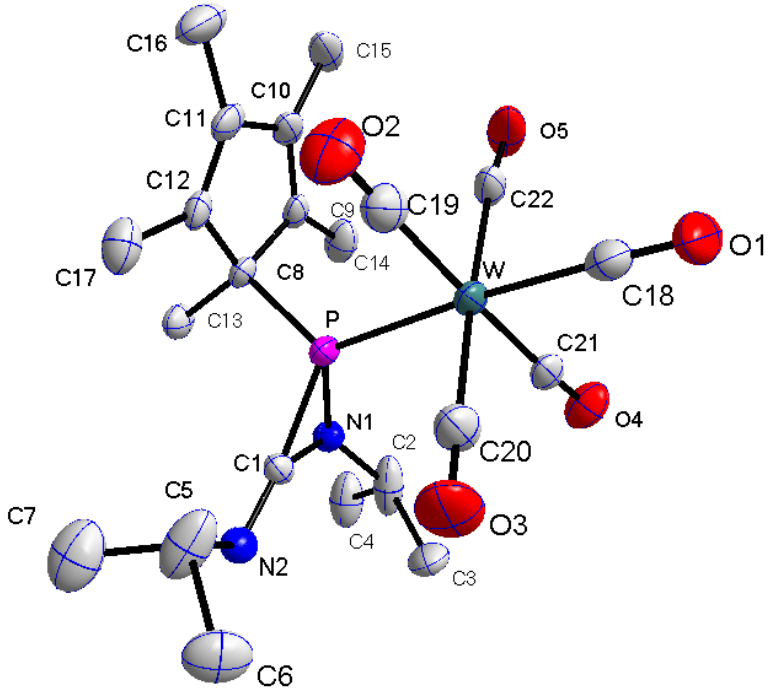

Table 8.6. Crystal data and structure refinement for **22a**.

Identification code	318 // GXray3299f
Device Type	Bruker X8-KappaApex-II
Empirical formula	$C_{22}H_{29}N_2O_5PW$
Formula weight	616.29
Temperature/K	100.15
Crystal system	Triclinic
Space group	P-1
a/Å	10.9909(5)
b/Å	11.0605(6)
c/Å	12.8740(10)
α/°	108.084(4)
β/°	95.194(4)
γ/°	118.186(2)
Volume/Å^3	1257.68(14)
Z	2
ρ_{calc}g/cm^3	1.627
μ/mm^{-1}	4.688
F(000)	608.0
Crystal size/mm^3	0.26 × 0.06 × 0.02
Absorption correction	empirical
Tmin; Tmax	0.5393; 0.7460
Radiation	MoKα (λ = 0.71073)

2Θ range for data collection/°	6.316 to 55.994°
Completeness to theta	0.996
Index ranges	$-14 \leq h \leq 14$, $-14 \leq k \leq 14$, $-16 \leq l \leq 16$
Reflections collected	12812
Independent reflections	6035 [R_{int} = 0.0322, R_{sigma} = 0.0489]
Data/restraints/parameters	6035/2/339
Goodness-of-fit on F^2	1.026
Final R indexes [I>=2σ (I)]	R_1 = 0.0290, wR_2 = 0.0569
Final R indexes [all data]	R_1 = 0.0409, wR_2 = 0.0610
Largest diff. peak/hole / e $Å^{-3}$	0.97/-1.27

8.7. Crystal data and structure refinement for **25**

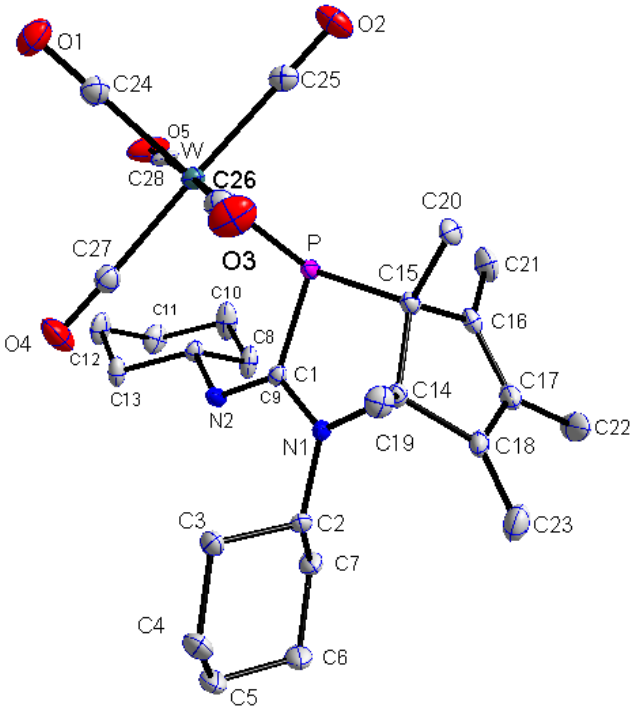

Table 8.7. Crystal data and structure refinement for **25**.

Identification code	GSTR270, 2433f
Device Type	Nonius KappaCCD
Empirical formula	C28 H39 N2 O5 P W
Formula weight	698.43
Temperature/K	123(2)
Crystal system	triclinic
Space group	P-1
a/Å	11.7278(12)
b/Å	12.0308(12)
c/Å	12.1600(12)
α/°	65.513(3)
β/°	72.612(4)
γ/°	69.370(4)
Volume/Å^3	1437.6(2)
Z	2
ρ_{calc}g/cm^3	1.614
μ/mm^{-1}	4.112
F(000)	700
Crystal size/mm^3	0.40 x 0.38 x 0.32
Absorption correction	empirical
Tmin; Tmax	0.3528; 0.2900

Radiation	MoKα (λ = 0.71073)
2Θ range for data collection/°	1.89 to 28.00°
Completeness to theta	0.999
Index ranges	-15 ≤ h ≤ 15, -15≤ k ≤ 15, -16 ≤ l ≤ 16
Reflections collected	80361
Independent reflections	6035 6938 [R(int) = 0.0279]
Data/restraints/parameters	6938 / 92 / 345
Goodness-of-fit on F^2	1.209
Final R indexes [I>=2σ (I)]	R1 = 0.0206, wR2 = 0.0460
Final R indexes [all data]	R1 = 0.0255, wR2 = 0.0502
Largest diff. peak/hole / e $Å^{-3}$	2.777/-1.659

Table 2. Atomic coordinates (x 10^4) and equivalent isotropic displacement parameters (A^2 x 10^3) for JMV227-iF3.
U(eq) is defined as one third of the trace of the orthogonalized Uij tensor.

	x	y	z	U(eq)
W	2258(1)	3890(1)	8749(1)	14(1)
P	2797(1)	1875(1)	8156(1)	12(1)
O(1)	1952(2)	5951(2)	9840(2)	31(1)
O(2)	523(2)	2527(2)	11143(2)	27(1)
O(3)	-154(2)	5566(2)	7567(2)	30(1)
O(4)	3811(2)	5358(2)	6277(2)	32(1)
O(5)	4726(2)	2433(3)	9877(2)	34(1)
N(1)	2814(2)	2435(2)	5778(2)	12(1)
N(2)	4641(2)	2474(2)	6157(2)	13(1)
C(1)	3499(2)	2303(2)	6545(2)	11(1)
C(2)	3159(2)	2878(2)	4418(2)	14(1)
C(3)	3307(3)	4229(3)	3862(2)	18(1)
C(4)	3528(3)	4665(3)	2455(3)	30(1)
C(5)	4628(4)	3745(3)	1974(3)	33(1)
C(6)	4455(3)	2410(3)	2539(3)	29(1)
C(7)	4259(3)	1941(3)	3942(3)	19(1)
C(8)	5556(2)	1894(2)	6973(2)	12(1)
C(9)	6090(3)	493(3)	7163(3)	21(1)
C(10)	7050(3)	-115(3)	8001(4)	31(1)
C(11)	8069(3)	567(3)	7507(3)	26(1)
C(12)	7528(3)	1966(3)	7305(3)	25(1)
C(13)	6572(3)	2575(3)	6457(3)	20(1)
C(14)	1540(2)	2230(2)	6350(2)	13(1)
C(15)	1555(2)	1544(2)	7756(2)	13(1)
C(16)	1906(2)	147(3)	7904(2)	16(1)
C(17)	1750(3)	23(3)	6883(3)	20(1)
C(18)	1399(2)	1228(3)	5965(3)	16(1)
C(19)	590(2)	3499(3)	5981(3)	18(1)
C(20)	291(2)	1857(3)	8569(3)	18(1)

C(21)	2256(3)	-856(3)	9021(3)	27(1)
C(22)	1878(4)	-1204(3)	6751(3)	31(1)
C(23)	955(3)	1472(3)	4930(3)	28(1)
C(24)	2044(3)	5207(3)	9432(3)	20(1)
C(25)	1157(3)	2998(3)	10294(2)	17(1)
C(26)	712(3)	4928(3)	7990(3)	18(1)
C(27)	3264(3)	4807(3)	7169(3)	18(1)
C(28)	3830(3)	2934(3)	9493(2)	18(1)

Table 3. Bond lengths [A] and angles [deg] for JMV227-iF3.

W-C(24)	1.987(3)
W-C(27)	2.026(3)
W-C(26)	2.036(3)
W-C(28)	2.045(3)
W-C(25)	2.050(3)
W-P	2.6253(7)
P-C(1)	1.810(3)
P-C(15)	1.874(3)
P-H(24)	1.41(3)
O(1)-C(24)	1.152(4)
O(2)-C(25)	1.137(3)
O(3)-C(26)	1.149(4)
O(4)-C(27)	1.146(4)
O(5)-C(28)	1.140(4)
N(1)-C(1)	1.333(3)
N(1)-C(2)	1.484(3)
N(1)-C(14)	1.509(3)
N(2)-C(1)	1.339(3)
N(2)-C(8)	1.470(3)
N(2)-H(25)	0.84(3)
C(2)-C(7)	1.529(4)
C(2)-C(3)	1.532(4)
C(2)-H(2A)	1.0000
C(3)-C(4)	1.534(4)
C(3)-H(3A)	0.9900
C(3)-H(3B)	0.9900
C(4)-C(5)	1.520(5)
C(4)-H(4A)	0.9900
C(4)-H(4B)	0.9900
C(5)-C(6)	1.526(4)
C(5)-H(5A)	0.9900
C(5)-H(5B)	0.9900
C(6)-C(7)	1.530(4)
C(6)-H(6A)	0.9900
C(6)-H(6B)	0.9900
C(7)-H(7A)	0.9900
C(7)-H(7B)	0.9900
C(8)-C(13)	1.516(4)
C(8)-C(9)	1.519(4)
C(8)-H(8A)	1.0000
C(9)-C(10)	1.526(4)
C(9)-H(9A)	0.9900

C(9)-H(9B)	0.9900
C(10)-C(11)	1.522(4)
C(10)-H(10A)	0.9900
C(10)-H(10B)	0.9900
C(11)-C(12)	1.514(4)
C(11)-H(11A)	0.9900
C(11)-H(11B)	0.9900
C(12)-C(13)	1.531(4)
C(12)-H(12A)	0.9900
C(12)-H(12B)	0.9900
C(13)-H(13A)	0.9900
C(13)-H(13B)	0.9900
C(14)-C(19)	1.518(4)
C(14)-C(18)	1.533(4)
C(14)-C(15)	1.563(3)
C(15)-C(16)	1.527(4)
C(15)-C(20)	1.535(4)
C(16)-C(17)	1.381(4)
C(16)-C(21)	1.447(4)
C(17)-C(18)	1.425(4)
C(17)-C(22)	1.500(4)
C(18)-C(23)	1.386(4)
C(19)-H(19A)	0.9800
C(19)-H(19B)	0.9800
C(19)-H(19C)	0.9800
C(20)-H(20A)	0.9800
C(20)-H(20B)	0.9800
C(20)-H(20C)	0.9800
C(21)-H(21A)	0.9800
C(21)-H(21B)	0.9800
C(21)-H(21C)	0.9800
C(22)-H(22A)	0.9800
C(22)-H(22B)	0.9800
C(22)-H(22C)	0.9800
C(23)-H(23A)	0.9800
C(23)-H(23B)	0.9800
C(23)-H(23C)	0.9800

C(24)-W-C(27)	90.42(11)
C(24)-W-C(26)	90.18(11)
C(27)-W-C(26)	88.28(11)
C(24)-W-C(28)	87.37(11)
C(27)-W-C(28)	90.03(11)
C(26)-W-C(28)	177.01(11)
C(24)-W-C(25)	90.53(11)
C(27)-W-C(25)	176.70(11)
C(26)-W-C(25)	88.56(11)
C(28)-W-C(25)	93.17(11)
C(24)-W-P	169.37(8)
C(27)-W-P	93.46(8)
C(26)-W-P	99.83(8)
C(28)-W-P	82.73(8)
C(25)-W-P	86.16(8)
C(1)-P-C(15)	87.96(11)
C(1)-P-W	106.66(8)
C(15)-P-W	118.95(9)
C(1)-P-H(24)	117.7(13)
C(15)-P-H(24)	113.1(13)

W-P-H(24)	110.8(13)
C(1)-N(1)-C(2)	125.3(2)
C(1)-N(1)-C(14)	116.3(2)
C(2)-N(1)-C(14)	118.15(19)
C(1)-N(2)-C(8)	121.9(2)
C(1)-N(2)-H(25)	117(2)
C(8)-N(2)-H(25)	117(2)
N(1)-C(1)-N(2)	122.3(2)
N(1)-C(1)-P	116.08(18)
N(2)-C(1)-P	121.57(19)
N(1)-C(2)-C(7)	113.3(2)
N(1)-C(2)-C(3)	113.0(2)
C(7)-C(2)-C(3)	112.9(2)
N(1)-C(2)-H(2A)	105.6
C(7)-C(2)-H(2A)	105.6
C(3)-C(2)-H(2A)	105.6
C(2)-C(3)-C(4)	109.8(2)
C(2)-C(3)-H(3A)	109.7
C(4)-C(3)-H(3A)	109.7
C(2)-C(3)-H(3B)	109.7
C(4)-C(3)-H(3B)	109.7
H(3A)-C(3)-H(3B)	108.2
C(5)-C(4)-C(3)	111.2(3)
C(5)-C(4)-H(4A)	109.4
C(3)-C(4)-H(4A)	109.4
C(5)-C(4)-H(4B)	109.4
C(3)-C(4)-H(4B)	109.4
H(4A)-C(4)-H(4B)	108.0
C(4)-C(5)-C(6)	111.2(3)
C(4)-C(5)-H(5A)	109.4
C(6)-C(5)-H(5A)	109.4
C(4)-C(5)-H(5B)	109.4
C(6)-C(5)-H(5B)	109.4
H(5A)-C(5)-H(5B)	108.0
C(5)-C(6)-C(7)	111.3(2)
C(5)-C(6)-H(6A)	109.4
C(7)-C(6)-H(6A)	109.4
C(5)-C(6)-H(6B)	109.4
C(7)-C(6)-H(6B)	109.4
H(6A)-C(6)-H(6B)	108.0
C(2)-C(7)-C(6)	109.4(2)
C(2)-C(7)-H(7A)	109.8
C(6)-C(7)-H(7A)	109.8
C(2)-C(7)-H(7B)	109.8
C(6)-C(7)-H(7B)	109.8
H(7A)-C(7)-H(7B)	108.2
N(2)-C(8)-C(13)	110.3(2)
N(2)-C(8)-C(9)	110.6(2)
C(13)-C(8)-C(9)	111.0(2)
N(2)-C(8)-H(8A)	108.3
C(13)-C(8)-H(8A)	108.3
C(9)-C(8)-H(8A)	108.3
C(8)-C(9)-C(10)	110.9(2)
C(8)-C(9)-H(9A)	109.5
C(10)-C(9)-H(9A)	109.5
C(8)-C(9)-H(9B)	109.5
C(10)-C(9)-H(9B)	109.5
H(9A)-C(9)-H(9B)	108.0
C(11)-C(10)-C(9)	111.3(3)

C(11)-C(10)-H(10A)	109.4
C(9)-C(10)-H(10A)	109.4
C(11)-C(10)-H(10B)	109.4
C(9)-C(10)-H(10B)	109.4
H(10A)-C(10)-H(10B)	108.0
C(12)-C(11)-C(10)	110.8(3)
C(12)-C(11)-H(11A)	109.5
C(10)-C(11)-H(11A)	109.5
C(12)-C(11)-H(11B)	109.5
C(10)-C(11)-H(11B)	109.5
H(11A)-C(11)-H(11B)	108.1
C(11)-C(12)-C(13)	111.6(2)
C(11)-C(12)-H(12A)	109.3
C(13)-C(12)-H(12A)	109.3
C(11)-C(12)-H(12B)	109.3
C(13)-C(12)-H(12B)	109.3
H(12A)-C(12)-H(12B)	108.0
C(8)-C(13)-C(12)	110.2(2)
C(8)-C(13)-H(13A)	109.6
C(12)-C(13)-H(13A)	109.6
C(8)-C(13)-H(13B)	109.6
C(12)-C(13)-H(13B)	109.6
H(13A)-C(13)-H(13B)	108.1
N(1)-C(14)-C(19)	108.4(2)
N(1)-C(14)-C(18)	108.7(2)
C(19)-C(14)-C(18)	114.2(2)
N(1)-C(14)-C(15)	105.41(19)
C(19)-C(14)-C(15)	116.2(2)
C(18)-C(14)-C(15)	103.3(2)
C(16)-C(15)-C(20)	108.7(2)
C(16)-C(15)-C(14)	102.8(2)
C(20)-C(15)-C(14)	113.7(2)
C(16)-C(15)-P	109.58(17)
C(20)-C(15)-P	112.22(18)
C(14)-C(15)-P	109.38(16)
C(17)-C(16)-C(21)	127.4(3)
C(17)-C(16)-C(15)	110.3(2)
C(21)-C(16)-C(15)	122.2(2)
C(16)-C(17)-C(18)	111.1(2)
C(16)-C(17)-C(22)	125.5(3)
C(18)-C(17)-C(22)	123.4(3)
C(23)-C(18)-C(17)	126.4(3)
C(23)-C(18)-C(14)	125.4(3)
C(17)-C(18)-C(14)	108.1(2)
C(14)-C(19)-H(19A)	109.5
C(14)-C(19)-H(19B)	109.5
H(19A)-C(19)-H(19B)	109.5
C(14)-C(19)-H(19C)	109.5
H(19A)-C(19)-H(19C)	109.5
H(19B)-C(19)-H(19C)	109.5
C(15)-C(20)-H(20A)	109.5
C(15)-C(20)-H(20B)	109.5
H(20A)-C(20)-H(20B)	109.5
C(15)-C(20)-H(20C)	109.5
H(20A)-C(20)-H(20C)	109.5
H(20B)-C(20)-H(20C)	109.5
C(16)-C(21)-H(21A)	109.5
C(16)-C(21)-H(21B)	109.5
H(21A)-C(21)-H(21B)	109.5

C(16)-C(21)-H(21C)	109.5
H(21A)-C(21)-H(21C)	109.5
H(21B)-C(21)-H(21C)	109.5
C(17)-C(22)-H(22A)	109.5
C(17)-C(22)-H(22B)	109.5
H(22A)-C(22)-H(22B)	109.5
C(17)-C(22)-H(22C)	109.5
H(22A)-C(22)-H(22C)	109.5
H(22B)-C(22)-H(22C)	109.5
C(18)-C(23)-H(23A)	109.5
C(18)-C(23)-H(23B)	109.5
H(23A)-C(23)-H(23B)	109.5
C(18)-C(23)-H(23C)	109.5
H(23A)-C(23)-H(23C)	109.5
H(23B)-C(23)-H(23C)	109.5
O(1)-C(24)-W	178.0(3)
O(2)-C(25)-W	178.4(2)
O(3)-C(26)-W	176.6(2)
O(4)-C(27)-W	178.1(3)
O(5)-C(28)-W	177.6(3)

Symmetry transformations used to generate equivalent atoms:

Table 4. Anisotropic displacement parameters (A^2 x 10^3) for JMV227-iF3.

The anisotropic displacement factor exponent takes the form:

-2 pi^2 [h^2 a*^2 U11 + ... + 2 h k a* b* U12]

	U11	U22	U33	U23	U13	U12
W	16(1)	14(1)	13(1)	-5(1)	-2(1)	-4(1)
P	11(1)	14(1)	10(1)	-4(1)	-2(1)	-5(1)
O(1)	39(1)	23(1)	35(1)	-16(1)	-9(1)	-5(1)
O(2)	22(1)	24(1)	23(1)	-2(1)	4(1)	-4(1)
O(3)	29(1)	27(1)	31(1)	-11(1)	-17(1)	5(1)
O(4)	35(1)	32(1)	22(1)	1(1)	0(1)	-18(1)
O(5)	22(1)	56(2)	28(1)	-24(1)	-11(1)	3(1)
N(1)	11(1)	14(1)	11(1)	-3(1)	-2(1)	-6(1)
N(2)	13(1)	17(1)	10(1)	-2(1)	-3(1)	-6(1)
C(1)	13(1)	9(1)	13(1)	-4(1)	-3(1)	-3(1)
C(2)	17(1)	17(1)	10(1)	-3(1)	-4(1)	-8(1)
C(3)	26(1)	14(1)	15(1)	-2(1)	-6(1)	-8(1)
C(4)	50(2)	26(2)	15(1)	3(1)	-9(1)	-21(2)
C(5)	57(2)	36(2)	14(1)	-7(1)	5(1)	-31(2)
C(6)	43(2)	34(2)	17(1)	-13(1)	5(1)	-22(2)
C(7)	24(1)	18(1)	17(1)	-10(1)	1(1)	-8(1)

C(8)	12(1)	12(1)	14(1)	-3(1)	-5(1)	-3(1)
C(9)	17(1)	13(1)	37(2)	-7(1)	-11(1)	-4(1)
C(10)	27(2)	16(1)	49(2)	-1(1)	-22(2)	-4(1)
C(11)	17(1)	27(2)	36(2)	-12(1)	-11(1)	-3(1)
C(12)	23(2)	24(2)	37(2)	-7(1)	-17(1)	-9(1)
C(13)	21(1)	13(1)	28(2)	-3(1)	-10(1)	-8(1)
C(14)	11(1)	14(1)	14(1)	-3(1)	-4(1)	-5(1)
C(15)	11(1)	16(1)	13(1)	-4(1)	-1(1)	-6(1)
C(16)	13(1)	17(1)	17(1)	-4(1)	0(1)	-8(1)
C(17)	20(1)	20(1)	22(1)	-9(1)	4(1)	-11(1)
C(18)	14(1)	19(1)	20(1)	-8(1)	-1(1)	-9(1)
C(19)	15(1)	18(1)	21(1)	-6(1)	-6(1)	-2(1)
C(20)	12(1)	27(1)	19(1)	-10(1)	2(1)	-8(1)
C(21)	26(2)	19(1)	33(2)	-3(1)	-4(1)	-11(1)
C(22)	51(2)	22(2)	26(2)	-10(1)	1(2)	-19(2)
C(23)	28(2)	32(2)	34(2)	-13(1)	-9(1)	-14(1)
C(24)	23(1)	19(1)	18(1)	-6(1)	-4(1)	-6(1)
C(25)	16(1)	14(1)	16(1)	-5(1)	-4(1)	1(1)
C(26)	21(1)	17(1)	17(1)	-8(1)	-4(1)	-3(1)
C(27)	21(1)	16(1)	19(1)	-5(1)	-6(1)	-4(1)
C(28)	21(1)	25(1)	13(1)	-13(1)	-1(1)	-4(1)

Table 5. Hydrogen coordinates (x 10^4) and isotropic displacement parameters (A^2 x 10^3) for JMV227-iF3.

	x	y	z	U(eq)
H(24)	3470(30)	800(30)	8990(30)	14
H(25)	4910(30)	2700(30)	5390(30)	16
H(2A)	2436	2918	4115	17
H(3A)	4016	4254	4125	22
H(3B)	2551	4806	4157	22
H(4A)	2778	4732	2192	36
H(4B)	3681	5514	2101	36
H(5A)	5392	3737	2171	40
H(5B)	4726	4032	1069	40
H(6A)	5194	1828	2229	34
H(6B)	3730	2404	2285	34
H(7A)	4097	1096	4289	23
H(7B)	5014	1864	4203	23
H(8A)	5128	1984	7788	15
H(9A)	6480	384	6359	26
H(9B)	5413	64	7532	26
H(10A)	6639	-89	8832	37
H(10B)	7420	-1013	8069	37
H(11A)	8643	193	8098	31
H(11B)	8547	454	6721	31
H(12A)	8203	2396	6939	30
H(12B)	7131	2080	8106	30

H(13A)	6207	3477	6376	24
H(13B)	6982	2533	5631	24
H(19A)	656	3840	5086	22
H(19B)	744	4089	6249	22
H(19C)	-244	3387	6369	22
H(20A)	37	2761	8453	22
H(20B)	354	1359	9433	22
H(20C)	-325	1652	8342	22
H(21A)	1683	-667	9733	32
H(21B)	3100	-920	9060	32
H(21C)	2221	-1660	9026	32
H(22A)	1065	-1246	6734	37
H(22B)	2209	-1912	7449	37
H(22C)	2444	-1254	5986	37
H(23A)	1631	1545	4219	34
H(23B)	298	2266	4781	34
H(23C)	622	778	5058	34

Table 6. Torsion angles [deg] for JMV227-iF3.

C(24)-W-P-C(1)	-123.2(5)
C(27)-W-P-C(1)	-12.02(12)
C(26)-W-P-C(1)	76.83(12)
C(28)-W-P-C(1)	-101.61(12)
C(25)-W-P-C(1)	164.69(11)
C(24)-W-P-C(15)	139.7(5)
C(27)-W-P-C(15)	-109.10(12)
C(26)-W-P-C(15)	-20.25(12)
C(28)-W-P-C(15)	161.31(12)
C(25)-W-P-C(15)	67.61(12)
C(2)-N(1)-C(1)-N(2)	-5.2(4)
C(14)-N(1)-C(1)-N(2)	-179.2(2)
C(2)-N(1)-C(1)-P	174.89(19)
C(14)-N(1)-C(1)-P	0.9(3)
C(8)-N(2)-C(1)-N(1)	-156.7(2)
C(8)-N(2)-C(1)-P	23.2(3)
C(15)-P-C(1)-N(1)	11.3(2)
W-P-C(1)-N(1)	-108.34(18)
C(15)-P-C(1)-N(2)	-168.6(2)
W-P-C(1)-N(2)	71.7(2)
C(1)-N(1)-C(2)-C(7)	68.0(3)
C(14)-N(1)-C(2)-C(7)	-118.1(2)
C(1)-N(1)-C(2)-C(3)	-62.0(3)
C(14)-N(1)-C(2)-C(3)	112.0(2)
N(1)-C(2)-C(3)-C(4)	-174.1(2)
C(7)-C(2)-C(3)-C(4)	55.8(3)
C(2)-C(3)-C(4)-C(5)	-55.1(3)
C(3)-C(4)-C(5)-C(6)	56.7(4)
C(4)-C(5)-C(6)-C(7)	-57.3(4)
N(1)-C(2)-C(7)-C(6)	173.9(2)
C(3)-C(2)-C(7)-C(6)	-56.1(3)
C(5)-C(6)-C(7)-C(2)	56.0(4)
C(1)-N(2)-C(8)-C(13)	-160.8(2)
C(1)-N(2)-C(8)-C(9)	76.0(3)

N(2)-C(8)-C(9)-C(10)	179.5(2)
C(13)-C(8)-C(9)-C(10)	56.7(3)
C(8)-C(9)-C(10)-C(11)	-55.6(4)
C(9)-C(10)-C(11)-C(12)	55.0(4)
C(10)-C(11)-C(12)-C(13)	-55.7(4)
N(2)-C(8)-C(13)-C(12)	-179.7(2)
C(9)-C(8)-C(13)-C(12)	-56.8(3)
C(11)-C(12)-C(13)-C(8)	56.6(3)
C(1)-N(1)-C(14)-C(19)	109.6(2)
C(2)-N(1)-C(14)-C(19)	-64.9(3)
C(1)-N(1)-C(14)-C(18)	-125.7(2)
C(2)-N(1)-C(14)-C(18)	59.8(3)
C(1)-N(1)-C(14)-C(15)	-15.5(3)
C(2)-N(1)-C(14)-C(15)	170.0(2)
N(1)-C(14)-C(15)-C(16)	-93.8(2)
C(19)-C(14)-C(15)-C(16)	146.2(2)
C(18)-C(14)-C(15)-C(16)	20.3(2)
N(1)-C(14)-C(15)-C(20)	148.9(2)
C(19)-C(14)-C(15)-C(20)	28.9(3)
C(18)-C(14)-C(15)-C(20)	-97.0(2)
N(1)-C(14)-C(15)-P	22.6(2)
C(19)-C(14)-C(15)-P	-97.4(2)
C(18)-C(14)-C(15)-P	136.67(18)
C(1)-P-C(15)-C(16)	92.62(18)
W-P-C(15)-C(16)	-159.42(14)
C(1)-P-C(15)-C(20)	-146.5(2)
W-P-C(15)-C(20)	-38.6(2)
C(1)-P-C(15)-C(14)	-19.40(18)
W-P-C(15)-C(14)	88.56(17)
C(20)-C(15)-C(16)-C(17)	104.9(3)
C(14)-C(15)-C(16)-C(17)	-15.9(3)
P-C(15)-C(16)-C(17)	-132.1(2)
C(20)-C(15)-C(16)-C(21)	-71.0(3)
C(14)-C(15)-C(16)-C(21)	168.2(2)
P-C(15)-C(16)-C(21)	52.0(3)
C(21)-C(16)-C(17)-C(18)	179.9(3)
C(15)-C(16)-C(17)-C(18)	4.3(3)
C(21)-C(16)-C(17)-C(22)	2.1(5)
C(15)-C(16)-C(17)-C(22)	-173.5(3)
C(16)-C(17)-C(18)-C(23)	-167.6(3)
C(22)-C(17)-C(18)-C(23)	10.2(5)
C(16)-C(17)-C(18)-C(14)	9.8(3)
C(22)-C(17)-C(18)-C(14)	-172.4(3)
N(1)-C(14)-C(18)-C(23)	-90.0(3)
C(19)-C(14)-C(18)-C(23)	31.3(4)
C(15)-C(14)-C(18)-C(23)	158.4(3)
N(1)-C(14)-C(18)-C(17)	92.6(2)
C(19)-C(14)-C(18)-C(17)	-146.2(2)
C(15)-C(14)-C(18)-C(17)	-19.0(3)
C(27)-W-C(24)-O(1)	-85(8)
C(26)-W-C(24)-O(1)	-173(8)
C(28)-W-C(24)-O(1)	5(8)
C(25)-W-C(24)-O(1)	98(8)
P-W-C(24)-O(1)	26(8)
C(24)-W-C(25)-O(2)	69(9)
C(27)-W-C(25)-O(2)	-38(10)
C(26)-W-C(25)-O(2)	-21(9)
C(28)-W-C(25)-O(2)	156(9)
P-W-C(25)-O(2)	-121(9)

C(24)-W-C(26)-O(3)	21(4)
C(27)-W-C(26)-O(3)	-70(4)
C(28)-W-C(26)-O(3)	-14(6)
C(25)-W-C(26)-O(3)	111(4)
P-W-C(26)-O(3)	-163(4)
C(24)-W-C(27)-O(4)	-38(8)
C(26)-W-C(27)-O(4)	52(8)
C(28)-W-C(27)-O(4)	-125(8)
C(25)-W-C(27)-O(4)	69(8)
P-W-C(27)-O(4)	152(8)
C(24)-W-C(28)-O(5)	-70(6)
C(27)-W-C(28)-O(5)	20(6)
C(26)-W-C(28)-O(5)	-36(7)
C(25)-W-C(28)-O(5)	-161(6)
P-W-C(28)-O(5)	113(6)

Symmetry transformations used to generate equivalent atoms:

8.8. Crystal data and structure refinement for **27**

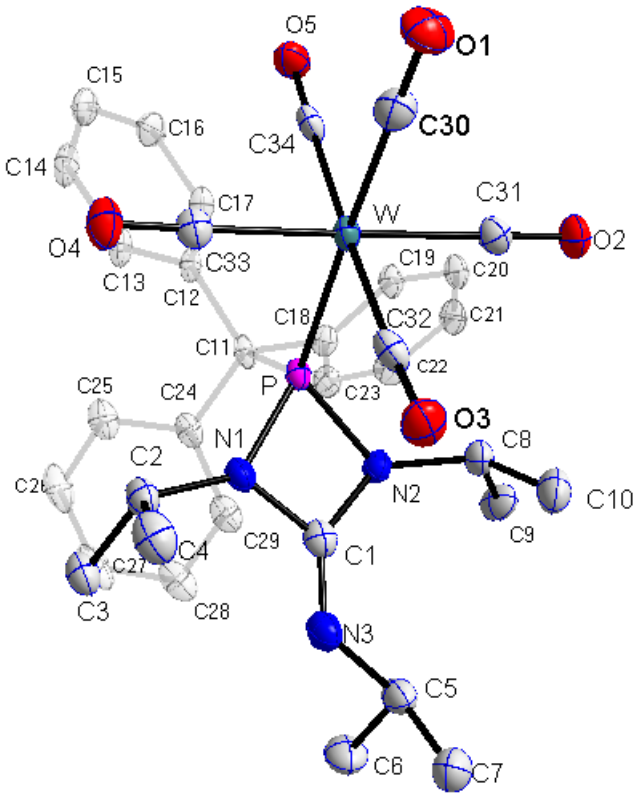

Table 8.8. Crystal data and structure refinement for **27**.

Identification code	GSTR381, 3700f
Empirical formula	$C_{34}H_{37}N_3O_5PW$
Formula weight	782.49
Temperature/K	100
Crystal system	triclinic
Space group	P-1
a/Å	9.4161(5)
b/Å	11.5014(6)
c/Å	15.6035(8)
α/°	86.325(2)
β/°	83.413(2)
γ/°	77.206(2)
Volume/Å^3	1635.69(15)
Z	2
ρ_{calc}g/cm^3	1.589
μ/mm^{-1}	3.625
F(000)	782.0
Crystal size/mm^3	0.15 × 0.06 × 0.04

Absorption correction	empirical
Tmin; Tmax	0.5544; 0.7460
Radiation	MoKα (λ = 0.71073)
2Θ range for data collection/°	5.1 to 56°
Completeness to theta	0.977
Index ranges	-12 ≤ h ≤ 12, -15 ≤ k ≤ 15, -20 ≤ l ≤ 19
Reflections collected	31825
Independent reflections	7732 [R_{int} = 0.0357, R_{sigma} = 0.0313]
Data/restraints/parameters	7732/0/403
Goodness-of-fit on F^2	1.159
Final R indexes [I>=2σ (I)]	R_1 = 0.0344, wR_2 = 0.0918
Final R indexes [all data]	R_1 = 0.0389, wR_2 = 0.0948
Largest diff. peak/hole / e $Å^{-3}$	3.89/-1.58
Identification code	GSTR381, 3700f

Table 2 Bond Lengths for 3700f.

Atom	Atom	Length/Å	Atom	Atom	Length/Å
W	P	2.5094(10)	C5	C7	1.527(7)
W	C30	2.017(5)	C8	C9	1.525(6)
W	C34	2.030(5)	C8	C10	1.541(6)
W	C31	2.065(4)	C11	C12	1.522(6)
W	C32	2.032(5)	C11	C18	1.549(5)
W	C33	2.050(4)	C11	C24	1.531(6)
P	N1	1.704(4)	C12	C13	1.402(6)
P	N2	1.713(4)	C12	C17	1.398(6)
P	C1	2.290(5)	C13	C14	1.387(7)
P	C11	1.962(4)	C14	C15	1.394(7)
O1	C30	1.129(6)	C15	C16	1.372(7)
O2	C31	1.129(5)	C16	C17	1.388(7)
O3	C32	1.154(6)	C18	C19	1.403(6)
O4	C33	1.143(5)	C18	C23	1.393(6)
O5	C34	1.154(6)	C19	C20	1.389(6)
N1	C1	1.400(6)	C20	C21	1.390(7)
N1	C2	1.470(5)	C21	C22	1.388(7)
N2	C1	1.442(5)	C22	C23	1.397(6)
N2	C8	1.477(5)	C24	C25	1.398(6)
N3	C1	1.249(6)	C24	C29	1.404(7)
N3	C5	1.456(6)	C25	C26	1.403(7)
C2	C3	1.524(6)	C26	C27	1.374(9)
C2	C4	1.532(6)	C27	C28	1.381(8)

C5	C6	1.532(7)	C28	C29	1.395(7)		

Table 3 Bond Angles for 3700f.

Atom	Atom	Atom	Angle/˚	Atom	Atom	Atom	Angle/˚
C30	W	P	176.33(13)	N3	C5	C6	106.6(4)
C30	W	C34	86.19(18)	N3	C5	C7	109.7(4)
C30	W	C31	87.08(18)	C7	C5	C6	111.1(4)
C30	W	C32	90.20(18)	N2	C8	C9	112.9(4)
C30	W	C33	89.27(17)	N2	C8	C10	113.5(4)
C34	W	P	97.48(12)	C9	C8	C10	112.3(4)
C34	W	C31	91.58(16)	C12	C11	P	108.2(3)
C34	W	C32	176.39(16)	C12	C11	C18	110.2(3)
C34	W	C33	90.54(17)	C12	C11	C24	111.8(3)
C31	W	P	92.72(12)	C18	C11	P	105.5(3)
C32	W	P	86.13(12)	C24	C11	P	109.9(3)
C32	W	C31	88.06(17)	C24	C11	C18	111.0(3)
C32	W	C33	89.58(17)	C13	C12	C11	120.3(4)
C33	W	P	90.77(12)	C17	C12	C11	122.2(4)
C33	W	C31	175.65(15)	C17	C12	C13	117.5(4)
N1	P	W	113.80(13)	C14	C13	C12	121.4(4)
N1	P	N2	76.38(17)	C13	C14	C15	119.6(4)
N1	P	C1	37.55(16)	C16	C15	C14	119.8(5)
N1	P	C11	109.25(17)	C15	C16	C17	120.6(4)
N2	P	W	118.72(13)	C16	C17	C12	121.0(4)
N2	P	C1	38.98(16)	C19	C18	C11	119.8(4)
N2	P	C11	104.43(18)	C23	C18	C11	122.1(4)
C1	P	W	121.62(11)	C23	C18	C19	117.9(4)
C11	P	W	124.16(13)	C20	C19	C18	121.3(4)
C11	P	C1	114.21(17)	C19	C20	C21	120.2(4)
C1	N1	P	94.6(3)	C22	C21	C20	119.2(4)
C1	N1	C2	128.3(4)	C21	C22	C23	120.5(4)
C2	N1	P	136.7(3)	C18	C23	C22	120.8(4)
C1	N2	P	92.7(3)	C25	C24	C11	121.6(4)
C1	N2	C8	133.0(4)	C25	C24	C29	117.4(4)
C8	N2	P	127.1(3)	C29	C24	C11	120.8(4)
C1	N3	C5	123.8(4)	C24	C25	C26	120.6(5)
N1	C1	P	47.9(2)	C27	C26	C25	121.1(5)
N1	C1	N2	96.0(3)	C26	C27	C28	119.1(5)
N2	C1	P	48.4(2)	C27	C28	C29	120.6(6)
N3	C1	P	172.3(4)	C28	C29	C24	121.2(5)
N3	C1	N1	125.1(4)	O1	C30	W	178.4(4)
N3	C1	N2	138.9(4)	O5	C34	W	174.4(4)
N1	C2	C3	111.3(4)	O2	C31	W	176.5(4)
N1	C2	C4	111.7(4)	O3	C32	W	177.2(4)
C3	C2	C4	111.2(4)	O4	C33	W	178.1(4)

Table 4 Torsion Angles for 3700f.

A	B	C	D	Angle/˚	A	B	C	D	Angle/˚
W	P	N1	C1	-111.5(2)	C11	C18	C23	C22	178.3(4)
W	P	N1	C2	61.3(4)	C11	C24	C25	C26	176.6(4)
W	P	N2	C1	105.9(2)	C11	C24	C29	C28	-177.3(4)
W	P	N2	C8	-47.2(4)	C12	C11	C18	C19	65.0(5)
W	P	C1	N1	88.7(2)	C12	C11	C18	C23	-110.2(4)
W	P	C1	N2	-97.8(2)	C12	C11	C24	C25	3.9(5)
W	P	C1	N3	64(3)	C12	C11	C24	C29	-179.8(4)
W	P	C11	C12	-29.4(3)	C12	C13	C14	C15	1.3(6)
W	P	C11	C18	88.5(3)	C13	C12	C17	C16	0.9(6)
W	P	C11	C24	-151.7(2)	C13	C14	C15	C16	0.1(7)
P	W	C30	O1	135(15)	C14	C15	C16	C17	-1.0(7)
P	W	C34	O5	164(4)	C15	C16	C17	C12	0.5(7)
P	W	C31	O2	-131(7)	C17	C12	C13	C14	-1.8(6)
P	W	C32	O3	123(9)	C18	C11	C12	C13	-164.5(4)
P	W	C33	O4	163(13)	C18	C11	C12	C17	18.0(5)
P	N1	C1	N2	-4.9(3)	C18	C11	C24	C25	-119.6(4)
P	N1	C1	N3	176.1(4)	C18	C11	C24	C29	56.7(5)
P	N1	C2	C3	124.0(4)	C18	C19	C20	C21	1.9(7)
P	N1	C2	C4	-111.0(5)	C19	C18	C23	C22	3.1(7)
P	N2	C1	N1	4.8(3)	C19	C20	C21	C22	1.1(7)
P	N2	C1	N3	-176.3(5)	C20	C21	C22	C23	-1.9(8)
P	N2	C8	C9	-126.6(4)	C21	C22	C23	C18	-0.2(7)
P	N2	C8	C10	104.1(4)	C23	C18	C19	C20	-3.9(7)
P	C11	C12	C13	-49.5(4)	C24	C11	C12	C13	71.6(4)
P	C11	C12	C17	133.0(3)	C24	C11	C12	C17	-105.9(4)
P	C11	C18	C19	-51.6(5)	C24	C11	C18	C19	-170.7(4)
P	C11	C18	C23	133.2(4)	C24	C11	C18	C23	14.2(6)
P	C11	C24	C25	124.0(4)	C24	C25	C26	C27	0.2(7)
P	C11	C24	C29	-59.7(4)	C25	C24	C29	C28	-0.8(6)
N1	P	N2	C1	-4.1(2)	C25	C26	C27	C28	0.2(7)
N1	P	N2	C8	-157.2(4)	C26	C27	C28	C29	-0.9(7)
N1	P	C1	N2	173.5(4)	C27	C28	C29	C24	1.2(7)
N1	P	C1	N3	-25(3)	C29	C24	C25	C26	0.1(6)
N1	P	C11	C12	109.5(3)	C30	W	P	N1	40(2)
N1	P	C11	C18	-132.6(3)	C30	W	P	N2	-47(2)
N1	P	C11	C24	-12.8(3)	C30	W	P	C1	-2(2)
N2	P	N1	C1	4.2(2)	C30	W	P	C11	178(2)
N2	P	N1	C2	177.0(4)	C30	W	C34	O5	-16(4)
N2	P	C1	N1	-173.5(4)	C30	W	C31	O2	45(7)
N2	P	C1	N3	162(3)	C30	W	C32	O3	-57(9)

N2	P	C11	C12	-170.2(3)	C30	W	C33	O4	-13(13)
N2	P	C11	C18	-52.3(3)	C34	W	P	N1	-141.06(18)
N2	P	C11	C24	67.5(3)	C34	W	P	N2	131.91(18)
C1	P	N1	C2	172.8(6)	C34	W	P	C1	177.19(17)
C1	P	N2	C8	-153.1(5)	C34	W	P	C11	-3.76(19)
C1	P	C11	C12	149.7(2)	C34	W	C30	O1	-43(16)
C1	P	C11	C18	-92.4(3)	C34	W	C31	O2	131(7)
C1	P	C11	C24	27.4(3)	C34	W	C32	O3	-54(10)
C1	N1	C2	C3	-65.2(6)	C34	W	C33	O4	-100(13)
C1	N1	C2	C4	59.8(6)	C31	W	P	N1	126.99(18)
C1	N2	C8	C9	91.6(5)	C31	W	P	N2	39.95(18)
C1	N2	C8	C10	-37.7(7)	C31	W	P	C1	85.24(17)
C1	N3	C5	C6	-109.5(5)	C31	W	P	C11	-95.71(18)
C1	N3	C5	C7	130.2(5)	C31	W	C30	O1	48(16)
C2	N1	C1	P	-173.7(5)	C31	W	C34	O5	-103(4)
C2	N1	C1	N2	-178.6(4)	C31	W	C32	O3	30(9)
C2	N1	C1	N3	2.4(7)	C31	W	C33	O4	20(14)
C5	N3	C1	P	-167(2)	C32	W	P	N1	39.12(19)
C5	N3	C1	N1	170.2(4)	C32	W	P	N2	-47.92(19)
C5	N3	C1	N2	-8.4(8)	C32	W	P	C1	-2.63(18)
C8	N2	C1	P	150.4(5)	C32	W	P	C11	176.42(19)
C8	N2	C1	N1	155.3(4)	C32	W	C30	O1	136(16)
C8	N2	C1	N3	-25.9(9)	C32	W	C34	O5	-19(5)
C11	P	N1	C1	105.0(3)	C32	W	C31	O2	-45(7)
C11	P	N1	C2	-82.3(4)	C32	W	C33	O4	77(13)
C11	P	N2	C1	-110.8(2)	C33	W	P	N1	-50.41(19)
C11	P	N2	C8	96.1(4)	C33	W	P	N2	-137.45(18)
C11	P	C1	N1	-90.5(3)	C33	W	P	C1	-92.16(18)
C11	P	C1	N2	83.0(3)	C33	W	P	C11	86.89(19)
C11	P	C1	N3	-115(3)	C33	W	C30	O1	-134(16)
C11	C12	C13	C14	-179.4(4)	C33	W	C34	O5	73(4)
C11	C12	C17	C16	178.5(4)	C33	W	C31	O2	12(8)
C11	C18	C19	C20	-179.3(4)	C33	W	C32	O3	-146(9)

8.9. Crystal data and structure refinement for **28a**

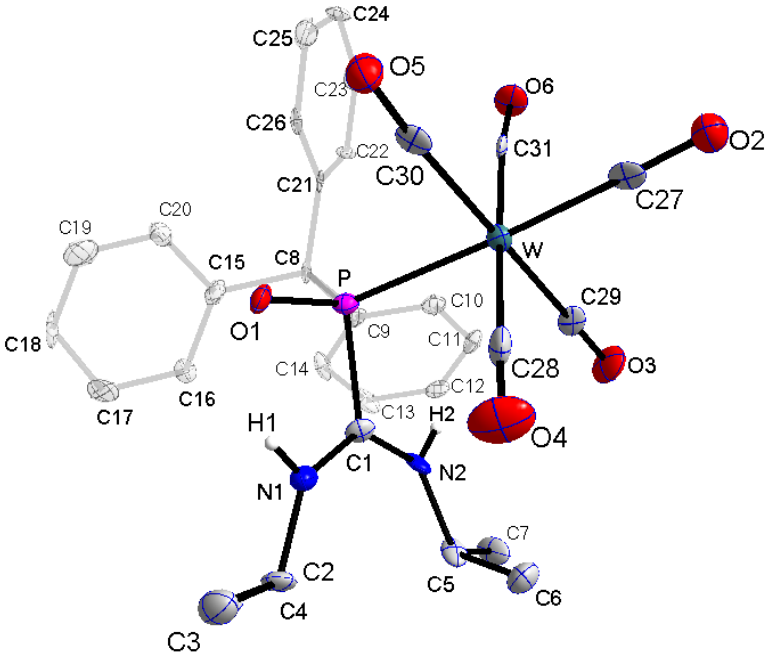

Table 8.9. Crystal data and structure refinement for **28a**.

Identification code	GSTR377, 3718
Empirical formula	$C_{31}H_{31}N_2O_6PW$
Formula weight	742.40
Temperature/K	123
Crystal system	monoclinic
Space group	$P2_1/c$
a/Å	17.7060(10)
b/Å	16.7883(13)
c/Å	9.9971(6)
α/°	90.00
β/°	94.217(5)
γ/°	90.00
Volume/Å^3	2963.6(3)
Z	4
ρ_{calc}g/cm^3	1.664
μ/mm^{-1}	3.998
F(000)	1472.0
Crystal size/mm^3	0.12 × 0.09 × 0.02

Absorption correction	integration
Tmin; Tmax	0.4446; 0.7315
Radiation	MoKα (λ = 0.71073)
2Θ range for data collection/°	5.38 to 56°
Completeness to theta	0.999
Index ranges	-23 ≤ h ≤ 23, -22 ≤ k ≤ 22, -13 ≤ l ≤ 1
Reflections collected	30626
Independent reflections	7156 [R_{int} = 0.2189, R_{sigma} = 0.3978]
Data/restraints/parameters	7156/42/374
Goodness-of-fit on F^2	0.459
Final R indexes [I>=2σ (I)]	R_1 = 0.0393, wR_2 = 0.0575
Final R indexes [all data]	R_1 = 0.1498, wR_2 = 0.0824
Largest diff. peak/hole / e $Å^{-3}$	1.14/-0.86

8.10. Crystal data and structure refinement for **29a**

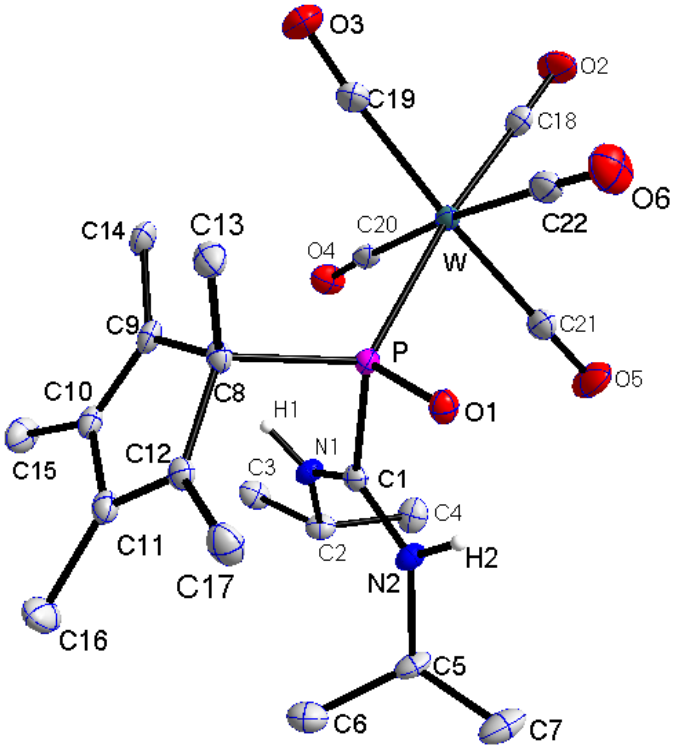

Table 8.10. Crystal data and structure refinement for **29a**.

Identification code	GSTR375, 3677f
Empirical formula	$C_{22}H_{31}N_2O_6PW$
Formula weight	634.31
Temperature/K	100
Crystal system	monoclinic
Space group	$P2_1/c$
a/Å	9.5748(5)
b/Å	27.7242(13)
c/Å	10.5851(5)
α/°	90.00
β/°	115.3400(10)
γ/°	90.00
Volume/Å^3	2539.5(2)
Z	4
ρ_{calc}g/cm^3	1.659
μ/mm^{-1}	4.649
F(000)	1256.0
Crystal size/mm^3	0.13 × 0.1 × 0.04
Absorption correction	empirical
Tmin; Tmax	0.5227; 0.7460

Radiation	MoKα (λ = 0.71073)
2Θ range for data collection/°	5.54 to 56°
Index ranges	-12 ≤ h ≤ 11, -36 ≤ k ≤ 36, -13 ≤ l ≤ 13
Reflections collected	19281
Independent reflections	6102 [R_{int} = 0.0297, R_{sigma} = 0.0302]
Data/restraints/parameters	6102/0/298
Goodness-of-fit on F^2	1.021
Final R indexes [I>=2σ (I)]	R_1 = 0.0205, wR_2 = 0.0462
Final R indexes [all data]	R_1 = 0.0248, wR_2 = 0.0476
Largest diff. peak/hole / e $Å^{-3}$	0.98/-0.63
Identification code	GSTR375, 3677f

8.11. Crystal data and structure refinement for **29b**

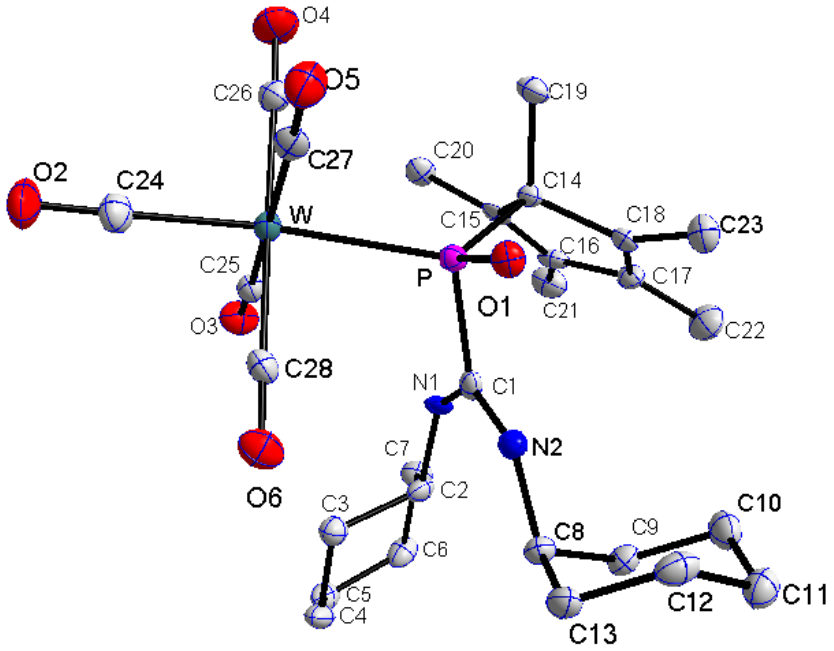

Table 8.11. Crystal data and structure refinement for **29b**.

Identification code	GSTR269, 2432
Device type	Nonius KappaCCD
Empirical formula	C28 H39 N2 O6 P W
Formula weight	714.43
Temperature/K	123(2)
Crystal system	monoclinic
Space group	$P2_1/c$
a/Å	10.9216(4)
b/Å	23.5529(11)
c/Å	14.5767(4)
α/°	90.00
β/°	126.717(2)
γ/°	90.00
Volume/Å^3	3005.7(2)
Z	4
ρ_{calc}g/cm^3	1.579
μ/mm^{-1}	3.938
F(000)	1432
Crystal size/mm^3	0.24 x 0.07 x 0.04
Absorption correction	empirical
Tmin; Tmax	0.5227; 0.7460

Radiation	MoKα (λ = 0. 0.7107)
2Θ range for data collection/°	2.57 to 28.00°
Completeness to theta	0.986
Index ranges	-11<=h<=14, -28<=k<=31, -19<=l<=19
Reflections collected	24433
Independent reflections	7162 [R(int) = 0.0803]
Data/restraints/parameters	7162 / 5 / 348
Goodness-of-fit on F^2	0.843
Final R indexes [I>=2σ (I)]	R1 = 0.0360, wR2 = 0.0545
Final R indexes [all data]	R1 = 0.0782, wR2 = 0.0631
Largest diff. peak/hole / e $Å^{-3}$	2.838/-2.320

8.12. Crystal data and structure refinement for **35**

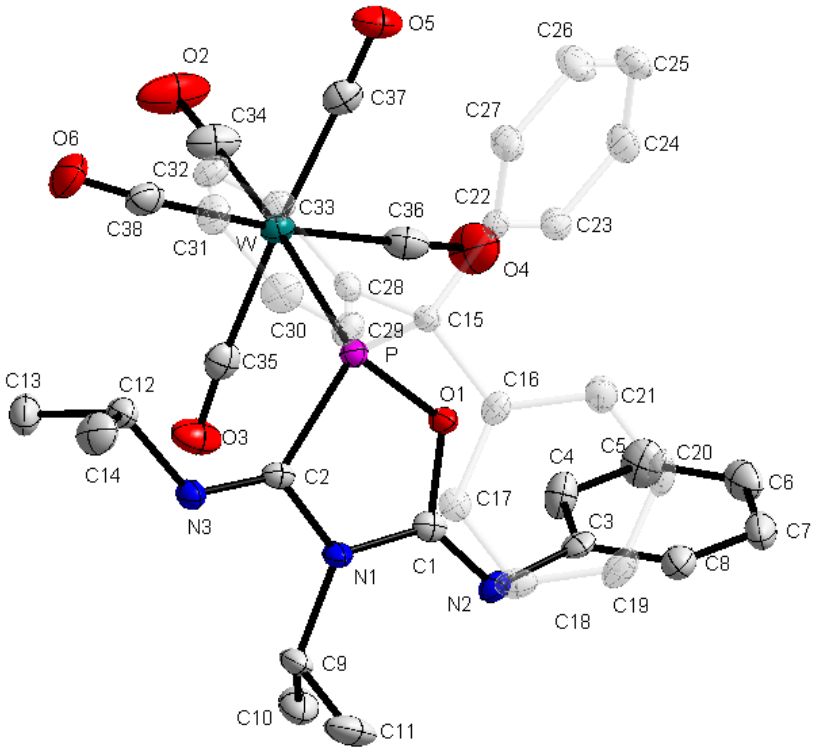

Table 8.12. Crystal data and structure refinement for **35**.

Identification code	GSTR373, 3628c
Empirical formula	$C_{38}H_{34}N_3O_6PW$
Formula weight	843.50
Temperature/K	123(2)
Crystal system	monoclinic
Space group	$P2_1/c$
a/Å	13.5927(4)
b/Å	9.9774(3)
c/Å	26.2734(7)
α/°	90.00
β/°	96.006(2)
γ/°	90.00
Volume/Å^3	3543.63(18)
Z	4
ρ_{calc}g/cm^3	1.581
μ/mm^{-1}	3.355
F(000)	1680.0
Crystal size/mm^3	0.12 × 0.09 × 0.03
Absorption correction	Integration
Tmin; Tmax	0.5755; 0.7572
Radiation	MoKα (λ = 0.71073)

2Θ range for data collection/°	5.22 to 56°
Index ranges	-15 ≤ h ≤ 17, -13 ≤ k ≤ 12, -34 ≤ l ≤ 24
Reflections collected	20867
Independent reflections	8465 [R_{int} = 0.0318, R_{sigma} = 0.0667]
Data/restraints/parameters	8465/0/446
Goodness-of-fit on F^2	0.764
Final R indexes [I>=2σ (I)]	R_1 = 0.0220, wR_2 = 0.0304
Final R indexes [all data]	R_1 = 0.0443, wR_2 = 0.0320
Largest diff. peak/hole / e $Å^{-3}$	1.10/-0.79

8.13. Crystal data and structure refinement for **36**

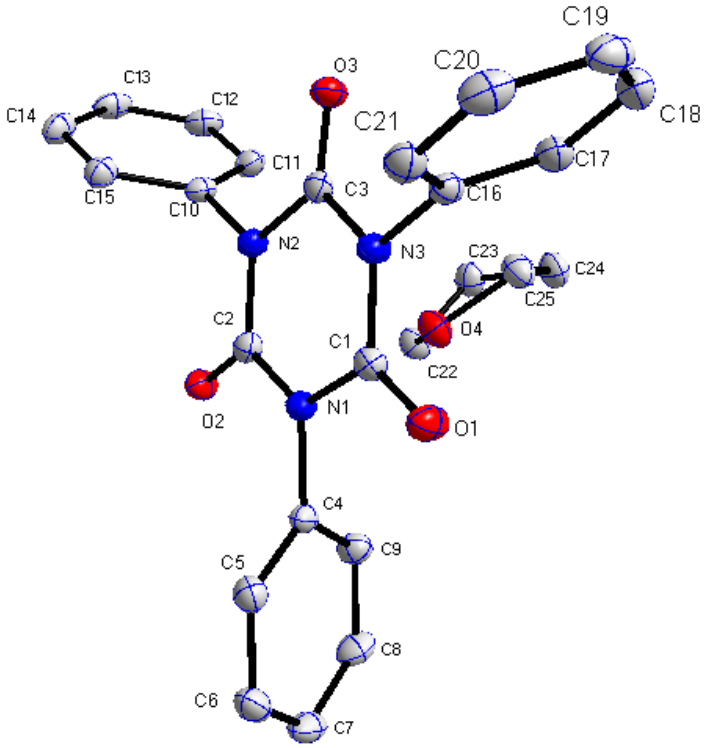

Table 8.13. Crystal data and structure refinement for **36**.

Identification code	GSTR283, 2484g
Device Type	Bruker X8-KappaApexII
Empirical formula	C25 H23 N3 O4
Moiety formula	C21 H15 N3 O3, C4 H8 O
Formula weight	429.46
Temperature/K	100(2)
Crystal system	Triclinic
Space group	P-1
a/Å	11.0468(6)
b/Å	11.1610(6)
c/Å	11.1665(6)
α/°	91.967(2)
β/°	113.625(2)
γ/°	118.811(2)
Volume/Å^3	1543.74(11)
Z	2
ρ_{calc}g/cm^3	1.653
μ/mm^{-1}	3.843
F(000)	760
Crystal size/mm^3	0.24 x 0.11 x 0.06
Absorption correction	Empirical
Tmin; Tmax	0.8022; 0.4590

Radiation	MoKα (λ = 0.71073)
2Θ range for data collection/°	2.76 to 28.00°
Completeness to theta	0.983
Index ranges	-12<=h<=11, -13<=k<=13, -23<=l<=23
Reflections collected	14631
Independent reflections	7318 [R(int) = 0.0498]
Data/restraints/parameters	7318 / 0 / 392
Goodness-of-fit on F^2	1.092
Final R indexes [I>=2σ (I)]	R1 = 0.0306, wR2 = 0.0774
Final R indexes [all data]	R1 = 0.0351, wR2 = 0.0789
Largest diff. peak/hole / e $Å^{-3}$	1.691 / -1.658

Table 2. Atomic coordinates (x 10^4) and equivalent isotropic displacement parameters (A^2 x 10^3) for JMV259.
U(eq) is defined as one third of the trace of the orthogonalized Uij tensor.

	x	y	z	U(eq)
C(1)	10157(2)	4869(1)	2925(1)	18(1)
C(2)	7590(1)	3192(1)	2777(1)	17(1)
C(3)	8255(2)	5577(1)	2508(1)	17(1)
C(4)	9397(2)	2454(1)	3020(1)	17(1)
C(5)	10487(2)	2499(1)	4229(1)	22(1)
C(6)	10778(2)	1415(2)	4263(1)	26(1)
C(7)	9982(2)	310(2)	3102(2)	26(1)
C(8)	8903(2)	292(2)	1894(2)	26(1)
C(9)	8608(2)	1367(1)	1848(1)	22(1)
C(10)	5774(2)	3921(1)	2467(1)	17(1)
C(11)	4557(2)	3486(1)	1163(1)	22(1)
C(12)	3090(2)	3099(1)	995(1)	25(1)
C(13)	2852(2)	3160(1)	2118(2)	25(1)
C(14)	4084(2)	3602(1)	3417(1)	24(1)
C(15)	5555(2)	3985(1)	3601(1)	21(1)
C(16)	10846(2)	7257(1)	2762(1)	17(1)
C(17)	10757(2)	7577(1)	1556(1)	22(1)
C(18)	11847(2)	8931(2)	1608(2)	27(1)
C(19)	13026(2)	9939(2)	2847(2)	28(1)
C(20)	13100(2)	9602(1)	4049(2)	25(1)
C(21)	12007(2)	8259(1)	4010(1)	22(1)
C(22)	5237(2)	1475(1)	-929(1)	25(1)
C(23)	4386(2)	1773(2)	-2215(1)	26(1)

C(24)	5743(2)	2846(2)	-2429(1)	28(1)
C(25)	7013(2)	3720(2)	-979(1)	27(1)
N(1)	9067(1)	3569(1)	2973(1)	17(1)
N(2)	7296(1)	4275(1)	2650(1)	17(1)
N(3)	9707(1)	5848(1)	2726(1)	18(1)
O(1)	11407(1)	5137(1)	3057(1)	26(1)
O(2)	6650(1)	2026(1)	2767(1)	22(1)
O(3)	7885(1)	6435(1)	2261(1)	22(1)
O(4)	6748(1)	2777(1)	-138(1)	26(1)

Table 3. Bond lengths [A] and angles [deg] for JMV259.

C(1)-O(1)	1.2059(15)
C(1)-N(1)	1.3897(16)
C(1)-N(3)	1.3928(16)
C(2)-O(2)	1.2078(15)
C(2)-N(1)	1.3905(16)
C(2)-N(2)	1.3932(15)
C(3)-O(3)	1.2101(15)
C(3)-N(2)	1.3881(16)
C(3)-N(3)	1.3926(16)
C(4)-C(9)	1.3789(18)
C(4)-C(5)	1.3815(18)
C(4)-N(1)	1.4525(15)
C(5)-C(6)	1.3911(19)
C(5)-H(5A)	0.9500
C(6)-C(7)	1.381(2)
C(6)-H(6A)	0.9500
C(7)-C(8)	1.3876(19)
C(7)-H(7A)	0.9500
C(8)-C(9)	1.3850(18)
C(8)-H(8A)	0.9500
C(9)-H(9A)	0.9500
C(10)-C(11)	1.3844(18)
C(10)-C(15)	1.3858(18)
C(10)-N(2)	1.4506(16)
C(11)-C(12)	1.3878(19)
C(11)-H(11A)	0.9500
C(12)-C(13)	1.386(2)
C(12)-H(12A)	0.9500
C(13)-C(14)	1.386(2)
C(13)-H(13A)	0.9500
C(14)-C(15)	1.3865(18)
C(14)-H(14A)	0.9500
C(15)-H(15A)	0.9500
C(16)-C(17)	1.3829(18)
C(16)-C(21)	1.3843(18)
C(16)-N(3)	1.4513(16)
C(17)-C(18)	1.3853(19)
C(17)-H(17A)	0.9500
C(18)-C(19)	1.383(2)
C(18)-H(18A)	0.9500
C(19)-C(20)	1.388(2)

C(19)-H(19A)	0.9500
C(20)-C(21)	1.3843(19)
C(20)-H(20A)	0.9500
C(21)-H(21A)	0.9500
C(22)-O(4)	1.4395(16)
C(22)-C(23)	1.5195(18)
C(22)-H(22A)	0.9900
C(22)-H(22B)	0.9900
C(23)-C(24)	1.521(2)
C(23)-H(23A)	0.9900
C(23)-H(23B)	0.9900
C(24)-C(25)	1.5135(19)
C(24)-H(24A)	0.9900
C(24)-H(24B)	0.9900
C(25)-O(4)	1.4381(16)
C(25)-H(25A)	0.9900
C(25)-H(25B)	0.9900

O(1)-C(1)-N(1)	122.52(11)
O(1)-C(1)-N(3)	122.32(12)
N(1)-C(1)-N(3)	115.15(11)
O(2)-C(2)-N(1)	122.54(11)
O(2)-C(2)-N(2)	122.27(11)
N(1)-C(2)-N(2)	115.14(10)
O(3)-C(3)-N(2)	122.82(11)
O(3)-C(3)-N(3)	122.36(11)
N(2)-C(3)-N(3)	114.77(10)
C(9)-C(4)-C(5)	121.35(12)
C(9)-C(4)-N(1)	118.91(11)
C(5)-C(4)-N(1)	119.74(11)
C(4)-C(5)-C(6)	119.13(13)
C(4)-C(5)-H(5A)	120.4
C(6)-C(5)-H(5A)	120.4
C(7)-C(6)-C(5)	120.17(12)
C(7)-C(6)-H(6A)	119.9
C(5)-C(6)-H(6A)	119.9
C(6)-C(7)-C(8)	119.82(12)
C(6)-C(7)-H(7A)	120.1
C(8)-C(7)-H(7A)	120.1
C(9)-C(8)-C(7)	120.44(13)
C(9)-C(8)-H(8A)	119.8
C(7)-C(8)-H(8A)	119.8
C(4)-C(9)-C(8)	119.07(12)
C(4)-C(9)-H(9A)	120.5
C(8)-C(9)-H(9A)	120.5
C(11)-C(10)-C(15)	121.34(12)
C(11)-C(10)-N(2)	119.39(11)
C(15)-C(10)-N(2)	119.24(11)
C(10)-C(11)-C(12)	118.97(12)
C(10)-C(11)-H(11A)	120.5
C(12)-C(11)-H(11A)	120.5
C(13)-C(12)-C(11)	120.41(13)
C(13)-C(12)-H(12A)	119.8
C(11)-C(12)-H(12A)	119.8
C(12)-C(13)-C(14)	119.88(13)
C(12)-C(13)-H(13A)	120.1
C(14)-C(13)-H(13A)	120.1
C(13)-C(14)-C(15)	120.37(13)

C(13)-C(14)-H(14A)	119.8
C(15)-C(14)-H(14A)	119.8
C(10)-C(15)-C(14)	119.03(12)
C(10)-C(15)-H(15A)	120.5
C(14)-C(15)-H(15A)	120.5
C(17)-C(16)-C(21)	121.16(12)
C(17)-C(16)-N(3)	119.74(11)
C(21)-C(16)-N(3)	119.10(11)
C(16)-C(17)-C(18)	118.96(13)
C(16)-C(17)-H(17A)	120.5
C(18)-C(17)-H(17A)	120.5
C(19)-C(18)-C(17)	120.65(13)
C(19)-C(18)-H(18A)	119.7
C(17)-C(18)-H(18A)	119.7
C(18)-C(19)-C(20)	119.72(13)
C(18)-C(19)-H(19A)	120.1
C(20)-C(19)-H(19A)	120.1
C(21)-C(20)-C(19)	120.22(13)
C(21)-C(20)-H(20A)	119.9
C(19)-C(20)-H(20A)	119.9
C(20)-C(21)-C(16)	119.28(12)
C(20)-C(21)-H(21A)	120.4
C(16)-C(21)-H(21A)	120.4
O(4)-C(22)-C(23)	106.16(11)
O(4)-C(22)-H(22A)	110.5
C(23)-C(22)-H(22A)	110.5
O(4)-C(22)-H(22B)	110.5
C(23)-C(22)-H(22B)	110.5
H(22A)-C(22)-H(22B)	108.7
C(22)-C(23)-C(24)	101.68(11)
C(22)-C(23)-H(23A)	111.4
C(24)-C(23)-H(23A)	111.4
C(22)-C(23)-H(23B)	111.4
C(24)-C(23)-H(23B)	111.4
H(23A)-C(23)-H(23B)	109.3
C(25)-C(24)-C(23)	101.91(11)
C(25)-C(24)-H(24A)	111.4
C(23)-C(24)-H(24A)	111.4
C(25)-C(24)-H(24B)	111.4
C(23)-C(24)-H(24B)	111.4
H(24A)-C(24)-H(24B)	109.3
O(4)-C(25)-C(24)	106.58(11)
O(4)-C(25)-H(25A)	110.4
C(24)-C(25)-H(25A)	110.4
O(4)-C(25)-H(25B)	110.4
C(24)-C(25)-H(25B)	110.4
H(25A)-C(25)-H(25B)	108.6
C(1)-N(1)-C(2)	124.60(10)
C(1)-N(1)-C(4)	117.30(10)
C(2)-N(1)-C(4)	117.38(10)
C(3)-N(2)-C(2)	124.64(10)
C(3)-N(2)-C(10)	118.32(10)
C(2)-N(2)-C(10)	116.47(10)
C(3)-N(3)-C(1)	124.87(11)
C(3)-N(3)-C(16)	117.76(10)
C(1)-N(3)-C(16)	117.37(10)
C(25)-O(4)-C(22)	109.06(10)

Symmetry transformations used to generate equivalent atoms:

Table 4. Anisotropic displacement parameters (A^2 x 10^3) for JMV259.

The anisotropic displacement factor exponent takes the form:

-2 pi^2 [h^2 a*^2 U11 + ... + 2 h k a* b* U12]

	U11	U22	U33	U23	U13	U12
C(1)	20(1)	19(1)	18(1)	7(1)	10(1)	11(1)
C(2)	16(1)	18(1)	16(1)	4(1)	8(1)	9(1)
C(3)	18(1)	17(1)	16(1)	4(1)	9(1)	9(1)
C(4)	18(1)	18(1)	22(1)	10(1)	13(1)	11(1)
C(5)	23(1)	25(1)	20(1)	9(1)	11(1)	14(1)
C(6)	26(1)	34(1)	28(1)	18(1)	14(1)	21(1)
C(7)	28(1)	24(1)	41(1)	17(1)	22(1)	19(1)
C(8)	24(1)	21(1)	33(1)	3(1)	14(1)	13(1)
C(9)	20(1)	24(1)	21(1)	6(1)	8(1)	13(1)
C(10)	17(1)	14(1)	24(1)	5(1)	11(1)	9(1)
C(11)	24(1)	23(1)	22(1)	5(1)	12(1)	15(1)
C(12)	21(1)	20(1)	29(1)	4(1)	8(1)	12(1)
C(13)	18(1)	19(1)	41(1)	8(1)	16(1)	11(1)
C(14)	25(1)	21(1)	32(1)	7(1)	19(1)	12(1)
C(15)	21(1)	18(1)	23(1)	5(1)	11(1)	10(1)
C(16)	16(1)	17(1)	24(1)	8(1)	11(1)	10(1)
C(17)	23(1)	24(1)	23(1)	8(1)	12(1)	15(1)
C(18)	35(1)	28(1)	34(1)	18(1)	25(1)	21(1)
C(19)	27(1)	18(1)	47(1)	12(1)	24(1)	13(1)
C(20)	18(1)	20(1)	32(1)	0(1)	9(1)	9(1)
C(21)	21(1)	24(1)	22(1)	7(1)	10(1)	14(1)
C(22)	23(1)	22(1)	25(1)	7(1)	10(1)	11(1)
C(23)	23(1)	31(1)	23(1)	9(1)	11(1)	14(1)
C(24)	31(1)	31(1)	23(1)	12(1)	14(1)	17(1)
C(25)	31(1)	22(1)	27(1)	10(1)	15(1)	13(1)
N(1)	17(1)	16(1)	20(1)	7(1)	10(1)	10(1)
N(2)	17(1)	17(1)	21(1)	7(1)	11(1)	10(1)
N(3)	17(1)	16(1)	24(1)	8(1)	11(1)	9(1)
O(1)	20(1)	25(1)	39(1)	14(1)	18(1)	14(1)
O(2)	22(1)	19(1)	29(1)	9(1)	15(1)	11(1)
O(3)	22(1)	20(1)	28(1)	10(1)	13(1)	14(1)
O(4)	25(1)	26(1)	21(1)	8(1)	8(1)	11(1)

Table 5. Hydrogen coordinates (x 10^4) and isotropic displacement parameters (A^2 x 10^3) for JMV259.

	x	y	z	U(eq)
H(5A)	11031	3261	5026	26
H(6A)	11526	1435	5088	31
H(7A)	10173	-435	3129	31
H(8A)	8362	-464	1093	31
H(9A)	7872	1357	1020	26
H(11A)	4724	3453	395	26
H(12A)	2242	2790	105	29
H(13A)	1847	2899	1998	30
H(14A)	3920	3643	4186	29
H(15A)	6400	4286	4490	25
H(17A)	9960	6880	704	26
H(18A)	11785	9168	786	32
H(19A)	13781	10859	2875	33
H(20A)	13903	10295	4901	30
H(21A)	12054	8026	4832	26
H(22A)	4641	1200	-414	30
H(22B)	5362	691	-1161	30
H(23A)	3818	2186	-2078	32
H(23B)	3636	898	-2994	32
H(24A)	6066	2366	-2881	33
H(24B)	5469	3443	-2974	33
H(25A)	8065	4102	-902	32
H(25B)	6949	4530	-697	32

Table 6. Torsion angles [deg] for JMV259.

C(9)-C(4)-C(5)-C(6)	-0.8(2)
N(1)-C(4)-C(5)-C(6)	179.24(11)
C(4)-C(5)-C(6)-C(7)	-0.1(2)
C(5)-C(6)-C(7)-C(8)	0.7(2)
C(6)-C(7)-C(8)-C(9)	-0.5(2)
C(5)-C(4)-C(9)-C(8)	0.9(2)
N(1)-C(4)-C(9)-C(8)	-179.07(12)
C(7)-C(8)-C(9)-C(4)	-0.3(2)
C(15)-C(10)-C(11)-C(12)	-0.39(19)
N(2)-C(10)-C(11)-C(12)	177.60(11)
C(10)-C(11)-C(12)-C(13)	0.56(19)
C(11)-C(12)-C(13)-C(14)	-0.4(2)
C(12)-C(13)-C(14)-C(15)	0.0(2)

C(11)-C(10)-C(15)-C(14)	0.03(19)
N(2)-C(10)-C(15)-C(14)	-177.96(11)
C(13)-C(14)-C(15)-C(10)	0.15(19)
C(21)-C(16)-C(17)-C(18)	-0.48(19)
N(3)-C(16)-C(17)-C(18)	179.63(11)
C(16)-C(17)-C(18)-C(19)	1.2(2)
C(17)-C(18)-C(19)-C(20)	-1.2(2)
C(18)-C(19)-C(20)-C(21)	0.5(2)
C(19)-C(20)-C(21)-C(16)	0.2(2)
C(17)-C(16)-C(21)-C(20)	-0.19(19)
N(3)-C(16)-C(21)-C(20)	179.70(11)
O(4)-C(22)-C(23)-C(24)	31.97(14)
C(22)-C(23)-C(24)-C(25)	-37.43(14)
C(23)-C(24)-C(25)-O(4)	30.80(14)
O(1)-C(1)-N(1)-C(2)	-177.57(11)
N(3)-C(1)-N(1)-C(2)	3.05(17)
O(1)-C(1)-N(1)-C(4)	-7.52(18)
N(3)-C(1)-N(1)-C(4)	173.10(10)
O(2)-C(2)-N(1)-C(1)	176.60(11)
N(2)-C(2)-N(1)-C(1)	-5.92(17)
O(2)-C(2)-N(1)-C(4)	6.55(17)
N(2)-C(2)-N(1)-C(4)	-175.97(10)
C(9)-C(4)-N(1)-C(1)	-102.62(14)
C(5)-C(4)-N(1)-C(1)	77.39(15)
C(9)-C(4)-N(1)-C(2)	68.17(15)
C(5)-C(4)-N(1)-C(2)	-111.82(13)
O(3)-C(3)-N(2)-C(2)	172.23(11)
N(3)-C(3)-N(2)-C(2)	-10.23(17)
O(3)-C(3)-N(2)-C(10)	1.23(18)
N(3)-C(3)-N(2)-C(10)	178.78(10)
O(2)-C(2)-N(2)-C(3)	-172.71(11)
N(1)-C(2)-N(2)-C(3)	9.81(17)
O(2)-C(2)-N(2)-C(10)	-1.56(17)
N(1)-C(2)-N(2)-C(10)	-179.05(10)
C(11)-C(10)-N(2)-C(3)	76.65(15)
C(15)-C(10)-N(2)-C(3)	-105.32(13)
C(11)-C(10)-N(2)-C(2)	-95.08(14)
C(15)-C(10)-N(2)-C(2)	82.95(14)
O(3)-C(3)-N(3)-C(1)	-175.53(12)
N(2)-C(3)-N(3)-C(1)	6.91(17)
O(3)-C(3)-N(3)-C(16)	5.02(18)
N(2)-C(3)-N(3)-C(16)	-172.54(10)
O(1)-C(1)-N(3)-C(3)	177.04(11)
N(1)-C(1)-N(3)-C(3)	-3.58(17)
O(1)-C(1)-N(3)-C(16)	-3.52(18)
N(1)-C(1)-N(3)-C(16)	175.87(10)
C(17)-C(16)-N(3)-C(3)	-82.30(15)
C(21)-C(16)-N(3)-C(3)	97.81(14)
C(17)-C(16)-N(3)-C(1)	98.21(14)
C(21)-C(16)-N(3)-C(1)	-81.68(15)
C(24)-C(25)-O(4)-C(22)	-11.20(15)
C(23)-C(22)-O(4)-C(25)	-13.33(14)

Symmetry transformations used to generate equivalent atoms:

8.14. Crystal data and structure refinement for **38**

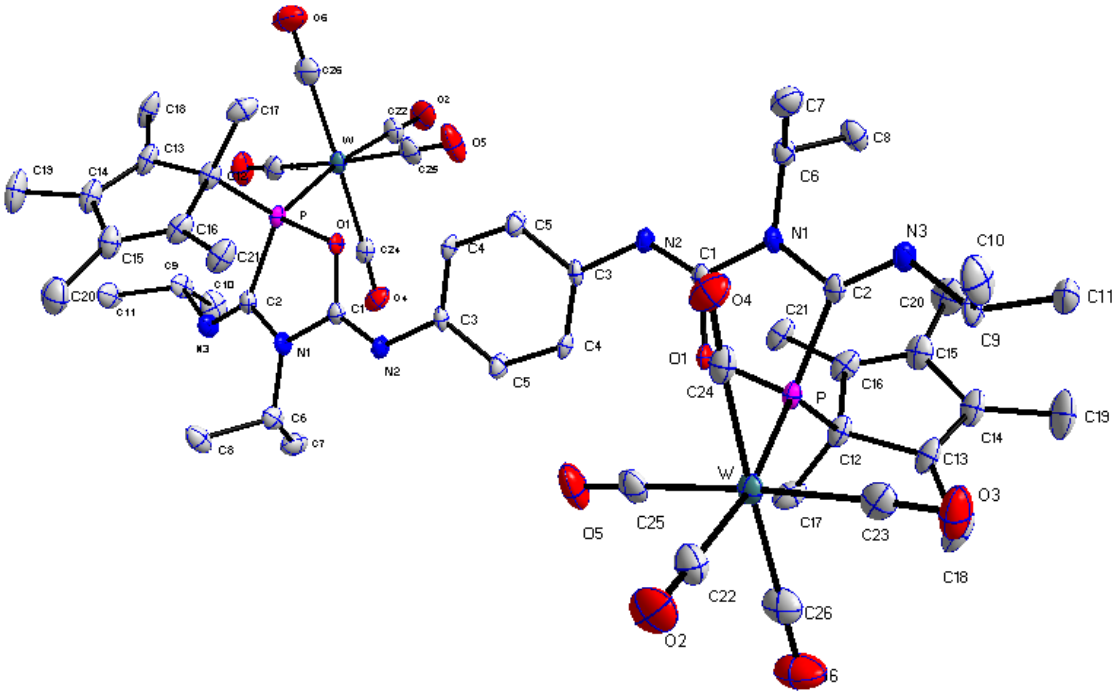

Table 8.14. Crystal data and structure refinement for **38**.

Identification code	GSTR400, JMV443 // GXray3943f
Device Type	Bruker X8-KappaApexII
Empirical formula	$C_{57}H_{74}N_6O_{12}P_2W_2$
Moiety formula	C52 H62 N6 O12 P2 W2, C5 H12
Formula weight	1464.86
Temperature/K	100
Crystal system	monoclinic
Space group	$P2_1/n$
a/Å	10.1110(6)
b/Å	21.9547(14)
c/Å	13.4351(9)
α/°	90
β/°	92.962(2)
γ/°	90
Volume/Å^3	2978.4(3)
Z	2
ρ_{calc}g/cm^3	1.633
μ/mm^{-1}	3.977
F(000)	1464.0
Crystal size/mm^3	0.12 × 0.1 × 0.08
Absorption correction	empirical
Tmin; Tmax	0.6437; 0.7460

Radiation	MoKα (λ = 0.71073)
2Θ range for data collection/°	5.482 to 56°
Completeness to theta	0.995
Index ranges	-13 ≤ h ≤ 10, -28 ≤ k ≤ 29, -17 ≤ l ≤ 17
Reflections collected	17418
Independent reflections	7150 [R_{int} = 0.0348, R_{sigma} = 0.0506]
Data/restraints/parameters	7150/61/374
Goodness-of-fit on F^2	1.036
Final R indexes [I>=2σ (I)]	R_1 = 0.0364, wR_2 = 0.0846
Final R indexes [all data]	R_1 = 0.0507, wR_2 = 0.0901
Largest diff. peak/hole / e $Å^{-3}$	2.16/-0.86

Table 2 Bond Lengths for 3943f.

Atom	Atom	Length/Å	Atom	Atom	Length/Å
W	P	2.4966(10)	C3	C4	1.399(6)
W	C22	2.023(5)	C3	C5	1.395(5)
W	C23	2.039(5)	C4	C5[1]	1.387(6)
W	C24	2.061(5)	C5	C4[1]	1.387(6)
W	C25	2.061(5)	C6	C7	1.531(6)
W	C26	2.039(5)	C6	C8	1.511(6)
P	O1	1.678(3)	C9	C10	1.516(6)
P	C2	1.859(4)	C9	C11	1.524(6)
P	C12	1.884(4)	C12	C13	1.514(6)
O1	C1	1.376(4)	C12	C16	1.532(6)
O2	C22	1.141(6)	C12	C17	1.528(6)
O3	C23	1.143(5)	C13	C14	1.342(6)
O4	C24	1.130(5)	C13	C18	1.480(6)
O5	C25	1.128(6)	C14	C15	1.498(6)
O6	C26	1.144(6)	C14	C19	1.495(6)
N1	C1	1.385(5)	C15	C16	1.340(6)
N1	C2	1.406(5)	C15	C20	1.488(6)
N1	C6	1.485(5)	C16	C21	1.504(6)
N2	C1	1.254(5)	C27	C28	1.481(10)
N2	C3	1.420(5)	C28	C29	1.498(10)
N3	C2	1.266(5)	C29	C30	1.470(10)
N3	C9	1.462(5)	C30	C31	1.487(10)

[1]2-X,2-Y,-Z

Table 3 Bond Angles for 3943f.

Atom	Atom	Atom	Angle/˚	Atom	Atom	Atom	Angle/˚
C22	W	P	170.74(14)	C5	C3	C4	117.3(4)
C22	W	C23	87.19(18)	C5[1]	C4	C3	120.2(4)
C22	W	C24	90.95(18)	C4[1]	C5	C3	122.5(4)
C22	W	C25	89.58(18)	N1	C6	C7	110.7(3)
C22	W	C26	88.45(19)	N1	C6	C8	111.6(3)
C23	W	P	99.69(12)	C8	C6	C7	113.3(4)
C23	W	C24	89.69(18)	N3	C9	C10	106.7(3)
C23	W	C25	176.06(17)	N3	C9	C11	109.6(4)
C23	W	C26	87.3(2)	C10	C9	C11	111.2(4)
C24	W	P	82.96(12)	C13	C12	P	109.0(3)
C25	W	P	83.76(12)	C13	C12	C16	103.3(3)
C25	W	C24	92.62(18)	C13	C12	C17	113.7(4)
C26	W	P	97.98(14)	C16	C12	P	110.6(3)
C26	W	C24	177.00(19)	C17	C12	P	108.0(3)
C26	W	C25	90.3(2)	C17	C12	C16	112.3(3)
O1	P	W	105.80(10)	C14	C13	C12	109.0(4)
O1	P	C2	90.19(16)	C14	C13	C18	127.1(4)
O1	P	C12	101.31(16)	C18	C13	C12	123.6(4)
C2	P	W	121.41(13)	C13	C14	C15	109.6(4)
C2	P	C12	103.87(19)	C13	C14	C19	128.2(4)
C12	P	W	126.13(14)	C19	C14	C15	121.9(4)
C1	O1	P	116.2(2)	C16	C15	C14	109.2(4)
C1	N1	C2	116.7(3)	C16	C15	C20	127.2(4)
C1	N1	C6	120.8(3)	C20	C15	C14	123.7(4)
C2	N1	C6	122.1(3)	C15	C16	C12	108.8(4)
C1	N2	C3	126.0(3)	C15	C16	C21	126.2(4)
C2	N3	C9	120.8(3)	C21	C16	C12	124.4(4)
O1	C1	N1	110.7(3)	O2	C22	W	178.8(4)
N2	C1	O1	125.9(4)	O3	C23	W	175.8(4)
N2	C1	N1	123.4(4)	O4	C24	W	177.2(4)
N1	C2	P	105.6(3)	O5	C25	W	178.7(4)
N3	C2	P	133.3(3)	O6	C26	W	176.4(5)
N3	C2	N1	121.0(4)	C27	C28	C29	141(3)
C4	C3	N2	126.5(3)	C30	C29	C28	113.7(10)
C5	C3	N2	116.1(4)	C29	C30	C31	106.3(9)

[1]2-X,2-Y,-Z

Table 4 Torsion Angles for 3943f.

A	B	C	D	Angle/˚	A	B	C	D	Angle/˚
W	P	O1	C1	-125.2(2)	C3	N2	C1	O1	0.5(7)
W	P	C2	N1	114.1(2)	C3	N2	C1	N1	178.4(4)
W	P	C2	N3	-63.7(5)	C4	C3	C5	C4[1]	-1.6(7)
W	P	C12	C13	70.9(3)	C5	C3	C4	C5[1]	1.5(7)

W	P	C12	C16	-176.2(2)	C6	N1	C1	O1	178.9(3)
W	P	C12	C17	-53.0(3)	C6	N1	C1	N2	0.8(6)
P	O1	C1	N1	-1.6(4)	C6	N1	C2	P	179.9(3)
P	O1	C1	N2	176.5(3)	C6	N1	C2	N3	-2.0(6)
P	C12	C13	C14	116.4(4)	C9	N3	C2	P	5.2(6)
P	C12	C13	C18	-68.7(5)	C9	N3	C2	N1	-172.3(4)
P	C12	C16	C15	-114.0(4)	C12	P	O1	C1	101.9(3)
P	C12	C16	C21	73.8(5)	C12	P	C2	N1	-96.3(3)
O1	P	C2	N1	5.4(3)	C12	P	C2	N3	85.9(5)
O1	P	C2	N3	-172.4(4)	C12	C13	C14	C15	-0.4(5)
O1	P	C12	C13	-169.8(3)	C12	C13	C14	C19	172.6(5)
O1	P	C12	C16	-56.9(3)	C13	C12	C16	C15	2.5(5)
O1	P	C12	C17	66.3(3)	C13	C12	C16	C21	-169.7(4)
N2	C3	C4	C5[1]	178.5(4)	C13	C14	C15	C16	2.1(6)
N2	C3	C5	C4[1]	-178.9(4)	C13	C14	C15	C20	-178.5(5)
C1	N1	C2	P	-7.7(4)	C14	C15	C16	C12	-2.8(5)
C1	N1	C2	N3	170.5(4)	C14	C15	C16	C21	169.3(4)
C1	N1	C6	C7	-107.9(4)	C16	C12	C13	C14	-1.2(5)
C1	N1	C6	C8	124.9(4)	C16	C12	C13	C18	173.7(4)
C1	N2	C3	C4	24.9(7)	C17	C12	C13	C14	-123.1(4)
C1	N2	C3	C5	-158.1(4)	C17	C12	C13	C18	51.8(6)
C2	P	O1	C1	-2.3(3)	C17	C12	C16	C15	125.4(4)
C2	P	C12	C13	-76.8(3)	C17	C12	C16	C21	-46.9(5)
C2	P	C12	C16	36.1(3)	C18	C13	C14	C15	-175.1(4)
C2	P	C12	C17	159.4(3)	C18	C13	C14	C19	-2.1(8)
C2	N1	C1	O1	6.4(5)	C19	C14	C15	C16	-171.4(4)
C2	N1	C1	N2	-171.8(4)	C19	C14	C15	C20	8.0(7)
C2	N1	C6	C7	64.2(5)	C20	C15	C16	C12	177.8(4)
C2	N1	C6	C8	-63.0(5)	C20	C15	C16	C21	-10.1(8)
C2	N3	C9	C10	109.5(4)	C27	C28	C29	C30	-70(5)
C2	N3	C9	C11	-130.1(4)	C28	C29	C30	C31	6(4)

8.15. Crystal data and structure refinement for **39**

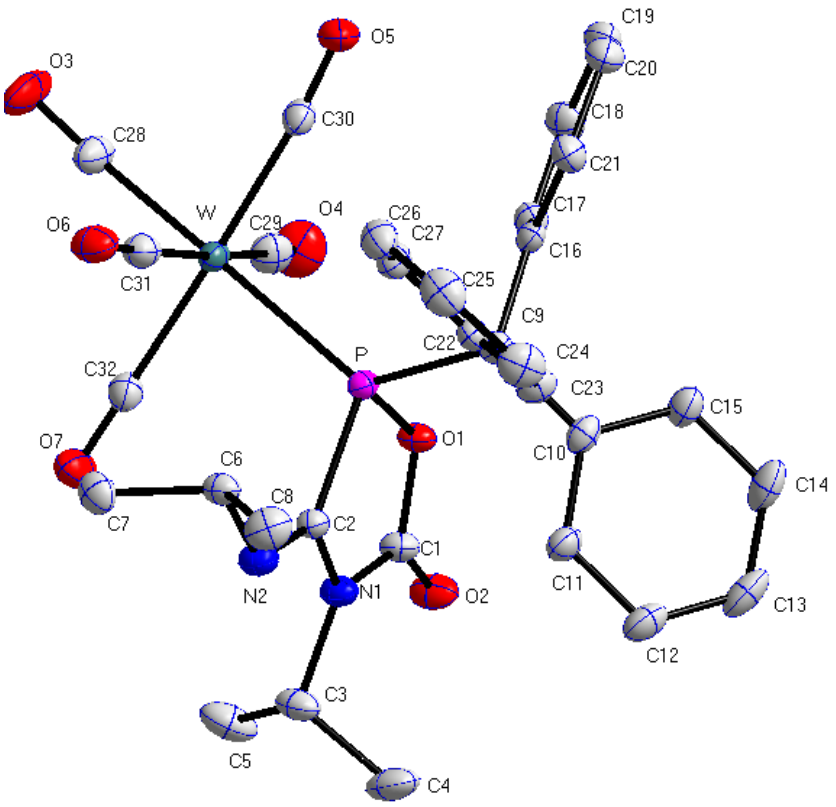

Table 8.15. Crystal data and structure refinement for **39**.

Identification code	GSTR295, 2671
Device Type	STOE IPDS2T
Empirical formula	C32 H29 N2 O7 P W
Moiety formula	C32 H29 N2 O7 P W
Formula weight	768.39
Temperature/K	123(2)
Crystal system	Triclinic
Space group	P-1
a/Å	9.1467(4)
b/Å	9.9353(4)
c/Å	17.7375(7)
α/°	74.768(3)
β/°	85.528(3)
γ/°	83.659(3)
Volume/Å^3	1.653
Z	2
ρ_{calc}g/cm^3	1.346
μ/mm^{-1}	0.093
F(000)	452
Crystal size/mm^3	0.10 x 0.10 x 0.05

Absorption correction	Empirical
Tmin; Tmax	0.9954; 0.9908
Radiation	MoKα (λ = 0.71073)
2Θ range for data collection/°	2.08 to 28.00°
Completeness to theta	0.987
Index ranges	-15 ≤ h ≤ 17, -13 ≤ k ≤ 12, -34 ≤ l ≤ 24
Reflections collected	9760
Independent reflections	5058 [R(int) = 0.0242]
Data/restraints/parameters	5058 / 1 / 289
Goodness-of-fit on F^2	1.062
Final R indexes [I>=2σ (I)]	R1 = 0.0415, wR2 = 0.0990
Final R indexes [all data]	R1 = 0.0578, wR2 = 0.1088
Largest diff. peak/hole / e $Å^{-3}$	0.281/-0.249

8.16. Crystal data and structure refinement for **44**

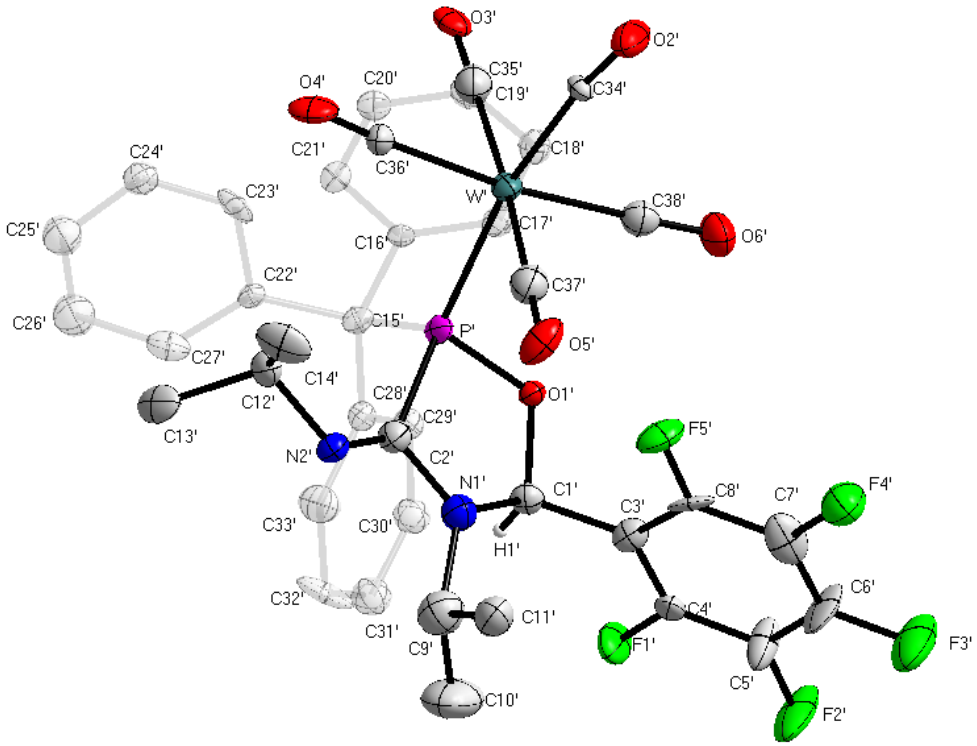

Table 8.16. Crystal data and structure refinement for **44**.

Identification code	GSTR417, JMV-452 // GXray4003_0t0
Device Type	Bruker X8-KappaApexII
Empirical formula	$C_{76}H_{61}F_{10}N_4O_{12}P_2W_2$
Moiety formula	C38 H31 F5 N2 O6 P W, C38 H30 F5 N2 O6 P W
Formula weight	1841.92
Temperature/K	100
Crystal system	monoclinic
Space group	C2/c
a/Å	43.742(5)
b/Å	9.4789(12)
c/Å	34.564(5)
α/°	90
β/°	94.132(6)
γ/°	90
Volume/Å^3	14294(3)
Z	8
ρ_{calc}g/cm^3	1.712
μ/mm^{-1}	3.353
F(000)	7272.0
Crystal size/mm^3	0.08 × 0.04 × 0.02
Absorption correction	empirical
Tmin; Tmax	0.482305; 0.745979

Radiation	MoKα (λ = 0.71073)
2Θ range for data collection/°	4.398 to 50.498°
Completeness to theta	0.843
Index ranges	-50 ≤ h ≤ 47, 0 ≤ k ≤ 11, 0 ≤ l ≤ 41
Reflections collected	22163
Independent reflections	22163 [R_{int} = 0.1698, R_{sigma} = 0.3047]
Data/restraints/parameters	22163/379/964
Goodness-of-fit on F^2	0.988
Final R indexes [I>=2σ (I)]	R_1 = 0.1024, wR_2 = 0.1869
Final R indexes [all data]	R_1 = 0.2372, wR_2 = 0.2392
Largest diff. peak/hole / e $Å^{-3}$	3.35/-3.11

Table 2 Bond Lengths for 4003_0t0.

Atom	Atom	Length/Å	Atom	Atom	Length/Å
W	P	2.528(6)	W'	P'	2.512(6)
W	C34	2.02(3)	W'	C34'	1.99(2)
W	C35	2.04(2)	W'	C35'	2.01(3)
W	C36	2.04(2)	W'	C36'	2.04(2)
W	C37	2.08(2)	W'	C37'	1.98(2)
W	C38	2.05(2)	W'	C38'	2.05(2)
P	O1	1.654(14)	P'	O1'	1.649(14)
P	C2	1.82(2)	P'	C2'	1.87(2)
P	C15	1.93(2)	P'	C15'	1.91(2)
F1	C4	1.33(2)	F1'	C4'	1.33(2)
F2	C5	1.34(2)	F2'	C5'	1.35(3)
F3	C6	1.32(2)	F3'	C6'	1.33(2)
F4	C7	1.30(2)	F4'	C7'	1.36(2)
F5	C8	1.37(2)	F5'	C8'	1.34(2)
O1	C1	1.47(2)	O1'	C1'	1.44(2)
O2	C34	1.13(2)	O2'	C34'	1.15(2)
O3	C35	1.14(2)	O3'	C35'	1.16(2)
O4	C36	1.15(2)	O4'	C36'	1.12(2)
O5	C37	1.12(2)	O5'	C37'	1.20(2)
O6	C38	1.14(2)	O6'	C38'	1.15(2)
N1	C1	1.45(3)	N1'	C1'	1.49(3)
N1	C2	1.37(2)	N1'	C2'	1.39(3)
N1	C9	1.50(2)	N1'	C9'	1.52(3)
N2	C2	1.32(3)	N2'	C2'	1.26(2)
N2	C12	1.47(3)	N2'	C12'	1.47(3)
C1	C3	1.48(3)	C1'	C3'	1.51(3)
C3	C4	1.40(3)	C3'	C4'	1.43(3)
C3	C8	1.36(3)	C3'	C8'	1.35(3)
C4	C5	1.38(3)	C4'	C5'	1.37(3)

C5	C6	1.39(3)	C5'	C6'	1.35(3)
C6	C7	1.37(3)	C6'	C7'	1.39(3)
C7	C8	1.43(3)	C7'	C8'	1.39(3)
C9	C10	1.61(3)	C9'	C10'	1.49(3)
C9	C11	1.54(3)	C9'	C11'	1.53(3)
C12	C13	1.49(3)	C12'	C13'	1.56(3)
C12	C14	1.48(3)	C12'	C14'	1.48(3)
C15	C16	1.53(3)	C15'	C16'	1.56(3)
C15	C22	1.57(3)	C15'	C22'	1.54(3)
C15	C28	1.54(3)	C15'	C28'	1.54(3)
C16	C17	1.37(3)	C16'	C17'	1.34(3)
C16	C21	1.42(3)	C16'	C21'	1.41(2)
C17	C18	1.38(3)	C17'	C18'	1.41(3)
C18	C19	1.39(3)	C18'	C19'	1.36(3)
C19	C20	1.39(3)	C19'	C20'	1.31(3)
C20	C21	1.36(3)	C20'	C21'	1.39(3)
C22	C23	1.40(3)	C22'	C23'	1.43(3)
C22	C27	1.35(3)	C22'	C27'	1.38(3)
C23	C24	1.36(3)	C23'	C24'	1.40(3)
C24	C25	1.40(3)	C24'	C25'	1.36(3)
C25	C26	1.33(3)	C25'	C26'	1.36(3)
C26	C27	1.40(3)	C26'	C27'	1.40(3)
C28	C29	1.39(3)	C28'	C29'	1.41(3)
C28	C33	1.41(3)	C28'	C33'	1.43(3)
C29	C30	1.38(3)	C29'	C30'	1.41(3)
C30	C31	1.40(3)	C30'	C31'	1.31(3)
C31	C32	1.40(3)	C31'	C32'	1.38(3)
C32	C33	1.37(3)	C32'	C33'	1.40(3)

Table 3 Bond Angles for 4003_0t0.

Atom	Atom	Atom	Angle/˚	Atom	Atom	Atom	Angle/˚
C34	W	P	172.0(7)	C34'	W'	P'	170.3(6)
C34	W	C35	87.6(9)	C34'	W'	C35'	91.0(9)
C34	W	C36	87.4(9)	C34'	W'	C36'	88.5(9)
C34	W	C37	86.6(9)	C34'	W'	C38'	85.5(9)
C34	W	C38	88.2(9)	C35'	W'	P'	95.6(7)
C35	W	P	88.0(6)	C35'	W'	C36'	83.7(9)
C35	W	C36	91.4(8)	C35'	W'	C38'	93.4(9)
C35	W	C37	174.2(9)	C36'	W'	P'	99.3(6)
C35	W	C38	89.8(8)	C36'	W'	C38'	173.3(9)
C36	W	P	86.0(6)	C37'	W'	P'	85.4(7)
C36	W	C37	89.3(8)	C37'	W'	C34'	88.7(9)
C36	W	C38	175.4(8)	C37'	W'	C35'	175.1(9)
C37	W	P	97.7(6)	C37'	W'	C36'	91.4(9)
C38	W	P	98.5(6)	C37'	W'	C38'	91.5(9)

C38	W	C37	89.1(9)	C38'	W'	P'	87.0(6)
O1	P	W	107.3(5)	O1'	P'	W'	108.1(5)
O1	P	C2	89.7(9)	O1'	P'	C2'	91.9(9)
O1	P	C15	100.5(8)	O1'	P'	C15'	100.7(8)
C2	P	W	117.6(7)	C2'	P'	W'	116.0(7)
C2	P	C15	108.3(9)	C2'	P'	C15'	108.0(9)
C15	P	W	125.4(7)	C15'	P'	W'	125.5(7)
C1	O1	P	116.6(12)	C1'	O1'	P'	116.5(12)
C1	N1	C9	122.4(17)	C1'	N1'	C9'	122.2(18)
C2	N1	C1	115.8(17)	C2'	N1'	C1'	117.5(18)
C2	N1	C9	119.9(18)	C2'	N1'	C9'	119(2)
C2	N2	C12	124(2)	C2'	N2'	C12'	123(2)
O1	C1	C3	105.8(16)	O1'	C1'	N1'	104.1(15)
N1	C1	O1	104.1(16)	O1'	C1'	C3'	107.8(16)
N1	C1	C3	116.9(17)	N1'	C1'	C3'	113.7(17)
N1	C2	P	109.7(16)	N1'	C2'	P'	105.4(16)
N2	C2	P	129.0(18)	N2'	C2'	P'	134.9(18)
N2	C2	N1	120(2)	N2'	C2'	N1'	119(2)
C4	C3	C1	123(2)	C4'	C3'	C1'	118.0(19)
C8	C3	C1	121(2)	C8'	C3'	C1'	126(2)
C8	C3	C4	116(2)	C8'	C3'	C4'	116(2)
F1	C4	C3	122.0(19)	F1'	C4'	C3'	119.2(19)
F1	C4	C5	117(2)	F1'	C4'	C5'	120(2)
C5	C4	C3	121(2)	C5'	C4'	C3'	121(2)
F2	C5	C4	120(2)	F2'	C5'	C4'	118(2)
F2	C5	C6	119(2)	F2'	C5'	C6'	120(2)
C4	C5	C6	122(2)	C6'	C5'	C4'	122(2)
F3	C6	C5	122(2)	F3'	C6'	C5'	122(2)
F3	C6	C7	118(2)	F3'	C6'	C7'	120(2)
C7	C6	C5	121(2)	C5'	C6'	C7'	119(2)
F4	C7	C6	123(2)	F4'	C7'	C6'	120(2)
F4	C7	C8	121(2)	F4'	C7'	C8'	120(2)
C6	C7	C8	116(2)	C8'	C7'	C6'	119(2)
F5	C8	C7	115(2)	F5'	C8'	C3'	120(2)
C3	C8	F5	119.4(19)	F5'	C8'	C7'	117(2)
C3	C8	C7	126(2)	C3'	C8'	C7'	123(2)
N1	C9	C10	108.8(17)	N1'	C9'	C11'	108.4(19)
N1	C9	C11	111.6(18)	C10'	C9'	N1'	115(2)
C11	C9	C10	111.2(19)	C10'	C9'	C11'	118(2)
N2	C12	C13	109.9(19)	N2'	C12'	C13'	107.3(17)
N2	C12	C14	110.1(18)	N2'	C12'	C14'	110.7(18)
C14	C12	C13	111(2)	C14'	C12'	C13'	113.5(19)
C16	C15	P	107.6(13)	C16'	C15'	P'	106.9(13)
C16	C15	C22	110.7(16)	C22'	C15'	P'	109.1(13)
C16	C15	C28	109.3(16)	C22'	C15'	C16'	110.8(16)
C22	C15	P	107.0(13)	C22'	C15'	C28'	111.3(17)
C28	C15	P	111.0(14)	C28'	C15'	P'	110.3(14)

C28	C15	C22	111.1(17)	C28'	C15'	C16'	108.3(17)
C17	C16	C15	121.1(19)	C17'	C16'	C15'	123.2(18)
C17	C16	C21	117(2)	C17'	C16'	C21'	118.0(19)
C21	C16	C15	121.9(17)	C21'	C16'	C15'	118.5(18)
C16	C17	C18	122(2)	C16'	C17'	C18'	121.8(19)
C17	C18	C19	122(2)	C19'	C18'	C17'	118(2)
C18	C19	C20	115(2)	C20'	C19'	C18'	122(2)
C21	C20	C19	123(2)	C19'	C20'	C21'	121(2)
C20	C21	C16	120(2)	C20'	C21'	C16'	119(2)
C23	C22	C15	119.8(18)	C23'	C22'	C15'	117.9(19)
C27	C22	C15	122.5(19)	C27'	C22'	C15'	126(2)
C27	C22	C23	118(2)	C27'	C22'	C23'	115.5(19)
C24	C23	C22	121(2)	C24'	C23'	C22'	121(2)
C23	C24	C25	120(2)	C25'	C24'	C23'	120(2)
C26	C25	C24	120(3)	C26'	C25'	C24'	120(2)
C25	C26	C27	119(2)	C25'	C26'	C27'	120(2)
C22	C27	C26	122(2)	C22'	C27'	C26'	122(2)
C29	C28	C15	124(2)	C29'	C28'	C15'	123.2(19)
C29	C28	C33	117(2)	C29'	C28'	C33'	117(2)
C33	C28	C15	118.8(19)	C33'	C28'	C15'	119.5(19)
C30	C29	C28	123(2)	C30'	C29'	C28'	119(2)
C29	C30	C31	119(2)	C31'	C30'	C29'	124(2)
C30	C31	C32	119(2)	C30'	C31'	C32'	119(2)
C33	C32	C31	121(2)	C31'	C32'	C33'	120(2)
C32	C33	C28	121(2)	C32'	C33'	C28'	120(2)
O2	C34	W	177(2)	O2'	C34'	W'	172.4(18)
O3	C35	W	177(2)	O3'	C35'	W'	176(2)
O4	C36	W	175.4(19)	O4'	C36'	W'	176(2)
O5	C37	W	176(2)	O5'	C37'	W'	178(2)
O6	C38	W	178(2)	O6'	C38'	W'	176(2)

Table 4 Torsion Angles for 4003_0t0.

A	B	C	D	Angle/˚	A	B	C	D	Angle/˚
W	P	O1	C1	-132.4(12)	W'	P'	O1'	C1'	-133.4(11)
W	P	C2	N1	110.4(13)	W'	P'	C2'	N1'	113.1(13)
W	P	C2	N2	-59(2)	W'	P'	C2'	N2'	-57(3)
P	O1	C1	N1	21.1(18)	P'	O1'	C1'	N1'	22.6(17)
P	O1	C1	C3	145.0(14)	P'	O1'	C1'	C3'	143.7(14)
P	C15	C16	C17	142.2(18)	P'	C15'	C16'	C17'	-40(2)
P	C15	C16	C21	-40(2)	P'	C15'	C16'	C21'	146.4(16)
P	C15	C22	C23	-69(2)	P'	C15'	C22'	C23'	-62(2)
P	C15	C22	C27	107(2)	P'	C15'	C22'	C27'	128.6(19)
P	C15	C28	C29	133.4(18)	P'	C15'	C28'	C29'	110(2)
P	C15	C28	C33	-56(2)	P'	C15'	C28'	C33'	-68(2)
F1	C4	C5	F2	2(3)	F1'	C4'	C5'	F2'	-1(4)

F1	C4	C5	C6	180(2)	F1'	C4'	C5'	C6'	-179(2)
F2	C5	C6	F3	1(3)	F2'	C5'	C6'	F3'	1(4)
F2	C5	C6	C7	-179(2)	F2'	C5'	C6'	C7'	178(2)
F3	C6	C7	F4	-2(3)	F3'	C6'	C7'	F4'	-1(4)
F3	C6	C7	C8	-180(2)	F3'	C6'	C7'	C8'	-180(2)
F4	C7	C8	F5	4(3)	F4'	C7'	C8'	F5'	1(3)
F4	C7	C8	C3	178(2)	F4'	C7'	C8'	C3'	180(2)
O1	P	C2	N1	1.0(14)	O1'	P'	C2'	N1'	1.8(14)
O1	P	C2	N2	-168(2)	O1'	P'	C2'	N2'	-168(2)
O1	C1	C3	C4	-59(3)	O1'	C1'	C3'	C4'	123(2)
O1	C1	C3	C8	118(2)	O1'	C1'	C3'	C8'	-55(3)
N1	C1	C3	C4	56(3)	N1'	C1'	C3'	C4'	-122(2)
N1	C1	C3	C8	-126(2)	N1'	C1'	C3'	C8'	60(3)
C1	N1	C2	P	12(2)	C1'	N1'	C2'	P'	12(2)
C1	N1	C2	N2	-177.9(18)	C1'	N1'	C2'	N2'	-176.8(19)
C1	N1	C9	C10	-103(2)	C1'	N1'	C9'	C10'	29(3)
C1	N1	C9	C11	20(3)	C1'	N1'	C9'	C11'	-106(2)
C1	C3	C4	F1	-6(3)	C1'	C3'	C4'	F1'	2(3)
C1	C3	C4	C5	177(2)	C1'	C3'	C4'	C5'	-180(2)
C1	C3	C8	F5	1(3)	C1'	C3'	C8'	F5'	-2(4)
C1	C3	C8	C7	-173(2)	C1'	C3'	C8'	C7'	179(2)
C2	P	O1	C1	-13.4(14)	C2'	P'	O1'	C1'	-15.2(13)
C2	N1	C1	O1	-20(2)	C2'	N1'	C1'	O1'	-21(2)
C2	N1	C1	C3	-136.4(19)	C2'	N1'	C1'	C3'	-138.4(19)
C2	N1	C9	C10	93(2)	C2'	N1'	C9'	C10'	-137(2)
C2	N1	C9	C11	-143.8(19)	C2'	N1'	C9'	C11'	89(2)
C2	N2	C12	C13	-114(2)	C2'	N2'	C12'	C13'	-117(2)
C2	N2	C12	C14	123(2)	C2'	N2'	C12'	C14'	118(2)
C3	C4	C5	F2	179.8(19)	C3'	C4'	C5'	F2'	-179(2)
C3	C4	C5	C6	-2(3)	C3'	C4'	C5'	C6'	4(4)
C4	C3	C8	F5	178.3(18)	C4'	C3'	C8'	F5'	179.5(19)
C4	C3	C8	C7	4(3)	C4'	C3'	C8'	C7'	0(3)
C4	C5	C6	F3	-177(2)	C4'	C5'	C6'	F3'	179(2)
C4	C5	C6	C7	3(4)	C4'	C5'	C6'	C7'	-4(4)
C5	C6	C7	F4	178(2)	C5'	C6'	C7'	F4'	-178(2)
C5	C6	C7	C8	0(3)	C5'	C6'	C7'	C8'	3(4)
C6	C7	C8	F5	-178.1(19)	C6'	C7'	C8'	F5'	180(2)
C6	C7	C8	C3	-4(4)	C6'	C7'	C8'	C3'	-1(4)
C8	C3	C4	F1	177.0(19)	C8'	C3'	C4'	F1'	-179.4(19)
C8	C3	C4	C5	-1(3)	C8'	C3'	C4'	C5'	-2(3)
C9	N1	C1	O1	175.5(15)	C9'	N1'	C1'	O1'	173.0(16)
C9	N1	C1	C3	59(3)	C9'	N1'	C1'	C3'	56(3)
C9	N1	C2	P	176.6(14)	C9'	N1'	C2'	P'	177.7(14)
C9	N1	C2	N2	-13(3)	C9'	N1'	C2'	N2'	-11(3)
C12	N2	C2	P	-10(3)	C12'	N2'	C2'	P'	-8(4)
C12	N2	C2	N1	-178.7(17)	C12'	N2'	C2'	N1'	-176.2(17)
C15	P	O1	C1	95.2(14)	C15'	P'	O1'	C1'	93.6(13)

C15	P	C2	N1	-100.0(15)	C15'	P'	C2'	N1'	-100.1(15)
C15	P	C2	N2	91(2)	C15'	P'	C2'	N2'	90(3)
C15	C16	C17	C18	179.8(19)	C15'	C16'	C17'	C18'	-177.5(19)
C15	C16	C21	C20	179.1(19)	C15'	C16'	C21'	C20'	176.1(18)
C15	C22	C23	C24	177.4(19)	C15'	C22'	C23'	C24'	180.0(17)
C15	C22	C27	C26	-177(2)	C15'	C22'	C27'	C26'	176(2)
C15	C28	C29	C30	176(2)	C15'	C28'	C29'	C30'	-177.6(18)
C15	C28	C33	C32	-176.0(18)	C15'	C28'	C33'	C32'	178(2)
C16	C15	C22	C23	174.2(17)	C16'	C15'	C22'	C23'	56(2)
C16	C15	C22	C27	-10(3)	C16'	C15'	C22'	C27'	-114(2)
C16	C15	C28	C29	-108(2)	C16'	C15'	C28'	C29'	-7(3)
C16	C15	C28	C33	63(2)	C16'	C15'	C28'	C33'	175.0(18)
C16	C17	C18	C19	1(3)	C16'	C17'	C18'	C19'	3(3)
C17	C16	C21	C20	-3(3)	C17'	C16'	C21'	C20'	3(3)
C17	C18	C19	C20	-2(3)	C17'	C18'	C19'	C20'	0(3)
C18	C19	C20	C21	1(3)	C18'	C19'	C20'	C21'	-2(3)
C19	C20	C21	C16	2(3)	C19'	C20'	C21'	C16'	0(3)
C21	C16	C17	C18	2(3)	C21'	C16'	C17'	C18'	-4(3)
C22	C15	C16	C17	-101(2)	C22'	C15'	C16'	C17'	-159.1(19)
C22	C15	C16	C21	77(2)	C22'	C15'	C16'	C21'	28(3)
C22	C15	C28	C29	14(3)	C22'	C15'	C28'	C29'	-129(2)
C22	C15	C28	C33	-174.6(18)	C22'	C15'	C28'	C33'	53(2)
C22	C23	C24	C25	-2(3)	C22'	C23'	C24'	C25'	4(3)
C23	C22	C27	C26	-1(3)	C23'	C22'	C27'	C26'	6(3)
C23	C24	C25	C26	2(3)	C23'	C24'	C25'	C26'	4(3)
C24	C25	C26	C27	-2(4)	C24'	C25'	C26'	C27'	-7(4)
C25	C26	C27	C22	1(4)	C25'	C26'	C27'	C22'	2(4)
C27	C22	C23	C24	1(3)	C27'	C22'	C23'	C24'	-9(3)
C28	C15	C16	C17	22(3)	C28'	C15'	C16'	C17'	79(2)
C28	C15	C16	C21	-160.7(19)	C28'	C15'	C16'	C21'	-95(2)
C28	C15	C22	C23	52(2)	C28'	C15'	C22'	C23'	176.6(18)
C28	C15	C22	C27	-132(2)	C28'	C15'	C22'	C27'	7(3)
C28	C29	C30	C31	-3(3)	C28'	C29'	C30'	C31'	-2(3)
C29	C28	C33	C32	-4(3)	C29'	C28'	C33'	C32'	0(3)
C29	C30	C31	C32	-1(3)	C29'	C30'	C31'	C32'	2(4)
C30	C31	C32	C33	2(3)	C30'	C31'	C32'	C33'	-2(4)
C31	C32	C33	C28	1(3)	C31'	C32'	C33'	C28'	1(4)
C33	C28	C29	C30	5(3)	C33'	C28'	C29'	C30'	1(3)

8.17. Crystal data and structure refinement for **45**

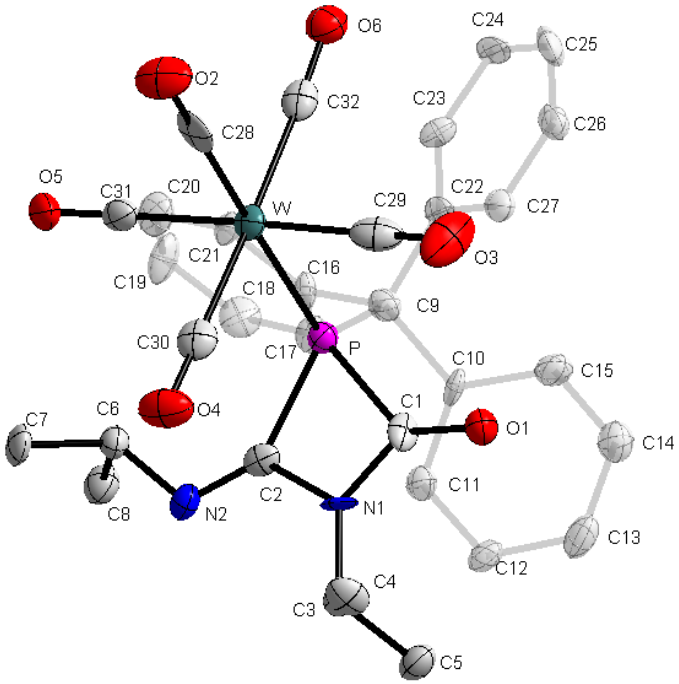

Table 8.17. Crystal data and structure refinement for **45**.

Identification code	GSTR414, JMV-460 // GXray4051g
Device Type	Bruker X8-KappaApexII
Empirical formula	$C_{32}H_{29}N_2O_6PW$
Moiety formula	C32 H29 N2 O6 P W
Formula weight	752.39
Temperature/K	100
Crystal system	triclinic
Space group	P-1
a/Å	9.5314(7)
b/Å	10.1118(7)
c/Å	17.1850(11)
α/°	96.218(4)
β/°	104.840(4)
γ/°	103.765(5)
Volume/Å^3	1529.58(19)
Z	2
ρ_{calc}g/cm^3	1.634
μ/mm^{-1}	3.874
F(000)	744.0
Crystal size/mm^3	0.12 × 0.11 × 0.04
Absorption correction	empirical

Tmin; Tmax	0.5810; 0.7460
Radiation	MoKα (λ = 0.71073)
2Θ range for data collection/°	5.272 to 50.498°
Completeness to theta	0.886
Index ranges	-11 ≤ h ≤ 11, -10 ≤ k ≤ 12, -20 ≤ l ≤ 20
Reflections collected	11086
Independent reflections	4918 [R_{int} = 0.1148, R_{sigma} = 0.2457]
Data/restraints/parameters	4918/66/383
Goodness-of-fit on F^2	0.964
Final R indexes [I>=2σ (I)]	R_1 = 0.0539, wR_2 = 0.0935
Final R indexes [all data]	R_1 = 0.1478, wR_2 = 0.1140
Largest diff. peak/hole / e $Å^{-3}$	3.00/-3.53

Table 2 Bond Lengths for 4051g.

Atom	Atom	Length/Å	Atom	Atom	Length/Å
W	P	2.510(3)	C6	C8	1.527(13)
W	C28	2.000(13)	C9	C10	1.535(12)
W	C29	2.032(13)	C9	C16	1.543(13)
W	C30	2.017(12)	C9	C22	1.532(12)
W	C31	2.046(11)	C10	C11	1.419(12)
W	C32	2.017(12)	C10	C15	1.410(12)
P	C1	1.916(10)	C11	C12	1.394(12)
P	C2	1.887(9)	C12	C13	1.366(12)
P	C9	1.946(10)	C13	C14	1.399(13)
O1	C1	1.207(10)	C14	C15	1.368(13)
O2	C28	1.168(11)	C16	C17	1.373(13)
O3	C29	1.154(13)	C16	C21	1.398(12)
O4	C30	1.167(11)	C17	C18	1.396(13)
O5	C31	1.156(11)	C18	C19	1.355(13)
O6	C32	1.180(11)	C19	C20	1.382(14)
N1	C1	1.326(11)	C20	C21	1.381(14)
N1	C2	1.455(12)	C22	C23	1.404(12)
N1	C3	1.452(11)	C22	C27	1.412(13)
N2	C2	1.255(11)	C23	C24	1.390(12)
N2	C6	1.486(12)	C24	C25	1.396(14)
C3	C4	1.517(13)	C25	C26	1.379(14)
C3	C5	1.512(12)	C26	C27	1.394(12)
C6	C7	1.533(12)			

Table 3 Bond Angles for 4051g.

Atom	Atom	Atom	Angle/˚	Atom	Atom	Atom	Angle/˚
C28	W	P	178.4(3)	C8	C6	C7	111.0(8)

C28	W	C29	91.6(4)	C10	C9	P	108.5(6)
C28	W	C30	92.4(4)	C10	C9	C16	111.6(8)
C28	W	C31	88.3(4)	C16	C9	P	109.2(6)
C28	W	C32	84.0(4)	C22	C9	P	103.2(6)
C29	W	P	86.8(3)	C22	C9	C10	111.1(7)
C29	W	C31	177.8(5)	C22	C9	C16	112.8(8)
C30	W	P	87.5(3)	C11	C10	C9	121.7(8)
C30	W	C29	90.2(4)	C15	C10	C9	121.9(8)
C30	W	C31	87.6(4)	C15	C10	C11	116.1(8)
C30	W	C32	176.4(4)	C12	C11	C10	120.8(9)
C31	W	P	93.3(3)	C13	C12	C11	121.2(9)
C32	W	P	96.1(3)	C12	C13	C14	119.2(9)
C32	W	C29	89.4(4)	C15	C14	C13	120.3(9)
C32	W	C31	92.8(4)	C14	C15	C10	122.4(9)
C1	P	W	110.9(3)	C17	C16	C9	122.0(9)
C1	P	C9	107.5(4)	C17	C16	C21	118.4(9)
C2	P	W	113.5(3)	C21	C16	C9	119.6(8)
C2	P	C1	69.9(4)	C16	C17	C18	120.4(9)
C2	P	C9	112.5(4)	C19	C18	C17	120.5(9)
C9	P	W	127.5(3)	C18	C19	C20	120.2(10)
C1	N1	C2	103.1(8)	C19	C20	C21	119.5(10)
C1	N1	C3	130.9(9)	C20	C21	C16	120.9(9)
C3	N1	C2	125.8(8)	C23	C22	C9	120.9(9)
C2	N2	C6	116.5(8)	C23	C22	C27	118.2(8)
O1	C1	P	132.5(8)	C27	C22	C9	120.6(8)
O1	C1	N1	132.6(10)	C24	C23	C22	120.9(9)
N1	C1	P	94.8(6)	C23	C24	C25	119.0(9)
N1	C2	P	91.9(6)	C26	C25	C24	121.9(9)
N2	C2	P	142.4(8)	C25	C26	C27	118.6(10)
N2	C2	N1	125.5(9)	C26	C27	C22	121.3(9)
N1	C3	C4	109.9(7)	O2	C28	W	179.5(9)
N1	C3	C5	110.6(8)	O3	C29	W	178.0(10)
C5	C3	C4	112.3(8)	O4	C30	W	178.7(9)
N2	C6	C7	106.8(8)	O5	C31	W	176.1(10)
N2	C6	C8	110.0(8)	O6	C32	W	174.6(8)

Table 4 Torsion Angles for 4051g.

A	B	C	D	Angle/˚	A	B	C	D	Angle/˚
W	P	C2	N1	-101.7(5)	C9	C22	C23	C24	-175.5(8)
W	P	C2	N2	71.9(13)	C9	C22	C27	C26	177.2(8)
P	C9	C10	C11	61.4(10)	C10	C9	C16	C17	-11.9(12)
P	C9	C10	C15	-124.0(9)	C10	C9	C16	C21	171.1(8)
P	C9	C16	C17	-131.8(8)	C10	C9	C22	C23	107.8(10)
P	C9	C16	C21	51.2(10)	C10	C9	C22	C27	-67.3(11)
P	C9	C22	C23	-136.1(8)	C10	C11	C12	C13	-1.6(15)

P	C9	C22	C27	48.8(10)	C11	C10	C15	C14	-1.2(14)
C1	P	C2	N1	3.1(5)	C11	C12	C13	C14	0.7(16)
C1	P	C2	N2	176.7(14)	C12	C13	C14	C15	0.0(15)
C1	N1	C2	P	-4.3(7)	C13	C14	C15	C10	0.3(16)
C1	N1	C2	N2	-179.5(9)	C15	C10	C11	C12	1.8(14)
C1	N1	C3	C4	55.0(12)	C16	C9	C10	C11	-58.9(11)
C1	N1	C3	C5	-69.5(12)	C16	C9	C10	C15	115.6(10)
C2	N1	C1	P	4.3(7)	C16	C9	C22	C23	-18.4(12)
C2	N1	C1	O1	-178.6(11)	C16	C9	C22	C27	166.6(8)
C2	N1	C3	C4	-119.5(10)	C16	C17	C18	C19	-0.6(15)
C2	N1	C3	C5	115.9(10)	C17	C16	C21	C20	2.8(14)
C2	N2	C6	C7	-122.7(9)	C17	C18	C19	C20	0.7(15)
C2	N2	C6	C8	116.8(9)	C18	C19	C20	C21	0.9(15)
C3	N1	C1	P	-171.2(8)	C19	C20	C21	C16	-2.7(15)
C3	N1	C1	O1	6.0(18)	C21	C16	C17	C18	-1.2(14)
C3	N1	C2	P	171.5(7)	C22	C9	C10	C11	174.2(9)
C3	N1	C2	N2	-3.8(15)	C22	C9	C10	C15	-11.2(12)
C6	N2	C2	P	6.6(17)	C22	C9	C16	C17	114.0(10)
C6	N2	C2	N1	178.7(8)	C22	C9	C16	C21	-62.9(11)
C9	P	C2	N1	104.4(6)	C22	C23	C24	C25	-1.1(14)
C9	P	C2	N2	-82.0(13)	C23	C22	C27	C26	2.0(13)
C9	C10	C11	C12	176.7(9)	C23	C24	C25	C26	0.9(15)
C9	C10	C15	C14	-176.0(9)	C24	C25	C26	C27	0.7(15)
C9	C16	C17	C18	-178.1(8)	C25	C26	C27	C22	-2.2(14)
C9	C16	C21	C20	179.8(9)	C27	C22	C23	C24	-0.3(13)

8.18. Crystal data and structure refinement for **26b**

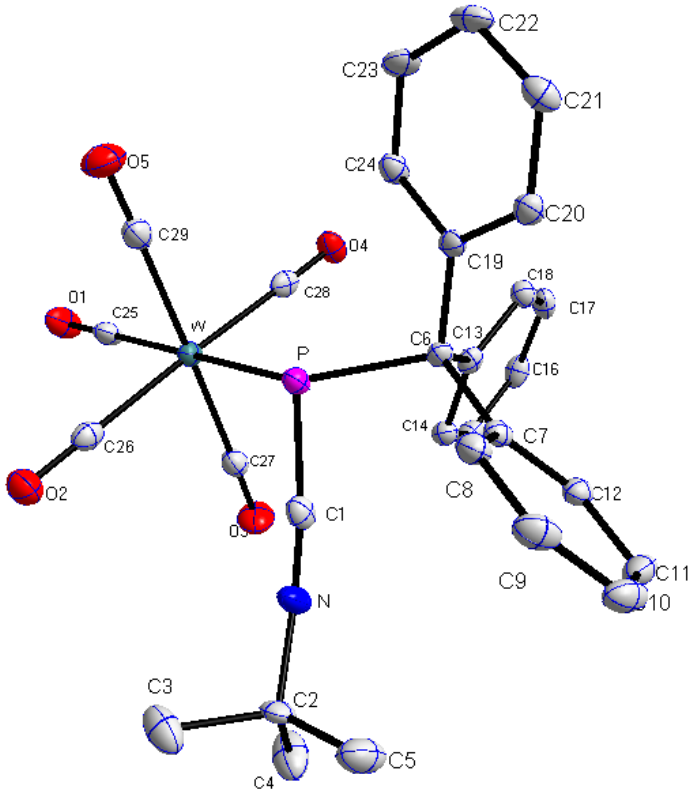

Table 8.18. Crystal data and structure refinement for **26b**.

Identification code	GSTR421, JMV474 // GXray4100f
Device Type	Bruker X8-KappaApexII
Empirical formula	$C_{29}H_{24}NO_5PW$
Moiety formula	C29 H24 N O5 P W
Formula weight	681.31
Temperature/K	100
Crystal system	monoclinic
Space group	$P2_1/n$
a/Å	13.1709(10)
b/Å	13.0975(9)
c/Å	15.6670(12)
α/°	90
β/°	91.408(2)
γ/°	90
Volume/Å^3	2701.8(3)
Z	4
ρ_{calc}g/cm^3	1.675
μ/mm^{-1}	4.373
F(000)	1336.0
Crystal size/mm^3	0.24 × 0.22 × 0.2

Absorption correction	empirical
Tmin; Tmax	0.4719; 0.7460
Radiation	MoKα (λ = 0.71073)
2Θ range for data collection/°	5.06 to 55.996°
Completeness to theta	0.995
Index ranges	-17 ≤ h ≤ 16, -17 ≤ k ≤ 14, -20 ≤ l ≤ 20
Reflections collected	26300
Independent reflections	6503 [R_{int} = 0.0405, R_{sigma} = 0.0355]
Data/restraints/parameters	6503/0/337
Goodness-of-fit on F^2	1.048
Final R indexes [I>=2σ (I)]	R_1 = 0.0220, wR_2 = 0.0470
Final R indexes [all data]	R_1 = 0.0268, wR_2 = 0.0483
Largest diff. peak/hole / e $Å^{-3}$	0.78/-0.63

Table 2 Bond Lengths for 4100f.

Atom	Atom	Length/Å	Atom	Atom	Length/Å
W	P	2.5908(7)	C6	C19	1.538(3)
W	C25	1.989(3)	C7	C8	1.404(3)
W	C26	2.043(3)	C7	C12	1.388(3)
W	C27	2.047(3)	C8	C9	1.383(4)
W	C28	2.048(3)	C9	C10	1.383(4)
W	C29	2.041(3)	C10	C11	1.377(4)
P	C1	1.747(3)	C11	C12	1.400(4)
P	C6	1.952(2)	C13	C14	1.401(3)
O1	C25	1.146(3)	C13	C18	1.391(3)
O2	C26	1.146(3)	C14	C15	1.376(3)
O3	C27	1.141(3)	C15	C16	1.392(4)
O4	C28	1.139(3)	C16	C17	1.379(4)
O5	C29	1.139(3)	C17	C18	1.391(3)
N	C1	1.156(3)	C19	C20	1.395(3)
N	C2	1.462(3)	C19	C24	1.399(3)
C2	C3	1.515(4)	C20	C21	1.386(3)
C2	C4	1.516(4)	C21	C22	1.387(4)
C2	C5	1.520(4)	C22	C23	1.389(4)
C6	C7	1.531(3)	C23	C24	1.385(3)
C6	C13	1.538(3)			

Table 3 Bond Angles for 4100f.

Atom	Atom	Atom	Angle/˚	Atom	Atom	Atom	Angle/˚
C25	W	P	172.40(8)	C19	C6	P	103.35(15)
C25	W	C26	88.75(10)	C8	C7	C6	119.6(2)
C25	W	C27	90.43(11)	C12	C7	C6	122.7(2)
C25	W	C28	91.96(10)	C12	C7	C8	117.7(2)
C25	W	C29	88.11(11)	C9	C8	C7	121.0(2)
C26	W	P	85.87(7)	C8	C9	C10	120.5(3)
C26	W	C27	88.74(10)	C11	C10	C9	119.5(3)
C26	W	C28	178.15(10)	C10	C11	C12	120.2(3)
C27	W	P	94.81(7)	C7	C12	C11	121.1(2)
C27	W	C28	89.55(10)	C14	C13	C6	121.0(2)
C28	W	P	93.58(7)	C18	C13	C6	121.2(2)
C29	W	P	86.61(8)	C18	C13	C14	117.8(2)
C29	W	C26	90.97(10)	C15	C14	C13	121.1(2)
C29	W	C27	178.52(10)	C14	C15	C16	120.5(2)
C29	W	C28	90.76(10)	C17	C16	C15	119.1(2)
C1	P	W	101.06(8)	C16	C17	C18	120.4(2)
C1	P	C6	98.57(11)	C13	C18	C17	121.1(2)
C6	P	W	124.25(7)	C20	C19	C6	122.3(2)
C1	N	C2	165.5(3)	C20	C19	C24	117.5(2)
N	C1	P	173.6(2)	C24	C19	C6	120.1(2)
N	C2	C3	106.5(2)	C21	C20	C19	120.9(2)
N	C2	C4	108.4(2)	C20	C21	C22	120.9(2)
N	C2	C5	106.4(2)	C21	C22	C23	118.8(2)
C3	C2	C4	109.4(2)	C24	C23	C22	120.2(2)
C3	C2	C5	112.7(2)	C23	C24	C19	121.6(2)
C4	C2	C5	113.2(2)	O1	C25	W	178.5(2)
C7	C6	P	106.54(15)	O2	C26	W	178.7(2)
C7	C6	C13	112.56(19)	O3	C27	W	177.6(2)
C7	C6	C19	111.01(19)	O4	C28	W	178.6(2)
C13	C6	P	112.01(16)	O5	C29	W	178.1(2)
C13	C6	C19	110.92(18)				

Table 4 Torsion Angles for 4100f.

A	B	C	D	Angle/˚	A	B	C	D	Angle/˚
P	C6	C7	C8	-52.9(3)	C10	C11	C12	C7	-1.1(4)
P	C6	C7	C12	130.1(2)	C12	C7	C8	C9	-0.4(4)
P	C6	C13	C14	-49.1(3)	C13	C6	C7	C8	-176.0(2)
P	C6	C13	C18	132.9(2)	C13	C6	C7	C12	6.9(3)
P	C6	C19	C20	125.6(2)	C13	C6	C19	C20	-114.2(2)
P	C6	C19	C24	-55.4(2)	C13	C6	C19	C24	64.8(3)
C1	N	C2	C3	55.5(11)	C13	C14	C15	C16	0.3(4)
C1	N	C2	C4	173.0(10)	C14	C13	C18	C17	1.2(4)
C1	N	C2	C5	-65.0(11)	C14	C15	C16	C17	0.5(4)
C6	C7	C8	C9	-177.5(2)	C15	C16	C17	C18	-0.5(4)

C6	C7	C12	C11	178.1(2)	C16	C17	C18	C13	-0.4(4)
C6	C13	C14	C15	-179.2(2)	C18	C13	C14	C15	-1.1(4)
C6	C13	C18	C17	179.3(2)	C19	C6	C7	C8	58.9(3)
C6	C19	C20	C21	-178.9(2)	C19	C6	C7	C12	-118.1(2)
C6	C19	C24	C23	179.3(2)	C19	C6	C13	C14	-164.0(2)
C7	C6	C13	C14	71.0(3)	C19	C6	C13	C18	18.0(3)
C7	C6	C13	C18	-107.1(3)	C19	C20	C21	C22	-0.7(4)
C7	C6	C19	C20	11.8(3)	C20	C19	C24	C23	-1.7(4)
C7	C6	C19	C24	-169.2(2)	C20	C21	C22	C23	-1.2(4)
C7	C8	C9	C10	-0.4(4)	C21	C22	C23	C24	1.6(4)
C8	C7	C12	C11	1.1(4)	C22	C23	C24	C19	-0.1(4)
C8	C9	C10	C11	0.4(4)	C24	C19	C20	C21	2.0(4)
C9	C10	C11	C12	0.3(4)					

8.19. Crystal data and structure refinement for **54**.

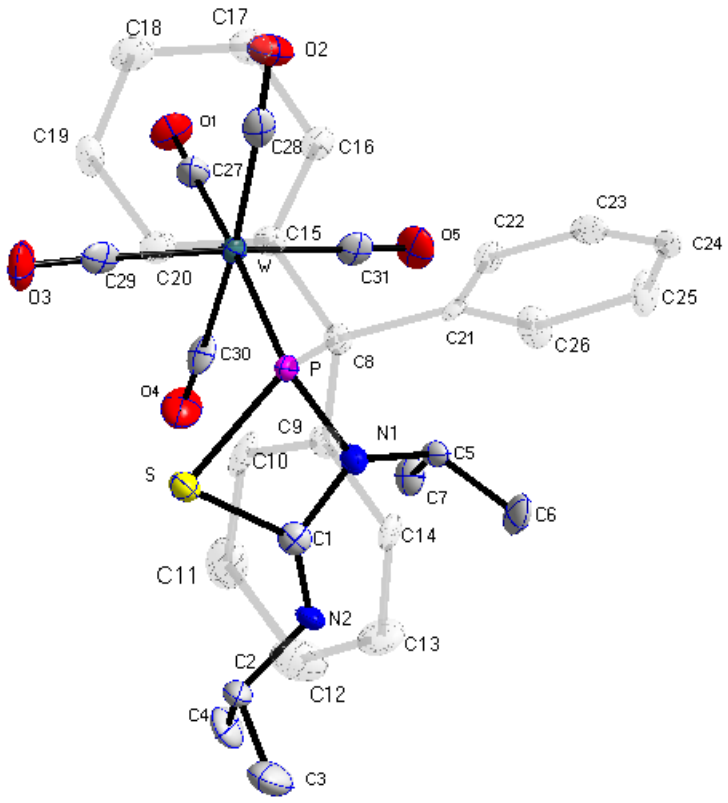

Table 8.19. Crystal data and structure refinement for **54**.

Identification code	GSTR386, JMV416 // GXray3815
Device Type	STOE IPDS 2T
Empirical formula	$C_{31}H_{29}N_2O_5PSW$
Formula weight	756.44
Temperature/K	123(2)
Crystal system	triclinic
Space group	P-1
a/Å	9.6390(6)
b/Å	9.9715(5)
c/Å	16.9758(11)
α/°	78.438(5)
β/°	89.320(5)
γ/°	73.325(4)
Volume/Å^3	1529.49(16)
Z	2
ρ_{calc}g/cm^3	1.643
μ/mm^{-1}	3.938
F(000)	748.0
Crystal size/mm^3	0.12 × 0.09 × 0.03

Absorption correction	integration
Tmin; Tmax	0.4692; 0.6566
Radiation	MoKα (λ = 0.71073)
2Θ range for data collection/°	5.22 to 50.5°
Completeness to theta	0.976
Index ranges	-11 ≤ h ≤ 11, -11 ≤ k ≤ 11, -20 ≤ l ≤ 19
Reflections collected	10474
Independent reflections	5403 [R_{int} = 0.0652, R_{sigma} = 0.1334]
Data/restraints/parameters	5403/0/374
Goodness-of-fit on F^2	0.899
Final R indexes [I>=2σ (I)]	R_1 = 0.0429, wR_2 = 0.0726
Final R indexes [all data]	R_1 = 0.0694, wR_2 = 0.0762
Largest diff. peak/hole / e $Å^{-3}$	1.27/-1.04

Table 2 Bond Lengths for 3815.

Atom	Atom	Length/Å	Atom	Atom	Length/Å
W	P	2.506(2)	C5	C7	1.507(11)
W	C27	2.005(9)	C8	C9	1.536(10)
W	C28	2.046(10)	C8	C15	1.544(9)
W	C29	2.058(9)	C8	C21	1.542(9)
W	C30	2.040(10)	C9	C10	1.400(10)
W	C31	2.039(9)	C9	C14	1.387(10)
S	P	2.132(3)	C10	C11	1.360(11)
S	C1	1.841(7)	C11	C12	1.379(12)
P	N1	1.707(6)	C12	C13	1.390(11)
P	C8	1.949(8)	C13	C14	1.372(11)
O1	C27	1.157(10)	C15	C16	1.382(10)
O2	C28	1.141(10)	C15	C20	1.401(10)
O3	C29	1.126(9)	C16	C17	1.390(10)
O4	C30	1.145(11)	C17	C18	1.396(11)
O5	C31	1.133(9)	C18	C19	1.387(11)
N1	C1	1.388(9)	C19	C20	1.387(10)
N1	C5	1.497(8)	C21	C22	1.389(10)
N2	C1	1.237(10)	C21	C26	1.399(10)
N2	C2	1.476(9)	C22	C23	1.383(10)
C2	C3	1.508(12)	C23	C24	1.358(12)
C2	C4	1.530(12)	C24	C25	1.386(11)
C5	C6	1.521(10)	C25	C26	1.383(10)

Table 3 Bond Angles for 3815.

Atom	Atom	Atom	Angle/˚	Atom	Atom	Atom	Angle/˚
C27	W	P	176.3(3)	C9	C8	P	109.1(5)
C27	W	C28	86.4(4)	C9	C8	C15	112.7(6)
C27	W	C29	91.0(3)	C9	C8	C21	110.0(6)
C27	W	C30	89.7(4)	C15	C8	P	105.2(5)
C27	W	C31	88.6(3)	C21	C8	P	109.8(5)
C28	W	P	97.0(2)	C21	C8	C15	110.0(6)
C28	W	C29	90.6(3)	C10	C9	C8	123.0(6)
C29	W	P	87.7(2)	C14	C9	C8	119.3(6)
C30	W	P	86.8(3)	C14	C9	C10	117.6(7)
C30	W	C28	174.8(4)	C11	C10	C9	120.8(7)
C30	W	C29	86.1(3)	C10	C11	C12	121.4(8)
C31	W	P	92.5(2)	C11	C12	C13	118.4(8)
C31	W	C28	93.3(3)	C14	C13	C12	120.4(7)
C31	W	C29	176.0(4)	C13	C14	C9	121.3(7)
C31	W	C30	90.0(4)	C16	C15	C8	122.2(6)
C1	S	P	75.6(3)	C16	C15	C20	119.3(6)
S	P	W	113.18(10)	C20	C15	C8	118.5(7)
N1	P	W	118.2(2)	C15	C16	C17	121.0(7)
N1	P	S	80.2(2)	C16	C17	C18	120.1(8)
N1	P	C8	106.5(3)	C19	C18	C17	118.7(7)
C8	P	W	124.6(2)	C18	C19	C20	121.5(7)
C8	P	S	105.0(2)	C19	C20	C15	119.5(8)
C1	N1	P	103.9(4)	C22	C21	C8	122.8(7)
C1	N1	C5	123.8(6)	C22	C21	C26	117.4(7)
C5	N1	P	129.7(5)	C26	C21	C8	119.6(6)
C1	N2	C2	119.2(6)	C23	C22	C21	120.8(7)
N1	C1	S	100.3(5)	C24	C23	C22	121.4(7)
N2	C1	S	131.4(6)	C23	C24	C25	119.0(7)
N2	C1	N1	128.3(7)	C26	C25	C24	120.3(8)
N2	C2	C3	108.4(7)	C25	C26	C21	121.0(7)
N2	C2	C4	107.8(7)	O1	C27	W	179.5(9)
C3	C2	C4	111.5(7)	O2	C28	W	174.3(8)
N1	C5	C6	110.4(6)	O3	C29	W	175.5(8)
N1	C5	C7	112.2(6)	O4	C30	W	177.6(7)
C7	C5	C6	112.0(6)	O5	C31	W	176.4(7)

Table 4 Torsion Angles for 3815.

A	B	C	D	Angle/˚	A	B	C	D	Angle/˚
W	P	N1	C1	-110.7(4)	C12	C13	C14	C9	0.2(13)
W	P	N1	C5	51.2(7)	C14	C9	C10	C11	-2.0(12)
W	P	C8	C9	156.3(3)	C15	C8	C9	C10	7.4(11)
W	P	C8	C15	35.2(5)	C15	C8	C9	C14	-173.4(7)
W	P	C8	C21	-83.1(5)	C15	C8	C21	C22	-81.7(8)
S	P	N1	C1	0.4(4)	C15	C8	C21	C26	93.8(8)

S	P	N1	C5	162.4(7)	C15	C16	C17	C18	0.3(13)
S	P	C8	C9	23.5(5)	C16	C15	C20	C19	1.3(12)
S	P	C8	C15	-97.6(4)	C16	C17	C18	C19	-0.2(12)
S	P	C8	C21	144.2(4)	C17	C18	C19	C20	0.7(12)
P	W	C27	O1	-104(100)	C18	C19	C20	C15	-1.3(12)
P	W	C28	O2	-172(7)	C20	C15	C16	C17	-0.8(12)
P	W	C29	O3	-109(9)	C21	C8	C9	C10	130.6(8)
P	W	C30	O4	115(22)	C21	C8	C9	C14	-50.3(9)
P	W	C31	O5	152(13)	C21	C8	C15	C16	-13.0(10)
P	S	C1	N1	0.4(4)	C21	C8	C15	C20	167.5(7)
P	S	C1	N2	-177.8(9)	C21	C22	C23	C24	-1.9(11)
P	N1	C1	S	-0.5(5)	C22	C21	C26	C25	-0.7(11)
P	N1	C1	N2	177.8(8)	C22	C23	C24	C25	-0.1(12)
P	N1	C5	C6	127.8(7)	C23	C24	C25	C26	1.6(13)
P	N1	C5	C7	-106.4(7)	C24	C25	C26	C21	-1.2(12)
P	C8	C9	C10	-109.0(8)	C26	C21	C22	C23	2.2(11)
P	C8	C9	C14	70.2(7)	C27	W	P	S	-27(4)
P	C8	C15	C16	-131.1(7)	C27	W	P	N1	64(4)
P	C8	C15	C20	49.4(8)	C27	W	P	C8	-156(4)
P	C8	C21	C22	33.5(8)	C27	W	C28	O2	6(7)
P	C8	C21	C26	-150.9(6)	C27	W	C29	O3	67(9)
N1	P	C8	C9	-60.5(5)	C27	W	C30	O4	-64(22)
N1	P	C8	C15	178.4(4)	C27	W	C31	O5	-25(13)
N1	P	C8	C21	60.2(5)	C28	W	P	S	132.1(2)
C1	S	P	W	116.2(3)	C28	W	P	N1	-136.8(3)
C1	S	P	N1	-0.3(3)	C28	W	P	C8	2.6(3)
C1	S	P	C8	-104.9(3)	C28	W	C27	O1	97(100)
C1	N1	C5	C6	-73.4(9)	C28	W	C29	O3	154(9)
C1	N1	C5	C7	52.4(9)	C28	W	C30	O4	-24(26)
C1	N2	C2	C3	-108.5(9)	C28	W	C31	O5	-111(13)
C1	N2	C2	C4	130.6(8)	C29	W	P	S	41.7(3)
C2	N2	C1	S	-3.7(12)	C29	W	P	N1	132.8(4)
C2	N2	C1	N1	178.6(7)	C29	W	P	C8	-87.8(4)
C5	N1	C1	S	-163.8(6)	C29	W	C27	O1	-173(100)
C5	N1	C1	N2	14.4(12)	C29	W	C28	O2	-85(7)
C8	P	N1	C1	103.3(5)	C29	W	C30	O4	27(22)
C8	P	N1	C5	-94.8(7)	C29	W	C31	O5	60(16)
C8	C9	C10	C11	177.2(8)	C30	W	P	S	-44.5(2)
C8	C9	C14	C13	-178.1(8)	C30	W	P	N1	46.7(3)
C8	C15	C16	C17	179.7(7)	C30	W	P	C8	-173.9(3)
C8	C15	C20	C19	-179.1(7)	C30	W	C27	O1	-87(100)
C8	C21	C22	C23	177.9(6)	C30	W	C28	O2	-35(11)
C8	C21	C26	C25	-176.5(7)	C30	W	C29	O3	-22(9)
C9	C8	C15	C16	110.2(8)	C30	W	C31	O5	65(13)
C9	C8	C15	C20	-69.3(9)	C31	W	P	S	-134.3(3)
C9	C8	C21	C22	153.5(7)	C31	W	P	N1	-43.2(4)
C9	C8	C21	C26	-30.9(9)	C31	W	P	C8	96.3(4)

C9	C10	C11	C12	1.6(15)	C31	W	C27	O1	3(100)
C10	C9	C14	C13	1.1(12)	C31	W	C28	O2	95(7)
C10	C11	C12	C13	-0.3(15)	C31	W	C29	O3	-17(13)
C11	C12	C13	C14	-0.6(14)	C31	W	C30	O4	-153(22)

8.20. Crystal data and structure refinement for **58**

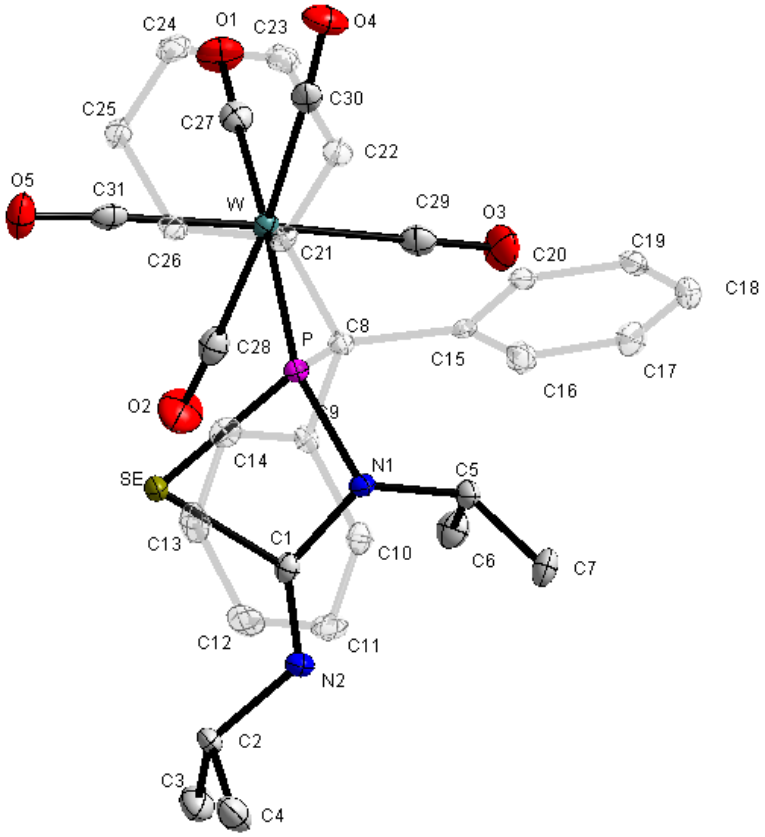

Table 8.20. Crystal data and structure refinement for **58**.

Identification code	GSTR421, JMV474 // GXray4100f
Device Type	Bruker X8-KappaApexII
Empirical formula	$C_{29}H_{24}NO_5PW$
Moiety formula	C29 H24 N O5 P W
Formula weight	681.31
Temperature/K	100
Crystal system	monoclinic
Space group	$P2_1/n$
a/Å	13.1709(10)
b/Å	13.0975(9)
c/Å	15.6670(12)
α/°	90
β/°	91.408(2)
γ/°	90
Volume/Å^3	2701.8(3)
Z	4
ρ_{calc}g/cm^3	1.675
μ/mm^{-1}	4.373

F(000)	1336.0
Crystal size/mm^3	0.24 × 0.22 × 0.2
Absorption correction	empirical
Tmin; Tmax	0.4719; 0.7460
Radiation	MoKα (λ = 0.71073)
2Θ range for data collection/°	5.06 to 55.996°
Completeness to theta	0.995
Index ranges	-17 ≤ h ≤ 16, -17 ≤ k ≤ 14, -20 ≤ l ≤ 20
Reflections collected	26300
Independent reflections	6503 [R_{int} = 0.0405, R_{sigma} = 0.0355]
Data/restraints/parameters	6503/0/337
Goodness-of-fit on F^2	1.048
Final R indexes [I>=2σ (I)]	R_1 = 0.0220, wR_2 = 0.0470
Final R indexes [all data]	R_1 = 0.0268, wR_2 = 0.0483
Largest diff. peak/hole / e Å^{-3}	0.78/-0.63

Table 2 Bond Lengths for 3902f.

Atom	Atom	Length/Å	Atom	Atom	Length/Å
W	P	2.5103(5)	C5	C7	1.527(3)
W	C27	2.003(2)	C8	C9	1.531(3)
W	C28	2.033(2)	C8	C15	1.536(3)
W	C29	2.038(2)	C8	C21	1.531(3)
W	C30	2.055(2)	C9	C10	1.401(3)
W	C31	2.046(2)	C9	C14	1.386(3)
Se	P	2.2719(6)	C10	C11	1.378(3)
Se	C1	1.987(2)	C11	C12	1.386(3)
P	N1	1.7125(17)	C12	C13	1.377(3)
P	C8	1.960(2)	C13	C14	1.394(3)
O1	C27	1.143(2)	C15	C16	1.397(3)
O2	C28	1.138(3)	C15	C20	1.391(3)
O3	C29	1.142(3)	C16	C17	1.388(3)
O4	C30	1.131(3)	C17	C18	1.383(3)
O5	C31	1.139(3)	C18	C19	1.379(3)
N1	C1	1.386(3)	C19	C20	1.389(3)
N1	C5	1.484(3)	C21	C22	1.394(3)
N2	C1	1.245(3)	C21	C26	1.395(3)
N2	C2	1.465(2)	C22	C23	1.389(3)
C2	C3	1.512(3)	C23	C24	1.380(3)
C2	C4	1.514(3)	C24	C25	1.384(3)
C5	C6	1.528(3)	C25	C26	1.383(3)

Table 3 Bond Angles for 3902f.

Atom	Atom	Atom	Angle/˚	Atom	Atom	Atom	Angle/˚
C27	W	P	176.36(6)	C9	C8	P	108.54(13)
C27	W	C28	90.07(8)	C9	C8	C15	110.40(15)
C27	W	C29	87.70(8)	C9	C8	C21	112.39(16)
C27	W	C30	86.16(8)	C15	C8	P	109.99(13)
C27	W	C31	90.64(8)	C21	C8	P	104.69(12)
C28	W	P	86.44(6)	C21	C8	C15	110.66(16)
C28	W	C29	90.09(9)	C10	C9	C8	119.14(18)
C28	W	C30	174.72(8)	C14	C9	C8	123.01(18)
C28	W	C31	85.90(9)	C14	C9	C10	117.84(19)
C29	W	P	93.32(6)	C11	C10	C9	121.0(2)
C29	W	C30	93.44(9)	C10	C11	C12	120.5(2)
C29	W	C31	175.66(9)	C13	C12	C11	119.3(2)
C30	W	P	97.26(6)	C12	C13	C14	120.3(2)
C31	W	P	88.09(6)	C9	C14	C13	121.0(2)
C31	W	C30	90.45(8)	C16	C15	C8	119.80(18)
C1	Se	P	71.27(6)	C20	C15	C8	122.51(17)
Se	P	W	113.12(2)	C20	C15	C16	117.47(18)
N1	P	W	117.43(6)	C17	C16	C15	121.0(2)
N1	P	Se	81.26(6)	C18	C17	C16	120.5(2)
N1	P	C8	106.65(8)	C19	C18	C17	119.3(2)
C8	P	W	124.31(6)	C18	C19	C20	120.2(2)
C8	P	Se	105.38(6)	C19	C20	C15	121.46(19)
C1	N1	P	106.60(13)	C22	C21	C8	122.30(17)
C1	N1	C5	123.18(16)	C22	C21	C26	117.60(18)
C5	N1	P	128.33(13)	C26	C21	C8	120.09(17)
C1	N2	C2	120.11(18)	C23	C22	C21	120.75(19)
N1	C1	Se	100.87(13)	C24	C23	C22	120.6(2)
N2	C1	Se	130.86(16)	C23	C24	C25	119.5(2)
N2	C1	N1	128.25(19)	C26	C25	C24	119.83(19)
N2	C2	C3	109.22(18)	C25	C26	C21	121.69(19)
N2	C2	C4	108.19(16)	O1	C27	W	179.10(18)
C3	C2	C4	111.81(18)	O2	C28	W	177.23(19)
N1	C5	C6	111.70(16)	O3	C29	W	177.42(19)
N1	C5	C7	111.17(17)	O4	C30	W	174.09(17)
C7	C5	C6	112.33(18)	O5	C31	W	176.64(19)

Table 4 Torsion Angles for 3902f.

A	B	C	D	Angle/˚	A	B	C	D	Angle/˚
W	P	N1	C1	-111.95(12)	C9	C8	C15	C16	-30.7(3)
W	P	N1	C5	52.55(17)	C9	C8	C15	C20	154.76(18)
Se	P	N1	C1	-0.38(11)	C9	C8	C21	C22	111.3(2)

Se	P	N1	C5	164.12(16)	C9	C8	C21	C26	-68.6(2)
P	N1	C1	Se	0.43(13)	C9	C10	C11	C12	0.1(3)
P	N1	C1	N2	179.05(18)	C10	C9	C14	C13	-2.0(3)
P	N1	C5	C6	-108.59(19)	C10	C11	C12	C13	-1.8(3)
P	N1	C5	C7	125.07(17)	C11	C12	C13	C14	1.6(3)
P	C8	C9	C10	70.23(19)	C12	C13	C14	C9	0.4(3)
P	C8	C9	C14	-110.30(18)	C14	C9	C10	C11	1.8(3)
P	C8	C15	C16	-150.41(16)	C15	C8	C9	C10	-50.4(2)
P	C8	C15	C20	35.0(2)	C15	C8	C9	C14	129.08(19)
P	C8	C21	C22	-131.08(17)	C15	C8	C21	C22	-12.6(3)
P	C8	C21	C26	49.0(2)	C15	C8	C21	C26	167.44(17)
C1	N1	C5	C6	53.6(2)	C15	C16	C17	C18	-0.9(3)
C1	N1	C5	C7	-72.8(2)	C16	C15	C20	C19	2.8(3)
C1	N2	C2	C3	129.8(2)	C16	C17	C18	C19	1.7(3)
C1	N2	C2	C4	-108.3(2)	C17	C18	C19	C20	-0.1(3)
C2	N2	C1	Se	-2.9(3)	C18	C19	C20	C15	-2.2(3)
C2	N2	C1	N1	178.85(18)	C20	C15	C16	C17	-1.3(3)
C5	N1	C1	Se	-165.06(14)	C21	C8	C9	C10	-174.47(16)
C5	N1	C1	N2	13.6(3)	C21	C8	C9	C14	5.0(3)
C8	P	N1	C1	103.16(13)	C21	C8	C15	C16	94.4(2)
C8	P	N1	C5	-92.34(17)	C21	C8	C15	C20	-80.2(2)
C8	C9	C10	C11	-178.74(18)	C21	C22	C23	C24	-0.7(3)
C8	C9	C14	C13	178.51(18)	C22	C21	C26	C25	1.1(3)
C8	C15	C16	C17	-176.12(19)	C22	C23	C24	C25	0.9(3)
C8	C15	C20	C19	177.53(18)	C23	C24	C25	C26	-0.2(3)
C8	C21	C22	C23	179.69(19)	C24	C25	C26	C21	-0.9(3)
C8	C21	C26	C25	-178.92(18)	C26	C21	C22	C23	-0.4(3)